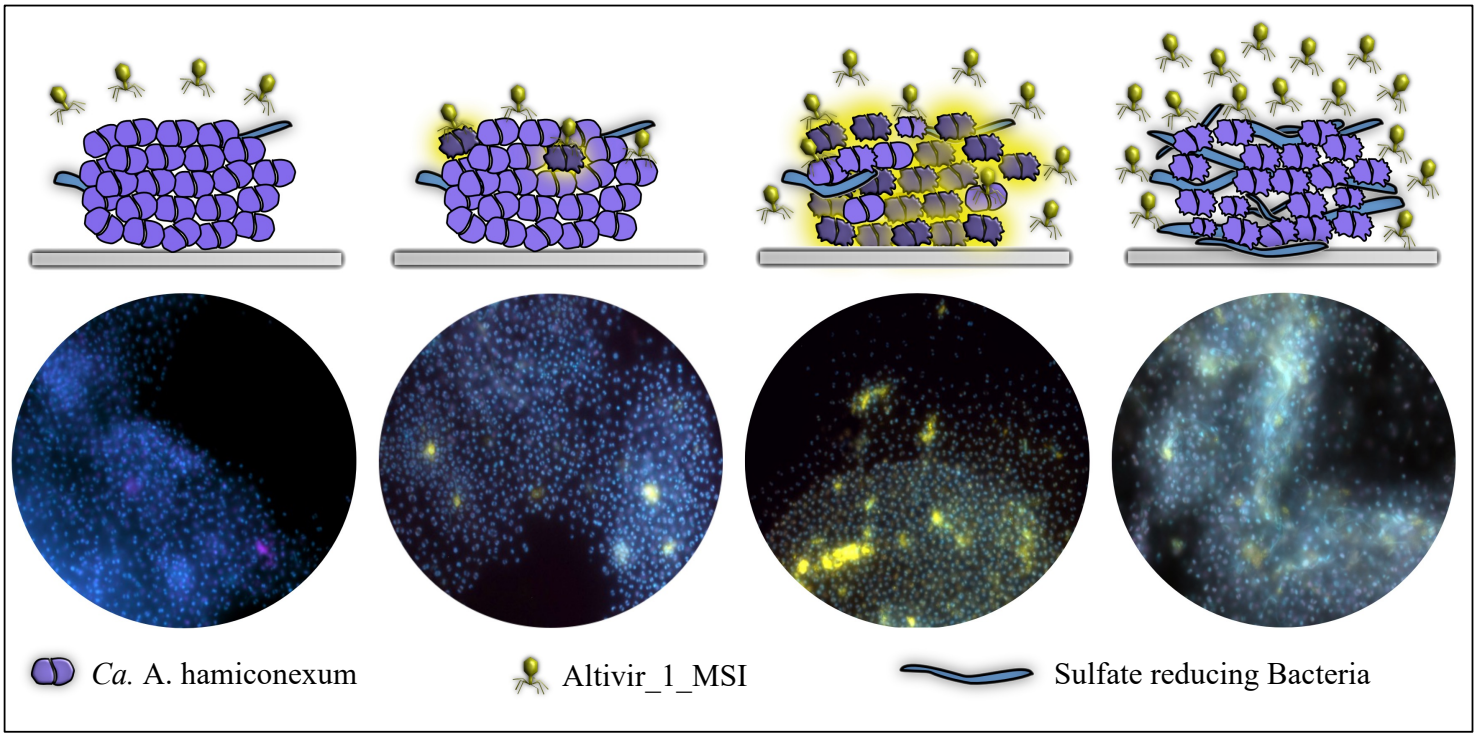

Hunting hidden archaeal viruses from the continental subsurface

DISSERTATION

Zur Erlangung des Doktorgrades der Naturwissenschaften (Dr. rer.nat.)

Der Fakultät für Chemie der

Universität Duisburg-Essen

vorgelegt von

Victoria Turzynski

aus Düsseldorf

2023

Image on title page: VirusFISH on *Ca.* Altiarchaea biofilms.
VirusFISH shows the temporal development of *Ca.* Altiarchaea biofilms during viral infections induced by Altivir_1_MSI I in the deep subsurface. © Image was created by Victoria Turzynski.

Das Promotionsgesuch wurde eingereicht am:		27.04.2023
Disputation erfolgte am:		27.10.2023
Diese Arbeit wurde angeleitet von:		Prof. Dr. Alexander J. Probst
Prüfungsausschuss:	Vorsitzender:	Prof. Dr. Kai S. Exner
1.	Gutachter:	Prof. Dr. Alexander J. Probst
2.	Gutachter:	Prof. Dr. Hans-Curt Flemming
3.	Gutachter:	Prof. Dr. David Prangishvili

_____

Unterschrift: Victoria Turzynski

DOI: 10.17185/duepublico/81303
URN: urn:nbn:de:hbz:465-20231204-071022-1

Hunting hidden archaeal viruses from the continental subsurface

DISSERTATION

For achieving the doctoral degree of natural sciences (Dr. rer. nat.)

At the faculty of Chemistry at the University of Duisburg-Essen

By

Victoria Turzynski

from Düsseldorf

2023

Key words:

Deep biosphere, microbial ecology, subsurface viruses, Altiarchaeota, fluorescence *in situ* hybridization, virusFISH, direct-geneFISH, microbial heterogeneity

This dissertation was performed under the auspices of

Prof. Dr. Alexander J. Probst (PhD supervisor)

At the Fakultät für Chemie under fullfillment of all guidelines according to the Promotionsordnung of the faculty

"The eye of a human being is a microscope,
which makes the world seem bigger than it really is."

(Khalil Gibran)

"Ravioli, ravioli. Give me the formuoli."

(Spongebob Schwammkopf)

"Life is like a box of chocolates,
you never know what you're going to get."

(Robert Zemeckis / Forrest Gump)

(The latter can also be transferred to imaging ☺)

Acknowledgements

First and foremost, I am extremely grateful to ***Prof. Dr. Alexander Probst*** for being my doctoral father and for giving me the opportunity for doing my thesis in his group. *Thank you!!!!!!!!*

His immense knowledge and plentiful experience have encouraged me in all the time of my academic research. By working on this super exiting project called "NOVAC": Novel viruses of terrestrial subsurface archaea impacting global carbon cycling – I was able to extend my previous research experiences from my Master thesis (also written in Prof. Dr. Probst group), resulting in not only great publications, but also in new ideas for further investigations and projects. Also, special thanks go to the ***Deutsche Forschungsgemeinschaft (DFG)*** for funding.

I would also like to thank ***Prof. Dr. Hans-Curt Flemming*** for being my second reviewer of my thesis. I could not imagine any other reviewer that has such an immense knowledge on biofilms and thus, represent the perfect fit for my thesis.

I deeply acknowledge the best direct-geneFISH/ CARD-FISH/ virusFISH trainer I ever had – ***Dr. Cristina Moraru*** – Many thanks that you trained me so good in these methods! Without your expertise, we probably would not have had such great results and publications!

In addition, I thank ***all co-authors*** who contributed significantly to my publications that made this PhD thesis possible.

I would like to thank ***all the members of the AG Probst group***. It is their kind help and support that have made my study and life a wonderful time.

Finally, I would like to express my gratitude to ***my mother***, and to ***my pets*** for entertainment at home ☺.

List of Publications

Victoria Turzynski has three first authorship publications, one second authorship publication (an additional one is in preparation for publication), and seven publications in total. The publications are listened below.

First authorship publications:

Rahlff, J., **Turzynski, V.,** Esser, S. P., Monsees, I., Bornemann, T. L. V., Figueroa-Gonzalez, P. A., Schulz, F., Woyke, T., Klingl, A., Moraru, C., Probst, A. J. Lytic archaeal viruses infect abundant primary producers in Earth's crust. ***Nature communications*** (2021)

Turzynski, V., Monsees, I., Moraru, C., Probst, A. J. Imaging techniques for detecting prokaryotic viruses in environmental samples. ***Viruses*** 13(11), (2021).

Turzynski, V., Griesdorn, L., Moraru, C., Soares, A., Simon, S. A., Stach, T. L., Rahlff, J., Esser, S. P., Probst, A. J. Virus-host dynamics in archaeal groundwater biofilms and the associated bacterial community composition. ***Viruses***, (2023).

Second authorship publications:

Monsees, I., **Turzynski, V.**, Esser, S. P., Soares, A., Timmermann, L., Weidenbach, K., Banas, J., Kloster, M., Beszteri, B., Schmidt-Streit, R., Probst, A. J. Label-free Raman microspectroscopy for identifying prokaryotic virocells. ***mSystems*** (2022).

Esser, S. P., **Turzynski, V.**, Plewka, J., Moore, C., Banas, I., Soares, A. R., Lee, J., Woyke, T., Probst, A. J. Differential expression of core metabolic functions in DPANN Archaea of distinct subsurface ecosystems. ***In preparation as brief communication to The ISME Journal*** (2023)

Other:

Bornemann, T. L. V., Adam, P. S., **Turzynski, V.**, Schreiber, U., Figueroa-Gonzalez, P. A., Rahlff, J., Koester, D., Schmidt, T. S., J., Schunk, R., Krauthausen, B., Probst, A. J. Genetic diversity in terrestrial subsurface ecosystems impacted by geological degassing. ***Nature communications*** (2022).

Banas, I., Esser, S. P., **Turzynski, V.,** Soares, A., Novikova, P., May, P., Moraru, C., Hasenberg, M., Wilmes, P., Klingl, A., Probst, A. J. Spatio-functional organization in virocells of small uncultivated archaea from the deep biosphere. ***In revision at The ISME Journal*** (2023)

Esser, S. P., Rahlff, J., Zhao, W., Predl, M., Plewka, J., Sures, K., Wimmer, F., Lee, J., Adam, P. S., McGonigle, J., **Turzynski, V.,** Banas, I., Schwank, K., Krupovic, M., Bornemann, T. L. V., Figueroa-Gonzalez, P. A., Jarett, J., Rattei, T., Amano, Y., Blaby, I. K., Cheng, J., Brazelton, W. J., Beisel, C. L., Woyke, T., Banfield, J. F., Zhang, Y., Probst, A. J. A CRISPR-mediated symbiosis between uncultivated archaea predicted from metagenomic data. ***In preparation for submitting to Nature Microbiology*** (2023)

Conference Proceedings

Victoria Turzynski contributed to different conferences.

Oral presentations

Turzynski, V., Rahlff, J., Moraru, C., Probst, A. J., 2020. Genome-informed microscopy reveals viral infections of uncultivated archaea in a terrestrial subsurface aquifer. *VAAM - Vereinigung für Allgemeine und Angewandte Mikrobiologie*, Leipzig, Deutschland

Turzynski, V., Rahlff, J., Esser, S., Monsees, I., Bornemann, T.L.V., Griesdorn, L., Figueroa-Gonzalez, P. A., Schulz, F., Woyke, T., Klingl, A., Moraru, C., Probst, A. J., 2021. Lytic archaeal viruses of the continental deep biosphere challenge a long-standing paradigm. *DOE Joint Genome Institute – Genomics of Energy & Environment Meeting,* Virtual conference

Turzynski, V., Rahlff, J., Esser, S., Monsees, I., Bornemann, T.L.V., Griesdorn, L., Figueroa-Gonzalez, P. A., Schulz, F., Woyke, T., Klingl, A., Moraru, C., Probst, A. J., 2021. Persistent viral infections of Altiarchaeota in the deep biosphere. *21st German Archaea Meeting*, Frankfurt, Deutschland

Poster First author

Turzynski, V., Griesdorn, L., Monsees, I., Moraru, C., Probst, A. J., 2022. Persistent viral infections of uncultivated subsurface archaea are associated with drastic morphological changes of the host. *VAAM - Vereinigung für Allgemeine und Angewandte Mikrobiologie*, Düsseldorf, Deutschland. Virtual conference. **(Poster Award)**

Poster co-author

Probst, A. J., Bornemann, T. L. V., Rahlff, J., Esser, S., **Turzynski, V.**, Monsees, I., Figueroa-Gonzalez, P. A., Adam, P., Schwank, K., Klingl, A., Moraru, C., 2019. Genome replication and effective CRISPR defense indicate a highly active microbiome in the continental subsurface.

Monsees, I., **Turzynski, V.,** Rahlff, J., Klingl, A., Moraru, C., Probst, A. J., 2019. Genome-informed microscopy: CLEM for studying viral infections of uncultivated archaea.

Monsees, I., **Turzynski, V.,** Probst, A. J., 2020. Studying bacteriophage infection using Raman microspectroscopy.

Monsees, I., **Turzynski, V.,** Esser, S., P., Soares, A., Timmermann, L., Kloser, M., Beszteri, B., Probst, A. J., 2021. Identification of virocell using Raman spectroscopy.

Esser, S. P., Monsees, I., **Turzynski, V.,** Probst, A. J., 2022. Identification/ Ultrastructure of novel archaeal viruses with help of multi-omics.

Esser, S. P., Beesley, T., Moore, C. J., Banas, **Turzynski, V.,** Probst, A. J., 2022. Microdiversity of archaeal viruses from a terrestrial subsurface aquifer.

Banas, I., **Turzynski V.,** Hasenberg M., Klingl A., Probst, A. J., 2022. CLEM reveals impact of viral infections on archaeal biofilm composition in groundwater.

Soares, A., Kaspareit, Y., **Turzynski V.,** Kallmeyer, J., Schnabel, E., Kitte, J. A., Okolski, S., Kutschera, E., Probst, A. J., 2022. Capturing virus-host interactions via long-read Hi-C metagenomics.

Table of Contents

I. Abstract

Viruses are ubiquitous and are important microbial predators that not only influence global biogeochemical cycles but also drive microbial evolution. Moreover, viruses cause significant mortality in prokaryotic communities, can modify the host diversity and abundance, but also alter the genetic content of their hosts via horizontal gene transfer or by expression of viral-encoded genes during viral infection. However, little is known about the role of viruses in the deep terrestrial subsurface that contains a large reservoir of organic carbon and hosts a large fraction of all microbes on Earth. Compared to various investigations focusing on the bacterial diversity, studies on archaea in the deep terrestrial subsurface are very limited. Culture-independent methods such as metagenomics have shown that, archaea like *Candidatus* Altiarchaea can dominate this difficult to access ecosystem. Due to the limitations of conventional culture techniques, the microbial distribution, and the interaction of microorganisms with, *e.g.,* viruses living in such an ecosystem, remain poorly understood. Studying viral infections can bolster our understanding in terms of the spatial and temporal distribution of viruses, the effects on the overall community composition, the microbial diversity, nutrient cycling, and carbon cycling in the deep biosphere.

The overarching objective of this study was to broaden the current knowledge on *Ca.* Altiarchaea and their microbial interactions within the deep subsurface. More specifically, this study focused on one specific sulfidic spring called the “Muehlbacher Schwefelquelle Isling (MSI)” located in Regensburg (Germany), that has been shown to harbor almost pure biofilms consisting of up to 95% of *Candidatus* Altiarchaeum hamiconexum (*Ca.* A. hamiconexum), a primary producer of the deep subsurface.

In this thesis, I report on one specific virus (here “Altivir_1_MSI”) hijacking *Ca.* A. hamiconexum and its respective viral lifestyle. This microbial “relationship” remained so far unexplored. Metagenomics coupled with fluorescence *in situ* hybridization (here “virusFISH”) enabled the investigation of this specific virus-host system in the deep subsurface. Moreover, this dissertation is the first one focusing on virus-host dynamics by using virusFISH in this rather difficult to access ecosystem at single-cell level. Analysis of the different infection stages using fluorescence microscopy revealed initial infections, advanced infections, as well as cell lysis of *Ca.* A. hamiconexum cells with the release of new virions. Through this linkage and the resulting stages of infection, a first indication of a lytic

replication cycle of Altivir_1_MSI was received. In addition, the virusFISH results evidenced a stable virus-host relationship over four years.

Furthermore, it can be assumed that this lytic virus might jump-start heterotrophic carbon cycling in this ecosystem by acting as a potential top-down and bottom-up controller. By having different virusFISH images at hand, an accumulation of sulfate-reducing bacteria on spots where a successful lysis event of *Ca.* A. hamiconexum cells occurred, was observed. Through a constant viral lysis of the primary producer, this "microbial loop" of the deep subsurface seems to be activated by a release of possible nutrients that other microbes like sulfate-reducing bacteria can utilize.

Overall, the results and findings of these investigations that make up this thesis, have contributed significantly to today's understanding of the interactions between archaeal viruses and their hosts, and their role in the deep subsurface. At the same time, this thesis is one of the first examples that showed how well these microbial interactions can be investigated by using today's current state-of-the-art-techniques in an ecosystem that is difficult to access.

II. General Introduction

1. *Around the world* – Prokaryotes and their distribution in the deep subsurface

Prokaryotes (bacteria and archaea) – the most ancient and most widespread forms of life on Earth represent not only an essential component of the Earth's biota, but also a large portion of life's genetic diversity (Whitman et al. 1998). They can be found in nearly all environments due to diverse metabolic processes and are responsible in many biogeochemical cycles, such as nitrogen and carbon cycles (Whitman et al. 1998). Microbial life depends on the constant supply of available nutrients (serving as electron donors and acceptors) that need to be constantly recycled, *e.g.,* by prokaryotes. Whitman and co-workers (1998) attempted to make a first estimation of the total prokaryotic number on Earth with $4–6\times10^{30}$ prokaryotic cells (Whitman et al. 1998). Most of Earth's prokaryotes, however, occur in the 'big five' habitats, *i.e.*, the open ocean (1×10^{29}), upper oceanic sediments (5×10^{28}), deep oceanic subsurface (4×10^{29}), soil (3×10^{29}), and deep continental subsurface (3×10^{29}) (see Figure II.1, Flemming and Wuertz 2019). However, quantification of Earth's prokaryotic biota, especially for the deep biosphere, remains extremely challenging in terms of, *e.g.,* the difficulty to obtain uncontaminated samples or the colonization of cells to surfaces (Flemming and Wuertz 2019).

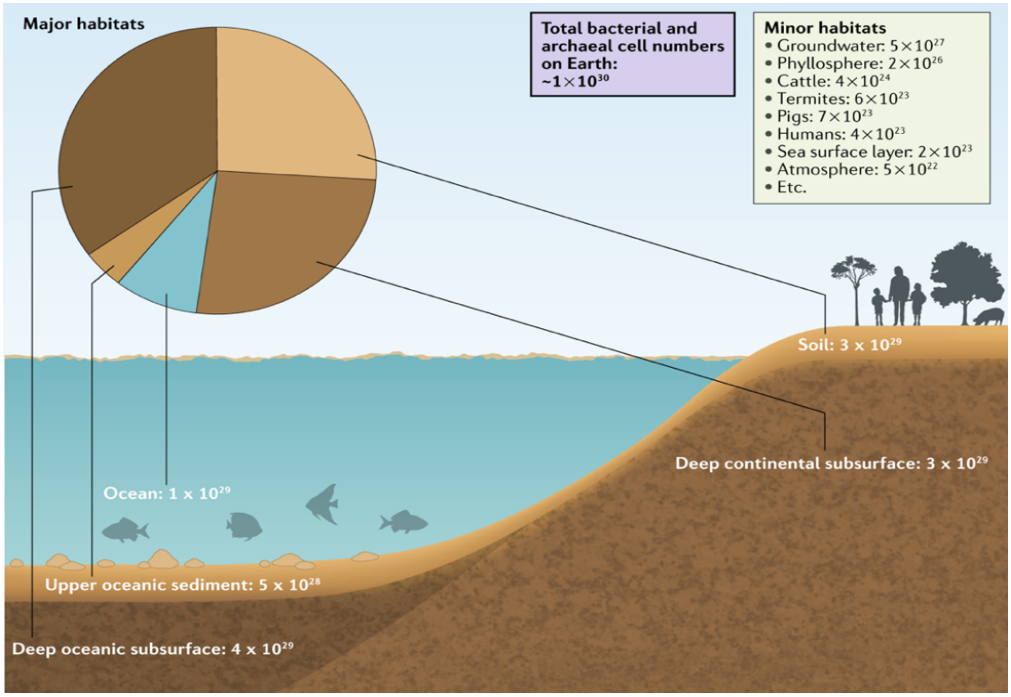

Figure II.1: Bacterial and archaeal abundances in the 'big five' habitats on Earth (taken from Flemming and Wuertz 2019).

Not every subsurface microbial habitat is yet explored and fully investigated. Today's understanding of microbial diversity and distribution patterns is still at an early stage, especially for the deep subsurface, as it has been assumed for the past 30 years that life is a surface phenomenon and that even active microbes are unable to live deeper than ten meters below the surface (Reith 2011). Today we know that life in the deep subsurface can be found down to a depth of 4,850 m and at temperatures up to 137°C (Beulig et al. 2022; Dai et al. 2021), however, the microbial abundance and diversity is decreasing with depth, a trend that was later also confirmed for, *e.g.,* archaeal viruses (Kyle et al. 2008).

It is not surprising that the microbial ecology of the deep biosphere has received increased research attention over the last two decades (Dai et al. 2021; D'Hondt et al. 2004; Fredrickson et al. 1995; Krumholz et al. 1997; Whitman et al. 1998) because the deep subsurface is ubiquitous and comprises ~12-20% of the total biomass of microorganisms on Earth (Fry et al. 2008; Kallmeyer et al. 2012; Magnabosco et al. 2018). Furthermore, this ecosystem includes a variety of subsurface habitats, *e.g.*, terrestrial deep aquifer systems or mines, marine sediments, deeply buried hydrocarbon reservoirs or the basaltic ocean crust (Teske et al. 2013). However, this barely studied ecosystem harbors by far the largest reservoir of organic carbon on Earth (Bar-On et al. 2018) with a yet uncharacterized microbial diversity, the so-called "microbial dark matter" (Rinke et al. 2013). Well adapted to the relatively stable subsurface environmental conditions with continuous darkness, anaerobic conditions, high pressure, limited energy and nutrient availability (Escudero et al. 2018), subsurface prokaryotes have developed "surviving strategies" for dealing with these conditions, albeit with a resulting slower metabolic activity (Jørgensen 2011). Due to the complex behavior in the microbial metabolism, it is still a major challenge to quantify, *e.g.*, microbial activity in subsurface environments for understanding their role in global biogeochemical cycles. The rate of microbial activity in subsurface seems to be several orders of magnitude lower than in surface environments, indicating that the energy flux and the availability of nutrients are one of the main limiting factors for microbial growth besides the other above mentioned abiotic factors (Chapelle and Lovley 1990; Miettinen et al. 2018; Parkes et al. 2000; Phelps et al. 1994; Wang et al. 2018). Miettinen and co-workers (2018) assumed that acetate and hydrogen (H_2) are key factors limiting the microbial metabolic activity in, *e.g.*, deep subsurface groundwaters (Miettinen et al. 2018). In many deep subsurface habitats, *e.g.*, deep aquifers or igneous-rock aquifers, acetate (*e.g.*, produced from carbon dioxide, CO_2, a possible carbon source) and hydrogen serve as energy source for

subsurface microbes indicating that autotrophic acetogenesis, methanogenesis, anaerobic methane oxidation, or sulfate reduction are thought to be relevant processes in the deep subsurface (Kotelnikova and Pedersen 1997; Stevens and McKinley 1995).

Since the deep biosphere is considered as the most energy limited ecosystem, the energy-conserving reductive acetyl-CoA (Wood-Ljungdahl) pathway is recognized as a key carbon fixation route in this special ecosystem (Momper et al. 2017; Probst et al. 2018; Stevens 1997). The study of Magnabosco et al. (2016) showed that this pathway occurs also at a depth of 3 km and was reported for a deep fracture fluid system accessed via the Tau Tona gold mine (Witwatersrand Basin, South Africa) (Magnabosco et al. 2016). However, the energy flux in some deep subsurface environments is so low (Jones et al. 2018) that microbes are forced to stop their growth and could enter, *e.g.,* into dormancy states for coping with perpetual energy limitation (Jones et al. 2018; Jørgensen 2011). Dormancy can preserve microbial diversity and is thought to be widespread among the subsurface biosphere (Jones et al. 2018; Jørgensen and Marshall 2016). Some techniques, like traditional metagenomic analyses cannot distinguish between active, dormant or dead microbes (Burkert et al. 2019), however, targeting and quantifying their ribosomes, a component of all living and active cells that is rapidly degraded upon their death (Davis et al. 1986), can be detected via fluorescence *in situ* hybridization (FISH) for identifying their "status" in the subsurface (Schippers et al. 2005) but also with other cell count methods, such as acridine orange direct counts (AODC) (Teske 2005). Besides this, more than 99% of bacterial and archaeal species have not been cultivated so far (Jiao et al. 2021), not only because of their microbial "status quo" (active/ dormant/ or dead) but also due to the limitations of conventional culture techniques or to the difficulty of sampling of such difficult to access environments. In addition, our ability to discover the full depth of the deep subsurface is currently hindered by technical issues to reach high depths (> 4 km), while providing sufficiently clean samples by avoiding any contaminations (Wilkins et al. 2014). It must also be recognized that accessing the deep biosphere is not completely without interactions from surface environments. For instance, the terrestrial subsurface is geological influenced by surface microbes that can transport not only nutrients, but also biomass from the surface to the subsurface biosphere. Several studies were conducted on, *e.g.*, the Äspö Hard Rock Laboratory (Sweden) located in an 1800-million-year-old Fennoscandian Shield bedrock that contains fractures bearing groundwaters of varying characteristics dependent on the connectivity to the surface, showing that surface microbes can infiltrate the microbiome of the deep biosphere (Holmfeldt et al. 2021; Hubalek

et al. 2016; Mathurin et al. 2012; Westmeijer et al. 2022). These numerous challenges that are involved in isolating and culturing deep subsurface microbes makes it difficult to actually characterize *in situ* subsurface microbial communities.

However, all studies on the deep biosphere conducted so far suggest that this ecosystem is microbial active and equally important for global biogeochemical cycles like, *e.g.,* surface environments.

1.1 *Prokaryotic predators* – Viruses

Despite the ecological and biogeochemical importance of prokaryotes in the deep biosphere, there is little information about their mortality and the regulation of their turnover. A potential cause of microbial mortality is viral lysis of their prokaryotic hosts, hence affecting benthic microbial processes and nutrient cycling within ecosystems (Danovaro et al. 2008; Fuhrman 1999; Suttle 2007, 1999; Weinbauer 2004). Viruses do not have their own metabolism and are found to be ubiquitous in every ecosystem studied to date, including the deep biosphere. Since viruses are depended on their hosts for completing their cycle of reproduction, either by lysing their hosts or by integrating viral genes into the host's genome without killing their hosts, viruses are suggested to act as a potential vector for horizontal gene transfer (HGT) by facilitating hosts manipulation and viral resistance (Irwin et al. 2021). In addition, HGT is hypothesized to be a major driver for prokaryotic evolution (Hall et al. 2020).

Viruses occur widespread with abundances that can sometimes exceeds the numbers of their bacterial or archaeal hosts as reported for, *e.g*., the deep sub-seafloor (Anderson et al. 2013; Engelhardt et al. 2014; Middelboe et al. 2011). Moreover, any variations in the viral and/ or prokaryotic numbers has effects also on the carbon content in the respective ecosystem (Engelhardt et al. 2014). Given the fact that counting environmental viruses and/ or their respective hosts represents a major challenge, a certain degree of uncertainty in these numbers still exist. It was estimated for, *e.g.,* deep sea ecosystems that ~0.37–0.63 gigatons of carbon (GtC) per year on a global scale are released through viral infections, a result that could indicate that viruses are essential key players in ecosystem's functioning (Danovaro et al. 2008; Gao et al. 2022). By killing their hosts, viruses convert organic matter from biomass to the pool of dissolved (DOM) and particulate organic matter (POM) (Proctor and Fuhrman 1992). This "viral shunt" has the effect of stimulating bacterial growth by providing a source of organic matter for their respiration (Suttle 2007). Thus, the viral shunt can mediate a

shuttle of organic carbon from autotrophic to heterotrophic microbial communities in the deep subsurface that are key microorganisms responsible for decomposition of dissolved organic carbon (DOC) and constitute a critical component in the so-called "microbial loop" (Fuhrman 1999; Suttle 2005). Thus, viruses control the host community composition in terms of nutrient availability by bottom-up processes and host abundance by lysis events (top-down) (Storesund et al. 2015).

However, the impact of the viral shunt on the deep biosphere depends on virus-to-cell ratios (Anderson et al. 2013). The virus-to-cell ratios or also termed as "virus-to-prokaryote ratio (VPR)" can vary according to depth and location (Danovaro et al. 2008; Kyle et al. 2008), resulting in difficulties in terms of calculating the overall impact of viruses on prokaryotic mortality in the deep subsurface (Anderson et al. 2013). Generally, it is considered that the viral abundance decreases with increasing depth by following the trend of prokaryotic abundance (Kyle et al. 2008; Middelboe et al. 2011), however, a study on, *e.g.,* deep sub-seafloor sediments showed the opposite (VPR increase with depth, Engelhardt et al. 2013). Another aspect is the predominant viral life cycle. The viral life cycles can be lytic, lysogenic or pseudolysogenic, but can also show chronic infections (reviewed in Weinbauer 2004). For instance, a high VPR in an ecosystem can be an indicator for an ongoing lytic viral process in contrast to lysogenic viruses (Parikka et al. 2017). During the lytic cycle of viral replication, viruses hijack the host's metabolic machinery, degrade the host chromosome, and release virions upon cell lysis (Mäntynen et al. 2021). For instance, ecosystems with a higher prokaryotic abundance would support a higher trend for lytic viral production (Rowe et al. 2008; Winget et al. 2011) by following the well-known "kill-the-winner" model, indicating that viruses prefer to lyse the most abundant organism and modify hosts diversity (Thingstad and Lignell 1997; Thingstad 2000). Estimates show that viral lysis removes approximately 20-40% of prokaryotic biomass, *e.g.,* in the ocean daily (Suttle 2007).

Besides lytic events, some viruses, *e.g.,* temperate phages/ viruses, can enter into a lysogenic state, if a low hosts abundance is given ($<10^6$ cells mL^{-1}), by integrating their genome into the host chromosome to become a prophage (Breitbart 2012; Brum et al. 2015; Paul 2008; Payet and Suttle 2013; Weinbauer 2004; Wommack and Colwell 2000). The virus persists in a "dormant state" until conditions favor their reactivation or persist as a plasmid and does not promote cell death due lysis or the production of virions as in the lytic cycle (Refardt 2011). Lysogeny has been previously hypothesized to be a preferable "survival strategy" for viruses, *e.g.,* in the deep subsurface (Anderson et al. 2013; Engelhardt et al.

2011). Recently, the newly proposed "piggyback-the-winner" model suggest that lysogeny would also be favored with a high microbial abundance (Chen et al. 2019b; Coutinho et al. 2017; Knowles et al. 2016). However, this model postulates that a high host abundance would favor a switch to the lysogenic life cycle (Silveira and Rohwer 2016). Viruses can switch between lysogenic to lytic or lytic to lysogenic, when stressful conditions appear (*e.g.*, DNA damage, temperature, pH change, cell density, phage density, nutrient availability etc. (Makky et al. 2021), the latter transition being less studied (Paul 2008; Williamson et al. 2002; Zhen et al. 2019). Both the lytic and the lysogenic cycles are present in all domains of life, eukarya, bacteria, and archaea (reviewed in Wirth and Young 2022). Another but less common viral life cycle is pseudolysogeny, in which the viral genome resides in an unstable, inactive state within its host and fails to replicate as in lytic production or to become a prophage as in the lysogenic state (Łoś and Węgrzyn 2012). Pseudolysogeny seems to play an important role in the long-term survival of viruses in nutrient-deprived environments (Ripp and Miller 1997), and was studied, *e.g.*, for the marine environment (Williamson et al. 2001) or freshwater lakes (Ripp and Miller 1997). Moreover, pseudolysogeny is most common where a constant production of phage in the presence of high host cell abundance is given (Ripp and Miller 1997; Williamson et al. 2001). Unlike lytic, lysogenic, and pseudolysogenic cycles, chronic infection leads to continuous virion production without lysis of the prokaryotic cell that was mainly reported for filamentous phages (reviewed in Mäntynen et al. 2021). Today we know that archaeal viruses can also cause chronic infections, *e.g.*, members of the *Fuselloviridae* family (*e.g.*, viruses of *Sulfolobus*, Xiang et al. 2005), or viruses of Haloarchaea (reviewed in Luk et al. 2014). For instance, a recent study on *Haloferax volcanii* pleomorphic virus 1 (HFPV-1) showed chronic infections on the model organism haloarchaeon *Haloferax volcanii* DS2 with a constant release of virions by using electron microscopy (Alarcón-Schumacher et al. 2022).

1.1.1 *Unique, special, exceptional* – A focus on archaeal viruses

Similar to members of the other two domains of life, archaea are also being infected by viruses that sometimes show distinct and special virion morphologies, many of which have never been reported for viruses infecting bacteria or eukaryotes (Krupovic et al. 2018; Prangishvili et al. 2017; Wirth and Young 2020). The majority of archaeal viruses show bottle-shaped, spindle-shaped, droplet-shaped, or fusiform morphologies (Prangishvili et al. 2006a). Additionally, archaeal viruses are divided into archaea specific viruses and

cosmopolitan viruses (Krupovic et al. 2018), whereby only cosmopolitan viruses possess structural and genetic features that are similar to those of bacterial and eukaryotic viruses (Iranzo et al. 2016; Krupovic et al. 2018). The first study on archaeal viruses was conducted in the 1980s by Wolfram Zillig and co-workers (Janekovic et al. 1983). Today, 40 years later, 117 known archaeal viruses have been isolated so far (reviewed in Dellas et al. 2014) from in total 6,300 viral isolates that infect also other prokaryotes. These approximately 1.85% of isolated archaeal viruses include viruses infecting, *e.g.*, hyperthermophiles and hyperhalophiles of the phyla *Crenarchaeaota* and *Euryarcheaota* (Luk et al. 2014; Prangishvili et al. 2017), but also methanogens (Pfister et al. 1998; Thiroux et al. 2021; Weidenbach et al. 2017; Wolf et al. 2019) and Thaumarchaea (Ahlgren et al. 2019; Chow et al. 2015; Danovaro et al. 2016; Kim et al. 2019; Krupovic et al. 2011b, 2019). Compared to extreme environments like hot springs, highly saline environments or hydrothermal vents, the number of archaeal viruses in mesophilic environments is still significantly lower, which could be due to the difficulty of culturing many of their microbial hosts (Munson-McGee et al. 2018).

Based on their diverse virion morphologies and genomic properties, archaeal viruses are currently classified into 17 families including members of the *Ampullaviridae, Spiraviridae, Fuselloviridae, Rudiviridae, Clavaviridae, Myoviridae,* etc. (Prangishvili et al. 2017). The majority of isolated archaeal viruses have linear or circular double stranded (ds) DNA genomes, but also single stranded (ss) DNA genomes were described (Mochizuki et al. 2012; Pietilä et al. 2010, 2009). To date, no archaeal RNA virus has been isolated so far, only detected via metagenomics (Bolduc et al. 2012). However, the number of archaeal viruses and their families will increase as more archaeal viruses are being discovered and characterized.

Special about archaeal viruses compared to those of bacterial viruses are the unique egress mechanisms that are, however, relatively unexplored. Most of these studies are focusing on viruses infecting archaea from the genus *Sulfolobales*. For instance, the formation of, *e.g.*, large pyramidal structures (virus-associated pyramids, VAPs) on the host cell surface were reported for viruses belonging to *Rudiviridae* (*Sulfolobus islandicus* rod-shaped virus 2, SIRV2, Bize et al. 2009), *Turriviridae* (*Sulfolobus* turreted icosahedral virus 1, STIV1, Brumfield et al. 2009), and *Ovaliviridae* (*Sulfolobus* ellipsoid virus 1, SEV1, Wang et al. 2018), all infecting hyperthermophilic or acidophilic archaea of *Sulfolobales*. Viral egress can also be performed via “budding” by maintaining the host cell membrane and a constant virion production without causing cell lysis. This egress mechanisms were described for

pleomorphic archaeal viruses of the family *Pleolipoviridae* isolated from halophilic archaeal strains belonging to the genera *Halorubrum*, *Haloarcula, Halogeometricum,* and *Natrinema* of the class Halobacteria (Demina and Oksanen 2020; Pietilä et al. 2009, 2010, 2012), but also for, *e.g.*, the spindle-shaped virus SSV1 from the family *Fuselloviridae*, infecting the hyperthermophilic members of the order *Sulfolobales* (Krupovic et al. 2014). These viral egress mechanisms remain exceptional for the domain archaea.

Currently, knowledge about virus-host interactions in archaea remains highly fragmented because most of the studies focusing on enrichment cultures. It is even more limited when it comes to viruses infecting, *e.g*., archaeal biofilms in ecosystems.

2. *Sticking and living together* – Biofilms

Prokaryotes alternate between two modes of growth, a unicellular life phase, in which the cells are planktonic (free-swimming), and a multicellular life phase, in which the cells are sessile and live in a so-called "biofilm". Generally, it has been estimated that 40–80% of the microbial cells on our planet reside in biofilms (Flemming and Wuertz 2019), however, factors controlling biofilm formation are poorly understood, especially for the deep subsurface. The term "biofilm" can be defined as heterogeneous structures comprising different microbial populations surrounded by a self-produced matrix (extracellular polymeric substances, EPS) that allows their attachment to each other and/ or to surfaces (Flemming and Wuertz 2019; Penesyan et al. 2021). Interactions among microbes that populate within a biofilm together with their protective EPS against environmental stressors, make these communities more robust than planktonic prokaryotes. In addition, the sticky EPS comprises 97% water, 2-5% microbial cells, 1-2% polysaccharides, 1-2% proteins and 1-2% DNA and RNA (Flemming and Wingender 2010; Sutherland 2001), holding their microbial inhabitants together, in contrast to their free-living planktonic counterparts (Flemming and Wuertz 2019). Moreover, the EPS account for 50-90% of the total organic carbon of the biofilm (Flemming 2016). The EPS composition determines important biofilm properties such as strength, elasticity, sorption properties, porosity, density, water content, charge, hydrophobicity, and mechanical stability (Flemming et al. 2007; Zhang and Bishop 2003). All these properties help to form a robust shelter that offers a protected and nutrient-rich ecological niche for the microbial survival (reviewed in Flemming et al. 2023). Thus, a biofilm provides a dynamic environment, assuming that the microbial cells are viable and metabolically active, which is also depending on their position in the biofilm matrix

(Sutherland et al. 2004). As mentioned previously, biofilms offer microorganisms the ability to adhere on surfaces, which can be seen as a survival strategy under energy conservation regarding the accumulation of nutrients on the biofilms (Flemming and Wingender 2010; Flemming and Wuertz 2019). Moreover, living in a biofilm can have many (ecological) advantages including genetic and metabolic exchange (*e.g.*, via horizontal gene transfer), cell-to-cell communication (*e.g.*, through quorum sensing), a more efficient nutrient recycling, protection against viral predation that is more depending on the gene expression patterns of sessile active cells, motility, and stress tolerance (Donlan 2002; Flemming and Wingender 2010; Pires et al. 2021).

Biofilm formation involves several steps and can be seen as a cyclic process that is divided into three distinct stages: attachment, maturation with active sessile cells forming cell clusters (stage I), and microcolonies (stage II), and dispersion of cells from the biofilm to the environment (stage III) (Figure II.2). The first step in the biofilm development is the adherence of prokaryotic cells to the surface through a reversible attachment via weak Van-der-Waals forces or electrostatic interactions (Mohamed Zuki et al. 2021). The attached cells proliferate and produce the EPS, in which microbial communication through biochemical signals (*e.g.*, for quorum sensing) and a genetic exchange is facilitated (Donlan 2002; Flemming and Wingender 2010; Pires et al. 2021). During the irreversible attachment of cells to the surface stronger hydrophilic/ hydrophobic interactions are developed through, *e.g.*, flagella, pili, exopolysaccharides, lipopolysaccharides, etc. (Flemming and Wingender 2010; Sauer et al. 2022; Yin et al. 2019), making a more stable cell cluster existence on the surface (Donlan 2002; Flemming and Wingender 2010). In the stages of the biofilm maturation, a spatial structuring of such cell clusters (Maturation I) occurs in all three dimensions, resulting in so-called “microcolonies” (Maturation II) (Sauer et al. 2022). The three-dimensional structure contains water channels for distributing nutrients and signaling molecules (*e.g.*, acylated homoserine lactones, AHL) within the biofilm matrix (Sauer et al. 2022; Yin et al. 2019). In the dispersal stage, microcolonies undergo cell death and lysis along with an active dispersal of motile cells and a degradation of the biofilm matrix components (Tolker-Nielsen 2015). The cells can be detached from the biofilm in clumps or as single, separated cells (Yin et al. 2019). In general, a biofilm maintains an equilibrium between growth and dispersal.

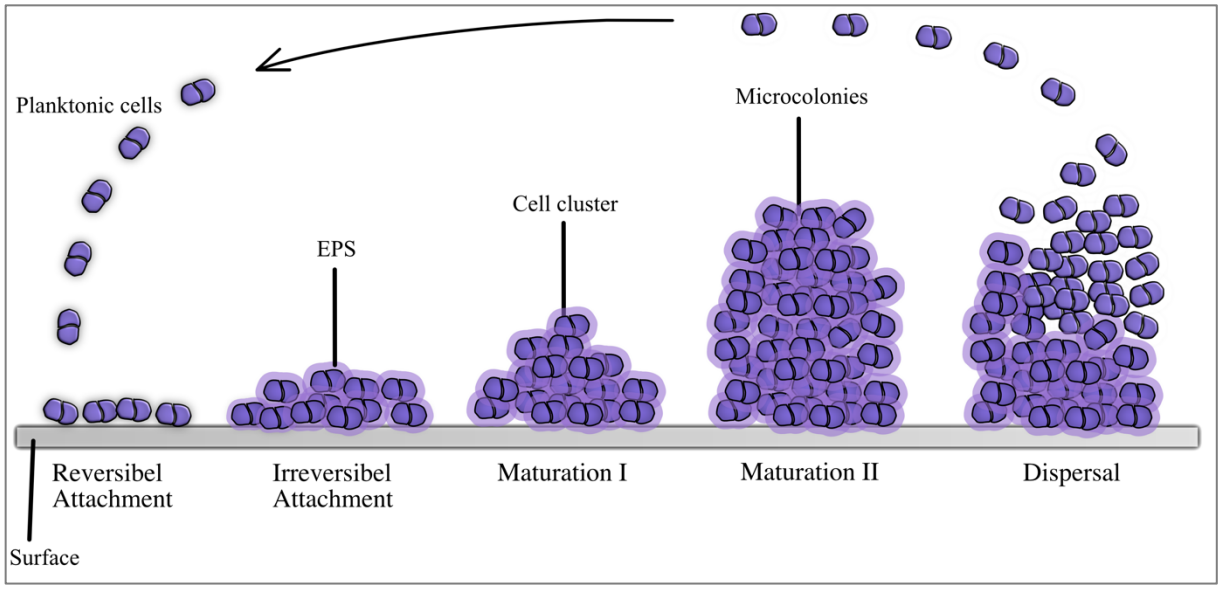

Figure II.2: Stages of biofilm development: Reversible attachment, Irreversible attachment, Maturation I, Maturation II, and Dispersal (adapted from Sauer et al. 2022).

During the biofilm life cycle, the EPS creates gradients for the emergence of microenvironments with specific physical and chemical properties and allows different types of microbes types an adaptation to that particular microenvironment (Penesyan et al. 2021). Thus, biofilms are not only dynamic but also organized in terms of their microbial community, which are composed of cells that are heterogeneous in space and time (Flemming 2016; Flemming and Wingender 2010; Penesyan et al. 2021). Heterogeneity in biofilms by having cells with different metabolic capacities (called "mixed-species biofilm community or multi-species biofilms", Penesyan et al. 2021), leads to a cooperation and establishment of gradients (electron acceptors and donors, redox conditions, etc.) within the biofilm (Flemming 2016). These features enable microbes to life in a specific niche within the biofilm based on its physiology and functional profile (Joshi et al. 2021; Penesyan et al. 2021). For instance, microbial species housing in microbial mats of shallow aquatic environments are organized according to their metabolic and energetic properties (Penesyan et al. 2021). The uppermost layers are dominated by aerobic photosynthetic organisms that are exposed to oxygen and light, while the deeper layers are mainly composed of anaerobic microorganisms (Penesyan et al. 2021). This phenomenon that multi-species biofilms are organized based on their microbial needs and not always randomly distributed on a population scale, was also shown in laboratory (Møller et al. 1998; Watnick and Kolter 2000). However, most species–species interactions in biofilms can be negative since cells are competing with each other for space and for a rapid nutrient uptake (resources). This competition can have the effect of a so-called

"Amensalim", where one population may produce compounds, such as acids, alcohols, antibiotics, extracellular membrane vesicles, and bacteriocins into the environment by affecting the growth of the other population (Berlanga and Guerrero 2016; Flemming 2016; Hibbing et al. 2010), potentially leading to a reduction of the biofilm structure and adhesion properties (Flemming 2016). Also, invaders like viruses can inhibit the biofilm formation by degradation of the EPS matrix, thus promoting its active dispersal (Flemming 2016).

Overall, understanding the temporal and spatial heterogeneity of biofilms and studying their invaders, and how all these aspects affect the evolution of social phenotypes is still at an early stage. However, most insights were gained with less complex biofilm communities in the laboratory by often neglecting these aspects (Flemming 2016).

2.1 *Altiarchaeota and their friendly neighbors* – A unique microbial community within deep subsurface biofilms

As mentioned in the previous chapters, several studies have shown that most deep subsurface microorganisms are likely surface-attached or live in biofilms (Flemming and Wuertz 2019; Jägevall et al. 2011; Magnabosco et al. 2018) like *Ca.* Altiarchaeum (Henneberger et al. 2006; Probst et al. 2013, 2014a, 2014b; Probst and Moissl-Eichinger 2015; Rudolph et al. 2001, 2004; Bird et al. 2016). *Ca.* Altiarchaeum (originally called the SM1, Probst et al. 2014b) is globally distributed and can be found in anoxic environments such as lake sediments, sulfidic aquifers, geothermal springs, deep sea sediments, mud volcanoes, and hydrothermal vents as well as industrial settings and drilled wells (Probst et al. 2014b). Based on 16S rRNA gene sequence analysis and phylogenomics, *Altiarchaeales* belong as uncultivated group of archaea to the Euryarchaeota phylum (Bird et al. 2016; Rudolph et al. 2001), more precisely close to the methanogen origin, most probably as a sister group to *Methanococcales* (Probst and Moissl-Eichinger 2015; Probst et al. 2014b). Special about *Ca.* Altiarchaea is that they belong to biofilm-forming archaea (Bird et al. 2016) (Figure II.3, A-E) besides *Sulfolobus* sp. from hot springs (Brock et al. 1972; Suzuki et al. 2002; Zillig et al. 1980), and uncultivated anaerobic methanotrophic (ANME) archaea from euxinic basins (Michaelis et al. 2002) and represents one of the few examples of archaea with a double cell membrane (Probst and Moissl-Eichinger 2015; Probst et al. 2014b). Moreover, *Altiarchaeales* can be divided into two clades, Alti-1 and Alti-2 (Bird et al. 2016). Members of Alti-1 and Alti-2 differ in their genomic characteristics and adaptations to different environments (Bird et al. 2016). For example, Alti-1 members like *Ca.* Altiarchaeum

hamiconexum, which is the most well-described representative of *Altiarchaeales* (Bird et al. 2016; Probst and Moissl-Eichinger 2015), have adaptations to form hooks and biofilms (Figure II.3, A-C), while Alti-2 residing in saline environments and have adaptations that make them specialized for a free-living state in sulfidic, saline environments (Bird et al. 2016). *Ca.* Altiarchaeum was first described as a nearly monoclonal biofilm in a cold terrestrial sulfidic spring called "Sippenauer Moor" (SM) in Regensburg (Germany) (Bird et al. 2016; Moissl et al. 2002; Rudolph et al. 2001). Here, a whitish string of pearls community was found, whereby the outer shell of the pearls consists of filamentous bacteria belonging to *Thiothrix* sp., a sulfide-oxidizing species (Moissl et al. 2002, 2003; Probst and Moissl-Eichinger 2015; Rudolph et al. 2001, 2004) that has been detected via FISH (Moissl et al. 2002; Probst et al. 2013). The interior of the pearls consists of up to 10^7 coccoid archaea (SM1 Euryarchaeon, Rudolph et al. 2001) that dominate the community.

Moreover, *Ca.* Altiarchaea were also found in the drilled Muehlbacher Schwefelquelle at Isling (MSI, image can be found in Henneberger et al. 2006) near Regensburg (Germany) (linear distance from MSI to the Sippenauer Moor: 20 km, Probst et al. 2014b) and is commonly referred to as SM1-MSI in the literature (Rudolph et al. 2001, 2004; Probst et al. 2014b). In contrast to the Sippenauer Moor, the white pearls of the biofilm of the Muehlbacher Schwefelquelle contain besides the predominant *Ca.* A. hamiconexum (95%), sulfate-reducing bacteria belonging to *Deltaproteobacteria* (5%) (Probst et al. 2013, 2014b; Probst and Moissl-Eichinger 2015; Henneberger et al. 2006). The potential bacterial partner in the MSI that surrounds the archaeal microcolony is suggested to be *Sulfuricurvum* sp., a sulfide-oxidizing microorganism that together with *Ca.* A. hamiconexum is important for the sulfur cycle in this ecosystem (Probst et al. 2013; Rudolph et al. 2004). The coexistence of *Ca.* A. hamiconexum with their bacterial partners suggests a syntrophic or symbiotic relationship including possible nutrient exchange (Henneberger et al. 2006; Moissl et al. 2002; Rudolph et al. 2004). *Ca.* Altiarchaeum has another feature of forming a regular three-dimensional arrangement of their cells (Figure II.3, B) to each other due to their filamentous cell appendages called "hami" (Moissl et al. 2005; Probst and Moissl-Eichinger 2015) (Figure II.3, C). These molecular barbed grappling hooks, which built up an entangled web between the cells (cell-cell distance of 4 µm), could be responsible for the attachment of cells to surfaces and for biofilm initiation and was described for both sulfidic springs (Henneberger et al. 2006).

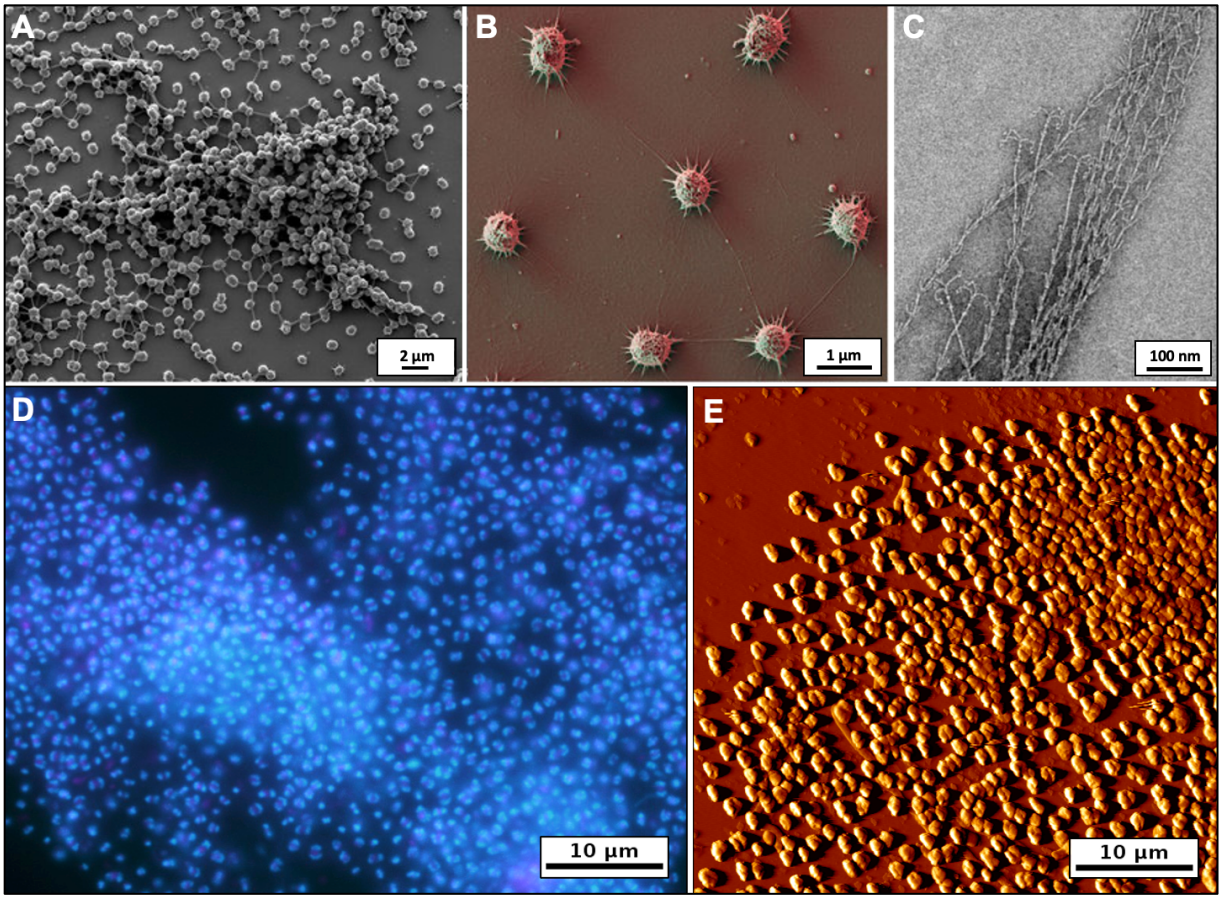

Figure II.3: (A, B) Scanning electron micrographs of *Ca.* A. hamiconexum cells (modified from Probst et al. 2014b). Bars: (A) 2 µm, (B) 1 µm. (C) *Ca.* A. hamiconexum cell surface appendages (modified from Probst and Moissl-Eichinger 2015). Bar: 100 nm. (D) Fluorescence micrograph and (E) atomic force micrograph of an *Ca.* A. hamiconexum biofilm taken by V. Turzynski. Bars: 10 µm.

However, compared to studies focusing on the bacterial diversity of diverse ecosystems around the globe, studies on archaea are rare, especially for the deep terrestrial subsurface (Bird et al. 2016; Lazar et al. 2017; O'Connell et al. 2003; Probst et al. 2013, 2014b, 2018; Purkamo et al. 2018; Takai et al. 2001; Waldron et al. 2007). A possible reason could be that studies on the deep subsurface often show that bacteria are more abundant in some subsurface environments than archaea (Lin et al. 2006; Rastogi et al. 2009; Schippers et al. 2005), only a limited number of studies exists that indicate that archaea predominate (*e.g.*, Biddle et al. 2006; Probst et al. 2014a; Probst and Moissl-Eichinger 2015). However, these few studies have profiled the archaeal diversity in the deep terrestrial biosphere, but their distribution and metabolic significance in biogeochemical cycles within the deep subsurface remains poorly understood. As mentioned in Chapter 1 (*Around the world* – Prokaryotes and their distribution in the deep subsurface) the deep terrestrial subsurface that also includes deep subsurface aquifers like the MSI, belongs to the most energy limited ecosystems on our planet (Probst et al. 2018). Archaea, like *Ca.* Altiarchaea that live here, have evolved a special

energy metabolism and are able to fix carbon from inorganic sources. *Ca.* Altiarchaea has been emerged as one of the best model organisms for studying microbial interactions within this energy-limited environment (Henneberger et al. 2006; Probst et al. 2013, 2014a, 2014b; Probst and Moissl-Eichinger 2015; Rudolph et al. 2001, 2004; Bird et al. 2016).

This microbe uses a special key carbon fixation route, the energy-conserving reductive acetyl-CoA (Wood-Ljungdahl) pathway that requires approximately 1 mol ATP for the generation of 1 mol pyruvate and is one of the most important pathways for carbon fixation (Probst and Moissl-Eichinger 2015; Probst et al. 2018). The reductive acetyl-CoA pathway has also been reported in various other ecosystems of the deep terrestrial biosphere (*e.g.,* Lau et al. 2016; Magnabosco et al. 2016; Nyyssönen et al. 2014; Rempfert et al. 2017). This pathway can be used either to degrade acetyl-CoA to carbon dioxide (CO_2) or to fix CO_2 to acetyl-CoA (Probst et al. 2014b). Such microorganisms like *Ca.* Altiarchaea that are capable of an autotrophic metabolism (modified WL-pathway without enzymes encoding for methanogenesis, (Probst et al. 2014b) are an integral part of the deep subsurface because they provide other microorganisms (*e.g.*, heterotrophs) an otherwise unavailable form of carbon (Berg et al. 2010). Carbon represents a key component of the global carbon cycle (Hügler and Sievert 2011). The carbon cycle is therefore important because the balance between autotrophy and heterotrophy (oxidation of organic carbon back into inorganic carbon) is significant for the CO_2 and O_2 concentration, *e.g.,* in the atmosphere, and hence also affects the Earth's redox balance (Hügler and Sievert 2011).

Besides, sulfate reduction, as well as methanogenesis (Kotelnikova 2002; Nyyssönen et al. 2014; Ward et al. 2004), anaerobic methane oxidation (Ino et al. 2018), acetogenesis (Kotelnikova and Pedersen 1997; Lever 2012), and reduction of iron (Haveman et al. 1999) can be found in the deep subsurface (Nuppunen-Puputti et al. 2018). In many anaerobic environments sulfate reducers and methanogens perform the final steps in the breakdown of complex organic matter (Jørgensen and Parkes 2010). By the decomposition of organic matter, acetate can be formed by, *e.g.*, acetogenic microbial communities (Nuppunen-Puputti et al. 2018) that can be further used by sulfate reducers (Pedersen et al. 2008). These acetogenic microbes may support further microbial groups, such as acetate-oxidizing sulfate reducing bacteria (Pedersen et al. 2008) or acetate utilizing methanogens (Kotelnikova and Pedersen 1997; Nuppunen-Puputti et al. 2018). The competition between sulfate reducing bacteria and methanogens for common substrates, *e.g.*, H_2 and acetate, is essentially depended by abiotic factors including substrate and sulfate concentrations (Lovley et al. 1982; Michas et

al. 2020). Until now, it is still unknown if the biofilm-forming *Ca.* Altiarchaeum is capable of methane oxidation or metanogenesis since the archaeal factor F_{420} was not yet identified in their metabolism (Moissl et al. 2003; Probst et al. 2013). However, methanogens are considered to be quickly outcompeted by sulfate reducers for hydrogen and organic substrates in such anoxic, sulfate-rich environments at high or limited amounts of sulfate (SM, MSI, Probst et al. 2013; Bell et al. 2020).

3. *Breaking down the architecture* – Virus based strategies of dispersing biofilms

Viral infections may be responsible for the high mortality of autotrophic and heterotrophic organisms in various ecosystems including the deep subsurface, resulting in effects on the carbon and nutrient cycle (Anderson et al. 2013; Danovaro et al. 2008; Suttle 2007). Prokaryotes live in multi-species and represent a spatially structured community that is ubiquitously in the microbial world (Flemming and Wuertz 2019; Penesyan et al. 2021). Such communities or biofilms, have a strong impact in the field of microbial ecology, however, very little attention has been paid on microbial interactions at the cellular scale, *e.g.*, that determine or destruct the overall biofilm structure. Biofilms have a so-called "open architecture" with water-filled channels (water channel model Wimpenny and Colasanti 1997) that allows viruses to directly access the interior of the biofilm and infect prokaryotes harbouring the biofilm (Wimpenny and Colasanti 1997; Sutherland et al. 2004). Since biofilms having a high cell density than, *e.g.*, the surrounding medium, they have the potential to be a hotspot for viral activity (Anderson et al. 2013). Investigating virus-host interactions within biofilms is depending on various factors, like the species composition, the number of viruses, the amount of biofilm biomass, the spatial heterogeneity, the composition of the biofilm matrix, and the microbial metabolic activity that can vary within the different layers of the biofilms (Abedon 2012, 2016). For instance, some bacterial species can secrete outer membrane vesicles (OMVs) containing phage receptors that can mediate phage entrapment by contributing to an irreversible binding of viruses, thereby preventing infections of biofilm cells (Manning and Kuehn 2011; Reyes-Robles et al. 2018; Pires et al. 2021).

The EPS matrix of a biofilm acts as a potential barrier against viral infection (Costerton et al. 1987; Roberts 1996; Weinbauer 2004; Wilkinson 1958), however, the EPS of biofilms cannot always prevent viral infections (Doolittle et al. 1995a; Hanlon et al. 2001; Weinbauer 2004), because viruses developed some strategies for penetrating this barrier, *e.g.,* due to enzymatic digestion (Weinbauer 2004). Viruses may enhance biofilm formation

through induction of polysaccharide production (Fernández et al. 2018; Secor et al. 2015) or have special enzymes that are involved in depolymerasing the biofilm matrix that are located in the virus tail or capsid (Weinbauer 2004). For instance, some viruses can produce enzymes that degrade the poly-γ-glutamic acid (γ-PGA) capsule of, *e.g.*, *Bacillus* spp. that represents a secreted polymeric substance that is similar to the EPS matrix in biofilms (Yu et al. 2016). The degradation of the biofilm matrix by associated enzymes and a direct viral lysis of their microbial hosts picture the normal component of the biofilm development and is a major factor for the release of new virions from the biofilm to the surrounding medium/ environment (Webb et al. 2003; Weinbauer 2004).

Moreover, active phages already trapped in the biofilm can eliminate newly arriving prokaryotic cells (Bond et al. 2021). Viruses can have different types of enzymes for, *e.g.*, degrading the surface polysaccharides of prokaryotes or the biofilm matrix by depolymerases, or destroying the prokaryotic cell wall by virion-associated peptidoglycan hydrolases (VAPGHs) and endolysins (Azeredo et al. 2021; Gutiérrez et al. 2017). These types of enzymes were reported for viruses hijacking bacteria (bacteriophages). Cell-wall containing archaea can also be lysed by special pseudomurein cleaving lysins reported for, *e.g.*, *Methanobacteriales* and *Methanopyrales* (reviewed in Visweswaran et al. 2010, 2011). However, archaeal viruses are able to employ other alternative mechanisms for infecting their hosts (see Chapter 1.2.1 *Unique, special, exceptional* - A focus on archaeal viruses) that are unique in the prokaryotic world, the most traditional method for analyzing virus-host interactions besides imaging and molecular biological techniques are computational methods based on data from laboratory experiments (cultured virus-host systems) (Jarett et al. 2020).

3.1 *Stayin' alive: an evolutionary arms race* – CRISPR Cas immune system vs. virus-encoded anti-CRISPR proteins

CRISPR-Cas systems represent a prokaryotic adaptive immunity mechanism against mobile genetic elements (MGEs), such as viruses or plasmids (Barrangou et al. 2007) and are widely conserved in both bacteria (up to 40%) and almost all archaea (90%) (Lier et al. 2015). CRISPR-Cas (clustered regularly interspaced short palindromic repeats) immunity involves three main stages (Figure II.4): 1) the adaptation stage in which virus/MGEs derived sequences (so-called "spacers") are inserted into the CRISPR locus, 2) the processing/ expression stage in which the CRISPR locus is transcribed and processed into separate CRISPR RNAs (crRNAs), and 3) the interference stage in which the detection and

degradation of MGEs by CRISPR RNA and Cas proteins happens (Rath et al. 2015). In the last step the crRNA binds to the assembled CRISPR effector complex (called "interference module") for recognizing and degrading DNA and/or RNA molecules containing the protospacer sequence (Rath et al. 2015). The CRISPR-Cas system can be divided into two broad classes and six distinct types (I-VI), which can be divided into several subtypes (Makarova et al. 2011; Pauly et al. 2019a). For instance, Class 1 contains Type I, III, and IV, whereby Class 2 CRISPR-Cas system covers Type II, V, VI (Hatoum-Aslan and Howell 2021). Class 1 CRISPR-Cas systems are widespread among bacteria and archaea; however, the less common Class 2 CRISPR-Cas systems are only found in bacterial species (Hatoum-Aslan and Howell 2021).

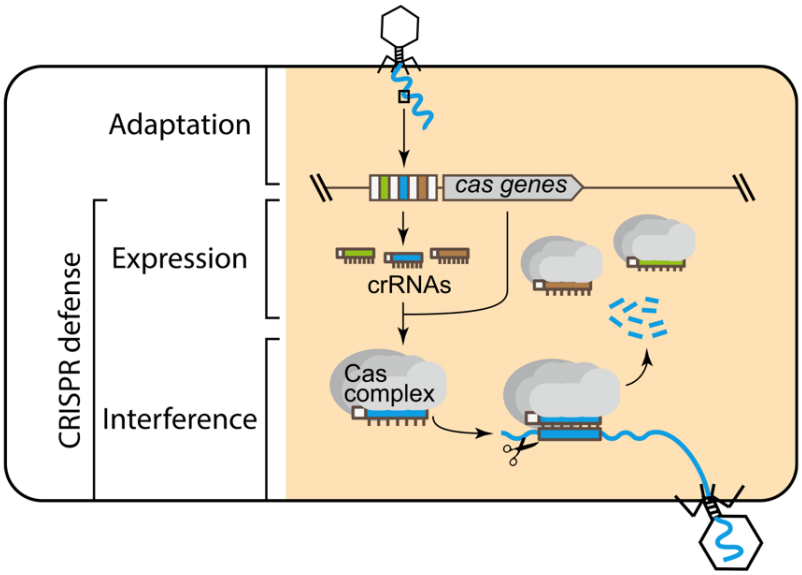

Figure II.4: The CRISPR-Cas system. Three major stages are involved for CRISPR immunity: adaptation, expression, and interference (taken from: Hatoum-Aslan and Howell 2021).

The fact, that up to 40% of bacteria and almost all archaea have a CRISPR-Cas system, suggests that viruses have effective mechanisms for overcoming this specific barrier. Viruses can stop the host's CRISPR-Cas complex from interrupting their phage life cycle by producing anti-CRISPR (Acr) proteins (consisting of 53-333 amino acids) (Wirth and Young 2022). For instance, it was shown that members of the *Rudiviruses* (specifically *Sulfolobus islandicus* rod-shaped virus, SIRV) constantly attack and infect archaea of the genus *Sulfolobus*. The CRISPR-Cas system of *Sulfolobus* is able to remember the viral DNA for a specific counterattack by breaking down the viral DNA before it can cause any harm within the host (He et al. 2018; Pauly et al. 2019a). However, it was shown that SIRV evolved strategies by using Acr proteins to evade the targeting by the host CRISPR-Cas adaptive

immunity (He et al. 2018). To date, only three archaeal Acr proteins have been characterized, all belonging to *Rudiviruses* (Athukoralage et al. 2020; Bhoobalan-Chitty et al. 2019; He et al. 2018), besides many investigations conducted for Acrs of bacteriophages (Bondy-Denomy et al. 2013; Borges et al. 2017; Davidson et al. 2020; Maxwell et al. 2016; Pawluk et al. 2014; Rauch et al. 2017; Wiegand et al. 2020).

Surprisingly, CRISPR-mediated defense systems can also appear to be employed by viruses for interviral conflicts. A recent study on archaeal viruses of the family *Portogloboviridae* isolated from a Japanese hot spring showed that *Sulfolobus polyhedral virus* 1 (SPV1) and 2 (SPV2) carry mini-CRISPR arrays with spacers targeting each other (Liu et al. 2018; Medvedeva et al. 2019). These interviral conflicts could represent a mechanism of heterotypic superinfection exclusion, in which a cell infected by one virus becomes resistant to another closely related virus (Medvedeva et al. 2019).

Over the past decade, basic insights into CRISPR-Cas mechanisms have been conducted with *in silico* analysis (*e.g.,* metagenomics) with the ongoing development of new powerful genetic and bioinformatic tools. A visual proof of whether the host's CRISPR-Cas system is active or not during a viral infection would be possible by using imaging techniques for detecting both — spacer and *cas* genes. Combining the information derived from metagenomics and imaging techniques (*e.g.,* via fluorescence *in situ* hybridization) could bolster our understanding in terms of an active arms race between viruses and their host within ecosystems.

4. Scope of the thesis and publication guide

The scope of the present thesis was to establish the virusFISH method for investigating the interaction between *Ca.* A. hamiconexum and their virus Altivir_1_MSI in the deep biosphere. This culture-independent method was previously used in several studies for pure cultures and less used for environmental samples. Within this thesis, I will show which potential this method has in terms of detecting viral infections, illustrating the viral lifestyle, and which effects viruses can have on the overall microbial community within the deep subsurface.

The next paragraphs summarize the content and main findings of the three publications generated during this thesis.

4.1 Which imaging methods can be used for studying virus-host interactions?

Rapid advances in imaging have fueled our enthusiasm for practical applications in detecting viruses, *e.g.,* in environmental samples. However, every imaging technique has certain limitations, but the development of new technologies and also the support of *in silico* analysis with novel tools, improved the ability for detecting these tiny predators. The advantages and disadvantages, as well as the sample preparation for each microscopy approach is summarized in manuscript 1 **"Imaging Techniques for Detecting Prokaryotic Viruses in Environmental Samples"**. In addition, advices on linking several imaging techniques for achieving the best resolution and image are given. In this manuscript, we report on the potential of the so-called "virusFISH" method for monitoring and quantifying viral infections for transferring this method to a difficult to access ecosystem, the deep terrestrial subsurface.

4.2 Establishment of virusFISH on *Ca.* A. hamiconexum and Altivir_1_MSI

A very good to study virus-host system is the primary producer *Ca.* A. hamiconexum and their virus Altivir_1_MSI, both found at the Muehlbacher Schwefelquelle (MSI). The establishment of the virusFISH method for this respective model system can be found in manuscript 2 entitled: **"Lytic archaeal viruses infect abundant primary producers in Earth's crust". ** By using virusFISH, which represent a method for linking viruses to their host, we showed active viral infections on *Ca*. A. hamiconexum with the indication for a lytic viral life cycle of Altivir_1_MSI. Moreover, we observed first hints of bacteria potentially benefitting from lysis events and jump-start the heterotrophic carbon cycle in this ecosystem.

4.3 Virus-host dynamics of *Ca.* A. hamiconexum and Altivir_1_MSI and the potential effects on the whole microbial community

The spatial and temporal distribution of Altivir_1_MSI was intensively studied in manuscript 3: **"Virus-host dynamics in archaeal groundwater biofilms and the associated bacterial community composition"** over a period of four years. Moreover, we calculated the virus-host ratios and determined the overall community of the MSI biofilm flocks. Since, we observed in manuscript 2 active bacteria that could benefit from lysing events, we were interested in determining which microbes these are. Our results achieved by Nanopore sequencing showed mainly sulfate-reducing bacteria. Moreover, the different stages of an

active biofilm development controlled by Altivir_1_MSI was also illustrated in this manuscript.

III. Publications

Overview

The present cumulative dissertation comprises three successfully published publications by Victoria Turzynski as first author. The first manuscript, and the third manuscript were published in the journal MDPI *Viruses,* whereby the latter was published in a special issue of MDPI called “Archaeal Virology”. The second manuscript was published in *Nature Communications*.

Supplementary information as well as additional data are supplied on the supporting CD (contents are described in Section VII).

Victoria Turzynski’s contributions to each of the manuscripts are as follows:

1. Turzynski et al., 2021: Victoria Turzynski wrote the manuscript, designed the Figures, prepared microscopy Figures, and incorporated revisions.

2. Rahlff, Turzynski et al., 2021: This manuscript was a shared first authorship, whereby both authors (J. Rahlff, and V. Turzynski) contributed equally.
   Victoria Turzynski wrote the manuscript, incorporated revisions, prepared microscopy Figures, performed the sampling, virusFISH and image analysis, as well as prepared the supplementary material.

3. Turzynski et al., 2023: Victoria Turzynski wrote the manuscript, performed the sampling, quantitative real-time PCR, and imaging (virusFISH, direct-geneFISH), prepared the Figures and the supplementary material, and incorporated revisions.

Review

I. Imaging Techniques for Detecting Prokaryotic Viruses in Environmental Samples

Victoria Turzynski [1,*], Indra Monsees [1], Cristina Moraru [2] and Alexander J. Probst [1,3*]

[1]Department of Chemistry, Environmental Microbiology and Biotechnology (EMB), University of Duisburg-Essen, Universitätsstraße 5, 45141 Essen, Germany
[2]Institute for Chemistry and Biology of the Marine Environment (ICBM), Carl-von-Ossietzky-University Oldenburg, Carl-von-Ossietzky-Straße 9-11, 26111 Oldenburg, Germany
[3]Centre of Water and Environmental Research (ZWU), University of Duisburg-Essen, Universitätsstraße 5, 45141, Essen, Germany

*Correspondence: victoria.turzynski@uni-due.de; alexander.probst@uni-due.de

Publication information:
Viruses 2021, 13(11), 2126; https://doi.org/10.3390/v13112126
Received: 20 September 2021 / Revised: 15 October 2021 / Accepted: 18 October 2021 / Published: 21 October 2021
Link: https://www.mdpi.com/1999-4915/13/11/2126

Abstract

Viruses are the most abundant biological entities on Earth with an estimate of 10^{31} viral particles across all ecosystems. Prokaryotic viruses—bacteriophages and archaeal viruses—influence global biogeochemical cycles by shaping microbial communities through predation, through the effect of horizontal gene transfer on the host genome evolution, and through manipulating the host cellular metabolism. Imaging techniques have played an important role in understanding the biology and lifestyle of prokaryotic viruses. Specifically, structure-resolving microscopy methods, for example, transmission electron microscopy, are commonly used for understanding viral morphology, ultrastructure, and host interaction. These methods have been applied mostly to cultivated phage–host pairs. However, recent advances in environmental genomics have demonstrated that the majority of viruses remain uncultivated, and thus microscopically uncharacterized. Although light- and structure-resolving microscopy of viruses from environmental samples is possible, quite often the link between the visualization and the genomic information of uncultivated prokaryotic viruses is missing. In this minireview, we summarize the current state of the art of imaging techniques available for characterizing viruses in environmental samples and discuss potential links between viral imaging and environmental genomics for shedding light on the morphology of uncultivated viruses and their lifestyles in Earth's ecosystems.

Keywords: fluorescence microscopy; electron microscopy; helium-ion microscopy; atomic force microscopy; metagenomics; viromics; fluorescence in situ hybridization; virusFISH; phageFISH; direct-geneFISH

1. Introduction

In the last few decades, it has been proven that viruses represent the most abundant components in Earth's ecosystems (Fuhrman 1999). Based on the molecular composition of their genome, these viral predators can be categorized into DNA and RNA viruses, whereas the respective genome can be single-stranded (ss) or double-stranded (ds). Current estimates based on aquatic and soil ecosystems suggest that the majority of prokaryotic viruses have dsDNA genomes (Srinivasiah et al. 2008). By influencing microbial communities on various levels, viruses impact carbon, nitrogen, sulfur, and phosphorous cycling in many ecosystems. For instance, up to 10^{28} viral infections are estimated to occur in the ocean per day (Suttle 2007), which convert cells into dissolved organic matter (DOM) and particulate organic matter (POM) (Suttle 2007), leading to a viral shunt and a redistribution of carbon compounds in the stratified ocean (Suttle 2005; Thingstad and Lignell 1997). Beyond the killing-the-winner hypothesis, based on which viruses modify host diversity (Thingstad and Lignell 1997) and microbial community composition, the piggy-back-the-winner hypothesis was recently proposed, highlighting the importance of viral lysogeny in microbial communities (Silveira and Rohwer 2016). Viruses alter biogeochemical cycling of microbes via horizontal gene transfer. Moreover, viruses can introduce auxiliary metabolic genes (AMGs) (Breitbart et al. 2007) to their prokaryotic host, adjusting the metabolism to their needs and likely increasing their burst size. Recent metagenomic studies have demonstrated that AMGs are diverse and abundant in marine viromes (Ahlgren et al. 2019; Anantharaman et al. 2014; Rahlff et al. 2021) but can also occur in archaeal and bacterial viruses in the deep subsurface (Anderson et al. 2014). For instance, viruses can heavily impact sulfur cycling in the deep ocean by transferring genes for sulfate reduction (Anantharaman et al. 2014). Furthermore, the presence of photosystem I genes in marine cyanophages results in a metabolism boost of Prochlorococcus and Synechococcus cells during viral reproduction (Sharon et al. 2009). While these findings were first documented using metagenomic studies (Fridman et al. 2017), the isolation of such viruses containing genes for photosystem I and II was successfully reported only eight years later, highlighting the necessity of studying uncultivated viruses directly in ecosystems. The Tara Ocean Project (Zhang and Ning 2015) was set out with the aim of investigating microbial interactions, their evolution, and viral infections (Brum et al. 2015) in the sea ecosystem. This project was based on an extraordinarily large dataset containing millions of newly discovered sequences from various oceanic microbes and viruses (Brum et al. 2015), and—along with the Pacific Ocean Virome (POV) (Duhaime and Sullivan 2012; Hurwitz et al. 2013) project and the Malaspina expedition (Roux et al. 2016)—revolutionized our view of genetic diversity of prokaryotic and eukaryotic viruses on Earth. Such datasets represent the best current means of documenting the taxonomic compositions of uncultivated and unknown viral communities (Hurwitz et al. 2013) in various ecosystems.

In contrast to uncultivated viruses, those that were cultivated in the laboratory have been extensively studied for decades, including via imaging techniques (Almeida et al. 2018), and have substantially broadened our knowledge regarding viral morphologies and ultrastructure. Fundamental insights regarding how viruses interact with their hosts and regarding the discovery of novel viruses can be gained from using epifluorescence

microscopy, electron microscopy (EM), helium-ion microscopy (HIM), and atomic force microscopy (AFM) (Figure 1, Table 1). For instance, virus enumeration (determined as virus-like particles, VLPs) is routinely performed via epifluorescence microscopy and EM for several ecosystems, *e.g.,* VLPs range from 10^7 to 10^8 mL^{-1} in marine and freshwater environments (Luef et al. 2009; Suttle 2005; Weinbauer 2004) and from 10^8 to 10^9 VLPs cm^{-3} in sediment (Danovaro et al. 2001; Engelhardt et al. 2014) and soil (Williamson et al. 2017, 2003). In addition, the combination of both imaging techniques (fluorescence and electron microscopy) —known as Correlative Light and Electron Microscopy "CLEM"—can be combined for the quantification of viruses and the visualization of virus–host associations (Jahn et al. 2021). The benefit of this technical linkage is that the observation of fluorescent-labeled viral particles can be easily identified and tracked as "real viruses" by using EM (Müller et al. 2019). For studying the viral entry and egress mechanisms, scanning electron microscopy (SEM) was identified as one of the most suitable imaging techniques (Bize et al. 2009). Analyses based on cryo-EM have provided important information not only on investigating and reconstructing the viral structure (Almeida et al. 2018; DiMaio et al. 2015; Prangishvili et al. 2006c) but also on the genome injection mechanisms of viruses (Guerrero-Ferreira and Wright 2013). Additionally, HIM and AFM have been applied for studying virus–host interactions under high resolution (Dubrovin et al. 2008; Leppänen et al. 2017).

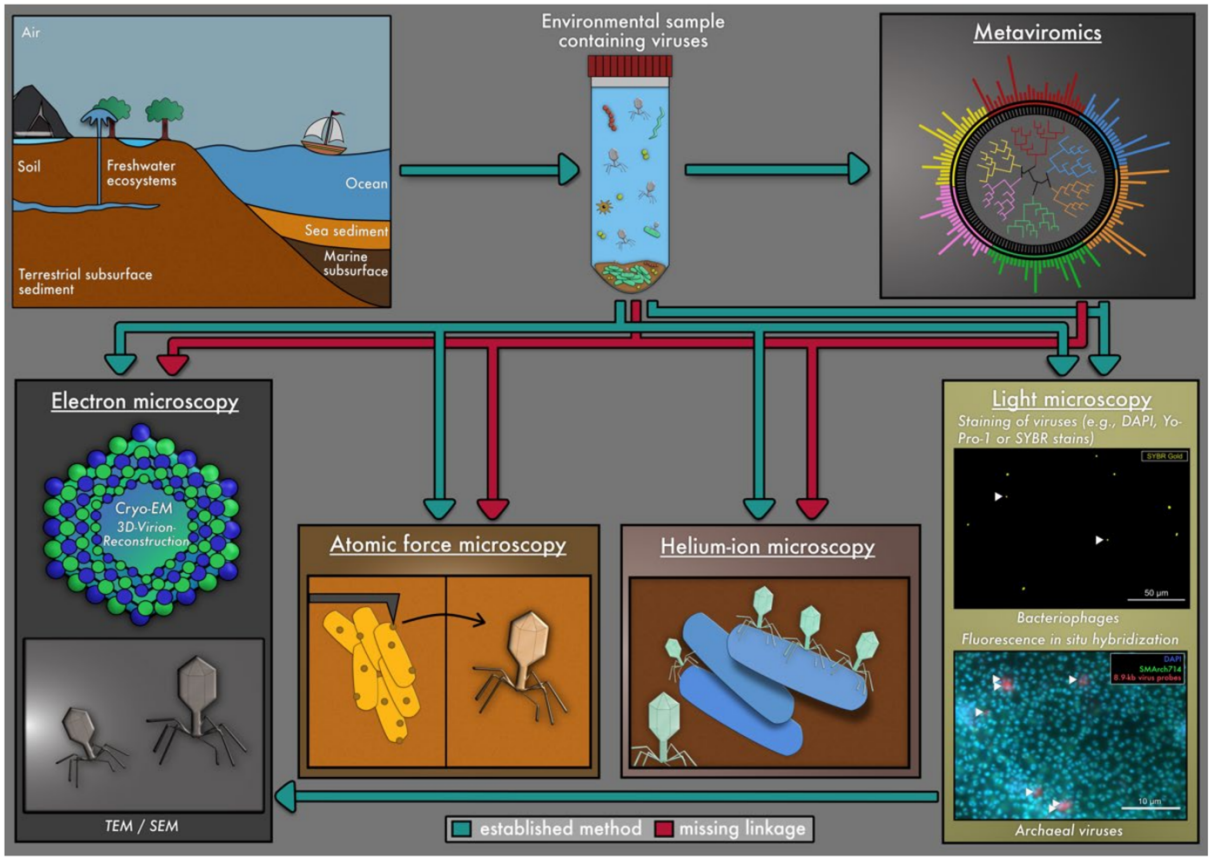

Figure 1: Overview of methods for detecting viruses in environmental samples and combinations thereof. Green arrows indicate commonly applied methods, which are described in the main text. Red arrows suggest potential couplings of methods that have not been performed to date. Coupling metaviromics with light microscopy has been performed in three studies (Hochstein et al. 2016; Jahn et al. 2021; Rahlff et al. 2021) and is elucidated

further in Figure 2. The origin of arrows in the figure is always associated with the environmental sample and the metaviromics analysis to indicate that both need to be combined to link viral structures to genome sequences.

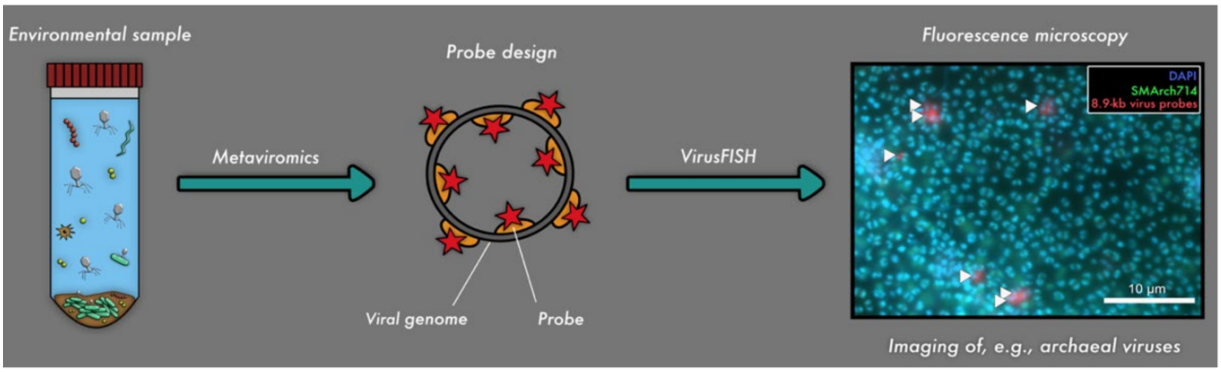

Figure 2: Linkage of metaviromics and fluorescence microscopy for detecting uncultivated viruses. The genome of the virus is detected in silico and used for respective probe design (Barrero-Canosa and Moraru 2019), followed by detection of the respective viral genomes in situ (*i.e.*, virusFISH, Rahlff et al. 2021).

Table 1: Overview of frequently used microscopy methods for studying viral abundance, viral morphology, and viral diversity.

Microscopy Technique	Advantages	Disadvantages	Resolution	Coupling With Following Techniques Has Been Performed
Fluorescence microscopy	- Powerful, cheap, and simple technique (Prata et al. 2012) for analyzing viruses with high accuracy and precision (Noble and Fuhrman 1998)	- Photobleaching - No structural resolution, only detection	- 300 nm for conventional light microscop techniques and 10 nm for super-resolution microscopy (SRM) (Hauser et al. 2017)	- Flow cytometry (Marie et al. 1999) -Ultracentrifugation (Thurber et al. 2009) - TEM (as CLEM) (Jahn et al. 2021)
Nucleic acid staining	- Estimation of total viral counts (more efficient than techniques such as TEM (Danovaro et al. 2001; Weinbauer and Suttle 1997) and can be carried out in the field (Noble and Fuhrman 1998)	- Some dyes have a long staining time or interfere with fixatives (Wen et al. 2004) - Small/large bacteria may be counted as viral particles (Danovaro e al. 2001) or bacterial cells (Pina et al. 1998) - Free nucleic acids can be recognized as viruses (Bettarel et al 2000)		
Fluorescence in situ hybridization (FISH) (direct-geneFISH (Barrero-Canosa et	- Precise localization of gene signals and virus-infected/ non-infected cells - Visualization of	- Requires an experienced and trained person		- Metagenomics/ viromics (Hochstein et al. 2016; Jahn et al. 2021; Rahlff et al. 2021)

al. 2017), *phageFISH* (Allers et al. 2013), *virusFISH* (Rahlff et al. 2021))	viral infections, *e.g.*, from an early infection stage to viral bursts (Allers et al. 2013; Zimmerman et al. 2019) and also used as culture-independent method			
Electron microscopy (EM)	- Highest resolution - High-quality images	- Expensive equipment and time-consuming - not possible in the field (Hennes and Suttle 1995)	- Subnanometer resolution (Hauser et al. 2017)	- Ultracentrifugation (Bachrach and Friedmann 1971; Bettstetter et al. 2003; Häring et al. 2005)
TEM, SEM and Cryo-EM	- Total viral counts, viral morphological characterization, viral infection frequencies, and burst size estimates can be obtained	- Underestimation of viral abundances (Hara et al. 1991; Noble and Fuhrman 1998; Weinbauer and Suttle 1997)		
Helium-ion microscopy (HIM)	- Imaging of various stages of viral infections - Coating and embedding of the sample are not required (uncoated samples show more ultra-structures) (Leppänen et al. 2017)	- Helium is a limited element on Earth, expensive imaging technique	- Higher imaging resolution than techniques such as EM (Leppänen et al. 2017) - Nanoscale imaging capacity with a higher depth of view compared to AFM (Leppänen et al. 2017)	
Atomic force microscopy (AFM)	- Inexpensive method with mechanically and electronically straightforward instruments (Kuznetsov and McPherson 2011) - Staining, labeling, and coating the samples is not necessary (Allison et al. 2010) - Analysis can be performed in fluids and in air (Kuznetsov and McPherson 2011) - Obtaining of viral morphology	- Recording an image is time consuming in contrast to fluorescence microscopy (Kuznetsov and McPherson 2011) - Limitation in scan range (Kuznetsov and McPherson 2011) - Debris can adhere to the AFM tip and can affect the image quality (Kuznetsov and McPherson 2011)	- Nanometer-scale resolution: imaging from molecular to cellular scale (Dubrovin et al. 2008)	- X-ray diffraction (Kuznetsov and McPherson 2011) - Ultracentrifugation (Dubrovin et al. 2004) - HIM (Andany et al. 2020)

The difficulty of culturing the majority of host organisms poses a huge problem for the analyses of their viruses (Munson-McGee et al. 2018), and thus, the majority of viruses

remains uncultivated and yet to be explored (Anderson et al. 2013; Suttle 2007; Williamson et al. 2003). To overcome the challenge of linking uncultivated microbial hosts to their uncultivated viruses, in-silico techniques like metaviromics have swiftly become keys in analyzing viral genomes from various ecosystems and linking them to prokaryotic genomes. Although metaviromics has been used with different microscopy techniques, such as epifluorescence microscopy (Hochstein et al. 2016; Rahlff et al. 2021) and EM (Hochstein et al. 2016; Rahlff et al. 2021) (Figure 1), a direct linkage of genome and microscopic image is seldomly achieved (Hochstein et al. 2016; Jahn et al. 2021; Rahlff et al. 2021) (Figure 2). Consequently, a major gap of knowledge exists regarding the morphology of uncultivated viruses, the stages of infection of their hosts, virus/host quantification, and the spatial localization of viruses and their host in ecosystems (*e.g.,* in terms of interactions with other prokaryotic/eukaryotic microbes or in biofilms). The major bottleneck for studying these uncultivated viruses is the disconnection of sequencing data (metagenomics and viromics) from uncultivated viruses and microscopy techniques. In this review, we summarize the current state of the art of visualization techniques for (cultivated) viruses and discuss their potential linkage to sequencing data in order to explore viruses directly in ecosystems.

2. Retrieving Viral Fractions from Ecosystems for Microscopy Analyses

Quite often, viruses in environmental samples need to be concentrated and purified before being analyzed with microscopy techniques, *e.g.,* for virus enumeration or identification of viral morphology. For this purpose, a careful removal of all contaminants like cellular organisms and debris is essential in order to obtain highly purified virus particles. Initially, viruses can be separated from contaminants, most often by size fractionation via filtration, but also via centrifugation (Table 1). The concentration and collection of viral particles can generally be performed either via tangential flow filtration (TFF), dead-end filtration or by using filters with pore sizes <0.02 µm, *e.g.,* Anodisc™ or Nuclepore™ (Budinoff et al. 2011; Noble and Fuhrman 1998). Analyses with Anodisc™ membranes provide an order of magnitude higher VLP abundance for seawater than Nuclepore™ membranes (Budinoff et al. 2011) and are thus likely better for collecting viral particles.

Concentrating viruses from environmental samples can be performed via TFF, in which the sample flows tangential to the filter surface (Wommack et al. 2010). Viruses from oligotrophic marine samples have been investigated using this concentration procedure in conjunction with ultrafiltration and transmission electron microscopy (TEM) analysis (Alonso et al. 1999). However, TFF can cause a loss in viral yield (Corinaldesi et al. 2010). An alternative method for concentrating and purifying viruses from pure cultures and environmental samples is ultracentrifugation. Ultracentrifugation has been used on a range of viruses (Thurber et al. 2009) and is conducted at more than 100.000× *g*, a centrifugal force that cannot be achieved by ordinary centrifuges. Thus, this technique requires an expensive ultracentrifuge, rotors, and special tubes (Nasukawa et al. 2017).

Recent protocols combine ultracentrifugation with a flocculation, filtration, and resuspension (FFR) method in order to most efficiently concentrate viruses from environmental samples (John et al. 2011). For instance, an iron-based virus FFR method

showed a marine virus recovery of >94 ± 1% by using $FeCl_3$, which represents an efficient, inexpensive, and non-toxic flocculant (John et al. 2011). This flocculation method is beneficial because it allows large amounts of water to be processed and is technically simple and fast with high viral recovery (John et al. 2011; Prata et al. 2012).

Ultracentrifugation can also be used in combination with polyethylene glycol (PEG). Usually, a PEG concentration of 10% (w/v) is commonly used for virus precipitation (Fouladvand et al. 2020). When combining PEG precipitation with density gradient ultracentrifugation, a gradient media is required. This can be iodixanol (Ford et al. 1994) ("Optiprep™"), cesium sulfate, sucrose, or cesium chloride (CsCl) (Bachrach and Friedmann 1971; Nasukawa et al. 2017), all easily removed after centrifugation by adding dialysis steps. CsCl represents the most widely used gradient media for achieving highly pure and concentrated virus solutions (Thurber et al. 2009). For instance, insight into different viral morphotypes of uncultivated viruses infecting members of the genus *Acidianus* in an enrichment culture obtained from a volcanic area in Italy was achieved by coupling PEG and CsCl density gradient ultracentrifugation with TEM (Häring et al. 2005). By using this method combination, *Acidianus* filamentous virus 1 (AFV1) was purified from an infected *Acidianus hospitalis* enrichment culture originally retrieved from hot springs (Bettstetter et al. 2003). These types of methods have been used so far in pure cultures and enrichments. The purification method based on the combination of PEG, CsCl density ultracentrifugation, and TEM has—to the best of our knowledge—not been applied directly to environmental samples.

3. Using Electron Microscopy for Virus Quantification and for Discovery of Previously Unknown Viral Morphologies and Ultrastructures

3.1. Sample Preparation for Transmission Electron Microscopy

Around the early 1930s, the first electron microscope was developed, and only eight years later the first electron micrograph of a virus was recorded in the literature (Kausche et al. 1939). Since then, TEM has been an integral part of the study of viruses for the determination of virion morphology and ultrastructure, as well as for virus quantification. For these purposes, two staining techniques are available—negative and positive staining (Barreto-Vieira and Barth 2015).

Prior to the staining procedure, the sample is frequently concentrated through (ultra-) centrifugation and filtration by using 0.2 µm-pore-size filters to get rid of debris and cellular organisms (see above) (Noble and Fuhrman 1998). Negative stains, phosphotungstic acid, ammonium molybdate, and uranyl acetate (also a fixative) are commonly used for staining the sample/phage solution deposited directly on the copper grid, whereby uranyl acetate is also used as a positive stain besides lead citrate for enhancing the contrast of samples (Reynolds 1963). The concentrated sample can also be embedded in epoxide or another resin. Thin sectioning of the embedded sample is performed by using a diamond knife to reveal the structures inside viruses and their hosts (Lundstrom et al. 1979; Milne and Trautner 1967).

As a result of the two staining techniques, the negative staining depicts light viral particles on a dark background, while positive staining results in dark particles on a bright background. For both staining techniques, the samples are incubated in heavy metal salt solutions (*e.g.,* uranyl acetate (Watson 1958)), whereby the salt can react with cellular structures (Watson 1958) or penetrate the viral tail (Proctor 1997), challenging the detection of fine viral structures. This paragraph just summarizes the superficial sample preparation for TEM that uses electron beams for the imaging of viruses, but correct preparation is essential for a thorough detection of viruses and elucidation of their morphologies. For further reading on viral preparation for TEM, the reader is referred to (Ackermann 2009; Belnap 2021).

3.2. Estimating Viral Abundances in Environmental Samples Using TEMs

The first quantification of viruses in environmental samples resulted in the detection of approximately 10 million putative viruses per milliliter of seawater (Bergh et al. 1989) and was conducted using TEM in 1989. Later, determining viral abundances via TEM was applied not only to seawater (Torrella and Morita 1979) but also to the slime of diatoms (Bratbak et al. 1990), marine snow particles (Peduzzi and Weinbauer 1993), hydrothermal vent systems (Williamson et al. 2008), deep granitic (Kyle et al. 2008) and shallow aquifers (Pan et al. 2017), and marine subsurface sediments (Engelhardt et al. 2014), resulting in a more general understanding of the distribution of viruses across Earth's biomes. Quantifying viruses based on their capsid morphology was conducted by combining TEM with metaviromics across six oceans and seas through the Tara Oceans Expedition (Brum et al. 2013). The aforementioned study resulted in the detection of four different viral morphotypes (*myoviral*, *podoviral*, *siphoviral*, and non-tailed icosahedral viruses), which were also analyzed on a genomic basis (Brum et al. 2013). These analyses provided evidence that non-tailed viruses dominate the upper water column of the global oceans, comprising 51–92% of the observed viral particles (Brum et al. 2013). TEM-based analyses of viral fractions did not only increase our understanding of the distribution of viral communities across ecosystems but also within ecosystems. For example, an increase in the viral abundance with depth was determined for marine sediment samples (Engelhardt et al. 2014), a trend that was also later confirmed for archaeal viruses in deep granitic groundwater (Kyle et al. 2008).

3.3. Determination of the Frequency of Visibly Infected Cells, Burst Sizes, and Spatial Distribution of Viruses

While the aforementioned studies focus on the detection of viral particles within the extracellular space, TEM can also be used for studying viruses within host cells. The frequency of visibly infected cells (FVIC) can be calculated for a sample by determining the number of visibly infected cells divided by the number of examined cells. FVIC is helpful in terms of estimating viral infections within cells, quantifying the number of infected cells, and determining the burst size (number of viral particles per cell). FVIC was calculated for several ecosystems, *e.g.,* for the surface of glaciers (Arctic cryoconite) (Bellas et al. 2013), various freshwater (Jasna et al. 2018; Peduzzi 2016), and marine ecosystems (Weinbauer and Peduzzi

1994). Although this method only detects cells in the late stage of infection (Castillo et al. 2020), it substantially increased our knowledge of naturally occurring virocells. For example, in marine ecosystems, the infection frequencies, burst size, capsid sizes, and the distribution patterns of viruses inside cells can vary between different bacterial morphotypes (Weinbauer and Peduzzi 1994). Moreover, coccoid and rod-shaped cells appeared to be more infected by viruses than, *e.g.,* spirilla, in marine ecosystems (Weinbauer and Peduzzi 1994), and likely also in alkaline lakes (Brum et al. 2005). Prokaryotic mortality was also shown to vary among seasons (pre-monsoon, monsoon, and post-monsoon) with an increase in mortality during the monsoon season, whereas rod-shaped bacteria were more infected during the dry season (Jasna et al. 2018). Across all seasons, myoviruses were the most dominant viral morphotype besides non-tailed viruses, miphoviruses, and podoviruses (Jasna et al. 2018). The results of this study led to the general assumption that seasonal dynamics of viruses impact the carbon and energy flow in tropical esturine ecosystems (Jasna et al. 2018).

3.4. Observing (Novel) Viral Morphologies

Viral morphology is one of the most studied viral features, usually by using TEM, because it offers information about how viruses are able to attach and penetrate the host cell. Furthermore, for a long time, morphological features determined by TEM, for example, tail type, capsid shape and size, and the presence or absence of envelopes and spikes (Norrby 1983), have been the main criteria used for viral classification, and, to a certain extent, they are still used today, together with the genomic information. For instance, until recently, the order *Caudovirales* (dsDNA viruses) comprised tailed viruses infecting bacteria and archaea, which were classified into three families (*Myoviridae*, *Siphoviridae*, and *Podoviridae*), based on their tail morphology (Krupovic et al. 2011a). Moreover, some viral particles have unique morphologies, such as lemon-shaped viruses (Prangishvili et al. 2006c; Zhang et al. 2019), and some viruses undergo spectacular extracellular developments (Häring et al. 2005). Most of these unique morphologies are associated with viruses that infect archaea. The biggest milestone for the study of archaeal viruses was the observation of the viruses in environmental samples via TEM in 1994 (Zillig et al. 1993). This analysis was quickly expanded to viruses infecting hyperthermophilic archaea in hot springs in the Yellowstone National Park (Wyoming, USA) (Bettstetter et al. 2003; Rachel et al. 2002). One study particularly focused on one specific virus (*Acidianus* filamentous virus 1, AFV1 (Bettstetter et al. 2003)), which infects only some representatives of the genus *Acidianus*. The authors revealed virus–host associations via EM pictures, which showed how AFV1 particles attach to the pili of *Acidianus hospitalis* and thus enable linking hosts and viruses in environmental samples (Bettstetter et al. 2003). Beyond the study of archaea-virus interactions with specific species in ecosystems, various morphotypes of hot spring viruses, ranging from filamentous, rod-shaped viruses to spindle-shaped viruses, were observed (Rachel et al. 2002). Ample research on hot spring viruses revealed a lemon-shaped *Acidianus* two-tailed virus with an astonishing extracellular morphological development (Häring et al. 2005). This virus develops long filamentous tails at its ends after being released from its host cell if the virus is exposed to the correct ecosystem temperature of ~75 °C (Häring et al. 2005).

3.5. Scanning Electron Microscopy for Studying Unique Viral Egress Mechanisms

A special viral egress mechanism of archaeal viruses was revealed using a combination of TEM and scanning electron microscopy (SEM) by focusing on their morphology during their proliferation (Bize et al. 2009). When exiting the *Sulfolobus* cell, the rod-shaped virus 2 (SIRV2 (Prangishvili et al. 1999)) caused the formation of virus-associated pyramids (Bize et al. 2009) (known as VAPs) on the surface of the host cell after 10 hours of infection. During this last stage of infection, huge apertures were created for releasing the newly matured viruses (Bize et al. 2009). Furthermore, the viral genome encoded the proteins that control the formation of VAPs (Bize et al. 2009). TEM analyses also showed a change of the host phenotype during infection, highlighted by the absence of its S-layer (Bize et al. 2009). The development of VAPs as virus release mechanisms was recently expanded to *Sulfolobus* turreted icosahedral virus (STIV) (Brumfield et al. 2009), suggesting that this complex exit mechanism is spread in the genus *Sulfolobus*, if not in other archaea as well.

3.6. Illustrating Virus–Host Associations by Using Cryo-Electron (Cryo-EM) Microscopy and Cryo-Electron Tomography (Cryo-ET)

Over the last 15 years, cryo-EM was established as the method to use when investigating in-depth and high-resolution viral structures (DiMaio et al. 2015; Mochizuki et al. 2012; Prangishvili et al. 2006c) or virus–host interactions (Dewey et al. 2010; Sun et al. 2014). Cryo-EM is ideally suited for exploring the three-dimensional architecture of viruses at molecular resolution down to sub-nanometer resolution (Chang et al. 2012a) (see Table 1 for a comparison with other EM techniques). For instance, cryo-EM enabled researchers to resolve the three-dimensional structure of the SIRV2 virion, revealing that the capsid protein wraps around the A-form viral DNA, to protect it (DiMaio et al. 2015). Moreover, cryo-EM revealed that the *Acidianus* two-tailed virus (ATV) has two types of virion structures—tail-less and two-tailed virions (Prangishvili et al. 2006c). The hyperthermophilic *Aeropyrum* coil-shaped virus (ACV) infects *Aeropyrum pernix* isolated from a coastal hot spring in Japan and has a single-stranded DNA genome (Mochizuki et al. 2012). TEM and cryo-TEM revealed that its virion is a rigid cylinder, a structure that has never been reported before for archaeal viruses (Mochizuki et al. 2012).

Parallel to cryo-EM, cryo-electron tomography (cryo-ET) has recently emerged as a powerful tool in the study of viruses and can also be used like cryo-ET for illustrating virus–host associations. Both techniques are central in terms of determining the high-resolution structures of several viral assemblies (Luque and Castón 2020). Combining cryo-ET with subtomogram averaging methods can provide detailed 3D information of the structure of molecules, viruses, and their viral proteins at sub-nanometer resolution (Briggs 2013; Luque and Castón 2020; Tu et al. 2017).

Recent advances in cryo-ET revealed various virus–host interactions and states of viral infections for bacteriophage Epsilon 15 and its hosts *Salmonella* (Chang et al. 2010), Phi29 and *B. subtilis* (Farley et al. 2017), T4 and T7 bacteriophages and *E.coli* (Hu et al. 2015,

2013), and for the cyanophage P-SSP7 and *Prochlorococcus marinus* (Liu et al. 2010). Furthermore, there is a large volume of published studies describing the role of cryo-ET in investigating archaeal viruses. For instance, the first 3D structure of a *Sulfolobus* spindle-shaped virus (SSV1) was achieved with cryo-ET by Stedman et al. (2015) (Stedman et al. 2015). Only one year later, the complete viral entry and egress mechanism of this specific virus SSV1 was illustrated by using this technique, showing that these mechanisms occur on the cellular cytoplasmic membrane of the host *Sulfolobus shibatae* B12 (Quemin et al. 2016).

A structural analysis of the filaments of *Acidianus* bottle-shaped virions (ABV) (Häring et al. 2005), the investigations of the tails of AFV3 virions (Vestergaard et al. 2008), and the structure of the spindle-shaped virus His1 and their structural proteins were analyzed using cryo-ET and subtomogram averaging (Hong et al. 2015), showing the broad range of this technique. Another study on archaeal viruses revealed the VAP structure (further described in Section 3.5) by using subtomogram averaging (Daum et al. 2014). The authors prepared sections by using the Tokuyasu method (Tokuyasu 1973) and used antibodies for immunolabeling against protein-forming virus-associated pyramids (PVAP) for TEM analysis (Daum et al. 2014). This study was the first that used the Tokuyasu method for TEM sample preparation on prokaryotic viruses, a method that uses a mild chemically fixation, freezing in sucrose and cutting the sample for cryo-sections. Despite the fact that the Tokuyasu method is not widely used in the area of prokaryotic viruses, this method has great potential when combined with CLEM for imaging and 3D structural determination of eukaryotic viruses as well (Vijayakrishnan et al. 2020).

Overall, electron microscopy has been used for three decades to study the morphology of viruses from environmental samples. It has proven to be a valuable technique that enables researchers to study not only the viral abundance in samples but also the details of viral proliferation, overcoming the limitations of light and fluorescence microscopy (Table 1). However, EM analyses are not only time-consuming and require more expensive consumables compared to light microscopy, but the microscopes themselves and their maintenance are costly. Furthermore, TEM analyses were shown to underestimate viral abundances due to uneven collection, problems during staining, washing off viral particles, and the generally low detection limit of the method (Bettarel et al. 2000; Hara et al. 1991; Noble and Fuhrman 1998). In addition, TEM is not suitable for high throughput sample analysis like light and fluorescence microscopy. Despite these disadvantages, this imaging technique has helped to gradually expand our understanding of viral morphology and virus–host interactions and has contributed significantly to the discovery of many previously unknown viruses, particularly in complex environmental samples.

4. Shedding Light on Viral Abundances in Ecosystems Using Epifluorescence Microscopy

Fluorescence microscopy is often used as a first step to investigate viruses in a given sample. It represents a powerful, cheap, and simple technique (Prata et al. 2012) that enables researchers to quantify viruses (Table 1). This technique advanced the field of viral ecology since the former standard assay of determining viral loads via plaque assays (Breitbart and

Rohwer 2005) required a cultivated host and known culture conditions of the respective viruses (Prata et al. 2012). Consequently, fluorescence microscopy is now the most frequently used technique for enumerating VLPs not only in pure cultures but also in environmental samples.

The first pioneer studies for determining the viral abundance in aquatic ecosystems via light microscopy were conducted in 1991 (Hara et al. 1991) and 1998 (Noble and Fuhrman 1998). Since then, scientists have applied different fluorescence dyes, such as 4′,6-Diamidin-2-phenylindol (DAPI) (Hara et al. 1991; Weinbauer and Suttle 1997; Wen et al. 2004), for enumerating viral particles, each with different advantages and disadvantages. For instance, T3 and T4 phage lysates and virus-sized particles in a high molecular weight concentrate (HMWC) of seawater were stained by using DAPI (Proctor and Fuhrman 1992). Because DAPI has low sensitivity when staining viruses, it was quickly substituted with Yo-Pro-1 (Hennes and Suttle 1995). Yo-Pro-1, a cyanine-based nucleic acid stain, is more stable and the fluorescence yield and binding coefficient for nucleic acids are higher (Hennes and Suttle 1995; Wen et al. 2004). Furthermore, this dye stains both DNA and RNA (Weinbauer 2004). When the viral abundance in seawater was determined by using both dyes, DAPI and Yo-Pro-1, similar estimates were obtained (Weinbauer and Suttle 1997). Another study reported that Yo-Pro-1 and light microscopy is the "best" method for enumerating viruses (Zimmerman et al. 2019). Nevertheless, Yo-Pro-1 interferes with aldehyde-based fixatives (Wen et al. 2004); therefore, it was eventually replaced by SYBR stains (Noble and Fuhrman 1998).

In 1998, a SYBR stain (SYBR Green I) was tested on marine water samples (containing viruses and bacteria) and was found to be an efficient dye for the field and for lab cultures (Noble and Fuhrman 1998). SYBR Green I can be used for enumerating viruses, whereby a brighter fluorescence for viruses compared to stained bacteria can be achieved (Noble and Fuhrman 1998). Later on, it was also applied to the quantification of micro-algal viruses, for example, the lytic virus PpV-01 infecting pure cultures of *Phaeocystis* (Marie et al. 1999). This enumeration method was also applied to environmental samples from different oceanic locations (*e.g.,* the English Channel, the Equatorial Pacific, and the Mediterranean Sea) (Marie et al. 1999). Ample research using this fluorescent dye followed, for instance, for marine viruses from high turbidity seawater (Sun et al. 2014) and marine sediment samples (Danovaro et al. 2001; Engelhardt et al. 2014), often combined with flow-cytometry (Chen et al. 2001; Marie et al. 1999) or confocal laser scanning microscopy (CLSM) (Luef et al. 2009). CLSM was applied to aggregates from the Danube River (Austria), in which 5.39×10^9 viruses cm^{-3} were found (Luef et al. 2009). The detection of aggregate-associated viruses was performed with SYBR Green I (Luef et al. 2009) , a stain that is frequently chosen for estimating viral abundances besides SYBR Gold (Chen et al. 2001). SYBR Gold is more sensitive than SYBR Green I for staining viruses (Chen et al. 2001). For example, viruses of surface marine and freshwater environments were investigated by using SYBR Gold (Chen et al. 2001). Comparisons of virus counts were performed between conventional fluorescence microscopy and those determined with CLSM, and no significant difference between the methods was obtained (Peduzzi et al. 2013). However, CLSM is not currently well established for enumerating viruses (Peduzzi et al. 2013), compared to the commonly applied epifluorescence microscopy.

Fluorescence microscopy also has disadvantages; for example, the detection sensitivity can be low in terms of the dyes (Proctor and Fuhrman 1992) and over-estimations in viral counts due to artifacts (Forterre et al. 2013). For instance, the presence of gene transfer agents of membrane vesicles can lead to overestimating the viral load in a sample (Soler et al. 2015). Moreover, small bacteria may be counted as viral particles (Danovaro et al. 2001); in turn, large viruses are confounded with microbial cells (Pina et al. 1998), and not every fluorescent signal corresponds to a real virus (*e.g.,* minerals can cause similar signals) (Weinbauer 2004). Overestimation, as well as underestimation, can interfere with viral quantification. For instance, a recent study reported on detection issues of ssDNA viruses when using DNA-binding stains and fluorescence microscopy, attributable to the genome type (ssDNA) and small size (Holmfeldt et al. 2012). Besides all these disadvantages, fluorescence microscopy offers an advantage in terms of speed and costs for sample preparation and analysis, as compared to EM.

To sum up, the studies mentioned above demonstrate that enumerating viruses by linking SYBR stains (Noble and Fuhrman 1998) with fluorescence microscopy is currently the most suitable method for estimating viral abundance in ecosystems. However, the actual confirmation of a VLP and the virus morphology cannot be studied in detail with light microscopy; thus, it requires a structure-resolving imaging technique like TEM, atomic force microscopy (AFM) or helium-ion microscopy (HIM).

5. Enhanced Surface Topography of Virus–Host Interactions Using Helium-Ion Microscopy

Helium-ion microscopy (HIM), an emerging technology, can be considered an ultra-high resolution "scanning" microscopy that uses helium atoms to scan the surface of a given sample (Ward et al. 2006). Similarly to SEM, it can be used to analyze the topography of biological structures (Leppänen et al. 2017). Sample preparation for HIM is simple, requiring no staining or embedding, which is a great advantage compared to conventional (S)EM. Furthermore, HIM has the potential to be used for investigating virus–host interactions (Leppänen et al. 2017) in terms of viral adsorption to the host cell and virus egression (Table 1).

To date, there is only one study that has investigated the association between viruses and their hosts in pure cultures by using HIM (Leppänen et al. 2017). The first step in the field of bacteriophages was the observation of the interaction of *Escherichia coli* and T4 phage by using HIM (Leppänen et al. 2017). Imaging of bacteria–phage interactions is difficult in terms of resolution limits, sample preparation, and the complexity of currently used microscopy techniques (Leppänen et al. 2017). However, HIM enables researchers to image microcolonies growing on agar plates, thus presenting a new opportunity in the field of imaging (Leppänen et al. 2017). For instance, active and individual infections of cells in plaques on agar plates were illustrated using this technique (Leppänen et al. 2017). In addition, the tailed morphology of T4 phages with an icosahedral shape of the capsid head and attaching phages on *E. coli* cells (Leppänen et al. 2017) and their complete lysis stage were observed. As a side note, bacteria–bacteria interactions (without phages) can also be

illustrated with HIM, as shown for the model organism *Flavobacterium columnare* B185 (Leppänen et al. 2017).

HIM application in environmental samples has been so far limited to a single study (Sharma et al. 2018) (Figure 1). In the aforementioned study, sediments and microbial mats from Himalayan hot springs were investigated using HIM and SEM to reveal the presence of tailed and non-tailed icosahedral viruses, and spindle-shaped viruses. This morphological assessment was supported by viral diversity data inferred from metagenomics.

Overall, HIM has great potential for deciphering viral structures and has the potential to slowly become a key instrument in the analyses of not only virus–host interactions but also microbe–microbe interactions. However, helium is a very limited element on our planet (Smith 2004), and extensive use of HIM might further shorten its availability.

6. Atomic Force Microscopy for Cost-Effective Scanning of Viral Structures

Atomic force microscopy (AFM), invented by Binning et al. in 1986 (Binnig et al. 1986), enables the visualization of the structural characteristics of viruses without pretreating the sample, similar to HIM. AFM integrates several imaging techniques (Allison et al. 2010), *e.g.,* scanning ion-conductance microscopy (SICM (Hansma et al. 1989)), scanning electrochemical microscopy (SECM (Bard et al. 1991)), Kelvin force microscopy (KFM (Nonnenmacher et al. 1991)), and scanning near-field ultrasound holography (SNFUH (Shekhawat 2005)). Given this array of techniques, AFM also has several disadvantages, which include, for instance, the extended time for recording an image compared to fluorescence microscopy (see Table 1). Furthermore, cell remnants and other debris can adhere on the AFM tip (as contamination) and may affect the quality of the overall image (Kuznetsov and McPherson 2011). Other disadvantages comprise forces acting between probe and sample, which can affect the image resolution (Dufrene 2002). Nevertheless, AFM currently represents the only technique that can image the surface of living cells at nanometer-scale and in real-time (Dufrene 2002). Moreover, AFM can also be combined (like EM) with X-ray diffraction, whereby a crystallized virus for the direct visualization of viral structures is required (Kuznetsov and McPherson 2011). A recent study demonstrated the potential of AFM by integrating this technique into a helium-ion microscope (Andany et al. 2020). Until now, no study on viruses has yet been conducted by using this powerful technical linkage, which could help characterize novel viruses in various ecosystems.

Using AFM, researchers investigated a variety of different viruses, *e.g.,* plant viruses (turnip yellow mosaic virus, TYMV (Kuznetsov and McPherson 2006), satellite tobacco mosaic virus (Kuznetsov et al. 2010a)), algal virus *Paramecium bursaria Chlorella* virus 1 (PBCV-1 (Kuznetsov et al. 2005b)), and the largest known virus, *Acanthamoeba polyphaga Mimivirus* (Kuznetsov et al. 2010b; Xiao et al. 2009). One study focused on important protocols for the investigation of different bacteria–phage interactions by using AFM (Dubrovin et al. 2008). This pioneering study includes protocols that span diverse host–phage systems including *E. coli* 057 and its lytic bacteriophage A157, *Salmonella enteritidis* 89 and its lytic phage 39, and *Bacillus thuringiensis* 393 and its V_f phage (Dubrovin et al. 2008). The abovementioned study visualized the ultrastructure of phage particles and compared bacterial

surfaces in different phases of infection via AFM (Dubrovin et al. 2008). Besides imaging the outer surface of bacteria in order to detect viral infections, the inside features of, *e.g.,* broken and intact viral capsids of bacteriophage ΦKZ (Matsko et al. 2001), as well as lysed bacteriophage capsids, *e.g.,* from phage T4 (Kolbe et al. 1992) due to osmotic shock or surface attachment, were also visualized by using AFM.

Phage–host interactions were also characterized by AFM in direct comparison with TEM, whereby more intact phages were found via AFM compared to TEM (Dubrovin et al. 2008), due to the fact that AFM provides a three-dimensional format of the image. In addition, phage DNA (Dubrovin et al. 2008) can also be visualized via AFM, which was also reported for PBCV-1 (Kuznetsov et al. 2005b) and for phage RNA of several icosahedral viruses (Kuznetsov et al. 2005a).

These examples demonstrate that extensive research with AFM has been carried out on phages grown under laboratory conditions; however, no study has—to the best of our knowledge—used AFM to investigate viruses of environmental samples so far.

To summarize, AFM is an inexpensive method (little maintenance, little costs for consumables compared to EM, a fairly cheap machine) for studying the presence and morphology of viruses (Kuznetsov et al. 2001). In general, AFM has different modes (contact mode, non-contact mode, and tapping mode), making it an ideal tool for studying living microbial systems in air, liquid, and solid samples (Kuznetsov and McPherson 2011). In general, AFM cannot replace the functions and information that can be obtained by light/fluorescence microscopy and EM (Chang et al. 2012b), as it is not as efficient as light/fluorescence microscopy, nor is its resolution comparable to EM or HIM. However, AFM provides a cheap and easy-to-use method for obtaining information on the viral morphology or illustrating the viral surface without complicated sample preparation.

7. Virus Discovery by (Meta)genomics and Microscopy

The majority of microorganisms cannot be cultured under defined laboratory conditions (Amann et al. 1991; Tyson and Banfield 2005). Therefore, it is not surprising that the majority of viruses have not been isolated so far, because this requires cultivated hosts (Munson-McGee et al. 2018). Studying the genetic inventory of complex microbial and viral communities can be accomplished by metagenomics, particularly if this technique is used to resolve genomes of populations from the ecosystem (Alneberg et al. 2020; Sharma et al. 2018). Although we demonstrated above that there exists a plethora of literature on studying viruses in environmental samples using microscopy, only a limited number of studies applied both environmental genomics of viral communities and respective microscopy techniques (Sharma et al. 2018; Wegley et al. 2007). In the following section, we discuss studies that performed metaviromics and microscopy separately, and which did not directly link the virus genome sequence and the viral morphology from environmental samples.

A recent study focusing on the hottest terrestrial geothermal spring in South Africa applied the combination of fluorescence microscopy, electron microscopy, and metagenomics (Zablocki et al. 2017). EM analysis on 74 VLPs revealed tailed bacteriophages of the order *Caudovirales* (Zablocki et al. 2017). The metagenome of this spring included a highly

abundant cyanophage genome and a genome fragment of a virus likely infecting *Gemmata* (Zablocki et al. 2017). However, the three methods were not linked; for instance, fluorescence microscopy was not applied on the exact same field of view as electron microscopy. Also, the visualization was not directly linked with genome information, which also applies to the following studies.

In another study, the viral diversity of Manikaran hot springs was investigated by using metagenomic profiling and SEM, revealing archaeal viruses with different morphotypes, mainly belonging to the *Fuselloviridae* family (Sharma et al. 2018). Four metagenomes from sediment samples of the hot spring were analyzed, by which 59 different archaeal viruses (including *Fuselloviridae, Siphoviridae* and *Podoviridae*) of varying abundances were identified. Two additional metagenomes of microbial mat samples aided in reconstructing another 65 bacteriophage genomes (Sharma et al. 2018). These studies highlight the general bottleneck in environmental viromics; viral morphology can provide only limited insight into virus taxonomic diversity (Brum et al. 2013), while the physiological characteristics of viruses can barely be extrapolated from their genetic sequences (Malki et al. 2015).

The first step in linking viral genomic information and morphological analyses from EM was recently performed in a study set out with the aim of investigating the microbial and viral diversity of five deep terrestrial subsurface locations (hydraulically fractured wells) (Daly et al. 2019). *Halanaerobium* spp., the most common species in this ecosystem, was in situ actively predated by viruses, as revealed by studying infection histories based on the host's CRISPR array (Daly et al. 2019). Viral genomic data revealed 50 viruses with a putative lysogenic lifestyle and 3 integrated prophages identified in isolate genomes of *Halanaerobium* retrieved via cultivation (Daly et al. 2019). The lysis of the cultivated *Halanaerobium* WG8 by its tail-less virus (burst size: 61 viruses per lytic event) was visualized by TEM (Daly et al. 2019) , representing an indirect linkage of metagenomics and TEM via cultivation assays.

Taken together, studies that used metagenomics and microscopy demonstrate the great potential of these techniques regarding the analysis of the uncultivated majority of viruses. Furthermore, linking these two technologies, *i.e.*, assigning infections or ultrastructure to genomic information, could further bolster our understanding of viral ecology; the abovementioned studies only realized this by cultivating the respective host.

8. A Promising Technique for Linking Environmental Genomics to Fluorescence Microscopy of Viruses

8.1. Fluorescence In Situ Hybridization (FISH) for Tracking Virus–Host Interactions

FISH uses genomic sequence information for probe design in order to identify biological entities in fluorescence microscopy (Allers et al. 2013). At the same time, this method also enables the quantification of microorganisms in samples (Danovaro et al. 2016; Teira et al. 2004) (Figure 1). In microbial ecology, FISH is widely used for the identification of microorganisms based on the ribosomal RNA of the small subunit (16S rRNA) (Amann et

al. 2001). In addition, several other FISH methods targeting rRNA, mRNA, and DNA have been developed (Allers et al. 2013; Barrero-Canosa et al. 2017; Kenzaka et al. 2010) (see Table 1).

Consequently, the idea of targeting viruses with oligonucleotide probes in FISH received much attention in recent years, as it would—in theory—enable researchers to visualize uncultivated viruses in their environment and determine their infection rate. A gap of knowledge relates to the linkage of genomic sequences to the morphology of uncultivated or previously unexplored viruses, the infection stages of their hosts, the viral lifestyle (lytic or lysogenic cycle), and virus enumeration in ecosystems. To perform such linkage, coupling FISH with TEM/HIM could help by filling these research gaps. However, the major bottleneck for studying viruses is the FISH protocol itself (*e.g.,* the permeabilization of the cells) because the sample preparation tends to destroy the ultrastructure of microbial cells (Knierim et al. 2012) and probably the viral morphology as well. Nevertheless, permeabilization is crucial in FISH since permeabilization of the cells allows the labeled oligonucleotides to diffuse through the cell envelope (Amann and Fuchs 2008).

Nowadays, different FISH methods exist for detecting viruses, *e.g.,* cycling primed in situ amplification-FISH (CPRINS-FISH) (Kenzaka et al. 2005) was developed for detecting individual genes in a bacterial cell, which was then optimized to visualize viral DNA and phage-mediated gene transfer in freshwater environments (Kenzaka et al. 2010). More recently, scientists developed PhageFISH (Allers et al. 2013) as an optimized technique of GeneFISH (Moraru et al. 2010). PhageFISH enables the visualization of viral infections from the early stage of infection to bursting cells (Allers et al. 2013). This type of method was further extended to eukaryotic microorganisms. For instance, the infection process of the eukaryotic algae *Ostreococcus lucimarinus* by Prasinoviruses was studied, whereby 200 infected cells with different stages of infection were counted (Zimmerman et al. 2019). In this study, virus-attached cells (viral signals detected on the margin of host signals), infected cells (the overlapping of virus and host signals), and lysed cells (concentrated viral signals and lost host signals) were observed (Zimmerman et al. 2019). More recently, PhageFISH and direct-geneFISH (Barrero-Canosa et al. 2017) were combined for applying virusFISH on the unicellular green algae *Ostreococcus tauri* and its virus *Ostreococcus tauri* 5 (OtV5) to monitor viral infections in pure cultures (Castillo et al. 2020). Furthermore, a new approach called Virocell-FISH (Vincent et al. 2020) showed the interaction of a giant virus chasing its host *Emiliania huxleyi*, an alga that is part of the ocean's biomass (Kenzaka et al. 2005). Consequently, there exists a great array of potential FISH methods for targeting viruses, whose potential has not yet been leveraged for exploring viral communities and their dynamics in ecosystems.

8.2. Coupling of Metaviromics with Fluorescence In Situ Hybridization

Although the knowledge gained through the variety of available microscopy techniques is astonishingly high regarding viruses in general, coupling meta-omics techniques with microscopy appears to be a major challenge and is consequently not frequently represented in the literature (see Figure 1). While some research has been carried out

regarding metaviromics and microscopy separately (mentioned in the previous section), there have been few studies that coupled both techniques directly. Crucial information for the design of probes that detect viruses in FISH results from metaviromics and thus aids in designing the detection of viruses in, *e.g.,* phageFISH (Allers et al. 2013). The linkage of metaviromics with imaging techniques was first described and performed for an environmental sample by Hochstein et al. (2016) (Hochstein et al. 2016). They identified a new archaeal *Acidianus* tailed spindle virus (ATSV, host: *Acidianus hospitalis* W1) with a 70.8 kb circular dsDNA viral genome in an acidic hot spring (Alice Spring) in the Yellowstone National Park (Wyoming, USA) (Hochstein et al. 2016). They sequenced the viral genome and designed probes to identify the virus within the ecosystem and confirmed this after isolating the virus and visualizing the ATSV virus particles in TEM as large, spindle-shaped virions (Hochstein et al. 2016). A comparative study also used genomic information to perform FISH targeting a viral genome in an enrichment culture (Wagner et al. 2017). An archaeal *Metallosphaera* turreted icosahedral virus (MTIV) (Wagner et al. 2017) was isolated from an acidic hot spring in the Yellowstone National Park (USA), and its icosahedral morphology was illustrated via TEM, cryo-electron tomography, and single-particle analysis. In order to verify their virus–host prediction, direct viral FISH (Barrero-Canosa et al. 2017) was performed on *Metallosphaera yellowstonensis* cultures (Wagner et al. 2017).

A recent investigation on the relationship of subsurface viruses targeting abundant primary producers (here Altiarchaeota) was conducted by Rahlff et al. (2021) (Rahlff et al. 2021). Intracellular and extracellular localizations of various stages of viral infections in Altiarchaeota biofilms by using virusFISH (Rahlff et al. 2021), a modified version of direct-geneFISH (Barrero-Canosa et al. 2017), were detected (Figure 2). Super-resolution microscopy was also performed on the Altiarchaeota biofilms, resulting in a better resolution of the viral infections (Rahlff et al. 2021) and representing the first time a super-resolution microscopy was used for the study of virus-infected cells. Applying direct-geneFISH on multiple samples from the ecosystem, the authors showed that the genome sequence detected by metaviromics belongs to a lytic virus and thus challenged a standing paradigm that the subsurface is mostly populated by lysogenic viruses.

Another example of coupling virusFISH with metagenomics was represented by replicating a lysogenic phage in a marine sponge holobiont (here *Aplysina aerophoba*) (Jahn et al. 2021). In this study, a new in situ microscopy approach called ‘PhageFISH-CLEM’ was developed that is based on a combination of imaging and bioinformatics for investigating virus–host interactions, providing new insights into virus ecology within marine sponges (Jahn et al. 2021). Phage-FISH-CLEM results showed phages within bacterial symbiont cells and in phagocytotic active sponge cells, indicating that lysogeny dominated this sponge microbiome (Jahn et al. 2021). For the first time, phageFISH was coupled directly with EM and enabled researchers not only the quantification of viruses but also the visualization of virus–host associations originally predicted from metagenomic data.

9. Conclusions

Viruses are a central component of Earth's biome and shape complex microbial communities and are crucial for ecosystem functioning (Anderson et al. 2013). Studying these tiny microbial predators in natural environments is necessary because so few of them can be cultivated under laboratory conditions. Over the last five decades, researchers have used microscopy to discover different viral lifestyles along with unique morphologies to demonstrate active viral infections across all domains of life. Research to date has consistently shown that viruses can be detected with various imaging techniques (epifluorescence microscopy, EM, CLEM, AFM, HIM). Applying metaviromics and microscopy, researchers have so far discovered only a small portion of the genetic and morphological diversity of viruses on our planet.

Tremendous advances have been made not only in the field of microscopy by developing higher resolution instruments, improved staining methods, and novel labeling strategies for FISH analyses, but also in the field of in-silico analyses of viromes for detecting sequences of novel viruses (VirSorter (Roux et al. 2015), VirFinder (Ren et al. 2017), Vibrant (Kieft et al. 2019)). The huge sequence data sets obtained through metagenomics and viromics, which, in particular, facilitate the development of new FISH probes that are essential for studying more and previously unexplored viruses in environments (Allers et al. 2013; Hochstein et al. 2016). Development of these technologies will in the future not only lead to the visualization of other novel viruses but could also lead to an improved understanding of the role viruses play in environmental communities, by, *e.g.,* quantifying viral infections in environmental samples.

We propose that linking (meta)viromics and FISH to AFM, HIM, and EM, *i.e.*, correlative light and electron microscopy (CLEM), for environmental samples will reveal the morphology of uncultivated viruses that have only been identified on a sequence basis so far. The plethora of different viral morphologies, particularly in the realm of archaeal viruses, promises many fascinating insights into viral diversity once CLEM becomes more applicable to ecosystems. For viruses that cannot be imaged via CLEM, there exists the possibility of identifying novel capsid proteins via proteomics of viral fractions followed by recombinant expression of the proteins and antibody generation for immunogold labeling in TEM (Hills et al. 1987). The overview as well as the new perspectives presented in this study will hopefully aid other researchers in the exploration of the morphology of cultivated and yet-to-be cultivated viruses on our planet in order to better understand their diversity and functioning in Earth's biomes.

Funding: This work received funding from the NOVAC project of the German Science Foundation (grant number DFG PR1603/2–1) and the Ministry of Culture and Science of North Rhine-Westphalia (Nachwuchsgruppe "Dr. Alexander Probst"). We acknowledge support from the Open Access Publication Fund of the University of Duisburg-Essen.

Conflicts of Interest: The authors declare no conflict of interest.

II. Lytic archaeal viruses infect abundant primary producers in Earth's crust

Janina Rahlff[1*†], Victoria Turzynski[1*], Sarah P. Esser[1], Indra Monsees[1], Till L.V. Bornemann[1], Perla Abigail Figueroa-Gonzalez[1], Frederik Schulz[2], Tanja Woyke[2], Andreas Klingl[3], Cristina Moraru[4], and Alexander J. Probst[1#]

[1]University of Duisburg-Essen, Department of Chemistry, Environmental Microbiology and Biotechnology (EMB), Group for Aquatic Microbial Ecology, Universitätsstraße 5, 45141 Essen, Germany
[2]DOE Joint Genome Institute, 1 Cyclotron Rd, Berkeley, CA, 94720, USA
[3]Plant Development & Electron Microscopy, Biocenter LMU Munich, Großhaderner Str. 2-4, 82152 Planegg-Martinsried, Germany
[4]Institute for Chemistry and Biology of the Marine Environment (ICBM), Carl-von-Ossietzky-University Oldenburg, PO Box 2503, Carl-von-Ossietzky-Straße 9-11, 26111, Oldenburg, Germany

†Present address: Centre for Ecology and Evolution in Microbial Model Systems (EEMiS), Department of Biology and Environmental Science, Linnaeus University, SE-39182, Kalmar, Sweden

*authors contributed equally

*Correspondence: alexander.probst@uni-due.de

Publication information:
Nature communications 2021, 12, 4642; https://doi.org/10.1038/s41467-021-24803-4
Received: 05 August 2020 / Accepted: 05 July 2021 / Published: 20 July 2021
Link: https://www.nature.com/articles/s41467-021-24803-4

Abstract

The continental subsurface houses a major portion of life's abundance and diversity, yet little is known about viruses infecting microbes that reside there. Here, we use a combination of metagenomics and virus-targeted direct-geneFISH (virusFISH) to show that highly abundant carbon-fixing organisms of the uncultivated genus Candidatus Altiarchaeum are frequent targets of previously unrecognized viruses in the deep subsurface. Analysis of CRISPR spacer matches display resistances of Ca. Altiarchaea against eight predicted viral clades, which show genomic relatedness across continents but little similarity to previously identified viruses. Based on metagenomic information, we tag and image a putatively viral genome rich in protospacers using fluorescence microscopy. VirusFISH reveals a lytic lifestyle of the respective virus and challenges previous predictions that lysogeny prevails as the dominant viral lifestyle in the subsurface. CRISPR development over time and imaging of 18 samples from one subsurface ecosystem suggest a sophisticated interplay of viral diversification and adapting CRISPR-mediated resistances of Ca. Altiarchaeum. We conclude

that infections of primary producers with lytic viruses followed by cell lysis potentially jump-start heterotrophic carbon cycling in these subsurface ecosystems.

1. Introduction

Earth's continental subsurface harbours 2-6 x 10^{29} prokaryotic cells (Flemming and Wuertz 2019; Magnabosco et al. 2018), which represent a major component of life's diversity on our planet (Anantharaman et al. 2016; Hug et al. 2016). Among these organisms are some of the most enigmatic archaea, including Aigarchaeota, Asgard archaea, Altiarchaeota and members of the DPANN radiation (Castelle et al. 2015; Nunoura et al. 2011; Probst et al. 2014b; Zaremba-Niedzwiedzka et al. 2017). Although the ecology and diversity of subsurface microorganisms has been under investigation in several studies, the fundamental question relating to how microbial diversity and composition in the deep subsurface change with virus infection remains mostly unanswered. Viruses have long been recognized as major drivers of microbial diversification (Weinbauer and Rassoulzadegan 2004), yet little is known about their lifestyle, activity and impact on oligotrophic subsurface ecosystems. Recent evidence demonstrated high numbers of virus-cell ratios in marine subsurface sediments (Engelhardt et al. 2014), suggesting ongoing viral proliferation in the deep biosphere. In oceanic surface sediments below 1000 m depth, virus-mediated lysis of archaea was estimated to be a major contributor to carbon release thus affecting global biogeochemical cycles (Danovaro et al. 2016). In addition, pronounced morphological diversity of bacteriophages with presumably lytic representatives has been found in granitic groundwater of up to 450 m depth (Kyle et al. 2008), and might be the result of recombination events, horizontal gene transfer and lysogeny known to shape microbial communities of the subsurface (Labonté et al. 2015). The recent recovery of two novel bacteriophage genera with lytic genes from groundwater highlights the potential of subsurface environments for being huge reservoirs of previously unknown viruses (Hylling et al. 2020). Furthermore, a study on predominant *Halanaerobium* spp. from anthropogenic subsurface communities (hydraulically fractured wells) suggested long-term host-virus dynamics, extensive viral predation and adaptive host immunity based on clustered regularly interspaced short palindromic repeats (CRISPR) spacer to protospacer matches (Daly et al. 2019). CRISPR systems function as defense mechanisms for bacteria and archaea against mobile genetic elements (MGEs), including viruses (Horvath and Barrangou 2010). The CRISPR locus is usually flanked by *cas* genes and interspaced by short variable DNA sequences termed spacers (Horvath and Barrangou 2010) previously acquired from invading MGEs. The diversification of CRISPR-Cas immunity in the host over geographical distances and time due to preceding viral infections and protospacer mutations has been well-documented, *e.g.,* for *Sulfolobus islandicus* (Pauly et al. 2019b).

Oligotrophic anaerobic subsurface environments can be populated by a variety of different microorganisms, some of them belonging to the phylum Altiarchaeota (Probst et al. 2014b, 2018). In fact, these organisms can reach high abundances in their ecosystems with up to 70% of the total community in the aquifer or with up to 95% within the biofilm (BF) they form (Henneberger et al. 2006; Probst et al. 2013). Members of the genus *Ca.* Altiarchaeum–the best-studied representative being *Ca.* A. hamiconexum (Probst et al. 2014b)–occur in

anoxic subsurface environments around the globe (Bird et al. 2016; Hernsdorf et al. 2017) and fix carbon via the reductive acetyl-CoA (Wood-Ljungdahl) pathway (Probst et al. 2014b). In certain ecosystems, *Ca.* Altiarchaea form nearly pure BFs, which are kept together by filamentous cell surface appendages called hami (singular: hamus) (Moissl et al. 2005). Studies to date demonstrated symbiotic relationships of *Ca.* Altiarchaea with bacterial partners *Thiothrix* sp. (Rudolph et al. 2001), and *Sulfuricurvum* sp. (Rudolph et al. 2004), but also a co-occurrence with the episymbiont *Ca.* Huberiarchaeum crystalense, belonging to the DPANN clade, has been recently reported (Probst et al. 2018; Schwank et al. 2019). A single transmission electron micrograph and the presence of CRISPR systems led to speculations on the existence of *Ca.* Altiarchaeum viruses in the subsurface (Probst and Moissl-Eichinger 2015). However, mesophilic archaeal viruses from the deep terrestrial subsurface remain highly enigmatic, despite the fact that mesophilic archaeal genomes contain more MGEs than their thermophilic counterparts (Makarova et al. 2014). The knowledge gap on archaeal viruses is fostered by a lack of their genome entries in public databases (Vik et al. 2017), missing marker genes for viruses (Anderson et al. 2013) and a bias towards viruses related to economical, medical or biotechnological activities (Rodrigues et al. 2017). In addition, only ~150 archaeal viruses have been isolated and described to date (Munson-McGee et al. 2018). Recent exhaustive metagenomic surveys aided the discovery of novel archaeal viruses (Paez-Espino et al. 2016) from multiple ecosystems, including the ocean (Philosof et al. 2017; Ahlgren et al. 2019), hot springs (Gudbergsdóttir et al. 2016; Zablocki et al. 2017; Munson-McGee et al. 2019) and soils (Emerson et al. 2018; Trubl et al. 2018), and eventually allowed targeting and visualization of an uncultivated virus based on its genome (Hochstein et al. 2016). More recently another correlative phageFISH imaging approach was used to visualize bacteriophages within sponge tissue (Jahn et al. 2021).

Due to their world-wide distribution and high abundance as the main primary producer in certain continental subsurface ecosystems, *Ca.* Altiarchaea represent the ideal model genus for studying viruses and their infection mechanisms of mesophilic microorganisms in the subsurface. This is especially relevant because the extent to which lytic infections occur in the continental subsurface is unknown, and lysogeny is assumed to be the predominant viral strategy (Anderson et al. 2011). In this work, we use metagenomics to predict viruses that infect *Ca.* Altiarchaea in subsurface ecosystems at four different sites across three continents (Europe, Asia, North America). Using virus-targeted direct-geneFISH (virusFISH), we visualize and characterize the most abundant putative virus from a sulfidic spring in Bavaria, Germany, providing novel insights into the lytic lifestyle of an uncultivated virus, whose genome shows little homologies with sequences in public databases and carries no viral hallmark genes. Our analyses further demonstrate the diversification of CRISPR systems of *Ca.* Altiarchaea along with a decline in virus abundances over six years. We conclude that the kill-the-winner theorem can play an important role in evolutionary and ecosystem processes of the deep biosphere.

2. Results

Globally distributed *Ca.* Altiarchaea have complex CRISPR systems with conserved DR sequences

Screening of 16S ribosomal RNA (rRNA) datasets and metagenomes within IMG (Chen et al. 2019a) confirmed a global distribution of organisms belonging to the phylum Altiarchaeota (Figure 1). We performed metagenomic analyses of four terrestrial subsurface ecosystems ranging from 37 to 352 m below ground that showed high abundance of the genus *Ca.* Altiarchaeum (Supplementary Table 1), previously also termed Alti-1 (Bird et al. 2016). These ecosystems included i) an anoxic aquifer accessible through an artesian well (Mühlbacher Schwefelquelle, Isling, MSI) (Rudolph et al. 2004) sampled in 2012 and 2018, and ii) a high-CO_2 geyser (Geyser Andernach, GA) (Bornemann et al. 2020a) both located in Germany, iii) a sulfidic spring in the US (Alpena County Library Fountain, ACLF) (Sharrar et al. 2017), and iv) a deep underground laboratory in Japan (Horonobe Underground Research Laboratory, HURL) at 140 and 250 m depth (Hernsdorf et al. 2017). All eight genomes of *Ca.* Altiarchaeum (Supplementary Data 1) carried genetic information for Type I-B-CRISPR-Cas immunity including proteins Cas5, Cas7, Cas8a. Although other Cas proteins were also present in the assembly but remained unbinned, we were able to confirm the presence of Cas3 (Supplementary Data 1) and Cas6 (Probst et al. 2014b) on scaffolds with the taxonomic annotation of Altiarchaea for the MSI site. Proteins of a Type III CRISPR-Cas immunity were found at the ACLF, HURL, and MSI site, including Repeat Associated Mysterious Proteins (RAMP, Cmr) of Type III-B and III-C, and Csm proteins of the Type III-A system (Supplementary Data 1). Confidence in binning CRISPR arrays and assigning direct repeat (DR) sequences to *Ca.* Altiarchaea arose from the 16 to 146-fold higher abundance of these organisms (and their CRISPR arrays) in the ecosystems than other microbes (Supplementary Figure 1 (Hernsdorf et al. 2017; Probst et al. 2014b; Sharrar et al. 2017)). Additionally, two versions of a CRISPR DR sequence assigned to *Ca.* Altiarchaea were highly conserved across these ecosystems (Supplementary Figure 2, Supplementary Data 1). DR sequence 1 occurred in all four ecosystems, whereas DR sequence 2 was only found at the HURL and the ACLF site (Supplementary Data 1). While all DR sequences from the four sites were previously unknown in the CRISPRmap database, DR sequence 1 in orientation 1 and DR sequence 2 in both orientations structurally resembled motif 13 and 12 of the database, respectively. All four sequences form thermodynamically favorable secondary structures and carry an AAA(N) motif (Supplementary Figure 2), indicating that both strands of the CRISPR array could theoretically be transcribed.

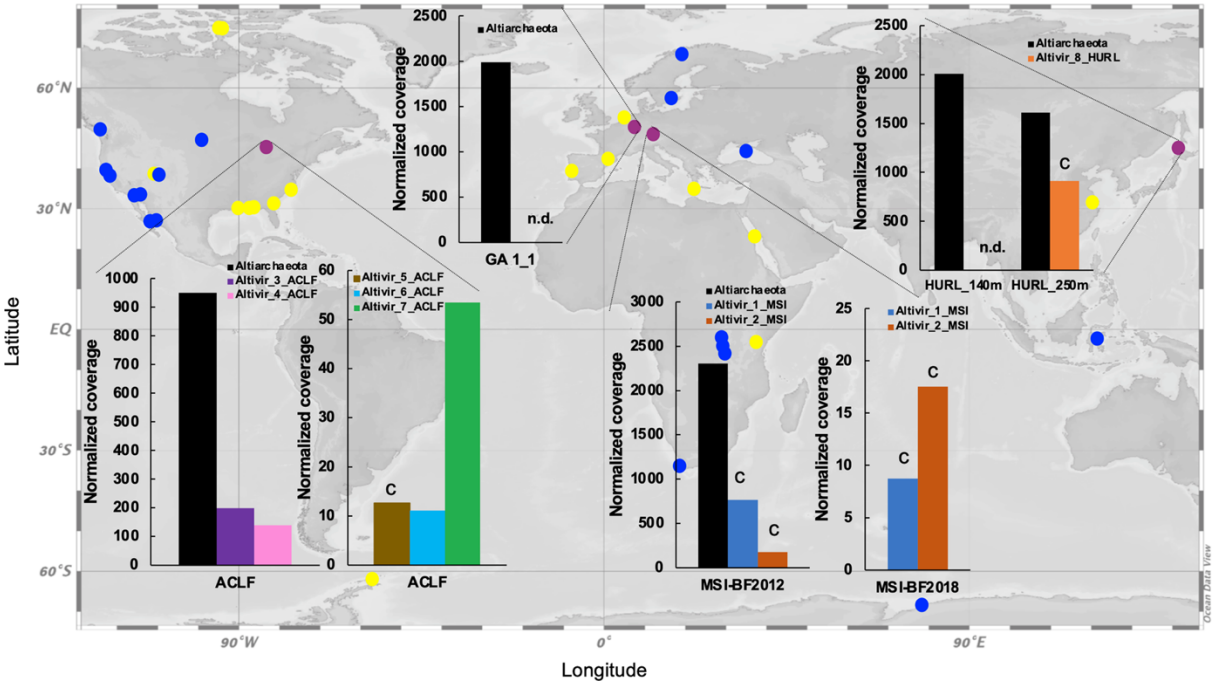

Figure 1: Global distribution of abundant Altiarchaeota (group Alti-1) and their predicted viruses in Altiarchaeota hot spots. Distribution analysis is based on 16S rRNA gene sequencing (yellow dots) and the detection of hamus genes in metagenomes from IMG (blue and purple dots). Purple dots correspond to the four investigated sites of this study. Normalized host and virus coverage are given for the four subsurface habitats: Alpena County Library Fountain (ACLF, Michigan, USA), Horonobe Underground Research Laboratory (HURL, Japan), Mühlbacher Schwefelquelle, Isling (MSI, Germany), and Geyser Andernach (GA, Germany). Percent relative abundance of dominant Altiarchaeota compared to other community members is shown in Supplementary Table 1. Only Altivir_1_MSI and Altivir_2_MSI obtained from biofilm (BF) samples are shown. The letter C indicates circular genomes. n.d. none detected. World map has been generated using Ocean Data View v.5.3.0 (Schlitzer 2015). Color explanation of bars representing normalized coverage: orange-red = Altivir_1_MSI (virus), blue = Altivir_2_MSI, purple = Altivir_3_ACLF, rose = Altivir_4_ACLF, brown = Altivir_5_ACLF, light blue = Altivir_6_ACLF, green = Altivir_7_ACLF, and black = Altiarchaeota (host).

Eight novel viral clades with genome relatedness across continents show infection histories with Altiarchaeota

Using matches of Altiarchaeota spacers to protospacers, we were able to identify 13 predicted viral genomes (termed *Ca.* Altiarchaeum virus Altivir_#, here further referred to as Altivir_# for short) in three out of the four sampling sites (Supplementary Table 2). No viruses targeted by *Ca.* Altiarchaea spacers could be predicted for GA and the HURL sites at 140 m depth. Only two out of the 13 predicted viral genomes, *i.e.*, the 20.8-kb long Altivir_2_MSI_BF_2012 and the 22.6-kb long Altivir_8_HURL, had hits in the Virus Orthologues Groups database (VOGDB, Supplementary Table 2), carried viral hallmark genes and were circular, prompting us to classify them as viruses. The others were designated as putative viruses according to our classification scheme (Supplementary Figure 3). All 13 (putative) viruses were categorized as lytic viruses according to VirSorter (Roux et al. 2015). Four predicted viruses were circular and thus complete in their genome sequence (Figure 1, Supplementary Table 2). The 13 viral genomes formed eight monophyletic clades based on VICTOR analysis (Figure 2), representing potentially eight individual genera (VICTOR

threshold for genus was 15.8% nucleotide based intergenomic similarity). Viral genomes in the Altivir_1_MSI and Altivir_2_MSI clades were recovered in all sampled time points from the MSI site (Supplementary Table 2), both in the cellular and virus enriched fractions. The Altivir_2_MSI genomes recovered from the virus enriched fraction (MSI_<0.1µm_2018) were fragmented and thus excluded from further analysis. Intergenomic pairwise similarities for the four Altivir_1_MSI varied between 99.3-99.7% (Supplementary Figure 4), this clade representing a single viral species (the threshold for species demarcation was 95% similarity). The three Altivir_2_MSI genomes had similarities between 87.0-96.1% and represented two viral species (Supplementary Figure 4). Using vConTACT, Altivir_1_MSI formed a cluster with Altivir_6_ACLF, a putative virus from ACLF, with whom it shared five protein clusters (Figure 2, Supplementary Figure 5). This relatedness between viruses from highly distant subsurface ecosystems was further supported by the VICTOR analysis, which placed them in the same monophyletic clade (Figure 2). All remaining viruses apart from Altivir_1_MSI, Altivir_2_MSI, and Altivir_6_ACLF were designated by vConTACT as unclustered singletons. Only one protein cluster was shared between Altivir_2_MSI, Altivir_4_ACLF, and Altivir_8_HURL, and no protein clusters between the remaining three viruses, indicating that all these viruses are distant from each other (Figure 2). In total, these eight viral genera were affiliated to seven vConTACT viral clusters (Altivir_1_MSI/Altivir_6_ACLF grouped together), which were unrelated with previously published viral genomes in the RefSeq94 database according to vConTACT criteria (Supplementary Figure 5). However, based on the phylogenetic analysis of the DNA polymerase B (for detailed annotations of viral proteins please see below; Supplementary Figure 6), Altivir_2_MSI is likely related to *Tectiviridae*, a dsDNA virus family in the *Varidnaviria* realm. The presence of a capsid portal protein in Altivir_4_ACLF (Supplementary Figure 7), a major tail tube protein in Altivir_7_ACLF (Supplementary Figure 8), and a terminase as well as a portal protein in Altivir_8_HURL (Supplementary Figures 9) indicate that these three viruses belong to the *Duplodnaviria* realm. Phylogenetic analysis of the aforementioned proteins suggests that Altivir_7_ACLF and Altivir_8_HURL potentially belong to the *Caudovirales* order. Altivir_4_ACLF is distantly related to eukaryotic viruses from *Herpesvirales*, suggesting a relationship with the known *Caudovirales*.

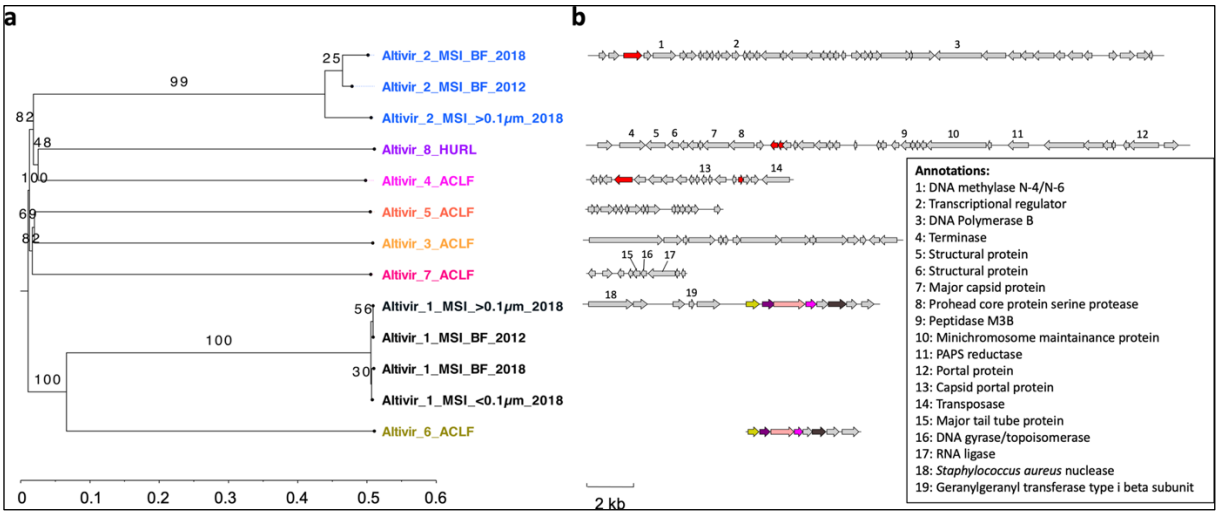

Figure 2: **Phylogenomic genome-BLAST distance phylogeny (GBDP) tree of *Ca.* Altiarchaeum viruses and viral proteins clusters. a** The tree was inferred using the distance formula D0 yielding average support of 69%. The numbers above branches are GBDP pseudo-bootstrap support values from 100 replications. The branch lengths of the resulting VICTOR (Meier-Kolthoff and Göker 2017) trees are scaled in terms of the respective distance formula used. The tree shows that the eight predicted viral genomes were assigned to the same family, to eight different genera, and ten species (which is the result of having multiple genomes included for Altivir_1_MSI and Altivir_2_MSI). **b** Protein clustering across all viruses revealed that Altivir_1_MSI_>0.1 µm_2018 and Altivir_6_ACLF, originating from different continents, have five protein clusters (2–6) in common. Altivir_2_MSI_BF_2012, Altivir_4_ACLF, and Altivir_8_HURL shared only one protein cluster (1). Open reading frames of the viral genomes were predicted using Prodigal v.2.6.3 (Hyatt et al. 2010) and further translated with the R package seqinr v.3.6.-1. Colors indicate shared protein clusters between genomes and numbers show nonhypothetical consensus annotations according to Supplementary Data 3. Color code for viral genomes: Altivir_1_MSI = black, Altivir_2_MSI = blue, Altivir_3_ACLF = yellow, Altivir_4_ACLF = pink, Altivir_5_ACLF = orange, Altivir_6_ACLF = olive-green, Altivir_7_ACLF = pink-red, and Altivir_8_HURL = purple.

Comparing the genomes of Altivir_1 and Altivir_2 individually across the samples from 2012 and 2018, we identified different developments of the two viral genomes. Altivir_2_MSI clade presented gene content variations between the genomes from different samples (Supplementary Figure 10), which agrees with the fact that it represents two viral species. By contrast, Altivir_1_MSI accumulated multiple single nucleotide polymorphisms (SNPs) and only represented strain level variations of the same species (Supplementary Figure 10, Supplementary Data 2).

Host-virus ratios (considering *Ca.* Altiarchaeum to be the host) based on metagenome read mapping varied greatly (between 1.8 and 301.9; Supplementary Table 2) with the smallest ratios of 1.8 for Altivir_8_HURL, followed by 2.3 for Altivir_1_MSI_>0.1µm_2018, 2.8 for Altivir_2_MSI_>0.1µm_2018 and 3.0 for Altivir_1_MSI_BF_2012. Abundance of in the planktonic fraction (>0.1µm) suggests high concentrations of *Ca.* Altiarchaeum BF on the 0.1 µm filter membrane during the filtration process. Relative abundance of viruses based on normalized coverage ranged between 9 (Altivir_1_MSI_BF_2018) and 913 (Altivir_8_HURL, Figure 1, Supplementary Table 2). The genomes of Altivir_2_MSI_BF_2018 and Altivir_8_HURL carried short CRISPR arrays with one spacer each, but spacers from these mini-CRISPR arrays did not match other viruses in the respective ecosystems.

Several viral proteins could be functionally annotated (see Figure 2B, Supplementary Table 2, Supplementary Data 3), belonging mostly to the circular Altivir_8_HURL genome. Altivir_8_HURL, bearing 36 genes, encoded for an auxiliary metabolic gene (AMG), namely the phosphoadenosine phosphosulfate reductase (PAPS, *CysH*) (phmmer, e value: 6.1e-48), which probably facilitates assimilatory sulfate reduction in the host, and is a common AMG of many viruses (Kieft et al. 2021). Altivir_1_MSI, of particular interest for this study because it was highly abundant in the MSI_BF-2012 metagenome, recruited many spacer hits and only 2 out of its 14 proteins could be annotated with enough certainty (Figure 2, Supplementary Table 2, Supplementary Data 3). These included a nuclease and a geranylgeranyl transferase. In sum, only 11.9% of the 159 proteins across all Altivir genomes have a putative function assigned rendering the remaining genes of yet unknown function as genetic dark matter (Figure 2, summary of annotations in Supplementary Table 2).

VirusFISH reveals a lytic lifestyle for Altivir_1_MSI

We selected the in silico predicted Altivir_1_MSI viral clade for visualization by virusFISH, due to its high abundance at the MSI site, and despite the lack of viral hallmark genes. VirusFISH with a probe containing eleven double stranded polynucleotides was successfully implemented to visualize the distribution of the circular genome of Altivir_1_MSI within altiarchaeal BF (Figure 3A, Supplementary Figure 11). In contrast to the negative control with a non-matching probe (Supplementary Figure 12), our target probes enabled us to detect altiarchaeal cells containing Altivir_1_MSI. Multiple cells were surrounded by halo signals, corresponding to a viral burst (Allers et al. 2013) and providing evidence for Altivir_1_MSI being an active virus and lysing Altiarchaeota cells.

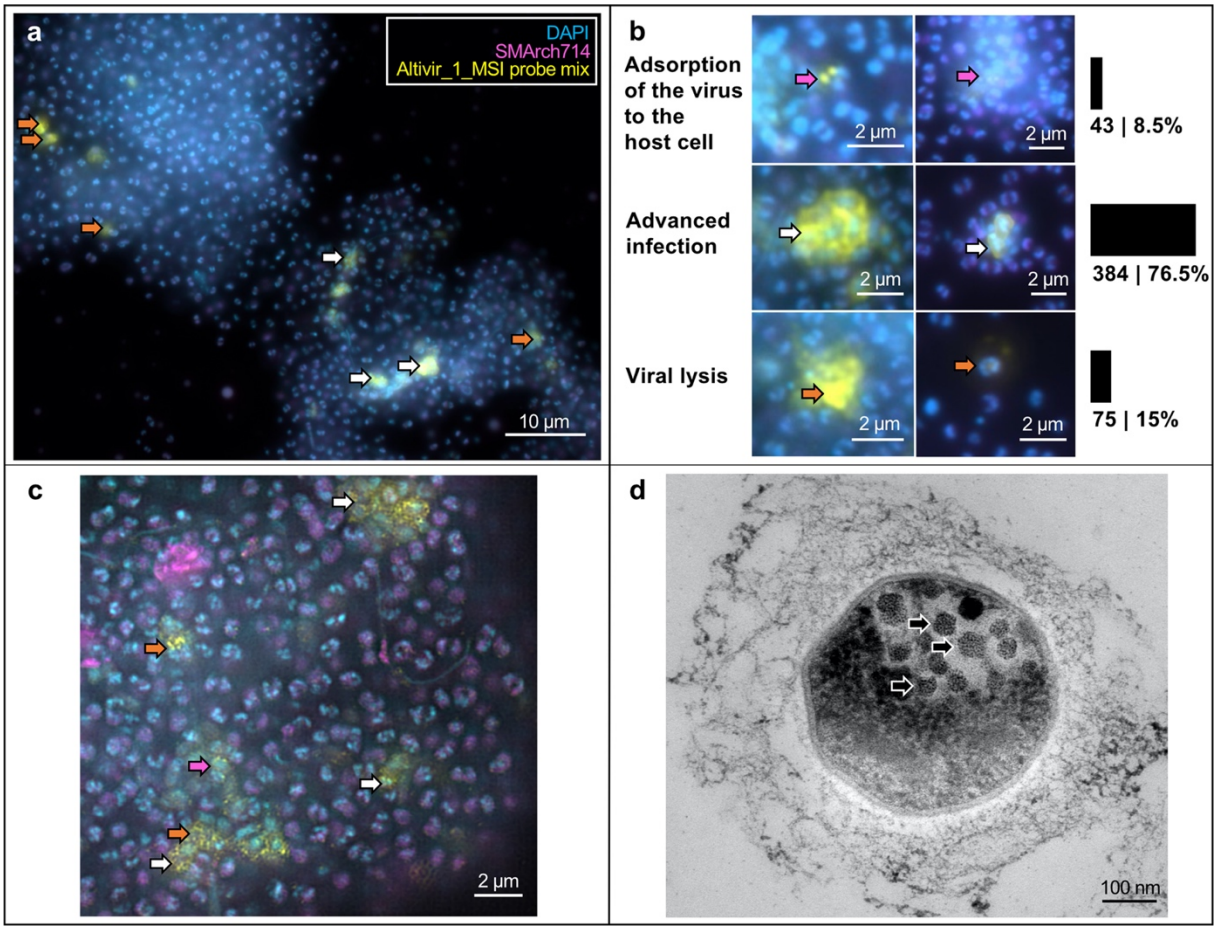

Figure 3: Visualization and quantification of *Ca.* Altiarchaeum virus Altivir_1_MSI-infected and noninfected Altiarchaeota biofilm (BF) cells from MSI site. For all virusFISH experiments shown here, an Altivir_1_MSI probe was used for detecting viral infections. BF material was visualized with filter sets for DAPI (blue, cells), ATTO 488 (purple, 16S rRNA signal), and Alexa 594 (yellow, viral genomes), and merged for analysis and display purposes. **a** VirusFISH displays the interactions between Altiarchaeota cells and their virus shown as yellow dots. For unmerged imaging data, see Supplementary Fig. 11. Scale bar: 10 µm. **b** Different infection stages with Altivir_1_MSI. The enumeration performed with a regular epifluorescence microscope was based on 18,411 archaeal cells and categorized into three infection stages. For the categorization we used in total 18 Altiarchaeota biofilms, whereby 17 biofilms were treated with the Altivir_1_MSI probe (n = 17) and one biofilm was treated with a Metallosphaera sp. virus probe (n = 1). Purple arrows indicate exemplary viruses that attach to host's cell surface, white arrows show advanced infections, and orange arrows bursting cells with free viruses. Scale bars: 2 µm. **c** Coupling virusFISH with structured illumination microscopy showed extracellular signals of tiny fluorescently labeled viral particles attaching to Altiarchaeota's cell surface but also in a free state as presumably released virions (n = 1). Scale bar: 2 µm. **d** Transmission electron microscopy revealed intracellular virus-like particles (n = 3). Scale bar: 100 nm.

A total of 18 411 altiarchaeal cells and 502 viral infections (co-localization of Altivir_1_MSI and *Ca.* Altiarchaea signals) across 18 samples/BF flocks were analyzed via fluorescence microscopy and categorized into three main infection stages: i) viral adsorption to the host cells (8.5%), ii) advanced infection with intracellular virus signals and ring-like signals around the cells (76.5%), and iii) cell lysis with bursting cells and release of virions (15%) (Figure 3B). Super-resolution microscopy further showed extracellular signals of small fluorescently labeled particles, which we interpret as individual viral particles (Figure 3C). This observation was further supported by ultra-thin sectioning and transmission electron microscopy, which revealed many intracellular virus-like particles associated with

Ca. Altiarchaea cells. These particles had an average diameter of 50 nm (SD ± 7 nm), as measured across eleven host cells (Figure 3D). The high percentage of cell lysis associated with the virus signals along with the high abundance of the virus in the planktonic and viral fraction suggests a lytic lifestyle for Altivir_1_MSI.

Spatio-temporal heterogeneity of predicted infections and CRISPR-Cas mediated immunity of *Ca.* Altiarchaea

To investigate the development of virus immunities over time, we compared the publicly available metagenome from MSI (taken in 2012) to a newly sequenced BF sample from 2018. We also analyzed the planktonic microbiome (>0.1 µm) and a viral fraction (<0.1 µm), *i.e.*, after 0.1 µm filtration and $FeCl_3$ precipitation. We compared the change in relative abundance (normalized coverages) of *Ca.* Altiarchaeum, Altivir_1_MSI, Altivir_2_MSI and *Ca.* Altiarchaeum CRISPR spacers across these samples (Figure 4) with *Ca.* Altiarchaeum being the most dominant microbe in each sample (Figure S1). While the planktonic microbiome showed a tremendous diversity based on *rpS3* sequences (238 different organisms, Figure 4), the diversity was quite restricted with 19 and 17 organisms in MSI_BF_2012 and MSI_BF_2018, respectively. Please note that there is a difference between the number of organisms detected in the rank abundance curves (Supplementary Figure 1) and those reported in Figure 4 as the latter were normalized to read abundance to ensure comparability.

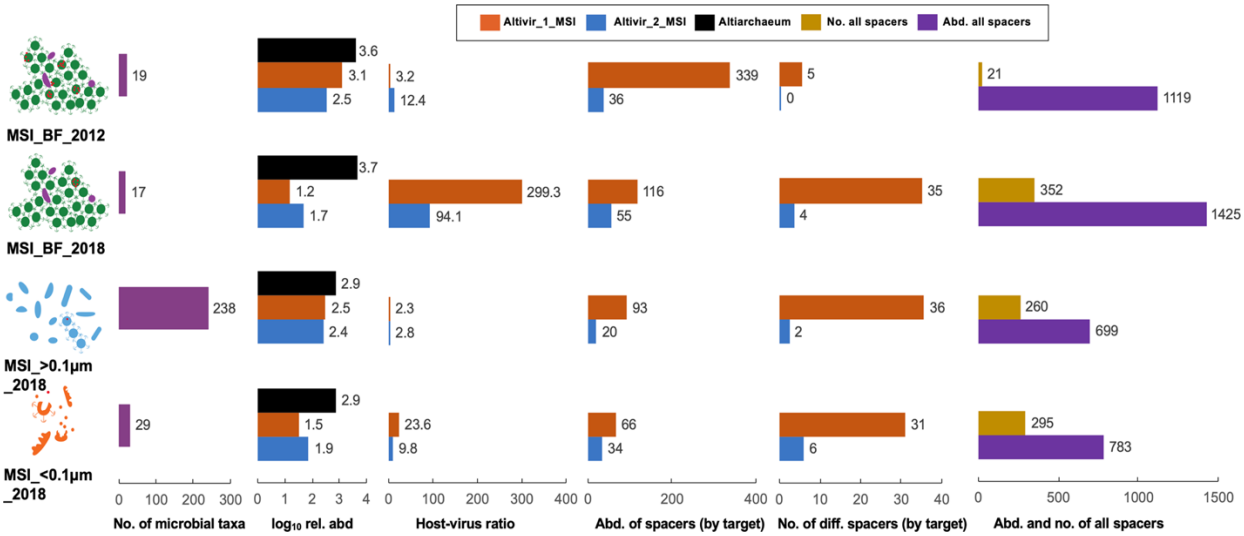

Figure 4: Development of host–virus and spacer dynamics from 2012 to 2018 based on metagenomics from the Mühlbacher Schwefelquelle, Isling (MSI). Predicted viruses Altivir_1_MSI and Altivir_2_MSI became less abundant from 2012 to 2018. Data are presented for biofilms (BF) from 2012 and 2018 as well as the planktonic fraction (>0.1 µm) and the viral fraction (<0.1 µm). Considering the BFs, total spacer abundance and numbers increased from 2012 to 2018 while those matching Altivir_1_MSI decreased in abundance but increased in numbers. Number (no.) of microbial taxa refers to the number of different prokaryotes in a sample detected via rpS3 rank abundance curves (normalized by sequencing depth). Host–virus ratio is calculated from host and virus coverage based on read mapping. Abundance and number of different spacers were normalized to minimum relative abundance (rel. abd.) of the host based on read mapping. Color definition of bars: violet = number of microbial taxa, orange-red = features of Altivir_1_MSI, blue = features of Altivir_2_MSI, black = log10 relative abundance of Altiarchaeum, ocher = number of all spacers, and purple = abundance of all spacers.

Both predicted viral genomes (Altivir_1_MSI_BF_2012, Altivir_2_MSI_BF_2012) declined in abundance when comparing the BF sample from 2018 to the sample from 2012, and at the same time the host:virus ratio increased (Figure 4). While Altivir_1_MSI was more abundant in 2012 (host-virus ratio=3.2) compared to Altivir_2_MSI relative to its host (host-virus ratio=12.4), the pattern reversed in 2018 for the BF sample (host-virus ratio=299.3 compared to 94.1 for Altivir_1_MSI and Altivir_2_MSI, respectively). Both, the total spacer abundance and the spacer diversity increased from 2012 to 2018 in BF samples, *i.e.*, from 21 to 352 (number of different spacers) including an ~20% increase in the number of spacer clusters that were singletons in the dataset (Supplementary Figure 13) and from 1 119 to 1 425 (abundance of spacers). The abundance of spacers matching the genome of Altivir_1_MSI_BF_2012 decreased from 339 to 116 spacers, whereas it increased from 36 to 55 for Altivir_2_MSI_BF_2012 in BF samples from 2012 to 2018. For both targets the number of different matching spacers increased over time (Supplementary Figure 14), in line with the development of the total spacers in this ecosystem (Figure 4). Because planktonic *Ca.* Altiarchaeum cells (diameter: 0.4-0.6 µm) cannot pass the 0.1 µm pore-size filters, it is more likely that lysed *Ca.* Altiarchaeum cells ended up in the <0.1 µm fraction in 2018 allowing binning of their genomes including the CRISPR system with low complexity of spacers from this fraction. The MSI_>0.1µm_2018 fraction and the MSI_<0.1µm_2018 contained about half the number of total spacers of the MSI_BF_2018 sample, although the number of different spacers displayed less variability. Spacers from these samples hitting the

viral targets were often reduced in abundance compared to BF-derived CRISPR spacers (Figure 4). MSI_BF_2018 had the most unique total spacer clusters (2599, Supplementary Figure 15 A) and also the most unique ones matching Altivir_1_MSI (Supplementary Figure 15 B) and Altivir_2_MSI as displayed as Venn diagrams in Supplementary Figure 15 C. The overlap of spacer clusters between years and samples was rather moderate (≤52 spacer clusters in common).

Congruent with the decline in relative abundance of Altivir_1_MSI based on metagenomic analysis, we also observed heterogeneous infections of BF flocks via imaging. Some BF showed no infection with Altivir_1_MSI at all (Figure 5A, Supplementary Figure 16), which aligns well with the decrease of the virus in the metagenomic data of the BF from 2012 to 2018. By contrast, we observed very few BF flocks that showed an extremely high infection and accumulation of rod-shaped microorganisms (Figure 5B, Supplementary Figure 17&18). The observed heterogeneity of infections in BF supports the aforementioned heterogeneity related to CRISPR resistances against Altivir_1_MSI with high spacer diversity dominated by singletons.

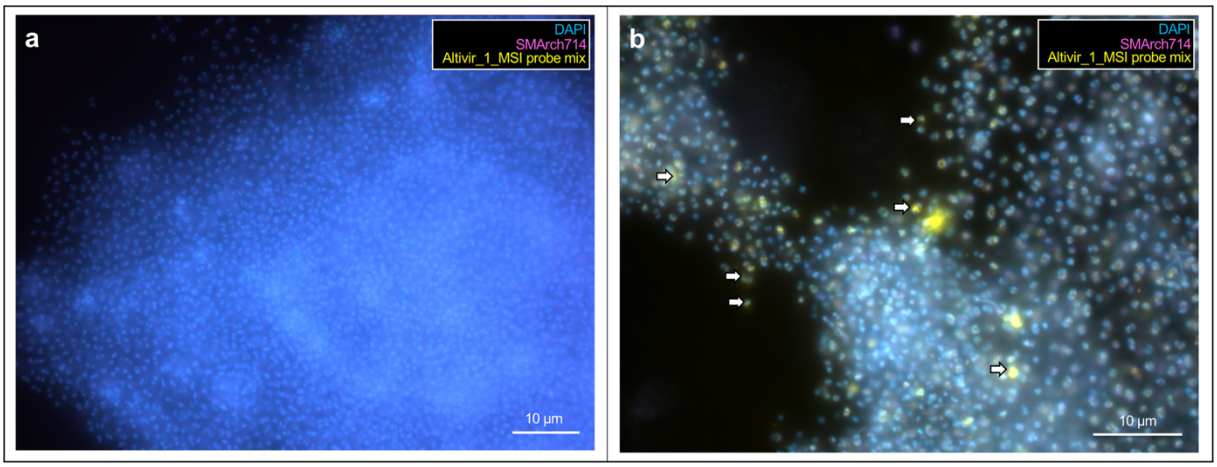

Figure 5: VirusFISH of two individual Altiarchaeota biofilm (BF) flocks depicting a) a dense BF flock without infections and b) one highly infected BF flock. For all virusFISH experiments, an Altivir_1_MSI probe was used for detecting viral infections. White arrows indicate exemplary virus–Altiarchaeota interactions (advanced infections). BF material was analyzed with filter sets for DAPI (blue, cells), ATTO 488 (purple, 16S rRNA signal), and Alexa 594 (yellow, viral genomes), and then the different fluorescent channels were merged for analysis and display purposes. For unmerged imaging data, see Supplementary Figs. 16 and 17. Scale bars: 10 µm.

3. Discussion

Although life in the deep subsurface contributes significantly to overall biomass and microbial biodiversity on our planet, its low accessibility leaves host-virus interactions—especially those of uncultivated hosts—highly enigmatic. Detection of novel and uncultivated viruses missing conserved sets of hallmark genes has been an ongoing challenge in viromics (Roux et al. 2019). Using a combination of bioinformatics and virusFISH, we were able to visualize infections of Altiarchaeota with a hitherto unknown, presumably lytic virus from a

subsurface ecosystem. We expanded the diversity of this virus detected in Germany (MSI) by identifying a distantly related viral genome infecting *Ca.* Altiarchaea in North America (ACLF site). This suggests genomic relatedness of archaeal viruses over long distances, a phenomenon known for bacteriophages (Breitbart and Rohwer 2005; Short and Suttle 2005). However, genomic relatedness and global distribution of bacteriophage genomes (and maybe also altiarchaeotal viruses) is in stark contrast to viruses infecting *Sulfolobus islandicus.* Viruses of this thermoacidophilic archaeon displayed a confined geographic distribution based on core gene sequence analysis and CRISPR-based host-virus interactions (Bautista et al. 2017; Held and Whitaker 2009), which demonstrated infections with local viruses for this host, and the geographical structuring of archaeal viral communities was recently extended by investigations of Italian hydrothermal environments (Baquero et al. 2020).

Altiarchaeota viruses do not represent an exception regarding the many genes that could not be annotated, and thus were classified as unknown ORFs or domains/genes of unknown function. Some proteins such as modification methylases or the phosphoadenosine phosphosulfate reductase were previously also detected on a *Methanosarcina* and other archaeal virus genomes (Molnár et al. 2020; Prangishvili et al. 2006b). Altiarchaeota can apparently employ two different CRISPR systems (Type I and III) with high similarity of their DR sequences across larger geographic distances; although the reasoning behind two independent CRISPR systems remains unclear, an additional Type III system might mediate resistance against plasmids carrying matching protospacers but lacking a protospacer-adjacent motif (Deng et al. 2013), or against viruses that overcome Type I systems as previously described for *Marinomonas mediterranea* (Silas et al. 2017) and *Sulfolobus islandicus* (Guo et al. 2019). Indeed, archaeal viruses found ways to interfere with CRISPR Type III systems by using anti-CRISPR proteins (Athukoralage et al. 2020; Bhoobalan-Chitty et al. 2019). However, we could not detect homologs of these proteins in viruses targeting *Ca.* Altiarchaeum.

Based on the metagenomic data collected in 2012 and 2018, it appears that the host prevailed in the arms race between Altiarchaeaota and the visualized virus (Altivir_1_MSI), whereas the arms race seems to be ongoing as at least parts of the host population still get infected. The number of different spacers matching this virus increased towards 2018 with a prominence of spacer singletons in the metagenome (Supplementary Figure 13), while the actual abundance of spacers matching Altivir_1_MSI decreased as did the abundance of the viral genome itself. CRISPR spacer diversification might be a successful response to an increasing number of variants in the genome of Altivir_1_MSI (Supplementary Figure 10) suggesting its mutations. As a trade-off, spacer diversification might allow the host to decrease the total abundance of spacers. We conclude that CRISPR spacers were diversifying to mediate a greater bandwidth of resistances against the virus, which worked in favor for the overall population of Altiarchaeota in this ecosystem. Moreover, the diversity of singleton spacers indicates a very heterogeneous Altiarchaeota population, which might be related to heterogeneous infections of the BF as visualized via virusFISH.

Our dual approach of coupling metagenomics to fluorescence microscopy enabled us to follow precisely the terrestrial subsurface predator-prey relationship of *Ca.* Altiarchaeum and one of its viruses. Our data suggests that the novel identified virus is lytic and challenge the

current paradigm that lysogeny prevails in the subsurface (Anderson et al. 2013, 2011). Instead, our data indicate that the kill-the-winner theorem–lytic viruses targeting abundant ecosystem key players (Thingstad and Lignell 1997)—also strongly applies to subsurface ecosystems. We currently do not know if this statement can be transferred to other subsurface ecosystems that have low cell counts (Magnabosco et al. 2018) as viruses might struggle with finding a new host. However, replication measures of bacteria in the ecosystem with the visualized virus suggest that microbial proliferation is similar to other oligotrophic systems (Bornemann et al. 2020a). Lytic infections in subsurface microbial hosts might thus launch heterotrophic carbon cycling similar to the viral shunt in the marine environment (Wilhelm and Suttle 1999). In fact, recent lipidomic analyses coupled to mass-balance calculations provide evidence that subsurface environments dominated by Altiarchaeota are completely fueled by these organisms' carbon fixation, transferring organic carbon to heterotrophs in the community (Probst et al. 2020). This process might be the basis for microbial loops (Dong et al. 2018) as we see the accumulation of rod-shaped microbes around Altiarchaeota when they are lysing due to viral attacks (Supplementary Figure 18).

Here, we provide underpinning evidence derived from metagenomic datasets of three continents for the frequent viral infection of a globally abundant, autotrophic key player of the subsurface carbon cycle. Using virusFISH for visualization, we show that one virus with a lytic lifestyle is even capable of infecting host cells in a dense BF, which is generally known to provide some protection from viral infection (Vidakovic et al. 2018). Subsurface ecosystems such as aquifers remain understudied regarding host-virus dynamics because of limited access, low microbial biomass and limited cultivation success. Our results presented here provide an experimental proof of concept for an ongoing host-virus arms race in the continental subsurface characterized by constant viral infections and cell lysis of subsurface microbes, followed by their own and their viruses' diversification.

4. Methods

Mining public metagenomes for Altiarchaeota

To get an overview of the global distribution of Altiarchaeota, we searched metagenomes in the IMG/M database (Chen et al. 2019a) (database accessed in July 2018) for Altiarchaeota contigs using DIAMOND BLASTp (v0.9.22) (Buchfink et al. 2015) with the putative *hamus* subunit (NCBI accession no CEG12198.1) as a query and an e-value and length cut-off of 1e-10 and 300 amino acids, respectively. The Altiarchaeota distribution based on 16S rRNA gene sequences was obtained from the SILVA SSU Parc database (Quast et al. 2013) based on all 16S rRNA genes classified as Altiarchaeota and for which geographic information was available (July 2018).

To investigate Altiarchaeota-virus relationships, we explored ecosystems where Altiarchaeota comprised the majority of the community. Therefore, metagenomic data from a microbial mat growing in the sulfidic groundwater-fed Alpena County Library Fountain (ACLF) (Alpena, MI, USA) were obtained from NCBI Sequence Read Archive (SRA)

repository (Sharrar et al. 2017) as were metagenome samples from Horonobe Underground Research Laboratory at 140 and 250 m depth (HURL, Hokkaido, Japan) (Hernsdorf et al. 2017). The analysis was complemented with three metagenomic datasets from CO_2-enriched groundwater erupted from a cold-water Geyser (Andernach, Middle Rhine Valley, Germany) (Bornemann et al. 2020a), and the metagenome of a sulfidic spring Mühlbacher Schwefelquelle Isling (MSI) in Regensburg, Germany (Probst et al. 2014b). All BioProject, BioSample accessions and information on sampling of MSI for various experiments are provided in Supplementary Table 1, 3, 4, respectively.

Re-sampling of MSI for virusFISH and metagenomic sequencing

BF samples were collected as previously described (Probst et al. 2013) from the 36.5 m deep, cold (~10 °C), sulfidic spring MSI in Regensburg, Germany (N 48° 59.142, E 012° 07.636) in January 2019, for which further geological description has been reported elsewhere (Probst et al. 2014a). Environmental parameters of the sulfidic spring were extensively investigated previously (Rudolph et al. 2004) and remained almost constant over years. In brief, hydrogen sulfide concentration in the spring hole was reported to be 0.85 mg L^{-1} (Probst et al. 2014a), dissolved carbon dioxide at 32 mg L^{-1} (Rudolph et al. 2004), and oxygen at 0.13 mg L^{-1} and later revised to be beyond detection limit of extremely sensitive probes (Probst et al. 2013; Rudolph et al. 2004). Chemical parameters of the spring water are presented in Supplementary Table 5.

For virusFISH, BF samples were fixed by addition of formaldehyde (3% v/v) and incubation at room temperature for one hour. For investigating infection stages, BF flocks were gently separated from several bigger flocks by using a pipette tip finally yielding 18 smaller flocks (range 170 – 5 870 µm^2). BF flocks for all microscopy experiments were subsequently washed three times in 1x phosphate buffered saline (PBS, pH 7.4) followed by dehydration via an ethanol gradient (50%, 70% v/v, and absolute ethanol, 10 min each). Samples were stored in absolute ethanol at -20 °C until further processing.

Three types of samples were collected for metagenomics: i) BF flocks; ii) the planktonic community (>0.1 µm pore-size fraction); and iii) the viruses and lysed cells (<0.1 µm pore-size fraction). Sampling of Altiarchaeota BF flocks for DNA extraction and metagenomic sequencing from the sulfidic spring (MSI) was performed in October 2018. For sampling the unfiltered planktonic microbial community, 70 L of groundwater were filtered onto a 0.1 µm pore-size PTFE membrane filter (Merck Millipore, Darmstadt, Germany). The flow-through was collected in a sterilized container, and a final concentration of 1 mg L^{-1} of iron (III) chloride (Carl Roth, Karlsruhe, Germany) was applied for chemical flocculation for 30 minutes (John et al. 2011). Flocculates were filtered onto 5 x 0.2 µm membrane filters (<0.1 µm fraction). DNA was extracted directly from collected BF samples using the RNeasy® PowerBiofilm Kit (Qiagen, Hilden, Germany) using a DNA-conform workflow. DNA from the 0.1 µm and pooled 0.2 µm membrane filters with iron flocculates was extracted using PowerMax Soil DNA Extraction Kit (Qiagen, Hilden, Germany), DNA was precipitated overnight and cleaned with 70% ethanol. Shotgun metagenome sequencing was

conducted within the Census of Deep Life Sequencing call 2018 and performed using the Illumina HiSeq platform at the Marine Biological Laboratory, Woods Hole, MA, USA.

Detection of viral genomes in metagenomes

Raw shotgun sequencing reads were trimmed and quality-filtered using bbduk (https://github.com/BioInfoTools/BBMap/blob/master/sh/bbduk.sh) and Sickle v.1.33 (Joshi and Fass 2011). Read assembly was conducted by using metaSPADes v.3.10 (Nurk et al. 2017) unless stated otherwise. Scaffolds <1 kb length were excluded from further analysis. Genes were predicted using prodigal v.2.6.3 (Hyatt et al. 2010) (meta mode) and functional annotations were determined by using DIAMOND v.0.9.9 (Buchfink et al. 2015) against UniRef100 (Feb. 2018) (Suzek et al. 2007). Public Altiarchaeota genomes were retrieved from databases (Bornemann et al. 2020a) and further cleaned or re-binned using%GC content, coverage distribution and taxonomy information (Bornemann et al. 2020b), which was necessary for all genomes except for Altiarchaeota from MSI_BF_2012 (Supplementary Table 1). Viral scaffolds >3 kb were identified by applying a combination of tools as presented in Supplementary Figure 1A. Predicted viruses were classified into viruses and putative viruses according to the classification system presented in Supplementary Figure 1B. Viral scaffolds were subsequently checked for mini-CRISPR arrays using default settings of CRISPRCasFinder (Couvin et al. 2018) as some archaeal viruses can bear mini-CRISPR arrays with 1-2 spacers having likely a role in interviral conflicts (Medvedeva et al. 2019; Iranzo et al. 2020).

CRISPR-Cas analysis of Altiarchaeota genomes

Cas genes and direct repeat (DR) sequences were identified in binned Altiarchaeota genomes via CRISPRCasFinder (Couvin et al. 2018) and genes were additionally confirmed via searches against UniRef100 (Suzek et al. 2007). CRISPR DR sequences were tested for formation of secondary structures using RNAfold (Denman 1993) and checked against the CRISPRmap database (v2.1.3-2014) (Lange et al. 2013) for formation of known motifs. The consensus DR sequence was used in both possible orientations to extract host-specific spacers from raw reads by using MetaCRAST (Moller and Liang 2017) with Cd-hit v.4.6 (Li and Godzik 2006) clustering at 99% identity. Spacers were filtered for minimum and maximum lengths of 20 and 60 nucleotides, respectively. Only spacers that were present on a read that contained at least one complete DR sequence with an exact match to the template were considered. Finally, spacers were further clustered with Cd-hit (Li and Godzik 2006) at 99% identity and matched to viral protospacers on the compiled output of viral identification tools using the BLASTn --short algorithm with a 80% similarity threshold. For comparing spacer dynamics (total abundance, diversity and matches to Altivir_1_MSI and Altivir_2_MSI genomes) of 2012 and 2018 samples from MSI, all spacers of the four respective MSI samples were clustered with Cd-hit (Li and Godzik 2006) at 99% identity and representative sequences of each cluster were matched to representative Altivir_1_MSI and Altivir_2_MSI

genomes from the BF of 2012 (Supplementary Table 2). All data arising from spacer counts were normalized by genome abundance of the respective Altiarchaeota genome.

Functional annotation of proteins and clustering of viral genomes

Coding sequences of predicted viral scaffolds were identified using prodigal (meta mode) (Hyatt et al. 2010). Furthermore, the proteins predicted by prodigal were grouped into clusters based on BLASTp similarity (Bischoff et al. 2019) and then functionally annotated by searching in several sequence databases and then manually curating and consolidating the results. The databases searched were the following: i) the NR database (Virus only section, https://blast.ncbi.nlm.nih.gov/) from NCBI was searched using BLASTp and DELTA-BLAST (if no BLASTp results were found, (Boratyn et al. 2012)); ii) the prokaryotic Viruses Orthologous Groups (pVOGs (Grazziotin et al. 2017)) was searched using HHblits v.3.3.0 (results kept only if the probability was >= 70%) (Remmert et al. 2011); iii) the VOGDB (Marz et al. 2014) (vog93, April 2019) was searched using HMMER with an e-value cut-off of 10^{-5}; iv) the InterPro database 82.0 (Finn et al. 2017) was searched using InterProScan integrated in Geneious prime 2020 (Kearse et al. 2012); v) UniRef100 (Feb. 2018) (Suzek et al. 2007) was searched using DIAMOND (Buchfink et al. 2015) with an e-value of 10^{-5}, and vi) PDB_mmCIFC70_4_Feb, Pfam-A v.32.0, NCBI_Conserved_Domains_v3.16 and TIGRFAMs v15.0 database were searched using HHpred (Söding et al. 2005; Zimmermann et al. 2018) with an e-value cut-off of 10^{-6}. For the two most abundant predicted *Ca.* Altiarchaeum viruses Altivir_1_MSI and Altivir_8_HURL we additionally applied DELTA-BLAST (Boratyn et al. 2012) searches against NCBI's non-redundant protein sequences (nr) and phmmer (Potter et al. 2018) against reference proteomes.

Predicted viral scaffolds carrying multiple hits against existing bacterial genomes in UniRef100 (Suzek et al. 2007) and no viral hallmark genes or carrying extensive CRISPR arrays (detected as false positives) were removed from further analyses.
Clustering of entire viral genomes on nucleic-acid level was performed with VICTOR (Meier-Kolthoff and Göker 2017) (https://ggdc.dsmz.de/victor.php) using the Genome-BLAST Distance Phylogeny method (Meier-Kolthoff et al. 2013) with distance formula d0 and OPTSIL clustering (Göker et al. 2009). A separate virus clustering was performed using vConTACT v.0.9.11 (Bin Jang et al. 2019; Bolduc et al. 2017) applying the database 'ProkaryoticViralRefSeq94' (Brister et al. 2015) and visualization of the viral network was performed in Cytoscape version 3.7.2 (Shannon et al. 2003). Intergenomic similarities between viral genomes and the corresponding heatmap were calculated using VIRIDIC accessible through http://viridic.icbm.de with default settings (Moraru et al. 2020). In order to further investigate the genetic relationship between the *Ca.* Altiarchaeum viruses Altivir_1 - Altivir_8, proteins of all viral genomes were clustered by first performing an all against all BLASTp with an e-value cut-off of 10^{-5} and a bitscore threshold of 50. Then, the results were loaded into the mcl program with the parameters -l --abc. The genomic maps were plotted using the genoPlotR v.0.8.9 (Guy et al. 2010) package of the R programming environment v.3.5.2 (R Core Team, 2019).

Single gene phylogenetic trees

Phylogenetic trees were constructed for viral hallmark proteins identified in different *Ca.* Altiarchaeum viruses: i) DNA polymerase B from Altivir_2_MSI; ii) capsid portal protein from Altivir_4_ACLF; iii) major tail tube protein from Altivir_7_ACLF and iv) terminase protein from Altivir_8_HURL. For each phylogenetic tree, the following workflow was performed. The respective viral hallmark protein was used as BLASTp query to search for related proteins in the viral section of the NR BLAST database from NCBI (https://blast.ncbi.nlm.nih.gov/). If no results were found with BLASTp (capsid protein from Altivir_4_ACLF, major tail tube protein from Altivir_7_ACLF), then DELTA-BLAST was used to search for distantly related proteins. Only hits with an e-value smaller than 0.0005 were kept. The selected proteins, including the query, were aligned using the Constraint-based Multiple Alignment Tool (COBALT, Papadopoulos and Agarwala 2007), using the online tool (https://www.ncbi.nlm.nih.gov/tools/cobalt/re_cobalt.cgi). The COBALT alignment was imported in Geneious prime 2020 (Papadopoulos and Agarwala 2007) for refinement using MUSCLE v.3.8.425 (Edgar 2004) and end trimmed. The tree for the Altivir_2_MSI was constructed using FastTree v.2.1.12 (Price et al. 2010) with the "Whelan and Goldman 20012" and "Optimize the Gamma20 likelihood" parameters. The trees for Altivir_4_ACLF, Altivir_7_ACLF and Altivir_8_HURL were calculated using the webserver phylogeny.fr. Here, the alignment was first curated with Gblocks (Castresana 2000) (option "Do not allow many contiguous non-conserved positions"). The tree was reconstructed using PhyML (Guindon et al. 2010) with the substitution model "WAG for protein" and the approximate likelihood-ratio test "SH-like" for calculating the branch support statistics. All trees were exported as ".newick" format, visualized with FigTree v.1.4.3 (Rambaut 2006), rooted at the midpoint, and further annotated in Inkscape v.1.0.2 (https://inkscape.org).

Relative abundance of viruses and hosts

Abundance of hosts and viruses was determined via read mapping respective genomes using Bowtie2 (Langmead and Salzberg 2012) in sensitive mode followed by mismatch filtering for host genomes (2%, depending on read length). Abundances were normalized to the total number of base pairs (bp) sequenced of each sample scaling to the sample with lowest counts, which is herein referred to as relative abundance or normalized coverage. Rank abundance curves were built based on the abundance of scaffolds carrying ribosomal protein S3 (*rpS3*) gene sequences predicted in metagenomic assemblies after running prodigal (meta mode) (Hyatt et al. 2010) and annotation (Buchfink et al. 2015) against UniRef100 (Suzek et al. 2007). For normalized rank abundance curves based on sequencing depth for the ecosystem MSI, we only considered *rpS3* gene sequences with a coverage >2.4 after normalization as this value represents the lowest coverage of any assembled *rpS3* gene sequence in the MSI dataset.

Design, synthesis and chemical labeling of gene probes

To target Altivir_1_MSI, a 8.9 kb putative viral genome recovered from the MSI_BF_2012 metagenomic dataset, eleven dsDNA polynucleotide probes of 300 nucleotides length were designed using genePROBER (gene-prober.icbm.de). In addition, a single 300 bp fragment of a *Metallosphaera* turreted icosahedral virus strain MTIV1 (NCBI accession no. MF443783.1) was designed as a negative control probe, because the *Metallosphaera* sp. virus was not detected in the metagenome of MSI_BF_2012. Sequences for all probes are given in Supplementary Table 6 and 7.

All probes were chemically synthesized by IDT (Integrated DNA Technologies, San Jose, CA, USA) as gBlocks® Gene Fragments (500 ng per polynucleotide), reconstituted in 5 mM Tris-HCl pH 8.0, 1 mM EDTA pH 8.0 and then labeled with the ULYSIS™ Alexa Fluor™ 594 nucleic acid labeling kit (Thermo Fisher Scientific, MA, USA) (Barrero-Canosa and Moraru 2021). Two µg of either an equimolar mixture of the eleven Altivir_1_MSI polynucleotides or of the single negative control polynucleotide were used in a single labeling reaction and then purified using NucAway Spin Columns (Thermo Fisher Scientific, USA). Before being used as probes for virus-targeted genome fluorescence *in situ* hybridization (virusFISH), the labeled probes were measured spectrophotometrically using a NanoDrop™ (Thermo Fisher Scientific, USA). The calculated labeling efficiency was 9.16 and 16.6 dyes per base for Altivir_1_MSI probe and negative control probe, respectively.

VirusFISH of MSI biofilms

VirusFISH was performed according to the direct-geneFISH protocol (Barrero-Canosa et al. 2017), with the modifications detailed further. In brief, Altiarchaeota BF, dehydrated in an ethanol series, were carefully placed in the middle of a press-to-seal silicone isolator (Sigma-Aldrich Chemie GmbH, Taufkirchen, Germany) mounted on Superfrost® Plus slides (Electron Microscopy Sciences, Hatfield, USA), and subsequently air-dried. Because Altiarchaeota lack the typical archaeal S-layer as outer sheath (Perras et al. 2015) and hence are more prone to membrane disintegration, no extra permeabilization step was required. Different formamide concentrations (20%, 30%, 50%) were tested to exclude false positive hybridization signals. In the final assay, 20% of formamide was used in the hybridization buffer that contained 5x SSC buffer (saline sodium citrate, pH 7.0), 20% (w/v) dextran sulfate, 20 mM EDTA, 0.25 mg mL^{-1} sheared salmon sperm DNA, 0.25 mg mL^{-1} yeast RNA, 1x blocking reagent, 0.1% (v/v) sodium dodecyl sulfate and nuclease-free water. The final NaCl concentration of 0.225M in the washing buffer corresponded to the 20% formamide in the hybridization buffer. As rRNA probes, the dual-Atto488-labeled probes NON338 (5'-ACTCCTACGGGAGGCAGC-3') (Wallner et al. 1993) and a SM1-Euryarchaeon-specific probe SMARCH714 (5'-GCCTTCGCCCAGATGGTC-3') (Moissl et al. 2003) were used. A volume of 45 µl hybridization mixture was used, with a final gene probe concentration of 330 pg μL^{-1} (30 pg μL^{-1} for each polynucleotide) and rRNA probe final concentration of 1 pmol μL^{-1}. In the hybridization chamber, 30 ml of formamide-water solution were added to keep a humid atmosphere. The denaturation and hybridization times were 30 min and 3 hours,

respectively. The post hybridization washing buffer contained 20 mM Tris-HCl (pH 8.0), 5 mM EDTA (pH 8.0), nuclease-free water, 0.01% SDS, and 0.225 M NaCl. A second washing step with 1x PBS (pH 7.4) for 20 min was performed. Then, the slides were transferred for one minute into molecular grade water and quickly rinsed in absolute ethanol. For staining, we used 15 µL of a mixture of 4',6-diamidin-2-phenylindole (4 µg mL^{-1}) in SlowFade Gold Antifade Mounting medium (both Thermo Fisher Scientific, Waltham, MA, USA). All solutions and buffers for virusFISH experiments were prepared with molecular grade water (Carl Roth, Karlsruhe, Germany). For the experiment with individual flocks, 17 out of 18 flocks were treated with the Altivir_1_MSI probe and one flock with the negative control probe.

The BF material was examined and imaged with an Axio Imager M2m epifluorescence microscope equipped with an Axio Cam MRm and a Zen 2 Pro software (version 2.0.0.0) (Carl Zeiss Microscopy GmbH, Jena, Germany). Channel mode visualization was performed by using the 110x/1.3 oil objective EC-Plan NEOFLUAR (Carl Zeiss Microscopy GmbH) and three different filter sets from Carl Zeiss: 49 DAPI for visualizing Altiarchaeota cells, 64 HE mPlum for the detection of viral infections, and 09 for achieving 16S rRNA signals. Enumeration of cells and viral signals was performed manually. Viral signals were categorized into three major groups, *i.e.*, viral adsorption on host cells, advanced infections and viral bursts.

Structured illumination microscopy

For structured illumination microscopy, the whole virusFISH protocol was carried out on a BF flock mounted on a cover slip (thickness No. 1.5H, Paul Marienfeld GmbH & Co. KG, Lauda-Königshofen, Germany). Staining was conducted without adding DAPI to the mounting medium. Samples were analyzed using an inverted epifluorescence microscope (Zeiss ELYRA PS.1) equipped with an α-Plan-Apochromat 100x/1.46 oil DIC M27 Elyra objective, F Set 77 He filter, and a Zen 2.3 SP1 FP3 black edition software (version 14.0.22.201), all obtained from the manufacturer Carl Zeiss Microscopy GmbH, Germany.

Transmission electron microscopy

BF flocks from MSI were pre-fixed in glutaraldehyde (Carl Roth, Karlsruhe, Germany) to a final concentration of 2.5% (v/v) and physically fixed via high-pressure freezing followed by freeze substitution, which was carried out with 0.2% (w/v) osmium tetroxide, 0.25% (w/v) uranyl acetate and 9.3% (v/v) water in acetone (Flechsler et al. 2020). After embedding in Epon resin and polymerization for 72 h, the samples were ultrathin sectioned and post-stained with 1% lead citrate for two minutes. Transmission electron microscopy was carried out on a Zeiss EM 912 (Zeiss, Oberkochen, Germany) with an integrated OMEGA-filter at 80 kV in the zero-loss mode. Imaging was done using a 2k x 2k pixel slow-scan CCD camera (TRS Tröndle Restlichtverstärkersysteme, Moorenweis, Germany) and an ImageSP software (version 1.2.9.77) (x64) (SysProg, Minsk, Belarus).

Data availability

Sequencing data generated and analyzed during this study are available at NCBI's sequence read archive and GenBank with accession codes as listed in Supplementary Table 1. Metagenomic reads are available from NCBI Bioprojects #PRJNA628506, Biosamples #SAMN14733005-07, Run #SRR11614986-88 (MSI_2018), Bioproject #PRJNA321556, Biosample #SAMN04999996-97, Run #SRR3546456-57 (HURL), Bioproject #PRJNA627655 (GA), Biosample #SAMN14680028-30, Run #SRR11600161-63 (GA), Bioproject #PRJNA340050, Biosample #SAMN05661201, Run #SRR4293692 (ACLF) as well as from ENA #PRJNA678866, Biosample #SAMEA2779769, Run accession #ERR628383 (MSI_2012). Metagenomic assemblies can be found under the above-mentioned Bioprojects/samples for MSI_2018 and GA. Exceptions represented MSI_2012, which was deposited under Bioproject #PRJNA678866, Biosample #SAMN16815598, HURL assemblies under Bioproject #PRJNA730881, Biosample #SAMN04999996-7, and the ACLF assembly under Bioproject #PRJNA730879, Biosample #SAMN05661201. Run accessions for these assemblies are JAEMOC000000000-JAEMOL000000000. *Ca.* Altiarchaeota genomes were deposited at GenBank under Bioproject #PRJNA628506, MAG Biosample #SAMN18220766, Run #JAGTWS000000000 (MSI_2018), Bioproject #PRJNA627655, MAG Biosamples #SAMN18220852-54, Run #JAGTWP000000000-JAGTWR000000000 (GA), Bioproject #PRJNA726854, MAG Biosample #SAMN18221259, Run #JAGWDR000000000 (ACLF), Bioproject #PRJNA726852, MAG Biosample #SAMN18220774-75, Run #JAGWDQ000000000 & #JAGWDP000000000 (HURL), and at ENA under #CCXY01000000 (MSI_2012). Viral genomes of *Ca.* Altiarchaeum virus Altivir_1 and 2 can be found under GenBank accessions #MW522970 and #MW522971, respectively. *Ca.* Altiarchaeum virus Altivir_3-8 genomes are available in the Third-Party Annotation Section of the DDBJ/ENA/GenBank databases under the accession numbers #BK059157-162.
Viral genomes of *Ca.* Altiarchaeum virus Altivir_3-8 can also be accessed via the scaffold accession numbers as given in Supplementary Table 4. Viral genomes can also be found at https://github.com/ProbstLab/viromics/tree/master/viruses/Altivir. Microscopy data can be obtained from the corresponding author upon reasonable request.

Code availability

Our tool EndMatcher for identification of circular sequences from metagenomes is available under https://github.com/ProbstLab/viromics/tree/master/Endmatcher.

Acknowledgements

This work received funding by the Alfred P. Sloan foundation (grant number G-2017-9955), the Ministry of Culture and Science of North Rhine-Westphalia (Nachwuchsgruppe "Dr. Alexander Probst"), and the NOVAC project of the German Science Foundation (grant number DFG PR1603/2-1). We acknowledge sampling logistics provided by the University of Regensburg, *i.e.*, by Harald Huber and Sebastien Ferreira-Cerca, and sequencing of MSI

metagenomes within the Census of Deep Life Sequencing call 2018, phase 14 project ”Development of novel archaeal viruses and the corresponding CRISPR arrays of a highly abundant carbon fixer in Earth’s crust”. We highly appreciate the technical assistance of Jannis Becker for protein annotations of viral scaffolds, Lea Griesdorn for assistance with data submission, Sabrina Eisfeld for laboratory maintenance, and Ken Dreger for server administration and maintenance. The work conducted by the U.S. Department of Energy Joint Genome Institute, a DOE Office of Science User Facility, is supported under Contract No. DE-AC02-05CH11231. Furthermore, we are also grateful to the Imaging Center Essen (IMCES) under the direction of Matthias Gunzer for access to an inverted epifluorescence microscope with structured illumination and for the respective training carried out by Alexandra Brenzel.

Author contributions

J. R., V. T., P. A. F. G., I. M., A. J. P. performed the sampling; J. R., S. P. E., T. L. V. B., A. J. P., F. S., T. W., A. J. P. carried out metagenomic analysis; J. R., V. T., I. M., A. K., C. M., A. J. P. performed virusFISH or related analysis; V. T., I. M., A. K. performed SIM and TEM microscopy; J. R. , V. T. , A. J. P. wrote the manuscript; all authors contributed to editing and proofreading of the manuscript; A. J. P. conceptualized the study.

Competing interests

The authors declare no competing interests.

Supplementary material

The supplementary material is available under https://www.nature.com/articles/s41467-021-24803-4#Sec21 as well as on the supplied CD (see section VII).

III. Virus-Host Dynamics in Archaeal Groundwater Biofilms and the Associated Bacterial Community Composition

Victoria Turzynski[1,2], Lea Griesdorn[1,2], Cristina Moraru[3], André R. Soares[1,2], Sophie A. Simon[1,2], Tom L. Stach[1,2], Janina Rahlff[1,†], Sarah P. Esser[1,2], and Alexander J. Probst[1,2,4,5#]

[1]Environmental Microbiology and Biotechnology (EMB), Department of Chemistry, Group for Aquatic Microbial Ecology, University of Duisburg-Essen, Universitätsstraße 5, 45141 Essen, Germany
[2]Environmental Metagenomics, Research Center One Health Ruhr of the University Alliance Ruhr, Faculty of Chemistry, University of Duisburg-Essen, Universitätsstraße 5, 45141 Essen, Germany
[3]Institute for Chemistry and Biology of the Marine Environment (ICBM), Carl-von-Ossietzky-University Oldenburg, PO Box 2503, Carl-von-Ossietzky-Straße 9-11, 26111, Oldenburg, Germany
[4]Centre of Water and Environmental Research (ZWU), University of Duisburg-Essen, Universitätsstraße 5, 45141 Essen, Germany
[5]Center for Medical Biotechnology (ZMB), University of Duisburg-Essen, Universitätsstraße 5, 45141 Essen, Germany

[†]Present address: Centre for Ecology and Evolution in Microbial Model Systems (EEMiS), Department of Biology and Environmental Science, Linnaeus University, SE-39182, Kalmar, Sweden

[#]Corresponding author: alexander.probst@uni-due.de, telephone: +49 201 183-7080

Publication information:
Viruses 2023, 15(4), 910; https://doi.org/10.3390/v15040910
Received: 03 February 2023 / Revised: 28 March 2023 / Accepted: 29 March 2023 / Published: 31 March 2023
Link: https://www.mdpi.com/1999-4915/15/4/910

Abstract

Spatial and temporal distribution of lytic viruses in deep groundwater remains unexplored so far. Here, we tackle this gap of knowledge by studying viral infections of Altivir_1_MSI in biofilms dominated by the uncultivated host Candidatus Altiarchaeum hamiconexum sampled from deep anoxic groundwater over a period of four years. Using virus-targeted direct-geneFISH (virusFISH) whose detection efficiency for individual viral particles was 15%, we show a significant and steady increase of virus infections from 2019 to 2022. Based on fluorescence micrographs of individual biofilm flocks, we determined different stages of viral infections in biofilms for single sampling events, demonstrating the progression of infection of biofilms in deep groundwater. Biofilms associated with many host cells undergoing lysis showed a substantial accumulation of filamentous microbes around

infected cells probably feeding off host cell debris. Using 16S rRNA gene sequencing across ten individual biofilm flocks from one sampling event, we determined that the associated bacterial community remains relatively constant and was dominated by sulfate-reducing members affiliated with Desulfobacterota. Given the stability of the virus-host interaction in these deep groundwater samples, we postulate that the uncultivated virus-host system described herein represents a suitable model system for studying deep biosphere virus-host interactions in future research endeavors.

Keywords: Deep biosphere, subsurface viruses, Altiarchaeota, fluorescence *in situ* hybridization, virusFISH, direct-geneFISH, microbial heterogeneity

1. Introduction

Microbes drive the biochemical cycling of nutrients and control food-web trophic interactions on Earth. The smallest biological entities, *i.e.*, viruses, manipulate microorganism-driven biogeochemical processes by impacting host metabolism, host evolution, and microbial community composition (Suttle 2007). By killing their hosts, viruses cause a transformation of microbial biomass into particulate organic matter (POM) and dissolved-organic matter (DOM) (Proctor and Fuhrman 1992). This "viral shunt" can mediate a shuttle of organic carbon from autotrophic to heterotrophic microbial communities for stimulating their growth (Suttle 2007) and generating a so-called "microbial loop" (Fuhrman 1999). However, not all viral lifestyles are involved in host lysis but can have different effects on the host ecology (Howard-Varona et al. 2017). While lytic viral infections are characterized by rapid production of new virions followed by lysis of the host cells, lysogenic viruses integrate their genome into the host chromosome and proliferate via cell division of the host. Thus, lysogeny has been suggested as a survival strategy of viruses living at low host density and/or at low nutrient content (Anderson et al. 2011; Fuhrman 1999; Howard-Varona et al. 2017). Lysogeny is found to be common in, *e.g.*, seawater, extreme environments, sediments, or hydrothermal vents (Anderson et al. 2011; Fuhrman 1999). As such, it has been proposed that lysogeny is the prevalent lifestyle of viruses in the deep (continental) biosphere (Anderson et al. 2011), because viruses are challenged with finding a host in the deep subsurface, where microbial biomass is generally low (Magnabosco et al. 2018). Based on metagenomic and virusFISH recent investigations as in Holmfeldt et al. (2021) and Rahlff et al. (2021) (Holmfeldt et al. 2021; Rahlff et al. 2021) demonstrated that lytic viruses can be abundant in the deep biosphere and even target main primary producers following the "kill-the-winner" model (Thingstad and Lignell 1997). For example, a drastic increase of virus-host ratios with depth was determined for marine sediment (Engelhardt et al. 2014) and deep granitic groundwater (Kyle et al. 2008). In the aforementioned study, viral abundance was correlated with bacterial abundance in a ratio of 10:1 in samples collected from 69 to 450 m depth (10^5-10^7 virus-like particles mL^{-1} and 10^4-10^6 total number of prokaryotic cells mL^{-1}, (Kyle et al. 2008)).

Viruses of Archaea—as they have been reported in deep granitic groundwater (Kyle et al. 2008)—are some of the least understood groups of viruses with unique morphologies

compared to eukaryotic viruses or bacteriophages (Attar 2016; Prangishvili et al. 2017) (also reviewed in Wirth and Young 2020). Knowledge on Altiarchaeota and their viruses has mainly been gained from the uncultivated genus *Candidatus* Altiarchaeum with the best studied representative *Ca.* Altiarchaeum hamiconexum (Probst and Moissl-Eichinger 2015), which is a frequent target of recently described lytic archaeal viruses in the deep subsurface (Rahlff et al. 2021). Due to their worldwide distribution and high abundance as main primary producers in the deep subsurface (carbon fixation via a modified reductive acetyl-CoA pathway (Probst et al. 2014b)) *Ca.* Altiarchaea have been heavily analyzed regarding their ecophysiology (Henneberger et al. 2006; Moissl et al. 2005; Perras et al. 2015; Probst et al. 2018, 2014b, 2014a; Rudolph et al. 2004, 2001). They often form nearly pure biofilms in the subsurface (>95% of the cells) (Henneberger et al. 2006) or streamers with a string-of-pearls-like morphology when associated with sulfur oxidizing bacteria in surface streams (Probst et al. 2018; Rudolph et al. 2004) and thus reach high abundances in their ecosystems constituting up to 70% of the total microbial community (Rahlff et al. 2021).

While the biology of viral attacks in biofilms is generally rather complex (Pires et al. 2021), biofilms also have the potential to be a hotspot for viral activity due to their high cell density (Thingstad and Lignell 1997). However, the extracellular polymeric substances (EPS) of biofilms can also act as barriers against viral infection (Weinbauer 2004). Furthermore, cell surface appendages as shown for the amyloid fiber network of *E.coli* can prevent viral infections with its lytic phage T7 (Vidakovic et al. 2018). At the same time, phages already trapped in the biofilm matrix may remain active and can also eliminate newly arriving prokaryotic cells (Bond et al. 2021). It has also been suggested that viruses may enhance biofilm formation through induction of polysaccharide production (Fernández et al. 2018; Secor et al. 2015). These examples illustrate the complexity of virus-host interactions in biofilms, yet little is known about how viruses affect biofilms and community structures in the deep biosphere. Biofilms with a high cell density could increase virus-host contacts enabling an easy spread of viral infections in the deep subsurface (Anderson et al. 2011), however, actual evidence to verify or falsify this hypothesis is still missing.

For the present study, we used naturally grown biofilms of the uncultivated host *Ca.* A. hamiconexum that can be accessed through the Muehlbacher Schwefelquelle (MSI, near Regensburg, Germany) to answer the question how virus-host ratios change over time and across individual biofilms. We took samples in four consecutive years from 2019 to 2022 (once per year) and applied virusFISH to biofilms dominated by the uncultivated virus Altivir_1_MSI and its host. Individual biofilm flocks from 2022 were analyzed using qPCR designed for detection of *Ca.* A. hamiconexum, Altivir_1_MSI, and bacteria and archaea in general (excluding the host). While virus-host ratios showed a constant increase over the years, we generally observed strong heterogeneity regarding the infections in biofilms. We consequently propose a temporal succession from little to no infections in the biofilm to high virus-host ratios that can be associated with the enrichment of filamentous microbes during cell lysis. Microbiome analyses based on full-length 16S ribosomal RNA (rRNA) gene analyses of individual flocks revealed a relatively constant community composition of the associated bacteriome in the biofilms.

2. Material and Methods

2.1 Sampling Procedure and DNA Extraction

Biofilm flocks from the deep subsurface were collected from the cold (~10°C), sulfidic spring (drilled to a depth of 36.5 m), Muehlbacher Schwefelquelle (Regensburg, Germany, N 48° 59.142, E 012° 07.636), as described previously (Probst et al. 2013). We used Schott flasks with two openings (fused by the university's glass blowing workshop) and inserted polyethylene nets for collecting enough biofilm flocks (~500 flocks per sampling event). The flask was placed on a funnel to make as much spring water flow through the nets as possible. This biofilm trapping system has the advantage that the biofilms directly stick to the nets due to the flow rate of the spring with ~5.50 $m^3 h^{-1}$ and due to their *hami* that represent cell surface appendage with nano-grappling hooks (Probst et al. 2014b). Each of the biofilm trapping systems were incubated for one day as deep as possible (~1 m) in the borehole. Further information on the environmental parameters of the sulfidic spring is described elsewhere and proved to be interannually constant (Probst et al. 2013; Rudolph et al. 2004).

For virusFISH, biofilms were collected in January 2019, August 2020, May 2021, and February 2022 (see Table S1). Biofilm samples for DNA extractions and quantitative polymerase chain reaction (qPCR) experiments were taken in February 2022.

Genomic DNA was extracted from biofilm samples using the RNeasy® PowerBiofilm Kit (Qiagen GmbH, Hilden, Germany) following the manufacturer's instruction and a DNA-conform workflow. For accurate quantification of genomic DNA, a Qubit high-sensitivity DNA assay kit and a Qubit Fluorometer (Qubit 4, both Thermo Fisher Scientific, Waltham, MA, USA) was used, and the genomic DNA was stored at −20 °C until further use.

2.2 VirusFISH for Enumerating Viral-Host Ratios

VirusFISH and imaging was performed on 18 Altiarchaeota biofilm flocks for each of the four sampling events (n total = 72 biofilm flocks; raw data are listened in Table S2) following the protocol of Rahlff et al. 2021 (Rahlff et al. 2021). For enumerating 72 *Ca.* A. hamiconexum biofilms, 68 biofilms were treated with the Altivir_1_MSI probe (n = 68) and four biofilms were treated with a *Metallosphaera* sp. virus probe (n = 4). Shortly, the biofilms were hybridized with Atto 488 labelled 16S rRNA probes, Alexa 594 labelled virus probes, and counterstained with 4′,6-diamidin-2-phenylindole (DAPI, 4 µg mL^{-1}, Thermo Fisher Scientific, Waltham, MA, USA). Of the 18 biofilms from each year, 17 were treated with the Altivir_1_MSI probe (n = 17; see Supplementary Information of Rahlff et al. 2021 (Rahlff et al. 2021)) and one served as negative control (*Metallosphaera* sp. virus probe (Wagner et al. 2017); (Rahlff et al. 2021), Figure S1). Imaging was performed with an Axio Imager M2m epifluorescence microscope (X-Cite XYLIS Broad Spectrum LED Illumination System, Excelitas, Ontario, Canada) equipped with an Axio Cam MRm and a Zen 3.4 Pro software (version 3.4.91.00000) (Carl Zeiss Microscopy GmbH, Jena, Germany). The visualization

was performed by using the 110×/1.3 oil objective EC-Plan NEOFLUAR (Carl Zeiss Microscopy GmbH) and three different filter sets from Carl Zeiss: #49 DAPI for detecting DNA, #64 HE mPlum for the detection of signals of probes targeting Alitvir_1_MSI, and #09 for visualizing 16S rRNA signals of *Ca.* A. hamiconexum. We calculated virus-host ratios by summarizing virus counts across all three defined infection stages and compared the value to the number of host cells in the specimen. We use this as a proxy for the infection frequency in a sample.

2.3 Determining the Detection Efficiencies of Direct-GeneFISH and VirusFISH

Three different probe sets targeting the pseudo-genome *Ca*. A. hamiconexum (NCBI acc. no. JAGTWS000000000.1), as assembled from the MSI (Rahlff et al. 2021), were designed for the experiments estimating the detection efficiency of direct-geneFISH (Barrero-Canosa et al. 2017). Each probe set contained eleven dsDNA polynucleotides, having 300 bps in length.

In preparation for probe design, four metagenomic datasets from 2012 and 2018 (Probst et al. 2014b; Rahlff et al. 2021) were mapped and run in sensitive mode using Bowtie2 (v2.3.5.1) (Langmead and Salzberg 2012) to the reference genome of the host *Ca.* A. hamiconexum and its virus Altivir_1_MSI, respectively. Then, for each metagenomic sample and each host/virus genome inStrain (v1.5.3) (Olm et al. 2021) was used to i) detect single nucleotide polymorphisms (SNPs), counting all positions that were classified as 'divergent sites'; and ii) calculate the per base coverage. For calculating the coverage, we removed i) all 0 coverage regions, resulted during the pseudocontig creation by joining scaffolds with 1000 Ns as insert regions in-between: and ii) all genome positions corresponding to an N.

Then, all genomic regions with high SNP counts (more than 5 SNPs in 300 base window, or more than 10 SNPs in a 30-base window) and/or low coverage (lower than the median coverage for the respective metagenome) were removed. Only regions that were found in all metagenomes were kept. For the remaining genomic regions, polynucleotides of 300 bases (N free) were generated. Only those polynucleotides with a G+C base content between 30% and 40% were kept, similar to the G+C base content of the polynucleotides used to target Altivir_1_MSI (Rahlff et al. 2021). Their melting profiles were predicted using the DECIPHER R package (Wright 2016). To further aid the probe selection, we plotted the remaining polynucleotides along the length of the pseudocontig, together with their corresponding SNP counts (number of SNPs per polynucleotide) and coverage, for each metagenome. The plots were inspected visually and the polynucleotides in the three probe sets (Table S4) were chosen using the following criteria: i) localization on the same scaffold and within a 10 000 bases region, to ensure a spatial proximity similar to that of the Altivir_1_MSI probes; ii) per polynucleotide SNP counts similar to that of the Altivir_1_MSI probes, for which the SNP counts ranged of between 0 and 2.7 (see plot of the Supplementary information 1&2); and iii) similar melting profiles (Table S5).

The polynucleotides were chemically synthesized by IDT (Integrated DNA Technologies, CA, USA) as gBlocks® Gene Fragments. All eleven polynucleotides from each probe set were mixed in equimolar ratios and then labelled as previously described

(Rahlff et al. 2021), using the ULYSIS™ Alexa Fluor™ 594 nucleic acid labeling kit (Thermo Fisher Scientific, MA, USA).

For targeting the 16S rRNA of *Ca*. A. hamiconexum a specific SM1- Euryarchaeon-probe "SMARCH714" (5'-GCCTTCGCCCAGATGGTC-3', Moissl et al. 2003) was used. As negative control for the experiment, also *E.coli* was used for applying the different amount of probe sets and their combinations (Figure S2). Five biofilm flocks for each of the three probe sets (probe set 1, 2, and 3) and each probe set combination (1+2, 2+3, 3+1, 1+2+3) were used (n=35 in total). For details, please see Table S3-6.

2.4 *Quantitative Real-time PCR (qPCR) Targeting Altivir_1_MSI and Archaeal as well as Bacterial 16S rRNA Gene Sequences*

A primer set for targeting the previously identified (Rahlff et al. 2021) viral genome "Altivir_1_MSI" (GenBank accession number #MW522970) was designed with Primer3 (Untergasser et al. 2012) resulting in Altivir_1_MSI_F (5'-CGATTACACTCACCGGCTTG-3') and Altivir_1_MSI_R (5'-CGCTCCAACCACGAATGATT-3') (Table S7). The new primer set was evaluated against NCBI's nr and available metagenomes of archaeal biofilm samples from the respective site (Probst et al. 2014b; Rahlff et al. 2021) using blastn (Altschul et al. 1990). Archaeal 16S rRNA genes were targeted with primer set 345aF (5'-CGGGGYGCASCAGGCGCGAA-3', Burggraf et al. 1997) and 517uR (5'-GWATTACCGCGGCKGCTG-3', Amann et al. 1995) and archaea- and bacteria-directed 16S rRNA genes with 515F (5'-GTGYCAGCMGCCGCGGTAA-3', Parada et al. 2016) and 806R (5'-GGACTACNVGGGTWTCTAAT-3', Apprill et al. 2015), which do not detect *Ca.* Altiarchaeum. qPCR standards were generated by amplifying the respective product from DNA from biofilms flocks, followed by cloning into *Escherichia coli* (TOPO® Cloning Kit, Thermo Fisher Scientific, MA, USA) and purifying the respective vector. Inserts of the vectors were confirmed via Sanger sequencing (Eurofins Genomics, Ebersberg, Germany).

Bacterial, archaeal, and Altivir_1_MSI abundances were estimated by qPCR in ten individual MSI biofilm flocks (42.6 to 126 ng of DNA per flock) collected in February 2022. DEPC-treated water was used as template for negative controls. Dilution series of the respective vectors were used as positive controls (see above). Reactions were performed in triplicates for all samples (here MSI biofilm flocks) and in duplicates or triplicates for the respective standards (10^{-1}–10^{-8} or 10^{1}–10^{9} copies μL^{-1}). The R^2 values of the standard curves ranged from 0.96 to 0.99 (see Table S8).

All qPCR reactions (20 µL) were performed in MIC tubes (Biozym Scientific GmbH, Hessisch Oldendorf, Germany) containing 18 µL master mix (2x qPCRBIO SyGreen Mix, PCR Biosystems Ltd., London, UK), 0.4 µM of the respective forward and reverse primer, 1 µL bovine serum albumin (BSA) per reaction (Simplebiotech GmbH, Leipzig, Germany), DEPC-treated water (Biozym Scientific GmbH, Hessisch Oldendorf, Germany) and 2 µL of DNA template. The thermal cycling steps were carried out by using a MIC qPCR cycler (Bio Molecular Systems, Queensland, Australia). For the primers targeting archaea and Altivir_1_MSI they consisted of 95°C for 2 min and 40 cycles at 95°C for 30 s, 60°C for 30 s, and 72°C for 30 s. The qPCR steps for the archaea- and bacteria-directed 16S rRNA gene

primers were set as follows: 95°C for 10 min and 35 cycles at 95°C for 10 s, 50°C for 30 s, and 72°C for 30 s.

2.5 Statistical Analysis

A Kruskal-Wallis test was used to find significant differences among the different data sets obtained by qPCR and virusFISH and was performed in R (version 4.1.2) (R Core Team, 2022). If significant differences ($p < 0.05$) were observed, the *post-hoc* Dunn's test was used (Table S9).

2.6 Full Length 16S rRNA Gene Sequencing from DNA of Individual MSI Biofilm Flocks by Using Nanopore Sequencing

For Nanopore sequencing of bacterial 16S rRNA gene amplicons, we used the forward primer (5'-ATCGCCTACCGTGAC-barcode-AGAGTTTGATCMTGGCTCAG-3') and the reverse primer (5'-ATCGCCTACCGTGAC-barcode-CGGTTACCTTGTTACGACTT -3') from the 16S Barcoding Kit (1-24 Kit SQK-16S024, Oxford Nanopore Technologies (ONT), Oxford, UK) with some modifications in the protocol. Full-length 16S rRNA gene PCR was carried out in a total volume of 50 µL containing 15 µL DNA template, 5 U μL^{-1} Taq DNA polymerase (Takara, CA, USA), 1x of PCR buffer (10x, Takara, CA, USA), 10 µL of barcoded primer set forward/ reverse from ONT, 200 µM deoxynucleotide triphosphates (dNTPs, Takara, CA, USA), 1 µg μL^{-1} BSA (Simplebiotech GmbH, Leipzig, Germany), 1% (v/v) dimethyl sulfoxide (DMSO, Carl Roth GmbH + Co. KG, Karlsruhe, Germany). Thermal cycling was carried out with an initial denaturation step (1) at 95°C for 10 min, (2) denaturation at 95°C for 30 s, (3) annealing at 54°C for 30 s, (4) extension 72°C for 2 min (2-24 cycles), followed by an extension at 72°C for 10 min. Resulting PCR products were purified using Agencourt AMPure® XP beads (Beckman Coulter, IN, USA). The incubation with the magnetic beads was extended from 5 to 10 min.

The PCR product concentration in ng μL^{-1} per barcode, with barcode sequences listed in Table S10. The 90.67 fmol of amplicons were loaded on a R9.4.1 FlowCell (ONT). Sequencing was performed for 48 h on a MinION1kB sequencing device (ONT). Base calling and demultiplexing were performed using Guppy (v6.0.7, super high accuracy model). Basic sequencing statistics were collected using NanoPlot (v1.32.1) (De Coster et al. 2018).

Demultiplexed reads were classified via a custom script by mapping to the SILVA 138 SSU (https://www.arb-silva.de/documentation/release-138/) database (Quast et al. 2013) (accessed on 13th of January 2023) via minimap2 (Li 2018) allowing for up to ten mismatches. Reads mapping to the database were then clustered, and an OTU table created with numbers of reads mapped to each reference sequence. The final OTU table contained SILVA 138 taxonomy for each reference sequence and the numbers of reads mapped to the reference sequence across all samples. In RStudio, OTUs assigned to "Chloroplast", "Mitochondria" or "Eukarya" were removed manually and relative abundances calculated. Finally, after summarizing total read numbers at genus level per sample (tidyverse, Wickham et al. 2019), ggplot2 (Wickham 2016) was used to generate heatmaps.

3. Results

3.1 VirusFISH Reveals an Increase in Viral Infections of Ca. Altiarchaeum hamiconexum Cells in the MSI over Four Years

We compared the virus-host ratio of Altivir_1_MSI and *Ca.* A. hamiconexum in samples across four consecutive years (2019-2022) using a virusFISH protocol (Rahlff et al. 2021), in which we detected simultaneously the Altivir_1_MSI virus by using a set of eleven dsDNA polynucleotide probes, and *Ca.* A. hamiconexum, its host by using rRNA targeted oligonucleotides. To analyze spatial heterogeneity, *i.e.*, different infection rates in individual biofilm flocks, we analyzed 18 biofilm flocks per sampling event. This resulted in the analysis of 55,827 individual cells, of which 2,854 were infected (Figure 1A). We found the same three main infection categories as previously described (Rahlff et al. 2021): i) initial infections, represented by small, dot-like signals and including the viral adsorption, genome in-jection and early replication phases; ii) advanced infections, displaying the so-called "halo" signals and including the advanced genome replication stages; and, iii) lysing infections, recognizable from the virion release around the cells. While the percentage of advanced infections decreased over the years from 76.5 to 54.4%, initial infections (8.6-13.3%) and lysing infections (14.9-32.3%) constantly increased, except for the year 2021 (Fig 1A). In general, the virus-host ratio increased from 0.12 to 0.28 throughout the years 2019 to 2022 (median; Figure 1B, Table S10). These absolute ratios agreed well with the virus-host ratios previously found in metagenomes of biofilms from 2012 and 2018 (Rahlff et al. 2021). While the ratio determined for the 2018 metagenome (0.0033) aligned well with the in-creasing trend in virusFISH from 2019 to 2022, the ratio of 0.312 from the 2012 meta-genome was extraordinarily high, however, still in the range of the virusFISH-based ratios observed across the years. In addition, we also calculated the virus-host ratio for ten individual biofilm flocks sampled in 2022 for analyzing the distribution of Altivir_1_MSI, *Ca.* A. hamiconexum, and the bacterial community composition (for more details please see section 3.4). Here, the virus-host ratio ranged from 0.001 to 0.492, similar to the ratio obtained for the 17 biofilm flocks (Figure 1B). In Figure 1B, significant differences between populations are marked with an asterisk showing a p-value ≤ 0.01.

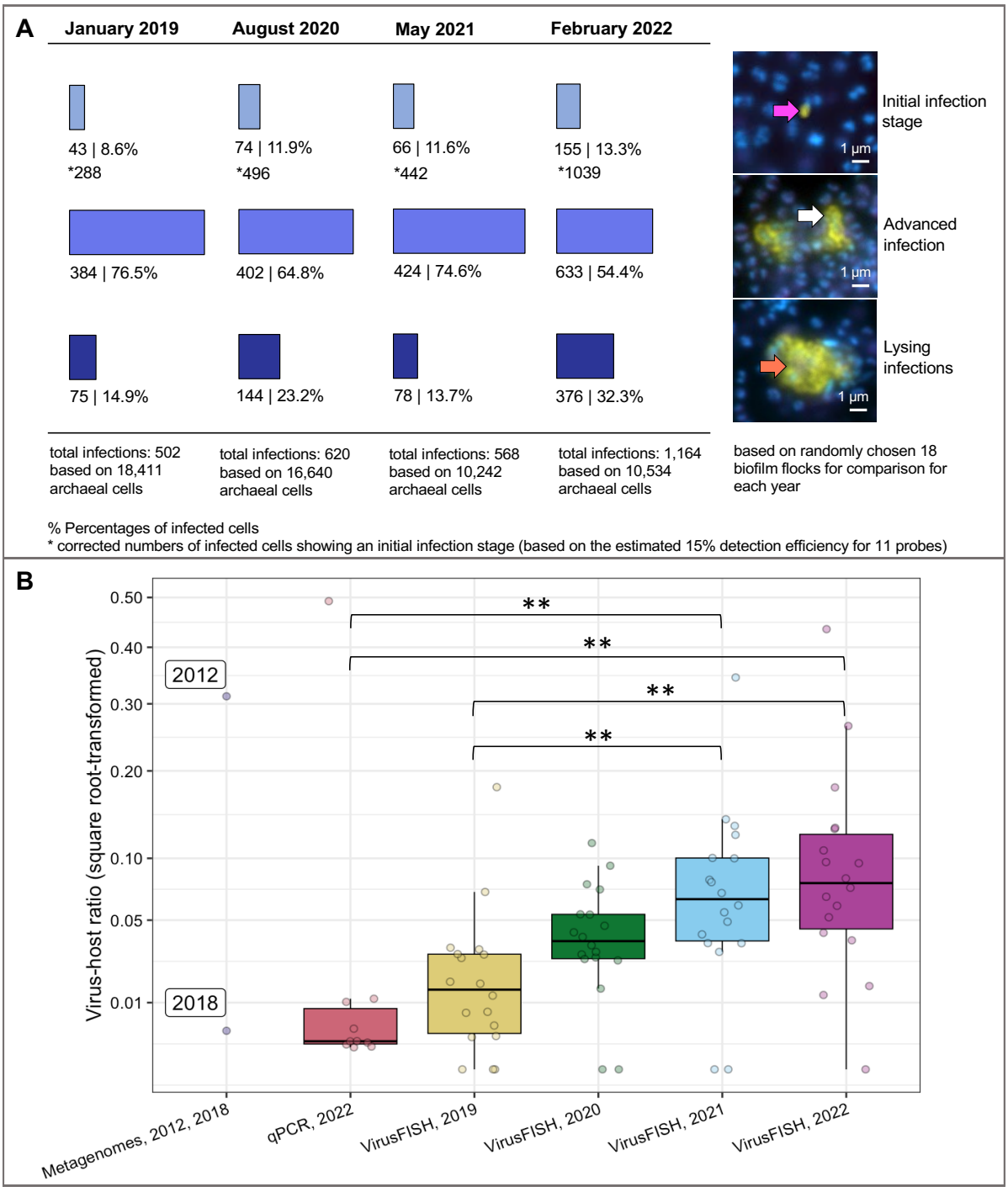

Figure 1: VirusFISH-based enumeration of infections of *Ca.* A. hamiconexum with Altivir_1_MSI across multiple years (A) and differences in virus-host ratios across techniques and years (B).

A. VirusFISH was performed by using a specific probe targeting Altivir_1_MSI within 18 altiar-chaeal biofilms from each year sampled from the MSI (Rahlff et al. 2021). The enumeration was conducted manually (data are listed in Table S11). The biofilms were visualized by using three different fluorescent channels: DAPI (blue, archaeal cells), ATTO 488 (purple, SMArch714, 16S rRNA signal), and Alexa 594 (yellow, the probe mix specific for the Altivir_1_MSI genome). The three fluorescent channels were merged for visualization (individual images available on FigShare). Each of the merged micrographs shown here

represent a different stage of viral infection. Purple arrow – virus attachment to the host's cell surface. White arrows – advanced infections with "halo" signals. Orange arrows – cell burst, and release of free virions, according to Rahlff et al. 2021). Scale bars: 1 μm. The number of initial infections were corrected (indicated by an asterisk) by a factor of ~6.7 (100% detection efficiency/15% calculated detection efficiency of direct-geneFISH), but not the number of advanced and lysing infections, which are expected to have more than ten viral genome copies per cell. For details on infection frequency please see next paragraph in the main text.
B. The distribution of virus-host ratios across biofilm samples was determined using: i) metagenomic read-mapping (data from Probst et al. 2013; Rahlff et al. 2021) on samples from 2012 and 2018; ii) qPCR on ten individual biofilm flocks from 2022; and, iii) the results obtained by virusFISH from 2019, 2020, 2021, and 2022 (data corresponds to panel A). The Kruskal-Wallis and *post-hoc* Dunn's test were used to compare the virus-host ratios across qPCR and virusFISH datasets. Highly significant differences between populations are indicated with asterisks ($p \leq 0.01$). For details, please see Table S8. Different colors indicate different years or methods.

3.2 Determining the Detection Efficiency of VirusFISH via Host-Directed Direct-GeneFISH

We observed striking differences in the abundance of the three infection categories across all years, with the abundance of the initial infection stage being the lowest (8.6%-13.3%; Figure 1A). The number of viral genomes per cell varies during the virus reproduction cycle. During the initial stage of infection, there can be as little as one viral genome copy per host cell. Because the detection of single copy targets in virusFISH is at the limit of sensitivity, potentially resulting in decreased detection efficiencies, we investigated here whether the low numbers of initial infections stem from a low detection efficiency. For this, we designed a direct-geneFISH protocol (on which the virusFISH is based) that compares the detection efficiency of *Ca.* A. hamiconexum cells by genome-targeted polynucleotide probes with the detection of *Ca.* A. hamiconexum by 16S rRNA probes. The latter is known to have a 100% detection efficiency, based on previous publications (Henneberger et al. 2006; Probst et al. 2014a, 2013). Three different *Ca.* A. hamiconexum probe sets were designed, each having eleven polynucleotides and other similar properties (G+C base content, polynucleotide length, etc. – see "Materials and methods" section) with the probe mix targeting Altivir_1_MSI. To avoid targeting individual strains of *Ca.* A. hamiconexum, which are known to exist in MSI (Probst et al. 2014b), the probe design was performed on genomic regions which had a coverage equal or larger than the median coverage in four metagenomes (Rahlff et al. 2021).

We first applied each probe set targeting the host genome individually and retrieved a detection efficiency of 15.0-16.1% compared to 16S rRNA geneFISH (see Figure 2). Hybridizing with combinations of two or three probe sets, to obtain probe mixtures of 22 and 33 polynucleotides, showed a linear increase of the detection efficiency. The highest efficiency was obtained for the 33-polynucleotide mixture, with an average detection efficiency of 43.5% (for the calculation see Table S7). Transferring these results to virusFISH, where we target a single Altivir_1_MSI genome by using eleven probes, means

that more than three viruses in close vicinity are needed to reach a detection efficiency greater than 50%. In other words, at least seven viruses in close vicinity are necessary to achieve a detection efficiency of 100% when extrapolating these findings. Therefore, it is likely that our virusFISH results have underestimated the number of initial infections (category 1) by a factor of ~6.7, but not the number of advanced and lysing infections, which are expected to have more than ten viral genome copies per cell.

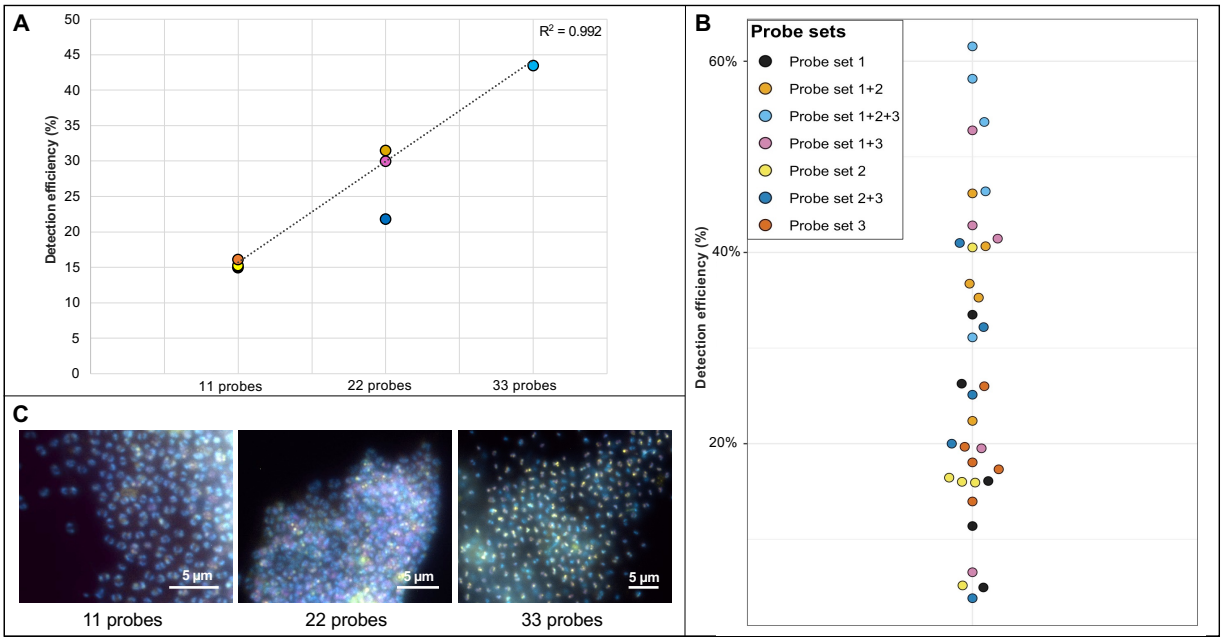

Figure 2: Determination of the detection efficiency of direct-geneFISH by using different probe sets targeting the genome of *Ca.* A. hamiconexum.

A. Three probe sets (probe set 1, 2 and 3 consisting of eleven probes each, Table S4) were designed based on the *Ca*. A. hamiconexum genome (see methods for details). The sets were combined to create probe mixtures with 22 polynucleotides (probe set 1+2, 2+3 and 3+1) and a probe set with 33 polynucleotides in total (1+2+3). For each probe set (1, 2, and 3) and probe set combination (1+2, 2+3, 3+1, 1+2+3), five biofilm flocks were used (n = 35). The different amounts of polynucleotides in a mixture were positively correlated with the detection efficiency (R^2 = 0.992, linear regression analysis).
B. Illustration of the detection efficiency in a bee swarm plot. The detection efficiency increases with increasing number of polynucleotides in a probe mixture (raw data can be found in Table S6&S7).
C. Visualization of the different detection efficiencies using fluorescence micrographs according to Figure 1. Biofilms were visualized by using three different fluorescent channels that were merged together: DAPI (blue, archaeal cells), ATTO 488 (purple, SMArch714, 16S rRNA signal), and Alexa 594 (yellow, probes targeting the *Ca*. A. hamiconexum genome). Scale bars: 5 µm. For unmerged imaging data see Supplementary material (Figure S3-S5). Raw image data available through FigShare. Scale bar 5 µm.

3.3 Filamentous Microorganisms Are Enriched in Areas of Vast Viral Lysis Suggesting a Development of Ca. A. hamiconexum Biofilms over Time

Using virusFISH, we observed different degrees of infection with Altivir_1_MSI of the *Ca.* A hamiconexum biofilms (n= 68). For some biofilm flocks (two out of 68), we observed a high accumulation of filamentous microorganisms in areas where *Ca.* A. hamiconexum showed heavy infections and viral lysis (Figure 3D). Although a similar

accumulation of bacteria was generally observed in biofilm flocks (Figure 3A-C), their abundance was low (Rahlff et al. 2021). In concert with results published previously (Rahlff et al. 2021), these results demonstrate that *Ca.* A. hamiconexum biofilms from MSI are homogeneous in terms of the associated bacterial community composition. We further suggest that the biofilms undergo a temporal development dependent on viral infections, with the main stages depicted in the individual panels in Figure 3. Initially, the biofilm shows no to very few viral infections (based on all infection categories, 17 out of 68 imaged flocks across 2019-2022, Figure 3A). Then, the infection frequency increases (47 out of 68, Figure 3B), until the vast majority of cells are infected (two out of 68 biofilm flocks, Fig 3C). And finally, many *Ca.* A hamiconexum cells lyse and filamentous microbes enrich along with the cell debris (two out of 68 biofilm flocks, Figure 3D). Out of 68 biofilms, 64 individual biofilms (94%) were infected, and four biofilms (6%) had no detectable infections (for raw data please see Table S2). Filamentous microbes that often appeared along with cell lysis are likely bacteria, as indicated by the previous identification as such of organisms with similar morphology (Probst et al. 2013), and by results based on 16S rRNA gene amplicon analysis (see below).

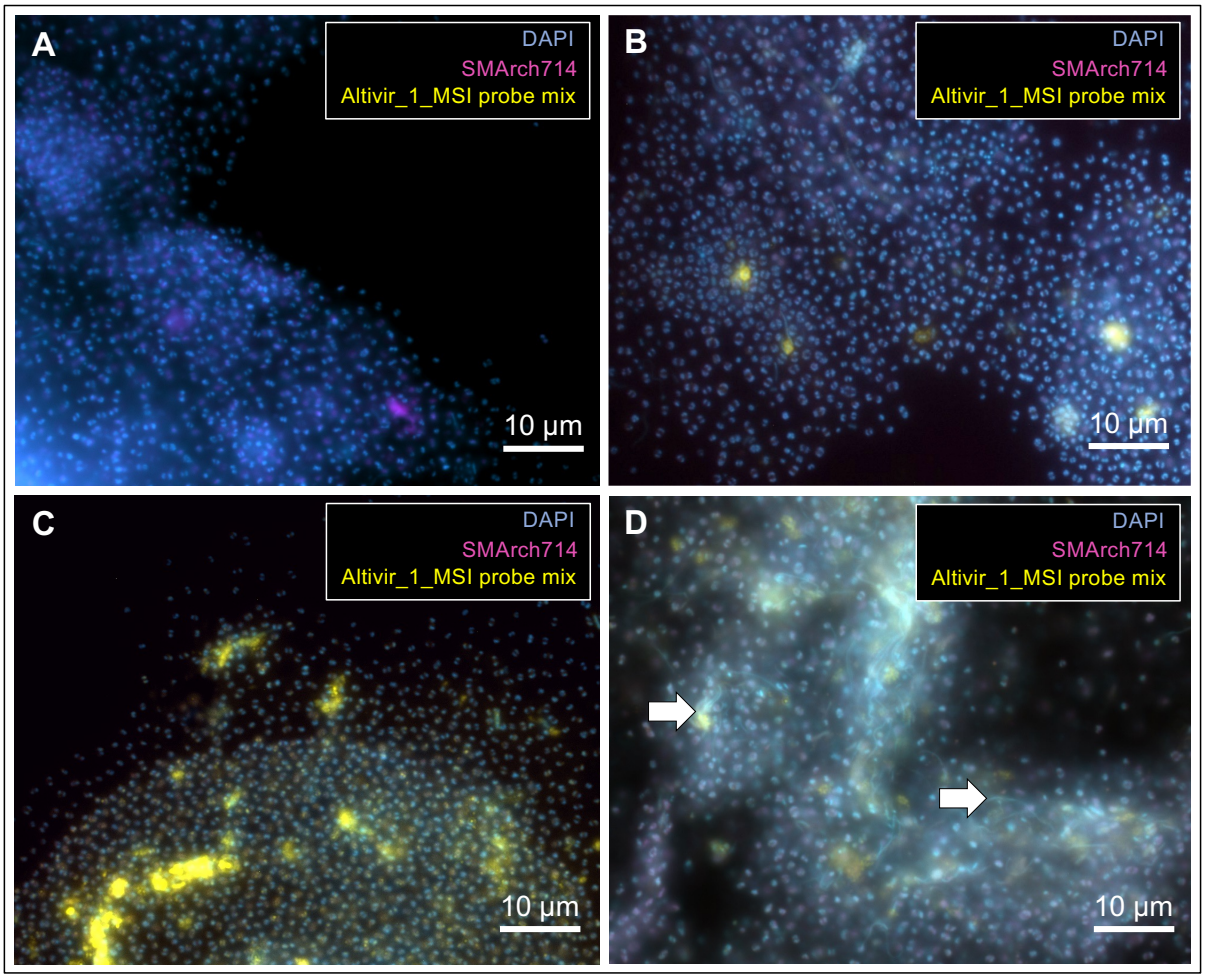

Figure 3: VirusFISH shows how infections of Altiarchaeota with Altivir_1_MSI in biofilms could progress over time. Here independent biofilm flocks with different infections frequencies are depicted. Infection frequencies are based on viral abundances derived from all infection categories (1-3).

A. Biofilms show no to very few viral infections (low infection frequency).
B. The infection frequency increases.
C. The vast majority of host cells are infected.
D. Lysis of *Ca.* A hamiconexum cells appears to promote the enrichment of filamentous microbes along with cell debris. White arrows indicate filamentous microbes. Micrographs were taken according to Figure 1 and raw data is available under FigShare. For unmerged imaging data see Supplementary material (Figure S6-S9). Scale bar: 10 µm.

3.4 Biofilm Flocks with Different Virus-Host Ratios Are Associated with a Constant Bacteriome

To investigate bacteria associated with biofilms with different infection frequency of the *Ca.* Altiarchaea cells, we sampled ten individual flocks from 2022 and investigated the virus-host ratio, bacterial abundance, and the bacterial community composition using near full-length 16S rRNA gene amplicon sequencing (Figure 4A, B). Our qPCR analysis (Figure 4A) displayed already a constant distribution of archaea (mainly *Ca.* A. hamiconexum) ranging from 7.07 x 10^8 to 2.52 x 10^9 copies per µL, Altivir_1_MSI from 1.26 x 10^6 to 4.52 x 10^8 copies per µL, and bacteria from 5.93 x 10^5 to 2.66 x 10^6 copies per µL in the ten individual biofilm flocks. The virus-host ratio varied from 0.001 to 0.492 based on specific qPCR assays. The ratio of *Ca.* A. hamiconexum to bacteria varied from 569.524 to 1,240.105 (raw data in Table S12). Besides *Ca.* A. hamiconexum, the community comprised only bacteria, and was dominated by organisms of the genus *Desulfocapsa*. However, there was no significant correlation between Altivir_1_MSI abundance and bacterial abundance, the community composition, or the top three most abundant organisms (Figure S10). *Proteobacteria* (class: *Desulfobacterota*) was the most predominant phylum, accounting for up to ~76% of the total relative abundance. *Desulfocapsa* was present in all ten biofilm samples with 20-75.7%. Six biofilms showed also hits for another, potentially sulfate-reducing bacterial clade belonging to *Desulfovibrio*, with a relative abundance between 5.4 and 14.4%. As a third group of organisms associated with sulfate-reducing bacteria, we detected a member of the *Desulfobacterium catecholicum group*, with 12.2% of the total relative abundance within one single biofilm. Other bacteria, *e.g.*, *Spirochaetota*, were also present in relatively low abundance (5.6%) in one single biofilm flock besides some uncultivated/ unclassified bacteria (rel. abundance between 5.0-32.7%). Next to many uncultivated bacteria, we also found hits for members of the phylum *Bacteroidota*, accounting for 11.3% of the relative abundance, and, *e.g.*, *Lentimicrobium* (also a representative of the phylum *Bacteroidota*) with a relative abundance of 10.2 and 11.8% detected in two biofilm flocks, in which the abundance of Altivir_1_MSI was also high. We conclude that the bacteriome of these ten individual biofilm flocks displayed a stable community consisting of heterotrophic and potentially sulfate-reducing bacteria.

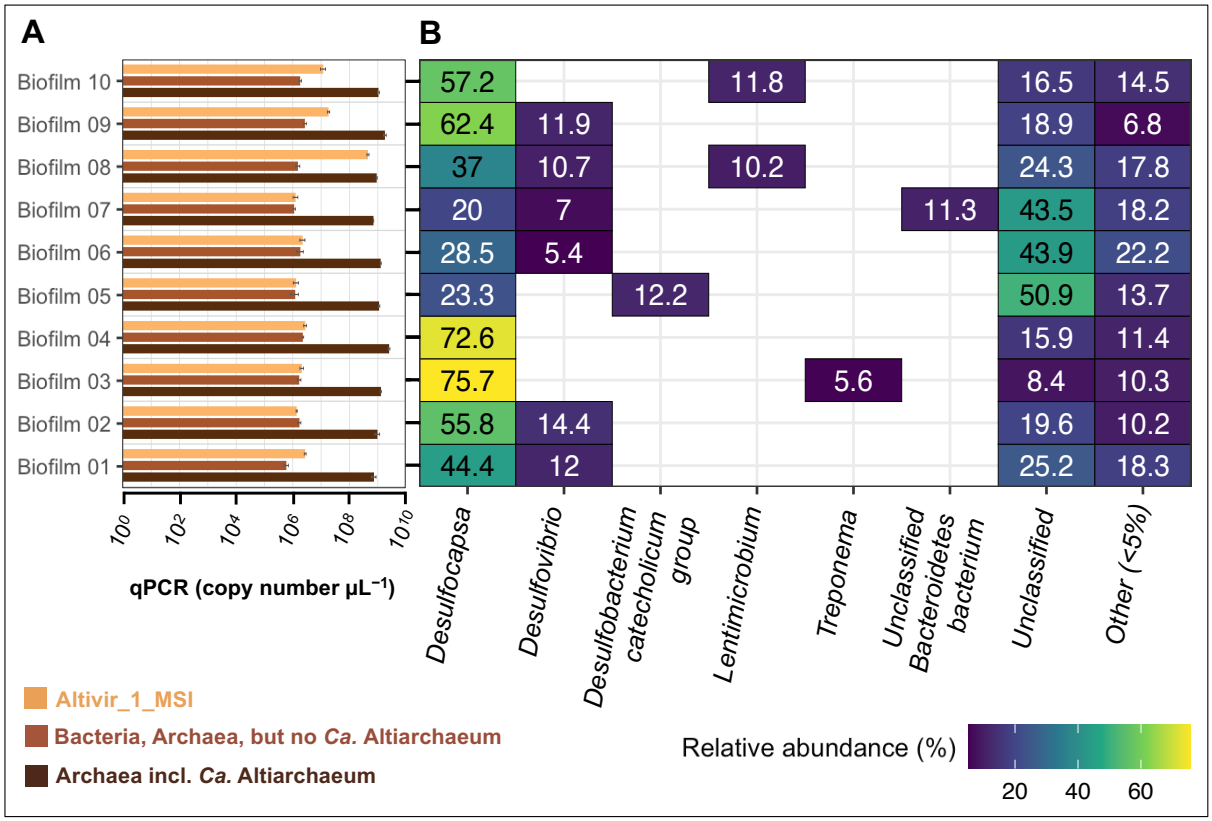

Figure 4: Quantification of microbes and bacterial community composition of ten individual biofilm flocks from MSI sampled in 2022.

A. qPCR data targeting archaea, bacteria, and Altivir_1_MSI of ten individual MSI biofilm flocks. For raw data please see Table S12.
B. Community heatmap depicting the relative abundance (%) of the bacterial taxa at the genus level based on 16S rRNA gene information derived from individual MSI biofilm flocks.

4. Discussion

The deep biosphere harbors by far the largest reservoir of organic carbon on Earth (Bar-On et al. 2018; Kallmeyer et al. 2012) and is estimated to contain of $6x10^{29}$ prokaryotic cells (Magnabosco et al. 2018), including members of not-yet cultivated bacteria and archaea. Despite the ecological and biogeochemical importance of prokaryotes in the deep biosphere, there is little information about the temporal succession and spatial distribution of their mortality due to viral attack. In a previous study, we linked metagenomics and virusFISH to study one specific virus-host system from the deep subsurface, here *Ca*. A. hamiconexum and its virus Altivir_1_MSI (Rahlff et al. 2021). Building upon this knowledge, we now investigated the stability of the virus-host system using virusFISH, over a period of four consecutive years. We have confirmed previous results on the different stages of viral infection on *Ca*. A. hamiconexum, but we also revealed a constant increase in virus-host ratios, *i.e.,* potential infection frequency, over the years 2019 until 2022.

Comparing the virusFISH results with those from other methods, *i.e.*, qPCR and metagenomics, revealed substantial differences, although results were in the same order of

magnitude. These differences likely stem from the different sampling times (see Figure 1B) and also, from the specific biases that each method has, *e.g.*, DNA extraction efficiency, primer binding efficiency, and labeling rate in fluorescence microscopy. Moreover, the size and the thickness of the biofilm can vary substantially, potentially leading to a reduction of virusFISH signals in thicker biofilm samples, due to the relatively strong autofluorescence of the EPS. However, we only used thin biofilm samples consisting of few cell layers for our analyses and their heterogeneity revealed via virusFISH showed significant differences in infection frequencies, *i.e.*, from no detectable infection to >94% of infections across different biofilms from different years. Consequently, the virus-host ratio determined via metagenomics—often based on sampling hundreds of biofilm flocks across several sampling campaigns (Probst et al. 2014b)—might rather reflect an average ratio, while qPCR is the more suitable technique to resolve virus-host ratios across individual biofilm flocks. However, qPCR does not allow to differentiate between the different infection stages within the biofilm. Since quantitative PCR methods and relative abundance measures of metagenomics usually correlate well for deep biosphere communities (Probst et al. 2018) and virusFISH helps to unravel the underlying infection stages, these approaches are complementary for determining the heterogeneity of such biofilms.

By investigating 68 individual biofilms flocks via virusFISH over four years, we identified two flocks that were heavily infected (nearly every cell with a virus signal) and another two with many lysis states. The latter two also revealed the accumulation of many filamentous microorganisms.

Moreover, *Ca.* A hamiconexum were previously found to be associated with filamentous bacteria identified as *Sulfuricurvum* sp*.,* which potentially lives in syntrophic relationship with *Ca.* A hamiconexum in oxygenated biofilms at the spring outflow (Rudolph et al. 2004). While the sulfur oxidation of *Sulfuricurvum* sp. is usually tied to oxygen reduction, species of this genus have been reported to oxidize sulfur compounds with nitrate (Kodama and Watanabe 2004), which has been reported in the spring water (Rudolph et al. 2004). Consequently, these filamentous structures around viral bursts could correspond to *Sulfuricurvum* sp*.,* as sequences classified as such were also detected in our 16S rRNA gene analysis.

Furthermore, Lentimicrobia, which are usually strictly fermentative bacteria (Zhang et al. 2017) but can also participate in sulfate reduction (Li et al. 2020), were found in two biofilms. However, none of the abundant bacterial taxa that were detected in the 16S rRNA gene survey correlated with the viral abundance from qPCR. (Figure S10). Nevertheless, we further suggest that some bacteria (*e.g.*, the unclassified and/ or other 5%) could also feed off cell remnants from lysed *Ca.* A. hamiconexum. These findings corroborate our previous hypothesis that viral lysis of primary producers likely jump-starts heterotrophic carbon cycling in the deep biosphere (Rahlff et al. 2021), and it may be a small fraction of the entire bacterial community that particularly benefits from virus-mediated nutrient release.

Having images of 68 biofilm flocks at hand, we developed a theory for the temporal succession of infection, starting with low to no viral signals, and ending up with many lysis states that involve filamentous microbes. We found that most infections were categorized as advanced infections, which is probably because this infection stage has the longest duration

and is consequently more often captured than initial infections or lysing infections. Not only the detection efficiency underestimates initial infections, but also the lower chance of observing such stages likely affected our results. Due to the proximity of cells in biofilms, viruses might easily jump between hosts without necessarily starting immediate infections. The biofilm itself could limit viral dispersion, since a study on virus-host dynamics in a microbial mat found that the lowered mobility in a biofilm would rather support lysogeny as the predominant viral lifestyle (Jarett et al. 2020), which is clearly not the case in the MSI ecosystem. Furthermore, Rahlff et al. 2021 described that *Ca.* A. hamiconexum uses adaptive immune defense in the form of clustered regularly interspaced short palindromic repeats (CRISPR)-Cas system to defend itself from Altivir_1_MSI, and hence we expected the observed oscillating infection frequencies being typical for a reasonably stable virus-host arms race (Rahlff et al. 2021). Active CRISPR defense will also mean that many viruses in adsorption stage (category 1), will finally not successfully replicate in the host. However, virus-host ratios clearly increased over the years as did the number of observed viruses undergoing adsorption. This suggests that the virus try to counteract the host defense by heavy proliferation, facilitating chances for mutations that would allow circumventing the host's armor. Increasing numbers of SNPs were already observed in Altivir_1_MSI between 2012 and 2018 (Rahlff et al. 2021).

The heterogeneity of infection frequencies in biofilms flocks of *Ca.* A hamiconexum further suggest that biofilms with a high cell density increase host cell contact, enabling a heavy spread of viruses after lysing their hosts. Consequently, these results support the hypothesis by Anderson et al. 2011, that this mode of viral dispersal and predation plays an important role in the deep biosphere (Anderson et al. 2011). Since previous studies about deep subsurface viruses do not provide information on ecosystem dynamics (Holmfeldt et al. 2021; Wirth and Young 2022), the year-long stability of *Ca.* A. hamiconexum and its virus Altivir_1_MSI described herein render their interaction, a perfect model system for studying virus-host interactions of aquatic samples from the deep biosphere.

5. Outlook

Despite the promising results of *Ca.* A. hamiconexum and its virus Altivir_1_MSI regarding their detection *in situ*, the virus-host ratio, and the infection frequency, many questions remain unanswered. First and foremost, the virion structure of Altivir_1_MSI has still not been identified and the current knowledge ends with bioinformatic analyses and virusFISH tagging. For linking the viral genome to the corresponding viral morphology, different possible approaches can be carried out in the future. One approach might be linking virusFISH and atomic force microscopy or scanning electron microscopy (SEM; (Turzynski et al. 2021)). Another promising approach could be Raman microspectroscopy for identification of infected *Ca.* A. hamiconexum cells (Monsees et al. 2022) and its coupling to embedding and transmission electron microscopy (TEM). While these approaches are based on correlative microscopy, traditional immunogold labeling of viral proteins in MSI biofilms will eventually lead to the discovery of the actual virion structure visualized by TEM. With a specific method for detecting Altivir_1_MSI virions in fluorescence microscopy at hand,

additional surveys regarding their occurrence and the accumulation of filamentous bacteria along with *Ca.* A. hamiconexum cell debris would bolster studying the viral ecology in this deep biosphere model ecosystem.

Author Contributions

Conceptualization of the work, A.J.P. with contribution by J.R.; Writing—original draft preparation, V.T., and A.J.P., specifically discussion section, V.T., J.R., and A.J.P. with input from all co-authors; Sampling, V.T., S.P.E., L.G., S.A.S.; VirusFISH, direct-geneFISH, image analysis, qPCR on archaea and Altivir_1_MSI, V.T., Enumeration of viral infections, V.T., L.G.; Probe design for virusFISH and direct-geneFISH, C.M.; qPCR with a universal primer for detecting bacteria in MSI biofilm flocks, and SNP identification in metagenomic data, T.L.S.; Full length 16S rRNA gene sequencing, S.A.S.; Classification of reads and R plotting, A.S. All authors have read and agreed to the published version of the manuscript.

Funding

This work received funding from the NOVAC project of the German Science Foundation (grant number DFG PR1603/2–1). A.J.P. was supported by the Ministry of Culture and Science of North Rhine-Westphalia (Nachwuchsgruppe “Dr. Alexander Probst”). We acknowledge support from the Open Access Publication Fund of the University of Duisburg-Essen.

Data Availability Statement

Microscopy and Nanopore data are available on Figshare (https://figshare.com/) (accessed on 23rd of March 2023) with the project title “Virus-host dynamics in archaeal groundwater biofilms and the associated bacterial community composition”.

Acknowledgements

The authors highly appreciate the technical assistance of Sabrina Eisfeld, Maximiliane Ackers, and Ines Pothmann for laboratory maintenance. Moreover, we thank Indra Banas for critical discussion of the data and the manuscript.

Competing Interest

The authors declare no conflict of interest.

Supplementary material

The supplementary material is available under https://www.mdpi.com/article/10.3390/v15040910/s1 as well as on the supplied CD (see Section VII)

IV. General Discussion

In this thesis, the interplay of *Ca.* Altiarchaea and their virus Altivir_1_MSI was investigated for one special ecosystem, a sulfidic spring called the Muehlbacher Schwefelquelle, which is located in Regensburg (Germany). For studying the interactions between this unique archaeon and their virus, cultivation-independent technologies, like metagenomics and imaging techniques, were used to obtain an original picture of this exceptional virus-host system. The direct linkage of information obtained via *in silico* analysis and the observations via *in situ* techniques enabled us to study how this virus can shape microbial communities within the deep terrestrial subsurface and how microbial interactions detected by these techniques can bolster our understanding in this less studied field of archaeal virology. By using virusFISH, we showed that *Ca.* Altiarchaea was continuously infected by the lytic virus Altivir_1_MSI with the effect that other microorganisms (here mainly sulfate-reducing bacteria) were benefitting from lysing events of bursting archaeal cells.

1. *Piracy in the deep subsurface* – the effects of Altivir_1_MSI on *Ca.* Altiarchaea

The advances in viral metagenomics and imaging (*e.g.,* in the field of FISH) have enabled us deeper investigations for the identification and characterization of viruses. By using transmission electron microscopy (TEM) and epifluorescence microscopy (EFM) first information that viruses represent a prevalent component of, *e.g.,* the deep subsurface can be obtained. For instance, seven years ago, advances in epifluorescence microscopy resulted in an approach called “virusFISH” for directly visualizing viruses in environmental samples. The studies herein were one of the first studies that successfully coupled metagenomics with virusFISH for displaying virus-host dynamics (here *Ca.* Altiarchaeum hamiconexum and its virus Altivir_1_MSI) within ecosystems. The first study was conducted by Hochstein and co-workers (2016) on the interaction between *Acidianus tailed spindle virus* (ATSV) and its host *Acidianus hospitalis* W1, both obtained and isolated from hot springs (Hochstein et al. 2016). This study made a major contribution to the research on archaeal large spindle viruses, which previously only included *Acidianus* two-tailed virus (ATV), *Sulfolobus tengchongensis* spindle-shaped virus 1 (STSV1), *Sulfolobus tengchongensis* spindle-shaped virus 2 (STSV2), and *Sulfolobus monocaudavirus* 1 (SMV1) (Hochstein et al. 2015), and now also the ATSV

virus (Hochstein et al. 2016). Furthermore, Jahn and co-workers (2021), and this is the second study that coupled metagenomic information with imaging, used a very promising approach called PhageFISH-CLEM (correlative light and electron microscopy: CLEM) for investigating the spatial distribution of viruses within sponge holobionts (Jahn et al. 2021). More research attention has been paid on exploring *in situ* viral-host interactions in enrichment cultures by using phageFISH (Allers et al. 2013) or direct-geneFISH (Barrero-Canosa et al. 2017). These techniques were quickly expanded to, *e.g.,* eukaryotic microorganisms like *Ostreococcus* by using phageFISH/ virusFISH (Castillo et al. 2021, 2020; Zimmerman et al. 2019) or by single-molecular FISH (smFISH) on *Emiliania huxleyi* (Vincent et al. 2021). Furthermore, a recent study that focused on marine phages from the North Sea successfully isolated a new ssDNA phage called "*Ascunsovirus oldenburgi* (ICBM5)" that uses a lytic and a carrier-state infection strategy (Zucker et al. 2022). By using direct-geneFISH on pure cultures, the authors could monitor viral infections on *Sulfitobacter dubius* SH24-1b (Zucker et al. 2022). However, the usage of culture-independent techniques on environmental samples (Castillo et al. 2021, 2020; Hochstein et al. 2016; Jahn et al. 2021; Rahlff et al. 2021; Vincent et al. 2021; Zimmerman et al. 2019) and in combination with metagenomics remains limited (Hochstein et al. 2016; Jahn et al. 2021; Rahlff et al. 2021). Until now, only two studies that formed a major part of the present thesis, in which virusFISH was used on environmental samples, focused also on the ecological effects that viruses might have after a successful cell lysis of their hosts (Rahlff et al. 2021; Turzynski et al. 2023).

Since the viral role in the deep terrestrial subsurface is rarely considered (Anderson et al. 2013), we have focused precisely on this specific, difficult to access ecosystem for obtaining information on virus-host interactions for filling specific knowledge gaps in this field. The present studies that dealt with metagenomics and virusFISH showed that *Ca.* Altiarchaea is continuously hijacked by their virus, evidence that eight years ago was still a hypothesis (Probst and Moissl-Eichinger 2015). At this time, only one single electron micrograph showed black dots adhering on the cell surface of *Ca.* Altiarchaea, suggesting putative viruses. However, their role in archaeal biofilms and their impact on the carbon cycle in the deep subsurface remained unclear (Probst and Moissl-Eichinger 2015). In the present thesis, it was shown that over a period of four years biofilms of *Ca.* Altiarchaea are constantly infected by Altivir_1_MSI. In addition, it was displayed that some biofilms showed no viral infections, and some were heavily infected. A review with the focus on archaeal viruses but in

hot springs reported the same: not all cells are constantly interacting with viruses (Munson-McGee et al. 2018), which could be true for cells living in deep subsurface biofilms.

While the complete lifecycle of most archaeal viruses remains unknown, there are several theories which putative lifestyles could be present in extreme environments (Anderson et al. 2011, 2013). For instance, ecosystems with a low nutrient flux like sediments or hydrothermal vents are considered to have high numbers of lysogenic hosts, thus the dominant viral lifestyle must be lysogenic (Anderson et al. 2011, 2013; Weinbauer 2004; Williamson et al. 2008; Paul 2008). Since we are in the "early days" in Archaeal Virology, studies on archaea, *e.g.,* in hot springs showed the controversy. The high prevalence of infections on archaea are chronic and represent the common viral lifestyle in environments with a low host cell density (Munson-McGee et al. 2018; Weitz et al. 2019). Until now, the statement that lysogeny is the common viral lifestyle in the deep subsurface represented a hypothesis (Anderson et al. 2011).

The virusFISH results showed a lytic viral lifestyle for Altivir_1_MSI, as indicated by three main infection stages: I) initial infection with the viral adsorption to the host cells, II) advanced infection with intracellular virus signals and ring-like signals around the host cells, and III) cell lysis with bursting cells and the release of new virions, similar to those three stages reported by Zimmerman et al. (2019) (Zimmerman et al. 2019). Our observed main infection stages displayed a lytic virus and contradict the aforementioned hypothesis of Anderson et al. (2011) that lysogeny prevails as the dominant vital lifestyle in the subsurface (Anderson et al. 2011). Furthermore, the advanced infection stage was the most dominant infection stage. If, *e.g.,* a chronic infection would be the favorable viral lifestyle as reported for ecosystems with a low host cell density (Munson-McGee et al. 2018; Weitz et al. 2019), a constant release of virions and no host cell lysis would be observed (Krupovic et al. 2018; Liu et al. 2017; Pietilä et al. 2016). Focusing on the biofilms of the Muehlbacher Schwefelquelle showed a high host cell density and cell lysing events by Altivir_1_MSI, both representing factors that contradict the theory of chronic infections of *Ca.* Altiarchaea.

For exploring the lytic lifestyle in detail, the structural resolution of Altivir_1_MSI and first high-resolution images of, *e.g.,* the release of new virions after a successful infection would be needed which are still missing. The power of correlative microscopy would advance our current understanding of viruses of *Ca.* Altiarchaea. First attempts were made by linking fluorescence microscopy to atomic-force microscopy (AFM) (Figure IV.1, A, B, unpublished results). It was found that the cell morphology and size of *Ca.* Altiarchaea changed during

viral infection. The cell morphology was irregular in shape and seems “swollen” (Figure IV.1, A). A recent study on the unique archaeal virus STSV2 that can induce cell gigantism of the host cells showed the same (Liu et al. 2021). After a successful infection, a dramatic increase of the host cell size was observed via AFM by becoming more than twice bigger in diameter compared to non-infected cells (Liu et al. 2021). However, research to date has not yet investigated if Altivir_1_MSI can induce cell gigantism on *Ca.* Altiarchaea cells.

In addition, some AFM pictures displayed potential viruses adhering on *Ca.* Altiarchaea cells (Figure IV.1, B), which likely appear to have an icosahedral and tailed structure. It can be assumed that based on the schemes of Ackermann and Prangishvili (2012) and Pietilä et al. (2014), Altivir_1_MSI could belong to the *Myoviridae*, *Siphoviridae* or *Podoviridae* family (Ackermann and Prangishvili 2012; Pietilä et al. 2014). However, higher resolution imaging techniques are required to confirm this hypothesis. According to the study of Ackermann and Prangishvili (2012), viruses belonging to, *e.g.,* the *Siphoviridae* family makes up to 57.3% of all prokaryotic viruses, besides *Myoviridae* with 24.8% or *Podoviridae* with 14.2% (Ackermann and Prangishvili 2012). However, viruses of the *Myoviridae* seem to be frequently found in relation to archaeal hosts (Ackermann and Prangishvili 2012). According to the genome size of the Altivir_1_MSI virus that is 8.9 kb, these virus do not seem to fit to the order *Caudovirales*, because all members of the three families belonging to *Caudovirales* show genome sizes of above 30 kb (Krupovic et al. 2018). At this point, Altivir_1_MSI would represent an archaeal specific virus with a small genome size according to the scheme of Krupovic et al. (2018) (Krupovic et al. 2018). In addition, a tailed structure of Altivir_1_MSI virions was not observed by using TEM (see Manuscript 3: Lytic archaeal viruses infect abundant primary producers in Earth’s crust, Rahlff et al. 2021), which would reject the hypothesis of having a virus belonging to the three above mentioned families.

Taken together, these AFM images must be interpreted with caution because with AFM I did not resolve any hami-structure of *Ca*. Altiarchaea. This would lead to the assumption that the AFM setting, or the treatment of the sample is not sufficient for AFM analysis. Thus, further work is required for resolving first the hami-structure of *Ca.* Altiarchaea cells via AFM in order to then investing archaeal viruses. For unraveling the viral morphology, coupling virusFISH to TEM/ SEM has to be performed. However, to the best of our knowledge, no study that focused on prokaryotic viruses in environmental samples has linked these two imaging techniques, which have shown great potential but still need to be optimized.

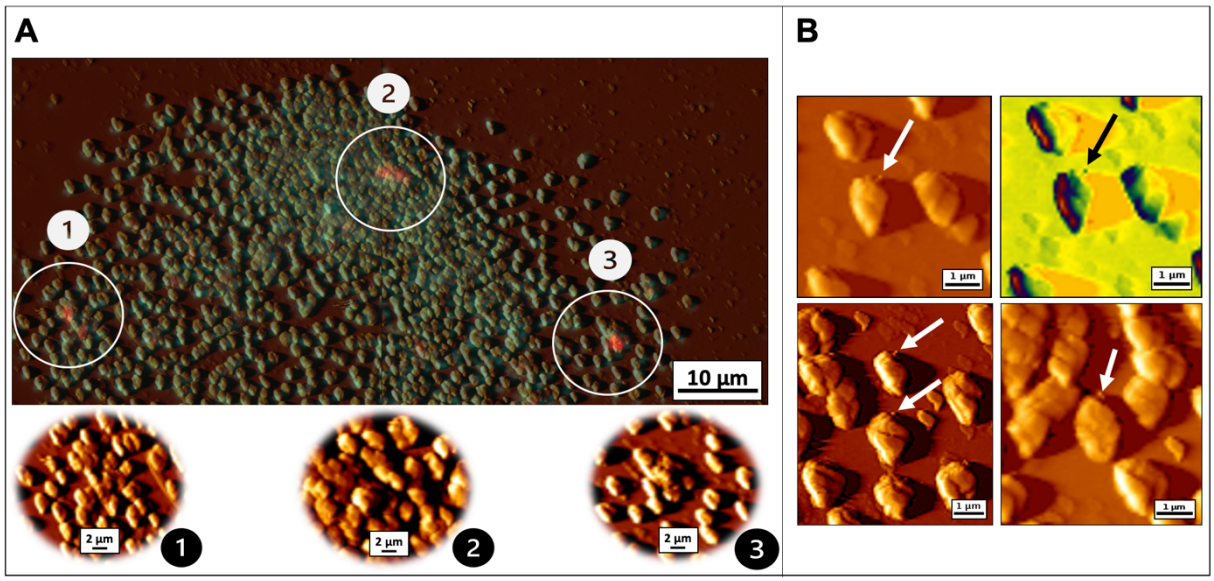

Figure IV.1: (A) Morphological changes of infected *Ca.* Altiarchaea cells achieved by linking epifluorescence microscopy (here virusFISH) to atomic-force microscopy (AFM). Biofilm material was analyzed with DAPI (blue, cells), ATTO 488 (green, 16S rRNA signal) and Alexa 594 (red, viral genomes of Altivir_1_MSI) and merged. Scale bars: 10 µm and 2 µm. (B) Putative viruses adhering on *Ca.* Altiarchaea cells. Scale bars: 1 µm.

Besides the lifestyle of Altivir_1_MSI, we also observed that infected cells were more abundant in certain regions of the biofilm where lower amounts of biofilm matrix were present (see Figure IV.2 A, B). This would lead to the assumption that the biofilm matrix can serve as a shield to protect the embedded *Ca.* A. hamiconexum cells from viral attack (Costerton et al. 1987; Roberts 1996; Weinbauer 2004; Wilkinson 1958). It is generally considered that the biofilm matrix (comprising of, *e.g.,* the EPS) act as a barrier for viruses. However, viruses can overcome this barrier by, *e.g.,* producing specific enzymes to infect their host, and damage the biofilm matrix (Doolittle et al. 1995b; Fernández et al. 2018; Hanlon et al. 2001; Secor et al. 2015; Webb et al. 2003; Weinbauer 2004; Yu et al. 2016). Research to date has not yet determined if Altivir_1_MSI uses enzymes for overcoming the EPS of *Ca.* Altiarchaea and remains an open question to be answered in future research.

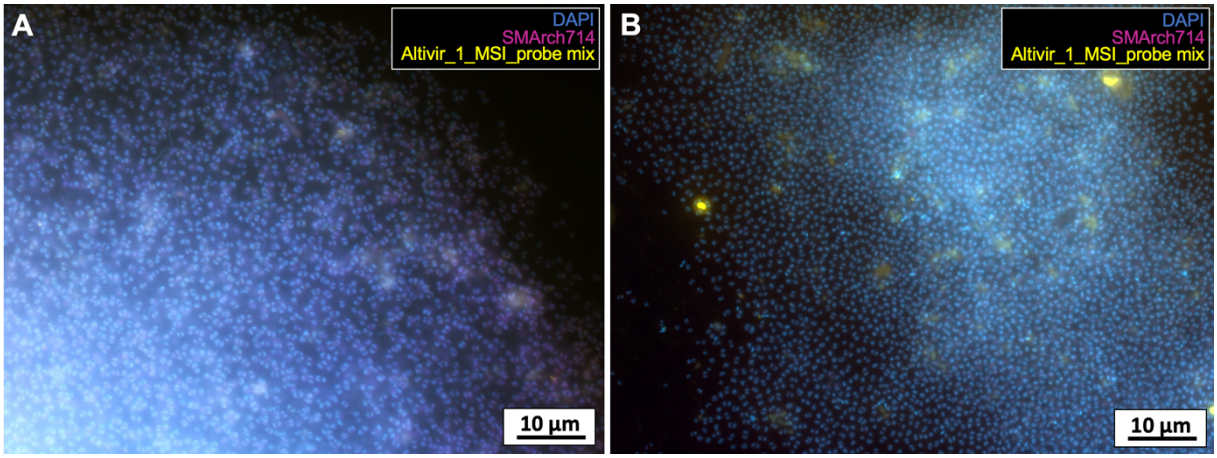

Figure IV.2: Viral infections of Altivir_1_MSI on *Ca.* Altiarchaea biofilms. (A) Minor viral infections due to multiple layers of the biofilm. (B) Biofilm with a less EPS matrix and many viral infections. Biofilm material was analyzed with DAPI (blue, cells), ATTO 488 (purple, 16S rRNA signal) and Alexa 594 (yellow, viral genomes of Altivir_1_MSI) and merged. Scale bars: 10 µm.

In addition, the spatial organization of the biofilm cells and the cell density can be also a determinant to the success of viral infection (reviewed in Pires et al. 2021) and can act as a "shield" by reducing the events of infections since viruses can also adsorb to exopolysaccharides or cell debris (Hansen et al. 2019). Moreover, due to the biofilm development, the thickness and the width of the biofilm, and the availability of nutrients within the biofilm gradually increase (reviewed in Xu et al. 2022). Nutrient gradients within a biofilm determine the different metabolic states of cells, *e.g.,* active, dead, stationary or being dormant (Morita 1999; Jørgensen 2011). For instance, the spatial organization of cells within biofilms lead to a localized growth and limited mobility creating cell clusters with dormant/ persisting cells (Hansen et al. 2019). It has been generally considered that cells with different metabolic activities in the microbial community cooperate to improve survival ability (Xu et al. 2022). In addition, the age of the biofilm is also an important factor for a successful viral infection. According to Ferriol-González and Domingo-Calap (2020) and Pires et al. (2021), the number of biofilm cells with a reduced metabolic activity is expected to increase with the biofilm age (Ferriol-González and Domingo-Calap 2020; Pires et al. 2021). Thus, older biofilms (most common in nature) will be less susceptible to viruses than younger biofilms (Sillankorva et al. 2008; Pires et al. 2021). Due to different sampling events and different biofilms floating out of the spring with a flow rate of about 5.50 m^3 h^{-1} (Henneberger et al. 2006), both, older and younger biofilms were to be included in our experimental approaches.

1.2. *Under Attack* – Ecological implications of infected *Ca.* Altiarchaea on the community composition

Research to date that focus on the usage of virusFISH has not yet determined the effects of viral infections on the whole microbial community in ecosystems. The virusFISH results showed that, due to the constant viral attack of Altivir_1_MSI on *Ca.* Altiarchaea, Altivir_1_MSI might act as a potential top-down controller by following the "killing the winner model" (Thingstad and Lignell 1997; Thingstad 2000), and possibly control the whole diversity of the host community in the MSI. Furthermore, this virus might stimulate the growth of the remaining community members through the regeneration of nutrients, thereby acting also as a bottom-up controller (Storesund et al. 2015). This "viral shunt" (*i.e.*, nutrient release after host cell lysis) facilitates bacterial growth by mediating a shuttle of organic carbon from autotrophs to heterotrophs in the subsurface, stimulate heterogeneity, and leads to a stable bacterial coexistence in this ecosystem. Hence it could conceivably be hypothesized that viruses, like Altivir_1_MSI, are essential key players in ecosystem's functioning and can control the carbon content in ecosystems due to viral infections, an observation which was recently reported for, *e.g.,* deep sea ecosystems (Danovaro et al. 2008; Gao et al. 2022).

Heterotrophs like sulfate reducing bacteria from the MSI (Henneberger et al. 2006; Probst et al. 2013) are important constituents of the deep terrestrial subsurface, represent often the dominant metabolic group where, *e.g.,* sulfate is present (Bell et al. 2020). Our 16S rRNA gene sequencing across individual biofilms of the MSI indicated that the associated bacterial community was dominated by sulfate reducing representatives of *Desulfobacterota*, for instance, of the class *Desulfocapsa* and *Desulfovibrio*, a similar trend that was also reported in the study of Probst et al. (2013) (Probst et al. 2013). What is very interesting is the fact that key enzymes for the Wood-Ljungdahl pathway and corresponding peptides were found in the proteome of , *e.g., Desulfocapsa*, suggesting that the acetyl-CoA pathway could also be used for the oxidation of small organic compounds in the deep subsurface (Bell et al. 2020). Moreover, both *Desulfocapsa* and *Desulfovibrio* are also able to grow on acetate (Finster et al. 1998) that is produced during the decomposition of organic matter by, *e.g*., acetogenic microbial communities (Nuppunen-Puputti et al. 2018), and can be further used by those sulfate reducers (Pedersen et al. 2008).

Sulfate reducers are the main driver of the sulfur cycle in the deep terrestrial subsurface and perform microbial sulfate reduction by producing sulfide. Our results display

an active microbial community not only consisting of sulfate reducing bacteria but also of sulfide oxidizing bacteria, suggesting that both together mediate the sulfur cycle in the MSI. The filamentous bacteria, which may benefit from viral lysis of *Ca.* Altiarchaea (Figure IV.3) could be associated with *Sulfuricurvum* sp. (Rudolph et al. 2004). Species of this genus have been reported to oxidize sulfur compounds with nitrate (Kodama and Watanabe 2004), can grow anaerobically on, *e.g.,* sulfide, has been reported in the MSI spring water (Rudolph et al. 2004) and were also detected in our 16S rRNA gene analysis.

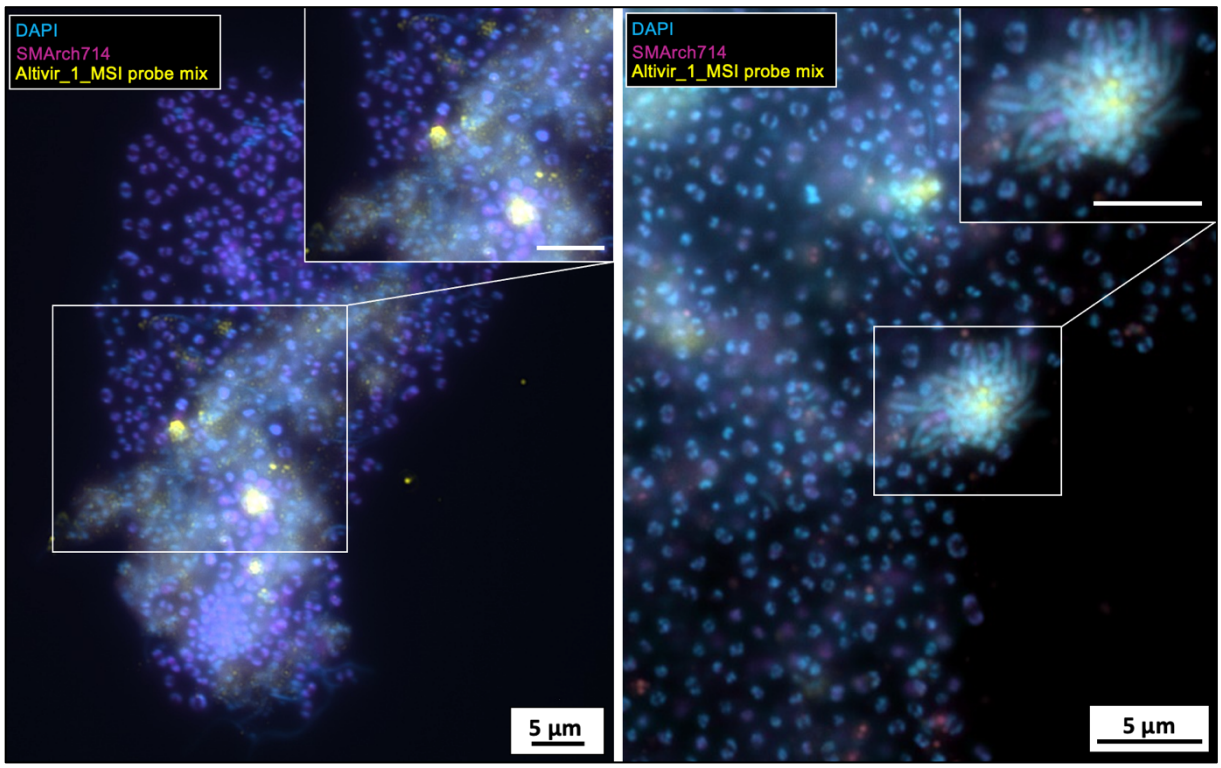

Figure IV.3: Viral infections of Altivir_1_MSI on *Ca.* Altiarchaea biofilms showing many filamentous bacteria putatively benefitting from cell debris and released nutrients from lysing *Ca.* Altiarchaea cells. Biofilm material was analyzed with DAPI (blue, cells), ATTO 488 (purple, 16S rRNA signal) and Alexa 594 (yellow, viral genomes of Altivir_1_MSI) and merged. Scale bars: 5 µm.

Since it was strictly assumed that Altivir_1_MSI has a lytic lifestyle according to the virusFISH results presented herein, and the main infection stages, environmental conditions can also influence the host physiology and can regulate the characteristics of a lytic viral infection (reviewed in Mojica and Brussaard 2014). For instance, after a successful infection, free virions are released from their hosts into the environment and are directly exposed to environmental factors that can reduce the infectivity, abundance by degradation or removal, or affect the new adsorption to their host by reducing the chance of a new successful infection (Mojica and Brussaard 2014). One main factor for viral inactivation is, *e.g.,* the temperature. It was shown for, *e.g.,* marine viruses that an increase in temperature lead to an induced loss

of viral infectivity or inactivation (Nagasaki and Yamaguchi 1998). Moreover, the optimal temperature for viral replication generally matches the temperature for host's growth because viruses are dependent on their hosts (Mojica and Brussaard 2014). It has been generally considered that the ideal temperature range for viruses is 4 to 10°C, where viruses are generally stable with pH values between 5 and 9 (Florent et al. 2022). These values are consistent with the environmental parameters of the MSI, which have been shown to be constant over several years (Rudolph et al. 2004) and provide ideal conditions for permanent viral infections on *Ca.* Altiarchaea. In addition, since the environmental parameters are constant in the MSI, the viral taxonomic composition should also be constant in this sulfidic spring. However, the temperature can also induce viral resistance (Kendrick et al. 2014) or influence the viral lifestyle by switching from lysogenic to lytic as reported for eukaryotic viruses (McDaniel et al. 2006; Wilson et al. 2001). Nevertheless, the impact of environmental factors on prokaryotic viruses remains largely unexplored for the deep terrestrial subsurface compared to, *e.g.,* soil environments (Adriaenssens et al. 2017; Lee et al. 2022) or aquatic environments (Gong et al. 2018).

1.3. *The endless cycle of defense and counter-defense* – Future perspectives for exploring the CRISPR-Cas system in *Ca.* Altiarchaea

CRISPR-Cas systems represent a prokaryotic adaptive immunity mechanism against mobile genetic elements (MGEs), such as viruses or plasmids (Barrangou et al. 2007) and are widely conserved in both bacteria (up to 40%) and almost all archaea (90%) (Makarova et al. 2020) suggests that viruses have effective mechanisms for overcoming this specific barrier. Nowadays, we have begun to realize that virus-virus competition for finding hosts is almost as important as host-virus interactions within ecosystems. For instance, CRISPR-mediated defense systems can also appear to be employed by viruses for interviral conflicts. A recent study on archaeal viruses of the family *Portogloboviridae* that were isolated from a Japanese hot spring showed that *Sulfolobus polyhedral virus* 1 (SPV1) and 2 (SPV2) carry mini-CRISPR arrays with spacers targeting each other (Liu et al. 2018; Medvedeva et al. 2019). Presumably both viruses, the 8.9 kb, and the 20.8 kb (which is also abundant in the MSI), could also fight for the same host that is *Ca.* Altiarchaea. These interviral conflicts could represent a mechanism of heterotypic superinfection exclusion, in which a cell infected by one virus becomes resistant to another closely related virus (Medvedeva et al. 2019). However, we did not study the 20.8 kb virus of *Ca.* Altiarchaea because we focused specifically on the one most abundant 8.9 kb virus Altivir_1_MSI. Nevertheless, it would be

perfect to also study this virus in regard to its viral lifestyle, infection potential, and for investigating interviral conflicts by having probes for the Altivir_1_MSI and Altivir_2_MSI at hand. According to our analysis of Altivir_2_MSI, it seems that this virus becomes more abundant over the last four years (see Manuscript 2: Rahlff et al. 2021, Figure 1). The idea of showing interviral conflicts on a single-cell level represents a new approach of virusFISH that no research to date has yet been investigated. In addition, also investigating the prokaryotic immune system after a successful viral infection by using virusFISH would become a milestone in the field of archaeal virology and would underline the strength of this unique *in situ t*echnique.

Over the past decade, basic insights into CRISPR-Cas mechanisms have only been conducted with *in silico* analysis (*e.g.,* metagenomics) with the ongoing development of new powerful genetic and bioinformatic tools. Until now, it is still unknown whether CRISPR systems interact on single-cell level with viruses in natural biofilms. A visual proof of whether the host's CRISPR-Cas system is active or not during a viral infection would be possible by using imaging techniques for detecting both — spacer (= sequences retained from past viral infections by CRISPR-Cas system) via spacerFISH including CARD-FISH steps, and the *cas* genes via mRNA-FISH. Therefore, attempts could be made to test if CRISPR systems are heterogeneously expressed in *Ca.* Altiarchaea biofilms. First experiments on the were conducted by designing oligonucleotide probes that target the spacers for detecting the expression within *Ca.* Altiarchaea cells (spacerFISH, Figure IV.4).

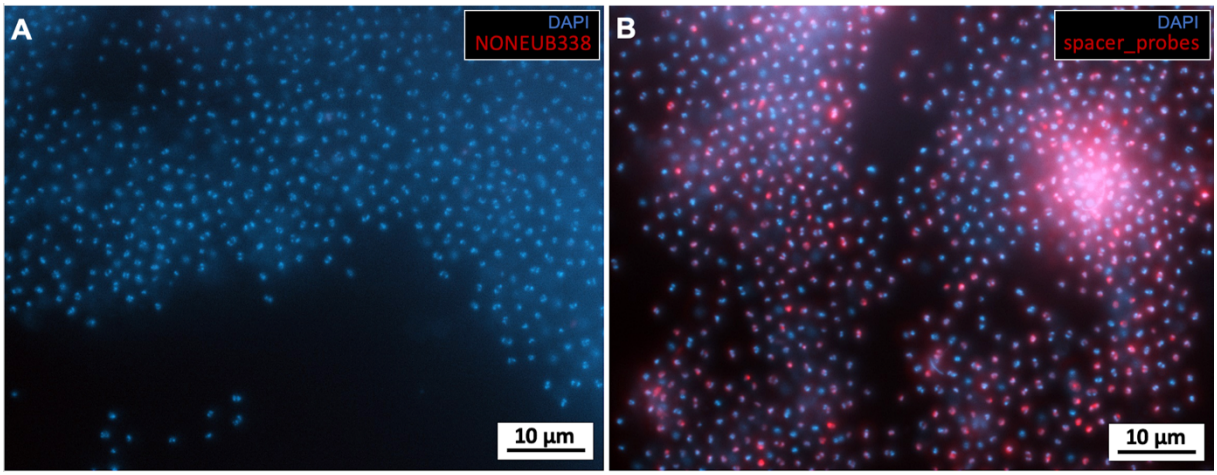

Figure IV.4: Detection of the expression of spacers within *Ca.* Altiarchaea biofilms on single-cell level by using spacerFISH. NONEUB338 probe was used as negative control (A). Putative heterogenous expression of the CRISPR system of *Ca.* Altiarchaea by using eleven spacer probes (B). Biofilm material was analyzed with DAPI (blue, cells, exposure time: 100 ms^{-1}), and Alexa 594 (red, NONEUB338 or spacers, exposure time: 500 ms^{-1}) and merged. Hybridization concentration was 0.001 µM, and one volume of tyramide was added in 500 volumes of amplification buffer. Scale bars: 10 µm.

Figure IV.4 displayed that not every cell has an active CRISPR system. The next step would be designing probes for targeting the *cas* genes and couple these methods with virusFISH. Thus, combining the information derived from metagenomics and imaging techniques (*e.g.,* via virusFISH, spacerFISH, and mRNA-FISH) could bolster our understanding in terms of an active arms race between viruses and their host within ecosystems with a potentially endless cycle of defense and counter-defense.

V. Zusammenfassung

Viren sind allgegenwärtig und wichtige mikrobielle Prädatoren, die nicht nur globale biogeochemische Zyklen beeinflussen, sondern auch die mikrobielle Evolution vorantreiben. Darüber hinaus verursachen Viren eine erhebliche Sterblichkeit prokaryotischer Gemeinschaften, können die Wirtsvielfalt und - abundanz modifizieren, aber auch die genetische Zusammensetzung ihrer Wirte durch horizontalen Gentransfer oder durch Expression viral kodierter Gene während einer Infektion verändern. Über die Rolle von Viren in der tiefen Biosphäre, die das mit Abstand größte Reservoir an organischem Kohlenstoff und einen großen Teil aller Mikroben der Erde beherbergt, die hauptsächlich in Biofilmen leben, ist nur wenig bekannt. Im Vergleich zu verschiedenen Untersuchungen, die sich auf die bakterielle Diversität konzentrieren, sind Studien zu Archaeen der tiefen Biosphäre sehr begrenzt. Kulturunabhängige Methoden, wie die Metagenomik haben gezeigt, dass beispielsweise Archaeen wie *Ca.* Altiarchaea dieses schwer zugängliche Ökosystem dominieren können. Aufgrund der Limitationen konventioneller Kultivierungstechniken bleiben die mikrobielle Verteilung und die Interaktionen von Mikroorganismen z.B. mit Viren, die in solch einem Ökosystemen leben, unverstanden. Die Untersuchung von Virusinfektionen aus der Perspektive eines Archaeums kann unser Verständnis hinsichtlich der räumlichen und zeitlichen Verteilung von Viren, der Auswirkungen auf die gesamte mikrobielle Gemeinschaft, der mikrobiellen Vielfalt, des Nährstoffkreislaufs und des Kohlenstoffkreislaufs der tiefen Biosphäre verbessern.

Das übergeordnete Ziel dieser Studie war es, das aktuelle Wissen über *Ca.* Altiarchaeum und dessen mikrobiellen Interaktionen im tiefen Untergrund zu erweitern. Genauer gesagt konzentrierte sich diese Studie auf eine bestimmte sulfidische Quelle namens „Muehlbacher Schwefelquelle Isling (MSI)“ in Regensburg (Deutschland), die nachweislich fast reine Biofilme enthält, die bis zu 95% aus *Candidatus* A. hamiconexum (*Ca.* A. hamiconexum), einem Primärproduzent des tiefen Untergrunds, bestehen.

In dieser Arbeit berichte ich über einen bestimmten Virus (hier Altivir_1_MSI) der *Ca.* Altiarchaeum infiziert und über dessen jeweiligen viralen Lebensstil. Diese mikrobielle „Beziehung“ blieb bisher unerforscht. Metagenomik gekoppelt mit Fluoreszenz-*in-situ*-Hybridisierung (hier virusFISH) ermöglichte die Untersuchung dieses spezifischen Virus-Wirt-Systems im tiefen Untergrund. Darüber hinaus ist diese Dissertation die erste, die sich

auf Einzelzellebene auf die Virus-Wirt-Interaktionen mittels virusFISH in diesem eher schwer zugänglichen Ökosystem fokussiert. Die Analyse der verschiedenen Infektionsstadien mittels Fluoreszenzmikroskopie ergab anfängliche Infektionen, fortgeschrittene Infektionen und Zelllyse von *Ca.* A. hamiconexum Zellen mit Freisetzung neuer Virionen. Durch diese Verknüpfung und die daraus resultierenden Infektionsstadien konnte ein erster Hinweis auf einen lytischen Replikationszyklus von Altivir_1_MSI erhalten werden. Die virusFISH-Ergebnisse zeigten eine stabile Virus-Wirt-Beziehung über vier Jahre.

Darüber hinaus gehen wir davon aus, dass dieses lytische Virus den heterotrophen Kohlenstoffkreislauf in diesem Ökosystem ankurbeln könnte, indem es als potenzieller Top-Down- und Bottom-Up-Controller fungiert. Anhand verschiedener virusFISH-Bilder konnte eine Ansammlung sulfat-reduzierender Bakterien an Stellen nachweisen werden, an denen eine erfolgreiche Lyse von *Ca.* A. hamiconexum Zellen aufgetreten ist. Durch eine ständige Lyse des Primärproduzenten scheint die „mikrobielle Schleife“ des tiefen Untergrunds durch die Freisetzung möglicher Nährstoffe aktiviert zu werden, die andere Mikroben wie sulfat-reduzierende Bakterien verwerten können.

Insgesamt haben die Ergebnisse und Erkenntnisse dieser Untersuchungen, aus denen sich diese Thesis zusammensetzt, wesentlich zum heutigen Verständnis der Interaktionen zwischen Viren und Archaeen beigetragen und deren Rolle im tiefen Untergrund aufgezeigt. Gleichzeitig konnte gezeigt werden, wie gut diese mikrobiellen Interaktionen in einem schwer zugänglichen Ökosystem mit dem heutigen, aktuellen Stand der Technik untersucht werden können.

VI. Bibliography

A

Abedon, S.T., 2016. Bacteriophage exploitation of bacterial biofilms: phage preference for less mature targets? *FEMS Microbiology Letters* **363**, fnv246. https://doi.org/10.1093/femsle/fnv246.

Abedon, S.T., 2012. Spatial Vulnerability: Bacterial Arrangements, Microcolonies, and Biofilms as Responses to Low Rather than High Phage Densities. *Viruses* **4**, 663–687. https://doi.org/10.3390/v4050663.

Ackermann, H.-W., 2009. Basic Phage Electron Microscopy. In 'Bacteriophages' 'Methods in Molecular Biology' (Eds. Clokie, M.R.J., Kropinski, A.M.). Humana Press, Totowa, NJ, pp. 113–126. https://doi.org/10.1007/978-1-60327-164-6_12.

Ackermann, H.-W., Prangishvili, D., 2012. Prokaryote viruses studied by electron microscopy. *Arch Virol* **157**, 1843–1849. https://doi.org/10.1007/s00705-012-1383-y.

Adriaenssens, E.M., Kramer, R., Van Goethem, M.W., Makhalanyane, T.P., Hogg, I., Cowan, D.A., 2017. Environmental drivers of viral community composition in Antarctic soils identified by viromics. *Microbiome* **5**, 83. https://doi.org/10.1186/s40168-017-0301-7.

Ahlgren, N.A., Fuchsman, C.A., Rocap, G., Fuhrman, J.A., 2019. Discovery of several novel, widespread, and ecologically distinct marine Thaumarchaeota viruses that encode amoC nitrification genes. *ISME J* **13**, 618–631. https://doi.org/10.1038/s41396-018-0289-4.

Alarcón-Schumacher, T., Naor, A., Gophna, U., Erdmann, S., 2022. Isolation of a virus causing a chronic infection in the archaeal model organism Haloferax volcanii reveals antiviral activities of a provirus. *Proceedings of the National Academy of Sciences* **119**, e2205037119. https://doi.org/10.1073/pnas.2205037119.

Allers, E., Moraru, C., Duhaime, M.B., Beneze, E., Solonenko, N., Barrero-Canosa, J., Amann, R., Sullivan, M.B., 2013. Single-cell and population level viral infection dynamics revealed by phageFISH, a method to visualize intracellular and free viruses: phageFISH - visualizing intracellular and free viruses. *Environ Microbiol* **15**, 2306–2318. https://doi.org/10.1111/1462-2920.12100.

Allison, D.P., Mortensen, N.P., Sullivan, C.J., Doktycz, M.J., 2010. Atomic force microscopy of biological samples. *WIREs Nanomed Nanobiotechnol* **2**, 618–634. https://doi.org/10.1002/wnan.104.

Almeida, G.MF., Leppänen, M., Maasilta, I.J., Sundberg, L.-R., 2018. Bacteriophage imaging: past, present and future. *Research in Microbiology* **169**, 488–494. https://doi.org/10.1016/j.resmic.2018.05.006.

Alneberg, J., Bennke, C., Beier, S., Bunse, C., Quince, C., Ininbergs, K., Riemann, L., Ekman, M., Jürgens, K., Labrenz, M., Pinhassi, J., Andersson, A.F., 2020. Ecosystem-wide metagenomic binning enables prediction of ecological niches from genomes. *Communications Biology* **3**, 1–10. https://doi.org/10.1038/s42003-020-0856-x.

Alonso, M.C., Rodríguez, J., Borrego, J.J., 1999. Enumeration and isolation of viral particles from oligotrophic marine environments by tangential flow filtration. *International Microbiology: The Official Journal of the Spanish Society for Microbiology* **2**, 227–232.

Altschul, S.F., Gish, W., Miller, W., Myers, E.W., Lipman, D.J., 1990. Basic local alignment search tool. *Journal of Molecular Biology* **215**, 403–410.

https://doi.org/10.1016/S0022-2836(05)80360-2

Amann, R., Fuchs, B.M., 2008. Single-cell identification in microbial communities by improved fluorescence in situ hybridization techniques. *Nature Reviews Microbiology* **6**, 339–348. https://doi.org/10.1038/nrmicro1888.

Amann, R., Fuchs, B.M., Behrens, S., 2001. The identification of microorganisms by fluorescence in situ hybridisation. *Current Opinion in Biotechnology* **12**, 231–236. https://doi.org/10.1016/S0958-1669(00)00204-4.

Amann, R., Springer, N., Ludwig, W., Görtz, H.D., Schleifer, K.H., 1991. Identification in situ and phylogeny of uncultured bacterial endosymbionts. *Nature* **351**, 161–164. https://doi.org/10.1038/351161a0.

Amann, R.I., Ludwig, W., Schleifer, K.-H., 1995. Phylogenetic Identification and In Situ Detection of Individual Microbial Cells without Cultivation. *MICROBIOL. REV.* **59**, 33.

Anantharaman, K., Brown, C.T., Hug, L.A., Sharon, I., Castelle, C.J., Probst, A.J., Thomas, B.C., Singh, A., Wilkins, M.J., Karaoz, U., Brodie, E.L., Williams, K.H., Hubbard, S.S., Banfield, J.F., 2016. Thousands of microbial genomes shed light on interconnected biogeochemical processes in an aquifer system. *Nat Commun* **7**, 13219. https://doi.org/10.1038/ncomms13219.

Anantharaman, K., Duhaime, M.B., Breier, J.A., Wendt, K.A., Toner, B.M., Dick, G.J., 2014. Sulfur Oxidation Genes in Diverse Deep-Sea Viruses. *Science* **344**, 757–760. https://doi.org/10.1126/science.1252229.

Andany, S.H., Hlawacek, G., Hummel, S., Brillard, C., Kangül, M., Fantner, G.E., 2020. An atomic force microscope integrated with a helium ion microscope for correlative nanoscale characterization. *Beilstein J. Nanotechnol.* **11**, 1272–1279. https://doi.org/10.3762/bjnano.11.111.

Anderson, R.E., Brazelton, W.J., Baross, J.A., 2013. The Deep Viriosphere: Assessing the Viral Impact on Microbial Community Dynamics in the Deep Subsurface. *Reviews in Mineralogy and Geochemistry* **75**, 649–675. https://doi.org/10.2138/rmg.2013.75.20.

Anderson, R.E., Brazelton, W.J., Baross, J.A., 2011. Is the Genetic Landscape of the Deep Subsurface Biosphere Affected by Viruses? *Front. Microbio.* **2**. https://doi.org/10.3389/fmicb.2011.00219.

Anderson, R.E., Sogin, M.L., Baross, J.A., 2014. Evolutionary Strategies of Viruses, Bacteria and Archaea in Hydrothermal Vent Ecosystems Revealed through Metagenomics. *PLoS ONE* **9**, e109696. https://doi.org/10.1371/journal.pone.0109696.

Apprill, A., McNally, S., Parsons, R., Weber, L., 2015. Minor revision to V4 region SSU rRNA 806R gene primer greatly increases detection of SAR11 bacterioplankton. *Aquat. Microb. Ecol.* **75**, 129–137. https://doi.org/10.3354/ame01753.

Athukoralage, J.S., McMahon, S.A., Zhang, C., Grüschow, S., Graham, S., Krupovic, M., Whitaker, R.J., Gloster, T.M., White, M.F., 2020. An anti-CRISPR viral ring nuclease subverts type III CRISPR immunity. *Nature* **577**, 572–575. https://doi.org/10.1038/s41586-019-1909-5.

Attar, N., 2016. Archaeal virus escapology. *Nat Rev Microbiol* **14**, 665–665. https://doi.org/10.1038/nrmicro.2016.147.

Azeredo, J., García, P., Drulis-Kawa, Z., 2021. Targeting biofilms using phages and their enzymes. *Current Opinion in Biotechnology* **68**, 251–261. https://doi.org/10.1016/j.copbio.2021.02.002.

B

Bachrach, U., Friedmann, A., 1971. Practical Procedures for the Purification of Bacterial Viruses. *Applied Microbiology* **22**, 706–715. https://doi.org/10.1128/AEM.22.4.706-715.1971.

Baquero, D.P., Contursi, P., Piochi, M., Bartolucci, S., Liu, Y., Cvirkaite-Krupovic, V., Prangishvili, D., Krupovic, M., 2020. New virus isolates from Italian hydrothermal environments underscore the biogeographic pattern in archaeal virus communities. *ISME J* **14**, 1821–1833. https://doi.org/10.1038/s41396-020-0653-z.

Bard, A.J., Fan, F.-R.F., Pierce, D.T., Unwin, P.R., Wipf, D.O., Zhou, F., 1991. Chemical Imaging of Surfaces with the Scanning Electrochemical Microscope. *Science* **254**, 68–74. https://doi.org/10.1126/science.254.5028.68.

Bar-On, Y.M., Phillips, R., Milo, R., 2018. The biomass distribution on Earth. *Proc. Natl. Acad. Sci. U.S.A.* **115**, 6506–6511. https://doi.org/10.1073/pnas.1711842115.

Barrangou, R., Fremaux, C., Deveau, H., Richards, M., Boyaval, P., Moineau, S., Romero, D.A., Horvath, P., 2007. CRISPR Provides Acquired Resistance Against Viruses in Prokaryotes. *Science* **315**, 1709–1712. https://doi.org/10.1126/science.1138140.

Barrero-Canosa, J., Moraru, C., 2021. Linking Microbes to Their Genes at Single Cell Level with Direct-geneFISH. *Methods Mol Biol* **2246**, 169–205. https://doi.org/10.1007/978-1-0716-1115-9_12.

Barrero-Canosa, J., Moraru, C., 2019. PhageFISH for Monitoring Phage Infections at Single Cell Level: Methods and Protocols, Volume IV. In 'Methods in Molecular Biology (Clifton, N.J.)'. pp. 1–26. https://doi.org/10.1007/978-1-4939-8940-9_1.

Barrero-Canosa, J., Moraru, C., Zeugner, L., Fuchs, B.M., Amann, R., 2017. Direct-geneFISH: a simplified protocol for the simultaneous detection and quantification of genes and rRNA in microorganisms. *Environ Microbiol* **19**, 70–82. https://doi.org/10.1111/1462-2920.13432.

Barrero-Canosa, J., Moraru, C., Zeugner, L., Fuchs, B.M., Amann, R., 2017. Direct-geneFISH: a simplified protocol for the simultaneous detection and quantification of genes and rRNA in microorganisms. *Environ Microbiol* **19**, 70–82. https://doi.org/10.1111/1462-2920.13432.

Barreto-Vieira, D.F., Barth, O.M., 2015. Negative and Positive Staining in Transmission Electron Microscopy for Virus Diagnosis. In 'Microbiology in Agriculture and Human Health' (Ed. Shah, M.M.). InTech. https://doi.org/10.5772/60511.

Bautista, M.A., Black, J.A., Youngblut, N.D., Whitaker, R.J., 2017. Differentiation and Structure in Sulfolobus islandicus Rod-Shaped Virus Populations. *Viruses* **9**, 120. https://doi.org/10.3390/v9050120.

Bell, E., Lamminmäki, T., Alneberg, J., Andersson, A.F., Qian, C., Xiong, W., Hettich, R.L., Frutschi, M., Bernier-Latmani, R., 2020. Active sulfur cycling in the terrestrial deep subsurface. *ISME J* **14**, 1260–1272. https://doi.org/10.1038/s41396-020-0602-x.

Bellas, C.M., Anesio, A.M., Telling, J., Stibal, M., Tranter, M., Davis, S., 2013. Viral impacts on bacterial communities in Arctic cryoconite. *Environ. Res. Lett.* **8**, 045021. https://doi.org/10.1088/1748-9326/8/4/045021.

Belnap, D.M., 2021. Detection of Bacteriophages: Electron Microscopy and Visualization. In 'Bacteriophages' (Eds. Harper, D.R., Abedon, S.T., Burrowes, B.H., McConville, M.L.). Springer International Publishing, Cham, pp. 561–620. https://doi.org/10.1007/978-3-319-41986-2_18.

Berg, I.A., Kockelkorn, D., Ramos-Vera, W.H., Say, R.F., Zarzycki, J., Hügler, M., Alber, B.E., Fuchs, G., 2010. Autotrophic carbon fixation in archaea. *Nat Rev Microbiol* **8**, 447–460. https://doi.org/10.1038/nrmicro2365.

Bergh, Ø., Børsheim, K.Y., Bratbak, G., Heldal, M., 1989. High abundance of viruses found in aquatic environments. *Nature* **340**, 467–468. https://doi.org/10.1038/340467a0.

Berlanga, M., Guerrero, R., 2016. Living together in biofilms: the microbial cell factory and its biotechnological implications. *Microbial Cell Factories* **15**, 165. https://doi.org/10.1186/s12934-016-0569-5.

Bettarel, Y., Sime-Ngando, T., Amblard, C., Laveran, H., 2000. A Comparison of Methods for Counting Viruses in Aquatic Systems. *Applied and Environmental Microbiology* **66**, 2283–2289. https://doi.org/10.1128/AEM.66.6.2283-2289.2000.

Bettstetter, M., Peng, X., Garrett, R.A., Prangishvili, D., 2003. AFV1, a novel virus infecting hyperthermophilic archaea of the genus acidianus. *Virology* **315**, 68–79. https://doi.org/10.1016/S0042-6822(03)00481-1.

Beulig, F., Schubert, F., Adhikari, R.R., Glombitza, C., Heuer, V.B., Hinrichs, K.-U., Homola, K.L., Inagaki, F., Jørgensen, B.B., Kallmeyer, J., Krause, S.J.E., Morono, Y., Sauvage, J., Spivack, A.J., Treude, T., 2022. Rapid metabolism fosters microbial survival in the deep, hot subseafloor biosphere. *Nat. Commun.* **13**, 312. https://doi.org/10.1038/s41467-021-27802-7.

Bhoobalan-Chitty, Y., Johansen, T.B., Di Cianni, N., Peng, X., 2019. Inhibition of Type III CRISPR-Cas Immunity by an Archaeal Virus-Encoded Anti-CRISPR Protein. *Cell* **179**, 448-458.e11. https://doi.org/10.1016/j.cell.2019.09.003.

Biddle, J.F., Lipp, J.S., Lever, M.A., Lloyd, K.G., Sørensen, K.B., Anderson, R., Fredricks, H.F., Elvert, M., Kelly, T.J., Schrag, D.P., Sogin, M.L., Brenchley, J.E., Teske, A., House, C.H., Hinrichs, K.-U., 2006. Heterotrophic Archaea dominate sedimentary subsurface ecosystems off Peru. *Proceedings of the National Academy of Sciences* **103**, 3846–3851. https://doi.org/10.1073/pnas.0600035103.

Bin Jang, H., Bolduc, B., Zablocki, O., Kuhn, J.H., Roux, S., Adriaenssens, E.M., Brister, J.R., Kropinski, A.M., Krupovic, M., Lavigne, R., Turner, D., Sullivan, M.B., 2019. Taxonomic assignment of uncultivated prokaryotic virus genomes is enabled by gene-sharing networks. *Nat Biotechnol* **37**, 632–639. https://doi.org/10.1038/s41587-019-0100-8.

Binnig, G., Quate, C.F., Gerber, Ch., 1986. Atomic Force Microscope. *Phys. Rev. Lett.* **56**, 930–933. https://doi.org/10.1103/PhysRevLett.56.930.

Bird, J.T., Baker, B.J., Probst, A.J., Podar, M., Lloyd, K.G., 2016. Culture Independent Genomic Comparisons Reveal Environmental Adaptations for Altiarchaeales. *Front Microbiol* **7**, 1221. https://doi.org/10.3389/fmicb.2016.01221.

Bischoff, V., Bunk, B., Meier-Kolthoff, J.P., Spröer, C., Poehlein, A., Dogs, M., Nguyen, M., Petersen, J., Daniel, R., Overmann, J., Göker, M., Simon, M., Brinkhoff, T., Moraru, C., 2019. Cobaviruses - a new globally distributed phage group infecting Rhodobacteraceae in marine ecosystems. *ISME J* **13**, 1404–1421. https://doi.org/10.1038/s41396-019-0362-7.

Bize, A., Karlsson, E.A., Ekefjard, K., Quax, T.E.F., Pina, M., Prevost, M.-C., Forterre, P., Tenaillon, O., Bernander, R., Prangishvili, D., 2009. A unique virus release mechanism in the Archaea. *Proceedings of the National Academy of Sciences* **106**, 11306–11311. https://doi.org/10.1073/pnas.0901238106.

Bolduc, B., Jang, H.B., Doulcier, G., You, Z.-Q., Roux, S., Sullivan, M.B., 2017. vConTACT: an iVirus tool to classify double-stranded DNA viruses that infect Archaea and Bacteria. *PeerJ* **5**, e3243. https://doi.org/10.7717/peerj.3243.

Bolduc, B., Shaughnessy, D.P., Wolf, Y.I., Koonin, E.V., Roberto, F.F., Young, M., 2012. Identification of novel positive-strand RNA viruses by metagenomic analysis of archaea-dominated Yellowstone hot springs. *J Virol* **86**, 5562–5573. https://doi.org/10.1128/JVI.07196-11.

Bond, M.C., Vidakovic, L., Singh, P.K., Drescher, K., Nadell, C.D., 2021. Matrix-trapped viruses can prevent invasion of bacterial biofilms by colonizing cells. *eLife* **10**, e65355. https://doi.org/10.7554/eLife.65355.

Bondy-Denomy, J., Pawluk, A., Maxwell, K.L., Davidson, A.R., 2013. Bacteriophage genes that inactivate the CRISPR/Cas bacterial immune system. *Nature* **493**, 429–432. https://doi.org/10.1038/nature11723.

Boratyn, G.M., Schäffer, A.A., Agarwala, R., Altschul, S.F., Lipman, D.J., Madden, T.L., 2012. Domain enhanced lookup time accelerated BLAST. *Biol Direct* **7**, 12. https://doi.org/10.1186/1745-6150-7-12.

Borges, A.L., Davidson, A.R., Bondy-Denomy, J., 2017. The Discovery, Mechanisms, and Evolutionary Impact of Anti-CRISPRs. *Annual Review of Virology* **4**, 37–59. https://doi.org/10.1146/annurev-virology-101416-041616.

Bornemann, T.L.V., Adam, P.S., Turzynski, V., Schreiber, U., Figueroa-Gonzalez, P.A., Rahlff, J., Köster, D., Schmidt, T.C., Schunk, R., Krauthausen, B., Probst, A.J., 2020a. Geological degassing enhances microbial metabolism in the continental subsurface. https://doi.org/10.1101/2020.03.07.980714.

Bornemann, T.L.V., Esser, S.P., Stach, T.L., Burg, T., Probst, A.J., 2020b. uBin – a manual refining tool for metagenomic bins designed for educational purposes. https://doi.org/10.1101/2020.07.15.204776.

Bratbak, G., Heldal, M., Norland, S., Thingstad, T.F., 1990. Viruses as Partners in Spring Bloom Microbial Trophodynamics. *Applied and Environmental Microbiology* **56**, 1400–1405. https://doi.org/10.1128/AEM.56.5.1400-1405.1990.

Breitbart, M., 2012. Marine Viruses: Truth or Dare. *Annu. Rev. Mar. Sci.* **4**, 425–448. https://doi.org/10.1146/annurev-marine-120709-142805.

Breitbart, M., Rohwer, F., 2005. Here a virus, there a virus, everywhere the same virus? *Trends in Microbiology* **13**, 278–284. https://doi.org/10.1016/j.tim.2005.04.003.

Breitbart, M., Thompson, L., Suttle, C., Sullivan, M., 2007. Exploring the Vast Diversity of Marine Viruses. *Oceanog.* **20**, 135–139. https://doi.org/10.5670/oceanog.2007.58.

Briggs, J.A., 2013. Structural biology in situ—the potential of subtomogram averaging. *Current Opinion in Structural Biology* **23**, 261–267. https://doi.org/10.1016/j.sbi.2013.02.003.

Brister, J.R., Ako-Adjei, D., Bao, Y., Blinkova, O., 2015. NCBI viral genomes resource. *Nucleic Acids Res* **43**, D571-577. https://doi.org/10.1093/nar/gku1207.

Brock, T.D., Brock, K.M., Belly, R.T., Weiss, R.L., 1972. Sulfolobus: a new genus of sulfur-oxidizing bacteria living at low pH and high temperature. *Arch Mikrobiol* **84**, 54–68. https://doi.org/10.1007/BF00408082.

Brum, J., Steward, G., Jiang, S., Jellison, R., 2005. Spatial and temporal variability of prokaryotes, viruses, and viral infections of prokaryotes in an alkaline, hypersaline lake. *Aquat. Microb. Ecol.* **41**, 247–260. https://doi.org/10.3354/ame041247.

Brum, J.R., Ignacio-Espinoza, J.C., Roux, S., Doulcier, G., Acinas, S.G., Alberti, A., Chaffron, S., Cruaud, C., de Vargas, C., Gasol, J.M., Gorsky, G., Gregory, A.C., Guidi, L., Hingamp, P., Iudicone, D., Not, F., Ogata, H., Pesant, S., Poulos, B.T., Schwenck, S.M., Speich, S., Dimier, C., Kandels-Lewis, S., Picheral, M., Searson, S., Tara Oceans Coordinators, Bork, P., Bowler, C., Sunagawa, S., Wincker, P., Karsenti, E., Sullivan, M.B., 2015. Patterns and ecological drivers of ocean viral communities. *Science* **348**, 1261498–1261498. https://doi.org/10.1126/science.1261498.

Brum, J.R., Schenck, R.O., Sullivan, M.B., 2013. Global morphological analysis of marine viruses shows minimal regional variation and dominance of non-tailed viruses. *The ISME Journal* **7**, 1738–1751. https://doi.org/10.1038/ismej.2013.67.

Brumfield, S.K., Ortmann, A.C., Ruigrok, V., Suci, P., Douglas, T., Young, M.J., 2009.

Particle Assembly and Ultrastructural Features Associated with Replication of the Lytic Archaeal Virus Sulfolobus Turreted Icosahedral Virus. *JVI* **83**, 5964–5970. https://doi.org/10.1128/JVI.02668-08.

Buchfink, B., Xie, C., Huson, D.H., 2015. Fast and sensitive protein alignment using DIAMOND. *Nature Methods* **12**, 59–60. https://doi.org/10.1038/nmeth.3176.

Budinoff, C.R., Loar, S.N., LeCleir, G.R., Wilhelm, S.W., Buchan, A., 2011. A protocol for enumeration of aquatic viruses by epifluorescence microscopy using Anodisc™ 13 membranes. *BMC Microbiol* **11**, 168. https://doi.org/10.1186/1471-2180-11-168.

Burggraf, S., Huber, H., Stetter, K.O., 1997. Reclassification of the Crenarchaeal Orders and Families in Accordance with 16S rRNA Sequence Data. *International Journal of Systematic Bacteriology* **47**, 657–660. https://doi.org/10.1099/00207713-47-3-657.

Burkert, A., Douglas, T.A., Waldrop, M.P., Mackelprang, R., 2019. Changes in the Active, Dead, and Dormant Microbial Community Structure across a Pleistocene Permafrost Chronosequence. *Appl Environ Microbiol* **85**, e02646-18. https://doi.org/10.1128/AEM.02646-18.

C

Castelle, C.J., Wrighton, K.C., Thomas, B.C., Hug, L.A., Brown, C.T., Wilkins, M.J., Frischkorn, K.R., Tringe, S.G., Singh, A., Markillie, L.M., Taylor, R.C., Williams, K.H., Banfield, J.F., 2015. Genomic expansion of domain archaea highlights roles for organisms from new phyla in anaerobic carbon cycling. *Curr Biol* **25**, 690–701. https://doi.org/10.1016/j.cub.2015.01.014.

Castillo, Y.M., Forn, I., Yau, S., Morán, X.A.G., Alonso-Sáez, L., Arandia-Gorostidi, N., Vaqué, D., Sebastián, M., 2021. Seasonal dynamics of natural Ostreococcus viral infection at the single cell level using VirusFISH. *Environmental Microbiology* **23**, 3009–3019. https://doi.org/10.1111/1462-2920.15504.

Castillo, Y.M., Sebastián, M., Forn, I., Grimsley, N., Yau, S., Moraru, C., Vaqué, D., 2020. Visualization of Viral Infection Dynamics in a Unicellular Eukaryote and Quantification of Viral Production Using Virus Fluorescence in situ Hybridization. *Front. Microbiol.* **11**, 1559. https://doi.org/10.3389/fmicb.2020.01559.

Castresana, J., 2000. Selection of conserved blocks from multiple alignments for their use in phylogenetic analysis. *Mol Biol Evol* **17**, 540–552. https://doi.org/10.1093/oxfordjournals.molbev.a026334.

Chang, J., Liu, X., Rochat, R.H., Baker, M.L., Chiu, W., 2012a. Reconstructing Virus Structures from Nanometer to Near-Atomic Resolutions with Cryo-Electron Microscopy and Tomography. In 'Viral Molecular Machines' 'Advances in Experimental Medicine and Biology' (Eds. Rossmann, M.G., Rao, V.B.). Springer US, Boston, MA, pp. 49–90. https://doi.org/10.1007/978-1-4614-0980-9_4.

Chang, J.T., Schmid, M.F., Haase-Pettingell, C., Weigele, P.R., King, J.A., Chiu, W., 2010. Visualizing the Structural Changes of Bacteriophage Epsilon15 and Its Salmonella Host during Infection. *Journal of Molecular Biology* **402**, 731–740. https://doi.org/10.1016/j.jmb.2010.07.058.

Chang, K.-C., Chiang, Y.-W., Yang, C.-H., Liou, J.-W., 2012b. Atomic force microscopy in biology and biomedicine. *Tzu Chi Medical Journal* **24**, 162–169. https://doi.org/10.1016/j.tcmj.2012.08.002.

Chapelle, F.H., Lovley, D.R., 1990. Rates of Microbial Metabolism in Deep Coastal Plain Aquifers. *Appl Environ Microbiol* **56**, 1865–1874. https://doi.org/10.1128/aem.56.6.1865-1874.1990.

Chen, F., Lu, J. -r., Binder, B.J., Liu, Y. -c., Hodson, R.E., 2001. Application of Digital Image

Analysis and Flow Cytometry To Enumerate Marine Viruses Stained with SYBR Gold. *Applied and Environmental Microbiology* **67**, 539–545. https://doi.org/10.1128/AEM.67.2.539-545.2001.

Chen, I.-M.A., Chu, K., Palaniappan, K., Pillay, M., Ratner, A., Huang, J., Huntemann, M., Varghese, N., White, J.R., Seshadri, R., Smirnova, T., Kirton, E., Jungbluth, S.P., Woyke, T., Eloe-Fadrosh, E.A., Ivanova, N.N., Kyrpides, N.C., 2019a. IMG/M v.5.0: an integrated data management and comparative analysis system for microbial genomes and microbiomes. *Nucleic Acids Res* **47**, D666–D677. https://doi.org/10.1093/nar/gky901.

Chen, X., Ma, R., Yang, Y., Jiao, N., Zhang, R., 2019b. Viral Regulation on Bacterial Community Impacted by Lysis-Lysogeny Switch: A Microcosm Experiment in Eutrophic Coastal Waters. *Frontiers in Microbiology* **10**. https://doi.org/10.3389/fmicb.2019.01763.

Chow, C.-E.T., Winget, D.M., White, R.A., Hallam, S.J., Suttle, C.A., 2015. Combining genomic sequencing methods to explore viral diversity and reveal potential virus-host interactions. *Frontiers in Microbiology* **6**. https://doi.org/10.3389/fmicb.2015.00265.

Corinaldesi, C., Dell'Anno, A., Magagnini, M., Danovaro, R., 2010. Viral decay and viral production rates in continental-shelf and deep-sea sediments of the Mediterranean Sea. *FEMS Microbiology Ecology* **72**, 208–218. https://doi.org/10.1111/j.1574-6941.2010.00840.x.

Costerton, J.W., Cheng, K.J., Geesey, G.G., Ladd, T.I., Nickel, J.C., Dasgupta, M., Marrie, T.J., 1987. Bacterial biofilms in nature and disease. *Annu Rev Microbiol* **41**, 435–464. https://doi.org/10.1146/annurev.mi.41.100187.002251.

Coutinho, F.H., Silveira, C.B., Gregoracci, G.B., Thompson, C.C., Edwards, R.A., Brussaard, C.P.D., Dutilh, B.E., Thompson, F.L., 2017. Marine viruses discovered via metagenomics shed light on viral strategies throughout the oceans. *Nat Commun* **8**, 15955. https://doi.org/10.1038/ncomms15955.

Couvin, D., Bernheim, A., Toffano-Nioche, C., Touchon, M., Michalik, J., Néron, B., Rocha, E.P.C., Vergnaud, G., Gautheret, D., Pourcel, C., 2018. CRISPRCasFinder, an update of CRISRFinder, includes a portable version, enhanced performance and integrates search for Cas proteins. *Nucleic Acids Res* **46**, W246–W251. https://doi.org/10.1093/nar/gky425.

D

Dai, X., Wang, Y., Luo, L., Pfiffner, S.M., Li, G., Dong, Z., Xu, Z., Dong, H., Huang, L., 2021. Detection of the deep biosphere in metamorphic rocks from the Chinese continental scientific drilling. *Geobiology* **19**, 278–291. https://doi.org/10.1111/gbi.12430.

Daly, R.A., Roux, S., Borton, M.A., Morgan, D.M., Johnston, M.D., Booker, A.E., Hoyt, D.W., Meulia, T., Wolfe, R.A., Hanson, A.J., Mouser, P.J., Moore, J.D., Wunch, K., Sullivan, M.B., Wrighton, K.C., Wilkins, M.J., 2019. Viruses control dominant bacteria colonizing the terrestrial deep biosphere after hydraulic fracturing. *Nat Microbiol* **4**, 352–361. https://doi.org/10.1038/s41564-018-0312-6.

Danovaro, R., Dell'Anno, A., Corinaldesi, C., Magagnini, M., Noble, R., Tamburini, C., Weinbauer, M., 2008. Major viral impact on the functioning of benthic deep-sea ecosystems. *Nature* **454**, 1084–1087. https://doi.org/10.1038/nature07268.

Danovaro, R., Dell'Anno, A., Corinaldesi, C., Rastelli, E., Cavicchioli, R., Krupovic, M., Noble, R.T., Nunoura, T., Prangishvili, D., 2016. Virus-mediated archaeal hecatomb in the deep seafloor. *Sci. Adv.* **2**, e1600492. https://doi.org/10.1126/sciadv.1600492.

Danovaro, R., Dell'Anno, A., Trucco, A., Serresi, M., Vanucci, S., 2001. Determination of Virus Abundance in Marine Sediments. *Applied and Environmental Microbiology* **67**, 1384–1387. https://doi.org/10.1128/AEM.67.3.1384-1387.2001.

Daum, B., Quax, T.E.F., Sachse, M., Mills, D.J., Reimann, J., Yildiz, Ö., Häder, S., Saveanu, C., Forterre, P., Albers, S.-V., Kühlbrandt, W., Prangishvili, D., 2014. Self-assembly of the general membrane-remodeling protein PVAP into sevenfold virus-associated pyramids. *Proc Natl Acad Sci USA* **111**, 3829–3834. https://doi.org/10.1073/pnas.1319245111.

Davidson, A.R., Lu, W.-T., Stanley, S.Y., Wang, J., Mejdani, M., Trost, C.N., Hicks, B.T., Lee, J., Sontheimer, E.J., 2020. Anti-CRISPRs: Protein Inhibitors of CRISPR-Cas Systems. *Annual Review of Biochemistry* **89**, 309–332. https://doi.org/10.1146/annurev-biochem-011420-111224.

Davis, B.D., Luger, S.M., Tai, P.C., 1986. Role of ribosome degradation in the death of starved Escherichia coli cells. *J Bacteriol* **166**, 439–445. https://doi.org/10.1128/jb.166.2.439-445.1986.

De Coster, W., D'Hert, S., Schultz, D.T., Cruts, M., Van Broeckhoven, C., 2018. NanoPack: visualizing and processing long-read sequencing data. *Bioinformatics* **34**, 2666–2669. https://doi.org/10.1093/bioinformatics/bty149.

Dellas, N., Snyder, J.C., Bolduc, B., Young, M.J., 2014. Archaeal Viruses: Diversity, Replication, and Structure. *Annu. Rev. Virol.* **1**, 399–426. https://doi.org/10.1146/annurev-virology-031413-085357.

Demina, T.A., Oksanen, H.M., 2020. Pleomorphic archaeal viruses: the family Pleolipoviridae is expanding by seven new species. *Arch Virol* **165**, 2723–2731. https://doi.org/10.1007/s00705-020-04689-1.

Deng, L., Garrett, R.A., Shah, S.A., Peng, X., She, Q., 2013. A novel interference mechanism by a type IIIB CRISPR-Cmr module in Sulfolobus. *Mol Microbiol* **87**, 1088–1099. https://doi.org/10.1111/mmi.12152.

Denman, R.B., 1993. Using RNAFOLD to predict the activity of small catalytic RNAs. *Biotechniques* **15**, 1090–1095.

Dewey, J.S., Savva, C.G., White, R.L., Vitha, S., Holzenburg, A., Young, R., 2010. Micron-scale holes terminate the phage infection cycle. *Proc Natl Acad Sci USA* **107**, 2219–2223. https://doi.org/10.1073/pnas.0914030107.

D'Hondt, S., Jørgensen, B.B., Miller, D.J., Batzke, A., Blake, R., Cragg, B.A., Cypionka, H., Dickens, G.R., Ferdelman, T., Hinrichs, K.-U., Holm, N.G., Mitterer, R., Spivack, A., Wang, G., Bekins, B., Engelen, B., Ford, K., Gettemy, G., Rutherford, S.D., Sass, H., Skilbeck, C.G., Aiello, I.W., Guèrin, G., House, C.H., Inagaki, F., Meister, P., Naehr, T., Niitsuma, S., Parkes, R.J., Schippers, A., Smith, D.C., Teske, A., Wiegel, J., Padilla, C.N., Acosta, J.L.S., 2004. Distributions of Microbial Activities in Deep Subseafloor Sediments. *Science* **306**, 2216–2221. https://doi.org/10.1126/science.1101155.

DiMaio, F., Yu, X., Rensen, E., Krupovic, M., Prangishvili, D., Egelman, E.H., 2015. A virus that infects a hyperthermophile encapsidates A-form DNA. *Science* **348**, 914–917. https://doi.org/10.1126/science.aaa4181.

Dong, X., Greening, C., Brüls, T., Conrad, R., Guo, K., Blaskowski, S., Kaschani, F., Kaiser, M., Laban, N.A., Meckenstock, R.U., 2018. Fermentative Spirochaetes mediate necromass recycling in anoxic hydrocarbon-contaminated habitats. *ISME J* **12**, 2039–2050. https://doi.org/10.1038/s41396-018-0148-3.

Donlan, R.M., 2002. Biofilms: Microbial Life on Surfaces. *Emerg. Infect. Dis.* **8**, 881–890. https://doi.org/10.3201/eid0809.020063.

Doolittle, M.M., Cooney, J.J., Caldwell, D.E., 1995a. Lytic infection of Escherichia coli

biofilms by bacteriophage T4. *Can. J. Microbiol.* **41**, 12–18. https://doi.org/10.1139/m95-002.

Doolittle, M.M., Cooney, J.J., Caldwell, D.E., 1995b. Lytic infection of *Escherichia coli* biofilms by bacteriophage T4. *Can. J. Microbiol.* **41**, 12–18. https://doi.org/10.1139/m95-002.

Dubrovin, E.V., Kirikova, M.N., Novikov, V.K., Drygin, Yu.F., Yaminsky, I.V., 2004. Study of the peculiarities of adhesion of tobacco mosaic virus by atomic force microscopy. *Colloid J* **66**, 673–678. https://doi.org/10.1007/s10595-005-0048-x.

Dubrovin, E.V., Voloshin, A.G., Kraevsky, S.V., Ignatyuk, T.E., Abramchuk, S.S., Yaminsky, I.V., Ignatov, S.G., 2008. Atomic Force Microscopy Investigation of Phage Infection of Bacteria. *Langmuir* **24**, 13068–13074. https://doi.org/10.1021/la8022612.

Dufrene, Y.F., 2002. Atomic Force Microscopy, a Powerful Tool in Microbiology. *Journal of Bacteriology* **184**, 5205–5213. https://doi.org/10.1128/JB.184.19.5205-5213.2002.

Duhaime, M.B., Sullivan, M.B., 2012. Ocean viruses: Rigorously evaluating the metagenomic sample-to-sequence pipeline. *Virology* **434**, 181–186. https://doi.org/10.1016/j.virol.2012.09.036.

E

Edgar, R.C., 2004. MUSCLE: a multiple sequence alignment method with reduced time and space complexity. *BMC Bioinformatics* **5**, 113. https://doi.org/10.1186/1471-2105-5-113.

Emerson, J.B., Roux, S., Brum, J.R., Bolduc, B., Woodcroft, B.J., Jang, H.B., Singleton, C.M., Solden, L.M., Naas, A.E., Boyd, J.A., Hodgkins, S.B., Wilson, R.M., Trubl, G., Li, C., Frolking, S., Pope, P.B., Wrighton, K.C., Crill, P.M., Chanton, J.P., Saleska, S.R., Tyson, G.W., Rich, V.I., Sullivan, M.B., 2018. Host-linked soil viral ecology along a permafrost thaw gradient. *Nat Microbiol* **3**, 870–880. https://doi.org/10.1038/s41564-018-0190-y.

Engelhardt, T., Kallmeyer, J., Cypionka, H., Engelen, B., 2014a. High virus-to-cell ratios indicate ongoing production of viruses in deep subsurface sediments. *ISME J* **8**, 1503–1509. https://doi.org/10.1038/ismej.2013.245.

Engelhardt, T., Sahlberg, M., Cypionka, H., Engelen, B., 2013. Biogeography of Rhizobium radiobacter and distribution of associated temperate phages in deep subseafloor sediments. *ISME J* **7**, 199–209. https://doi.org/10.1038/ismej.2012.92.

Engelhardt, T., Sahlberg, M., Cypionka, H., Engelen, B., 2011. Induction of prophages from deep-subseafloor bacteria: Phages in the deep-subseafloor. *Environmental Microbiology Reports* **3**, 459–465. https://doi.org/10.1111/j.1758-2229.2010.00232.x.

Escudero, C., Oggerin, M., Amils, R., 2018. The deep continental subsurface: the dark biosphere. *Int Microbiol* **21**, 3–14. https://doi.org/10.1007/s10123-018-0009-y.

F

Farley, M.M., Tu, J., Kearns, D.B., Molineux, I.J., Liu, J., 2017. Ultrastructural analysis of bacteriophage Φ29 during infection of Bacillus subtilis. *Journal of Structural Biology* **197**, 163–171. https://doi.org/10.1016/j.jsb.2016.07.019.

Fernández, L., Rodríguez, A., García, P., 2018. Phage or foe: an insight into the impact of viral predation on microbial communities. *ISME J* **12**, 1171–1179. https://doi.org/10.1038/s41396-018-0049-5.

Ferriol-González, C., Domingo-Calap, P., 2020. Phages for Biofilm Removal. *Antibiotics (Basel)* **9**, 268. https://doi.org/10.3390/antibiotics9050268.

Finn, R.D., Attwood, T.K., Babbitt, P.C., Bateman, A., Bork, P., Bridge, A.J., Chang, H.-Y., Dosztányi, Z., El-Gebali, S., Fraser, M., Gough, J., Haft, D., Holliday, G.L., Huang, H., Huang, X., Letunic, I., Lopez, R., Lu, S., Marchler-Bauer, A., Mi, H., Mistry, J., Natale, D.A., Necci, M., Nuka, G., Orengo, C.A., Park, Y., Pesseat, S., Piovesan, D., Potter, S.C., Rawlings, N.D., Redaschi, N., Richardson, L., Rivoire, C., Sangrador-Vegas, A., Sigrist, C., Sillitoe, I., Smithers, B., Squizzato, S., Sutton, G., Thanki, N., Thomas, P.D., Tosatto, S.C.E., Wu, C.H., Xenarios, I., Yeh, L.-S., Young, S.-Y., Mitchell, A.L., 2017. InterPro in 2017-beyond protein family and domain annotations. *Nucleic Acids Res* **45**, D190–D199. https://doi.org/10.1093/nar/gkw1107.

Finster, K., Liesack, W., Thamdrup, B., 1998. Elemental Sulfur and Thiosulfate Disproportionation by Desulfocapsa sulfoexigens sp. nov., a New Anaerobic Bacterium Isolated from Marine Surface Sediment. *Appl Environ Microbiol* **64**, 119–125. https://doi.org/10.1128/AEM.64.1.119-125.1998.

Flechsler, J., Heimerl, T., Pickl, C., Rachel, R., Stierhof, Y.-D., Klingl, A., 2020. 2D and 3D immunogold localization on (epoxy) ultrathin sections with and without osmium tetroxide. *Microscopy Research and Technique* **83**, 691–705. https://doi.org/10.1002/jemt.23459.

Flemming, H.-C., 2016. EPS-Then and Now. *Microorganisms* **4**, 41. https://doi.org/10.3390/microorganisms4040041.

Flemming, H.-C., Neu, T.R., Wozniak, D.J., 2007. The EPS Matrix: The "House of Biofilm Cells". *J Bacteriol* **189**, 7945–7947. https://doi.org/10.1128/JB.00858-07.

Flemming, H.-C., Wingender, J., 2010. The biofilm matrix. *Nat Rev Microbiol* **8**, 623–633. https://doi.org/10.1038/nrmicro2415.

Flemming, H.-C., Wuertz, S., 2019. Bacteria and archaea on Earth and their abundance in biofilms. *Nat Rev Microbiol* **17**, 247–260. https://doi.org/10.1038/s41579-019-0158-9.

Flemming, H.-C., van Hullebusch, E.D., Neu, T.R., Nielsen, P.H., Seviour, T., Stoodley, P., Wingender, J., Wuertz, S., 2023. The biofilm matrix: multitasking in a shared space. *Nat. Rev. Microbiol.* **21**, 70–86. https://doi.org/10.1038/s41579-022-00791-0.

Florent, P., Cauchie, H.-M., Herold, M., Jacquet, S., Ogorzaly, L., 2022. Soil pH, Calcium Content and Bacteria as Major Factors Responsible for the Distribution of the Known Fraction of the DNA Bacteriophage Populations in Soils of Luxembourg. *Microorganisms* **10**, 1458. https://doi.org/10.3390/microorganisms10071458.

Ford, T., Graham, J., Rickwood, D., 1994. Iodixanol: A Nonionic Iso-osmotic Centrifugation Medium for the Formation of Self-Generated Gradients. *Analytical Biochemistry* **220**, 360–366. https://doi.org/10.1006/abio.1994.1350.

Forterre, P., Soler, N., Krupovic, M., Marguet, E., Ackermann, H.-W., 2013. Fake virus particles generated by fluorescence microscopy. *Trends in Microbiology* **21**, 1–5. https://doi.org/10.1016/j.tim.2012.10.005.

Fouladvand, F., Bemani, P., Mohammadi, M., Amini, R., Azizi Jalilian, F., 2020. A Review of the Methods for Concentrating M13 Phage. *J Apple Biotechnol Rep* **7**. https://doi.org/10.30491/jabr.2020.105916.

Fredrickson, J.K., Mckinley, J.P., Nierzwicki-Bauer, S.A., White, D.C., Ringelberg, D.B., Rawson, S.A., Li, S.-M., Brockman, F.J., Bjornstad, B.N., 1995. Microbial community structure and biogeochemistry of Miocene subsurface sediments: implications for long-term microbial survival. *Molecular Ecology* **4**, 619–626. https://doi.org/10.1111/j.1365-294X.1995.tb00262.x.

Fridman, S., Flores-Uribe, J., Larom, S., Alalouf, O., Liran, O., Yacoby, I., Salama, F., Bailleul, B., Rappaport, F., Ziv, T., Sharon, I., Cornejo-Castillo, F.M., Philosof, A., Dupont, C.L., Sánchez, P., Acinas, S.G., Rohwer, F.L., Lindell, D., Béjà, O., 2017. A myovirus encoding both photosystem I and II proteins enhances cyclic electron flow

in infected Prochlorococcus cells. *Nat Microbiol* **2**, 1350–1357. https://doi.org/10.1038/s41564-017-0002-9.

Fry, J.C., Parkes, R.J., Cragg, B.A., Weightman, A.J., Webster, G., 2008. Prokaryotic biodiversity and activity in the deep subseafloor biosphere: Diversity and activity in the deep subseafloor biosphere. *FEMS Microbiology Ecology* **66**, 181–196. https://doi.org/10.1111/j.1574-6941.2008.00566.x.

Fuhrman, J.A., 1999a. Marine viruses and their biogeochemical and ecological effects. *Nature* **399**, 541–548. https://doi.org/10.1038/21119.

G

Gao, Y., Lu, Y., Dungait, J.A.J., Liu, J., Lin, S., Jia, J., Yu, G., 2022. The "Regulator" Function of Viruses on Ecosystem Carbon Cycling in the Anthropocene. *Front. Public Health* **10**, 858615. https://doi.org/10.3389/fpubh.2022.858615.

Göker, M., García-Blázquez, G., Voglmayr, H., Tellería, M.T., Martín, M.P., 2009. Molecular taxonomy of phytopathogenic fungi: a case study in Peronospora. *PLoS One* **4**, e6319. https://doi.org/10.1371/journal.pone.0006319.

Gong, Z., Liang, Y., Wang, M., Jiang, Y., Yang, Q., Xia, J., Zhou, X., You, S., Gao, C., Wang, J., He, J., Shao, H., McMinn, A., 2018. Viral Diversity and Its Relationship With Environmental Factors at the Surface and Deep Sea of Prydz Bay, Antarctica. *Frontiers in Microbiology* **9**. https://doi.org/10.3389/fmicb.2018.02981.

Grazziotin, A.L., Koonin, E.V., Kristensen, D.M., 2017. Prokaryotic Virus Orthologous Groups (pVOGs): a resource for comparative genomics and protein family annotation. *Nucleic Acids Res* **45**, D491–D498. https://doi.org/10.1093/nar/gkw975.

Gudbergsdóttir, S.R., Menzel, P., Krogh, A., Young, M., Peng, X., 2016. Novel viral genomes identified from six metagenomes reveal wide distribution of archaeal viruses and high viral diversity in terrestrial hot springs: Novel viral genomes from acidic hot springs. *Environ Microbiol* **18**, 863–874. https://doi.org/10.1111/1462-2920.13079.

Guerrero-Ferreira, R.C., Wright, E.R., 2013. Cryo-electron tomography of bacterial viruses. *Virology* **435**, 179–186. https://doi.org/10.1016/j.virol.2012.08.022.

Guindon, S., Dufayard, J.-F., Lefort, V., Anisimova, M., Hordijk, W., Gascuel, O., 2010. New algorithms and methods to estimate maximum-likelihood phylogenies: assessing the performance of PhyML 3.0. *Syst Biol* **59**, 307–321. https://doi.org/10.1093/sysbio/syq010.

Guo, T., Han, W., She, Q., 2019. Tolerance of Sulfolobus SMV1 virus to the immunity of I-A and III-B CRISPR-Cas systems in Sulfolobus islandicus. *RNA Biol* **16**, 549–556. https://doi.org/10.1080/15476286.2018.1460993.

Gutiérrez, D., Fernández, L., Martínez, B., Ruas-Madiedo, P., García, P., Rodríguez, A., 2017. Real-Time Assessment of Staphylococcus aureus Biofilm Disruption by Phage-Derived Proteins. *Frontiers in Microbiology* **8**. https://doi.org/10.3389/fmicb.2017.01632.

Guy, L., Kultima, J.R., Andersson, S.G.E., 2010. genoPlotR: comparative gene and genome visualization in R. *Bioinformatics* **26**, 2334–2335. https://doi.org/10.1093/bioinformatics/btq413.

H

Hall, R.J., Whelan, F.J., McInerney, J.O., Ou, Y., Domingo-Sananes, M.R., 2020. Horizontal Gene Transfer as a Source of Conflict and Cooperation in Prokaryotes. *Front.*

Microbiol. **11**, 1569. https://doi.org/10.3389/fmicb.2020.01569.

Hanlon, G.W., Denyer, S.P., Olliff, C.J., Ibrahim, L.J., 2001. Reduction in exopolysaccharide viscosity as an aid to bacteriophage penetration through Pseudomonas aeruginosa biofilms. *Appl Environ Microbiol* **67**, 2746–2753. https://doi.org/10.1128/AEM.67.6.2746-2753.2001.

Hansen, M.F., Svenningsen, S.L., Røder, H.L., Middelboe, M., Burmølle, M., 2019. Big Impact of the Tiny: Bacteriophage-Bacteria Interactions in Biofilms. *Trends Microbiol* **27**, 739–752. https://doi.org/10.1016/j.tim.2019.04.006.

Hansma, P., Drake, B., Marti, O., Gould, S., Prater, C., 1989. The scanning ion-conductance microscope. *Science* **243**, 641–643. https://doi.org/10.1126/science.2464851.

Hara, S., Terauchi, K., Koike, I., 1991. Abundance of Viruses in Marine Waters: Assessment by Epifluorescence and Transmission Electron Microscopy. *Applied and Environmental Microbiology* **57**, 2731–2734. https://doi.org/10.1128/AEM.57.9.2731-2734.1991.

Häring, M., Vestergaard, G., Rachel, R., Chen, L., Garrett, R.A., Prangishvili, D., 2005. Independent virus development outside a host. *Nature* **436**, 1101–1102. https://doi.org/10.1038/4361101a.

Hatoum-Aslan, A., Howell, O.G., 2021. CRISPR-Cas Systems and Anti-CRISPR Proteins: Adaptive Defense and Counter-Defense in Prokaryotes and Their Viruses. In 'Encyclopedia of Virology'. Elsevier, pp. 242–251. https://doi.org/10.1016/B978-0-12-809633-8.20962-X.

Hauser, M., Wojcik, M., Kim, D., Mahmoudi, M., Li, W., Xu, K., 2017. Correlative Super-Resolution Microscopy: New Dimensions and New Opportunities. *Chem. Rev.* **117**, 7428–7456. https://doi.org/10.1021/acs.chemrev.6b00604.

Haveman, S.A., Pedersen, K., Ruotsalainen, P., 1999. Distribution and metabolic diversity of microorganisms in deep igneous rock aquifers of Finland. *Geomicrobiology Journal* **16**, 277–294. https://doi.org/10.1080/014904599270541.

He, F., Bhoobalan-Chitty, Y., Van, L.B., Kjeldsen, A.L., Dedola, M., Makarova, K.S., Koonin, E.V., Brodersen, D.E., Peng, X., 2018. Anti-CRISPR proteins encoded by archaeal lytic viruses inhibit subtype I-D immunity. *Nat Microbiol* **3**, 461–469. https://doi.org/10.1038/s41564-018-0120-z.

Held, N.L., Whitaker, R.J., 2009. Viral biogeography revealed by signatures in Sulfolobus islandicus genomes. *Environ Microbiol* **11**, 457–466. https://doi.org/10.1111/j.1462-2920.2008.01784.x.

Henneberger, R., Moissl, C., Amann, T., Rudolph, C., Huber, R., 2006. New Insights into the Lifestyle of the Cold-Loving SM1 Euryarchaeon: Natural Growth as a Monospecies Biofilm in the Subsurface. *Appl Environ Microbiol* **72**, 192–199. https://doi.org/10.1128/AEM.72.1.192-199.2006.

Hennes, K.P., Suttle, C.A., 1995. Direct counts of viruses in natural waters and laboratory cultures by epifluorescence microscopy. *Limnol. Oceanogr.* **40**, 1050–1055. https://doi.org/10.4319/lo.1995.40.6.1050.

Hernsdorf, A.W., Amano, Y., Miyakawa, K., Ise, K., Suzuki, Y., Anantharaman, K., Probst, A., Burstein, D., Thomas, B.C., Banfield, J.F., 2017. Potential for microbial H2 and metal transformations associated with novel bacteria and archaea in deep terrestrial subsurface sediments. *ISME J* **11**, 1915–1929. https://doi.org/10.1038/ismej.2017.39.

Hibbing, M.E., Fuqua, C., Parsek, M.R., Peterson, S.B., 2010. Bacterial competition: surviving and thriving in the microbial jungle. *Nat Rev Microbiol* **8**, 15–25. https://doi.org/10.1038/nrmicro2259.

Hills, G.J., Plaskitt, K.A., Young, N.D., Dunigan, D.D., Watts, J.W., Wilson, T.M.A., Zaitlin, M., 1987. Immunogold localization of the intracellular sites of structural and

nonstructural tobacco mosaic virus proteins. *Virology* **161**, 488–496. https://doi.org/10.1016/0042-6822(87)90143-7.

Hochstein, R., Bollschweiler, D., Engelhardt, H., Lawrence, C.M., Young, M., 2015. Large Tailed Spindle Viruses of Archaea: a New Way of Doing Viral Business. *J. Virol.* **89**, 9146–9149. https://doi.org/10.1128/JVI.00612-15.

Hochstein, R.A., Amenabar, M.J., Munson-McGee, J.H., Boyd, E.S., Young, M.J., 2016. Acidianus Tailed Spindle Virus: a New Archaeal Large Tailed Spindle Virus Discovered by Culture-Independent Methods. *J. Virol.* **90**, 3458–3468. https://doi.org/10.1128/JVI.03098-15.

Holmfeldt, K., Nilsson, E., Simone, D., Lopez-Fernandez, M., Wu, X., de Bruijn, I., Lundin, D., Andersson, A.F., Bertilsson, S., Dopson, M., 2021. The Fennoscandian Shield deep terrestrial virosphere suggests slow motion 'boom and burst' cycles. *Commun Biol* **4**, 307. https://doi.org/10.1038/s42003-021-01810-1.

Holmfeldt, K., Odić, D., Sullivan, M.B., Middelboe, M., Riemann, L., 2012. Cultivated Single-Stranded DNA Phages That Infect Marine Bacteroidetes Prove Difficult To Detect with DNA-Binding Stains. *Appl. Environ. Microbiol.* **78**, 892–894. https://doi.org/10.1128/AEM.06580-11.

Hong, C., Pietilä, M.K., Fu, C.J., Schmid, M.F., Bamford, D.H., Chiu, W., 2015. Lemon-shaped halo archaeal virus His1 with uniform tail but variable capsid structure. *Proc Natl Acad Sci USA* **112**, 2449–2454. https://doi.org/10.1073/pnas.1425008112.

Horvath, P., Barrangou, R., 2010. CRISPR/Cas, the Immune System of Bacteria and Archaea. *Science* **327**, 167–170. https://doi.org/10.1126/science.1179555.

Howard-Varona, C., Hargreaves, K.R., Abedon, S.T., Sullivan, M.B., 2017. Lysogeny in nature: mechanisms, impact and ecology of temperate phages. *ISME J* **11**, 1511–1520. https://doi.org/10.1038/ismej.2017.16.

Hu, B., Margolin, W., Molineux, I.J., Liu, J., 2015. Structural remodeling of bacteriophage T4 and host membranes during infection initiation. *Proc Natl Acad Sci USA* **112**, E4919–E4928. https://doi.org/10.1073/pnas.1501064112.

Hu, B., Margolin, W., Molineux, I.J., Liu, J., 2013. The bacteriophage t7 virion undergoes extensive structural remodeling during infection. *Science* **339**, 576–579. https://doi.org/10.1126/science.1231887.

Hubalek, V., Wu, X., Eiler, A., Buck, M., Heim, C., Dopson, M., Bertilsson, S., Ionescu, D., 2016. Connectivity to the surface determines diversity patterns in subsurface aquifers of the Fennoscandian shield. *ISME J* **10**, 2447–2458. https://doi.org/10.1038/ismej.2016.36.

Hug, L.A., Baker, B.J., Anantharaman, K., Brown, C.T., Probst, A.J., Castelle, C.J., Butterfield, C.N., Hernsdorf, A.W., Amano, Y., Ise, K., Suzuki, Y., Dudek, N., Relman, D.A., Finstad, K.M., Amundson, R., Thomas, B.C., Banfield, J.F., 2016. A new view of the tree of life. *Nat Microbiol* **1**, 16048. https://doi.org/10.1038/nmicrobiol.2016.48.

Hügler, M., Sievert, S.M., 2011. Beyond the Calvin Cycle: Autotrophic Carbon Fixation in the Ocean. *Annual Review of Marine Science* **3**, 261–289. https://doi.org/10.1146/annurev-marine-120709-142712.

Hurwitz, B.L., Deng, L., Poulos, B.T., Sullivan, M.B., 2013. Evaluation of methods to concentrate and purify ocean virus communities through comparative, replicated metagenomics: Viral community concentration and purification. *Environmental Microbiology* **15**, 1428–1440. https://doi.org/10.1111/j.1462-2920.2012.02836.x.

Hyatt, D., Chen, G.-L., LoCascio, P.F., Land, M.L., Larimer, F.W., Hauser, L.J., 2010. Prodigal: prokaryotic gene recognition and translation initiation site identification. *BMC Bioinformatics* **11**, 119. https://doi.org/10.1186/1471-2105-11-119.

Hylling, O., Carstens, A.B., Kot, W., Hansen, M., Neve, H., Franz, C.M.A.P., Johansen, A., Ellegaard-Jensen, L., Hansen, L.H., 2020. Two novel bacteriophage genera from a groundwater reservoir highlight subsurface environments as underexplored biotopes in bacteriophage ecology. *Sci Rep* **10**, 11879. https://doi.org/10.1038/s41598-020-68389-1.

I

Ino, K., Hernsdorf, A.W., Konno, U., Kouduka, M., Yanagawa, K., Kato, S., Sunamura, M., Hirota, A., Togo, Y.S., Ito, K., Fukuda, A., Iwatsuki, T., Mizuno, T., Komatsu, D.D., Tsunogai, U., Ishimura, T., Amano, Y., Thomas, B.C., Banfield, J.F., Suzuki, Y., 2018. Ecological and genomic profiling of anaerobic methane-oxidizing archaea in a deep granitic environment. *ISME J* **12**, 31–47. https://doi.org/10.1038/ismej.2017.140.

Iranzo, J., Faure, G., Wolf, Y.I., Koonin, E.V., 2020. Game-Theoretical Modeling of Interviral Conflicts Mediated by Mini-CRISPR Arrays. *Front Microbiol* **11**, 381. https://doi.org/10.3389/fmicb.2020.00381.

Iranzo, J., Koonin, E.V., Prangishvili, D., Krupovic, M., 2016. Bipartite Network Analysis of the Archaeal Virosphere: Evolutionary Connections between Viruses and Capsidless Mobile Elements. *J Virol* **90**, 11043–11055. https://doi.org/10.1128/JVI.01622-16.

Irwin, N.A.T., Pittis, A.A., Richards, T.A., Keeling, P.J., 2021. Systematic evaluation of horizontal gene transfer between eukaryotes and viruses. *Nat. Microbiol.* **7**, 327–336. https://doi.org/10.1038/s41564-021-01026-3.

J

Jägevall, S., Rabe, L., Pedersen, K., 2011. Abundance and diversity of biofilms in natural and artificial aquifers of the Äspö Hard Rock Laboratory, Sweden. *Microb Ecol* **61**, 410–422. https://doi.org/10.1007/s00248-010-9761-z.

Jahn, M.T., Lachnit, T., Markert, S.M., Stigloher, C., Pita, L., Ribes, M., Dutilh, B.E., Hentschel, U., 2021. Lifestyle of sponge symbiont phages by host prediction and correlative microscopy. *ISME J*. https://doi.org/10.1038/s41396-021-00900-6.

Janekovic, D., Wunderl, S., Holz, I., Zillig, W., Gierl, A., Neumann, H., 1983. TTV1, TTV2 and TTV3, a family of viruses of the extremely thermophilic, anaerobic, sulfur reducing archaebacterium Thermoproteus tenax. *Molec Gen Genet* **192**, 39–45. https://doi.org/10.1007/BF00327644.

Jarett, J.K., Džunková, M., Schulz, F., Roux, S., Paez-Espino, D., Eloe-Fadrosh, E., Jungbluth, S.P., Ivanova, N., Spear, J.R., Carr, S.A., Trivedi, C.B., Corsetti, F.A., Johnson, H.A., Becraft, E., Kyrpides, N., Stepanauskas, R., Woyke, T., 2020. Insights into the dynamics between viruses and their hosts in a hot spring microbial mat. *ISME J* **14**, 2527–2541. https://doi.org/10.1038/s41396-020-0705-4.

Jasna, V., Pradeep Ram, A.S., Parvathi, A., Sime-Ngando, T., 2018. Differential impact of lytic viruses on prokaryotic morphopopulations in a tropical estuarine system (Cochin estuary, India). *PLoS ONE* **13**, e0194020. https://doi.org/10.1371/journal.pone.0194020.

Jiao, J.-Y., Liu, L., Hua, Z.-S., Fang, B.-Z., Zhou, E.-M., Salam, N., Hedlund, B.P., Li, W.-J., 2021. Microbial dark matter coming to light: challenges and opportunities. *National Science Review* **8**, nwaa280. https://doi.org/10.1093/nsr/nwaa280.

John, S.G., Mendez, C.B., Deng, L., Poulos, B., Kauffman, A.K.M., Kern, S., Brum, J., Polz, M.F., Boyle, E.A., Sullivan, M.B., 2011. A simple and efficient method for concentration of ocean viruses by chemical flocculation: Virus concentration by

flocculation with iron. *Environmental Microbiology Reports* **3**, 195–202. https://doi.org/10.1111/j.1758-2229.2010.00208.x.

Jones, R.M., Goordial, J.M., Orcutt, B.N., 2018. Low Energy Subsurface Environments as Extraterrestrial Analogs. *Frontiers in Microbiology* **9**.

Jørgensen, B.B., 2011. Deep subseafloor microbial cells on physiological standby. *Proc. Natl. Acad. Sci. U.S.A.* **108**, 18193–18194. https://doi.org/10.1073/pnas.1115421108.

Jørgensen, B.B., Parkes, R.J., 2010. Role of sulfate reduction and methane production by organic carbon degradation in eutrophic fjord sediments (Limfjorden, Denmark). *Limnol. Oceanogr.* **55**, 1338–1352. https://doi.org/10.4319/lo.2010.55.3.1338.

Jørgensen, B.B., Marshall, I.P.G., 2016. Slow Microbial Life in the Seabed. *Annual Review of Marine Science* **8**, 311–332. https://doi.org/10.1146/annurev-marine-010814-015535

Joshi, N., Fass, J., 2011. Sickle: A sliding-window, adaptive, quality-based trimming tool for FastQ files (Version 1.33)[Software].

Joshi, R.V., Gunawan, C., Mann, R., 2021. We Are One: Multispecies Metabolism of a Biofilm Consortium and Their Treatment Strategies. *Frontiers in Microbiology* **12**. https://doi.org/10.3389/fmicb.2021.635432.

K

Kallmeyer, J., Pockalny, R., Adhikari, R.R., Smith, D.C., D'Hondt, S., 2012. Global distribution of microbial abundance and biomass in subseafloor sediment. *Proc. Natl. Acad. Sci. U.S.A.* **109**, 16213–16216. https://doi.org/10.1073/pnas.1203849109.

Kausche, G.A., Pfankuch, E., Ruska, H., 1939. Die Sichtbarmachung von pflanzlichem Virus im Übermikroskop. *Naturwissenschaften* **27**, 292–299. https://doi.org/10.1007/BF01493353.

Kearse, M., Moir, R., Wilson, A., Stones-Havas, S., Cheung, M., Sturrock, S., Buxton, S., Cooper, A., Markowitz, S., Duran, C., Thierer, T., Ashton, B., Meintjes, P., Drummond, A., 2012. Geneious Basic: an integrated and extendable desktop software platform for the organization and analysis of sequence data. *Bioinformatics* **28**, 1647–1649. https://doi.org/10.1093/bioinformatics/bts199.

Kendrick, B.J., DiTullio, G.R., Cyronak, T.J., Fulton, J.M., Mooy, B.A.S.V., Bidle, K.D., 2014. Temperature-Induced Viral Resistance in Emiliania huxleyi (Prymnesiophyceae). *PLOS ONE* **9**, e112134. https://doi.org/10.1371/journal.pone.0112134.

Kenzaka, T., Tamaki, S., Yamaguchi, N., Tani, K., Nasu, M., 2005. Recognition of Individual Genes in Diverse Microorganisms by Cycling Primed In Situ Amplification. *Applied and Environmental Microbiology* **71**, 7236–7244. https://doi.org/10.1128/AEM.71.11.7236-7244.2005.

Kenzaka, T., Tani, K., Nasu, M., 2010. High-frequency phage-mediated gene transfer in freshwater environments determined at single-cell level. *ISME J* **4**, 648–659. https://doi.org/10.1038/ismej.2009.145.

Kieft, K., Breister, A.M., Huss, P., Linz, A.M., Zanetakos, E., Zhou, Z., Rahlff, J., Esser, S.P., Probst, A.J., Raman, S., Roux, S., Anantharaman, K., 2021. Virus-associated organosulfur metabolism in human and environmental systems. *Cell Rep* **36**, 109471. https://doi.org/10.1016/j.celrep.2021.109471.

Kieft, K., Zhou, Z., Anantharaman, K., 2019. VIBRANT: Automated recovery, annotation and curation of microbial viruses, and evaluation of virome function from genomic sequences. *bioRxiv* 855387. https://doi.org/10.1101/855387.

Kim, J.-G., Kim, S.-J., Cvirkaite-Krupovic, V., Yu, W.-J., Gwak, J.-H., López-Pérez, M., Rodriguez-Valera, F., Krupovic, M., Cho, J.-C., Rhee, S.-K., 2019. Spindle-shaped

viruses infect marine ammonia-oxidizing thaumarchaea. *Proc Natl Acad Sci U S A* **116**, 15645–15650. https://doi.org/10.1073/pnas.1905682116.

Knierim, B., Luef, B., Wilmes, P., Webb, R.I., Auer, M., Comolli, L.R., Banfield, J.F., 2012. Correlative microscopy for phylogenetic and ultrastructural characterization of microbial communities: Correlative TEM and CARD-FISH imaging. *Environmental Microbiology Reports* **4**, 36–41. https://doi.org/10.1111/j.1758-2229.2011.00275.x.

Knowles, B., Silveira, C.B., Bailey, B.A., Barott, K., Cantu, V.A., Cobián-Güemes, A.G., Coutinho, F.H., Dinsdale, E.A., Felts, B., Furby, K.A., George, E.E., Green, K.T., Gregoracci, G.B., Haas, A.F., Haggerty, J.M., Hester, E.R., Hisakawa, N., Kelly, L.W., Lim, Y.W., Little, M., Luque, A., McDole-Somera, T., McNair, K., de Oliveira, L.S., Quistad, S.D., Robinett, N.L., Sala, E., Salamon, P., Sanchez, S.E., Sandin, S., Silva, G.G.Z., Smith, J., Sullivan, C., Thompson, C., Vermeij, M.J.A., Youle, M., Young, C., Zgliczynski, B., Brainard, R., Edwards, R.A., Nulton, J., Thompson, F., Rohwer, F., 2016. Lytic to temperate switching of viral communities. *Nature* **531**, 466–470. https://doi.org/10.1038/nature17193.

Kodama, Y., Watanabe, K., 2004. Sulfuricurvum kujiense gen. nov., sp. nov., a facultatively anaerobic, chemolithoautotrophic, sulfur-oxidizing bacterium isolated from an underground crude-oil storage cavity. *International Journal of Systematic and Evolutionary Microbiology* **54**, 2297–2300. https://doi.org/10.1099/ijs.0.63243-0.

Kolbe, W.F., Ogletree, D.F., Salmeron, M.B., 1992. Atomic force microscopy imaging of T4 bacteriophages on silicon substrates. *Ultramicroscopy* **42–44**, 1113–1117. https://doi.org/10.1016/0304-3991(92)90411-C.

Kotelnikova, S., 2002. Microbial production and oxidation of methane in deep subsurface. *Earth-Science Reviews* **58**, 367–395. https://doi.org/10.1016/S0012-8252(01)00082-4.

Kotelnikova, S., Pedersen, K., 1997. Evidence for methanogenic Archaea and homoacetogenic Bacteria in deep granitic rock aquifers. *FEMS Microbiology Reviews* **20**, 339–349. https://doi.org/10.1111/j.1574-6976.1997.tb00319.x.

Krumholz, L.R., McKinley, J.P., Ulrich, G.A., Suflita, J.M., 1997. Confined subsurface microbial communities in Cretaceous rock. *Nature* **386**, 64–66. https://doi.org/10.1038/386064a0.

Krupovic, M., Cvirkaite-Krupovic, V., Iranzo, J., Prangishvili, D., Koonin, E.V., 2018. Viruses of archaea: Structural, functional, environmental and evolutionary genomics. *Virus Research* **244**, 181–193. https://doi.org/10.1016/j.virusres.2017.11.025.

Krupovic, M., Makarova, K.S., Wolf, Y.I., Medvedeva, S., Prangishvili, D., Forterre, P., Koonin, E.V., 2019. Integrated mobile genetic elements in Thaumarchaeota. *Environ Microbiol* **21**, 2056–2078. https://doi.org/10.1111/1462-2920.14564.

Krupovic, M., Prangishvili, D., Hendrix, R.W., Bamford, D.H., 2011a. Genomics of Bacterial and Archaeal Viruses: Dynamics within the Prokaryotic Virosphere. *Microbiology and Molecular Biology Reviews* **75**, 610–635. https://doi.org/10.1128/MMBR.00011-11.

Krupovic, M., Quemin, E.R.J., Bamford, D.H., Forterre, P., Prangishvili, D., 2014. Unification of the Globally Distributed Spindle-Shaped Viruses of the Archaea. *J Virol* **88**, 2354–2358. https://doi.org/10.1128/JVI.02941-13.

Krupovic, M., Spang, A., Gribaldo, S., Forterre, P., Schleper, C., 2011b. A thaumarchaeal provirus testifies for an ancient association of tailed viruses with archaea. *Biochem Soc Trans* **39**, 82–88. https://doi.org/10.1042/BST0390082.

Kuznetsov, Y.G., Daijogo, S., Zhou, J., Semler, B.L., McPherson, A., 2005a. Atomic Force Microscopy Analysis of Icosahedral Virus RNA. *Journal of Molecular Biology* **347**, 41–52. https://doi.org/10.1016/j.jmb.2005.01.006.

Kuznetsov, Y.G., Dowell, J.J., Gavira, J.A., Ng, J.D., McPherson, A., 2010a. Biophysical and atomic force microscopy characterization of the RNA from satellite tobacco mosaic

virus. *Nucleic Acids Research* **38**, 8284–8294. https://doi.org/10.1093/nar/gkq662.

Kuznetsov, Y.G., Gurnon, J.R., Van Etten, J.L., McPherson, A., 2005b. Atomic force microscopy investigation of a chlorella virus, PBCV-1. *Journal of Structural Biology* **149**, 256–263. https://doi.org/10.1016/j.jsb.2004.10.007.

Kuznetsov, Y.G., McPherson, A., 2011. Atomic Force Microscopy in Imaging of Viruses and Virus-Infected Cells. *Microbiology and Molecular Biology Reviews* **75**, 268–285. https://doi.org/10.1128/MMBR.00041-10.

Kuznetsov, Y.G., Xiao, C., Sun, S., Raoult, D., Rossmann, M., McPherson, A., 2010b. Atomic force microscopy investigation of the giant mimivirus. *Virology* **404**, 127–137. https://doi.org/10.1016/j.virol.2010.05.007.

Kuznetsov, Yu.G., Malkin, A.J., Lucas, R.W., Plomp, M., McPherson, A., 2001. Imaging of viruses by atomic force microscopy. *Journal of General Virology* **82**, 2025–2034. https://doi.org/10.1099/0022-1317-82-9-2025.

Kuznetsov, Yu.G., McPherson, A., 2006. Atomic force microscopy investigation of Turnip Yellow Mosaic Virus capsid disruption and RNA extrusion. *Virology* **352**, 329–337. https://doi.org/10.1016/j.virol.2006.04.008.

Kyle, J.E., Eydal, H.S.C., Ferris, F.G., Pedersen, K., 2008. Viruses in granitic groundwater from 69 to 450 m depth of the Äspö hard rock laboratory, Sweden. *ISME J* **2**, 571–574. https://doi.org/10.1038/ismej.2008.18.

L

Labonté, J.M., Field, E.K., Lau, M., Chivian, D., Van Heerden, E., Wommack, K.E., Kieft, T.L., Onstott, T.C., Stepanauskas, R., 2015. Single cell genomics indicates horizontal gene transfer and viral infections in a deep subsurface Firmicutes population. *Front Microbiol* **6**, 349. https://doi.org/10.3389/fmicb.2015.00349.

Lange, S.J., Alkhnbashi, O.S., Rose, D., Will, S., Backofen, R., 2013. CRISPRmap: an automated classification of repeat conservation in prokaryotic adaptive immune systems. *Nucleic Acids Res* **41**, 8034–8044. https://doi.org/10.1093/nar/gkt606.

Langmead, B., Salzberg, S.L., 2012. Fast gapped-read alignment with Bowtie 2. *Nat Methods* **9**, 357–359. https://doi.org/10.1038/nmeth.1923.

Lau, M.C.Y., Kieft, T.L., Kuloyo, O., Linage-Alvarez, B., van Heerden, E., Lindsay, M.R., Magnabosco, C., Wang, W., Wiggins, J.B., Guo, L., Perlman, D.H., Kyin, S., Shwe, H.H., Harris, R.L., Oh, Y., Yi, M.J., Purtschert, R., Slater, G.F., Ono, S., Wei, S., Li, L., Sherwood Lollar, B., Onstott, T.C., 2016. An oligotrophic deep-subsurface community dependent on syntrophy is dominated by sulfur-driven autotrophic denitrifiers. *Proceedings of the National Academy of Sciences* **113**, E7927–E7936. https://doi.org/10.1073/pnas.1612244113.

Lazar, C.S., Stoll, W., Lehmann, R., Herrmann, M., Schwab, V.F., Akob, D.M., Nawaz, A., Wubet, T., Buscot, F., Totsche, K.-U., Küsel, K., 2017. Archaeal Diversity and CO2 Fixers in Carbonate-/Siliciclastic-Rock Groundwater Ecosystems. *Archaea* **2017**, 2136287. https://doi.org/10.1155/2017/2136287.

Lee, S., Sorensen, J.W., Walker, R.L., Emerson, J.B., Nicol, G.W., Hazard, C., 2022. Soil pH influences the structure of virus communities at local and global scales. *Soil Biology and Biochemistry* **166**, 108569. https://doi.org/10.1016/j.soilbio.2022.108569.

Leppänen, M., Sundberg, L.-R., Laanto, E., de Freitas Almeida, G.M., Papponen, P., Maasilta, I.J., 2017. Imaging Bacterial Colonies and Phage-Bacterium Interaction at Sub-Nanometer Resolution Using Helium-Ion Microscopy. *Adv. Biosys.* **1**, 1700070. https://doi.org/10.1002/adbi.201700070.

Lever, M., 2012. Acetogenesis in the Energy-Starved Deep Biosphere – A Paradox? *Frontiers*

in Microbiology **2**. https://doi.org/10.3389/fmicb.2011.00284.

Li, H., 2018. Minimap2: pairwise alignment for nucleotide sequences. *Bioinformatics* **34**, 3094–3100. https://doi.org/10.1093/bioinformatics/bty191.

Li, J., Liang, Y., Miao, Y., Wang, D., Jia, S., Liu, C.-H., 2020. Metagenomic insights into aniline effects on microbial community and biological sulfate reduction pathways during anaerobic treatment of high-sulfate wastewater. *Sci Total Environ* **742**, 140537. https://doi.org/10.1016/j.scitotenv.2020.140537.

Li, W., Godzik, A., 2006. Cd-hit: a fast program for clustering and comparing large sets of protein or nucleotide sequences. *Bioinformatics* **22**, 1658–1659. https://doi.org/10.1093/bioinformatics/btl158.

Lier, C., Baticle, E., Horvath, P., Haguenoer, E., Valentin, A.-S., Glaser, P., Mereghetti, L., Lanotte, P., 2015. Analysis of the type II-A CRISPR-Cas system of Streptococcus agalactiae reveals distinctive features according to genetic lineages. *Frontiers in Genetics* **6**. https://doi.org/10.3389/fgene.2015.00214.

Lin, L.-H., Wang, P.-L., Rumble, D., Lippmann-Pipke, J., Boice, E., Pratt, L.M., Lollar, B.S., Brodie, E.L., Hazen, T.C., Andersen, G.L., DeSantis, T.Z., Moser, D.P., Kershaw, D., Onstott, T.C., 2006. Long-Term Sustainability of a High-Energy, Low-Diversity Crustal Biome. *Science* **314**, 479–482. https://doi.org/10.1126/science.1127376.

Liu, J., Cvirkaite-Krupovic, V., Baquero, D.P., Yang, Y., Zhang, Q., Shen, Y., Krupovic, M., 2021. Virus-induced cell gigantism and asymmetric cell division in archaea. *Proceedings of the National Academy of Sciences* **118**, e2022578118. https://doi.org/10.1073/pnas.2022578118.

Liu, X., Zhang, Q., Murata, K., Baker, M.L., Sullivan, M.B., Fu, C., Dougherty, M.T., Schmid, M.F., Osburne, M.S., Chisholm, S.W., Chiu, W., 2010. Structural changes in a marine podovirus associated with release of its genome into Prochlorococcus. *Nat Struct Mol Biol* **17**, 830–836. https://doi.org/10.1038/nsmb.1823.

Liu, Y., Ishino, S., Ishino, Y., Pehau-Arnaudet, G., Krupovic, M., Prangishvili, D., 2017. A Novel Type of Polyhedral Viruses Infecting Hyperthermophilic Archaea. *J Virol* **91**, e00589-17. https://doi.org/10.1128/JVI.00589-17.

Liu, Y., Osinski, T., Wang, F., Krupovic, M., Schouten, S., Kasson, P., Prangishvili, D., Egelman, E.H., 2018. Structural conservation in a membrane-enveloped filamentous virus infecting a hyperthermophilic acidophile. *Nat Commun* **9**, 3360. https://doi.org/10.1038/s41467-018-05684-6.

Łoś, M., Węgrzyn, G., 2012. Pseudolysogeny. *Adv Virus Res* **82**, 339–349. https://doi.org/10.1016/B978-0-12-394621-8.00019-4.

Lovley, D.R., Dwyer, D.F., Klug, M.J., 1982. Kinetic Analysis of Competition Between Sulfate Reducers and Methanogens for Hydrogen in Sedimentst. *Appl Environ Microbiol* **43**. https://doi.org/10.1128/aem.43.6.1373-1379.1982.

Luef, B., Neu, T.R., Peduzzi, P., 2009. Imaging and quantifying virus fluorescence signals on aquatic aggregates: a new method and its implication for aquatic microbial ecology: Viruses on riverine aggregates. *FEMS Microbiology Ecology* **68**, 372–380. https://doi.org/10.1111/j.1574-6941.2009.00675.x.

Luk, A.W.S., Williams, T.J., Erdmann, S., Papke, R.T., Cavicchioli, R., 2014. Viruses of Haloarchaea. *Life (Basel)* **4**, 681–715. https://doi.org/10.3390/life4040681.

Lundstrom, K.H., Bamford, D.H., Palva, E.T., Lounatmaa, K., 1979. Lipid-containing Bacteriophage PR4: Structure and Life Cycle. *Journal of General Virology* **43**, 583–592. https://doi.org/10.1099/0022-1317-43-3-583.

Luque, D., Castón, J.R., 2020. Cryo-electron microscopy for the study of virus assembly. *Nat Chem Biol* **16**, 231–239. https://doi.org/10.1038/s41589-020-0477-1.

M

Magnabosco, C., Lin, L.-H., Dong, H., Bomberg, M., Ghiorse, W., Stan-Lotter, H., Pedersen, K., Kieft, T.L., van Heerden, E., Onstott, T.C., 2018. The biomass and biodiversity of the continental subsurface. *Nature Geosci* **11**, 707–717. https://doi.org/10.1038/s41561-018-0221-6.

Magnabosco, C., Ryan, K., Lau, M.C.Y., Kuloyo, O., Sherwood Lollar, B., Kieft, T.L., van Heerden, E., Onstott, T.C., 2016. A metagenomic window into carbon metabolism at 3 km depth in Precambrian continental crust. *ISME J* **10**, 730–741. https://doi.org/10.1038/ismej.2015.150.

Makarova, K.S., Haft, D.H., Barrangou, R., Brouns, S.J.J., Charpentier, E., Horvath, P., Moineau, S., Mojica, F.J.M., Wolf, Y.I., Yakunin, A.F., van der Oost, J., Koonin, E.V., 2011. Evolution and classification of the CRISPR–Cas systems. *Nat Rev Microbiol* **9**, 467–477. https://doi.org/10.1038/nrmicro2577.

Makarova, K.S., Wolf, Y.I., Forterre, P., Prangishvili, D., Krupovic, M., Koonin, E.V., 2014. Dark matter in archaeal genomes: a rich source of novel mobile elements, defense systems and secretory complexes. *Extremophiles* **18**, 877–893. https://doi.org/10.1007/s00792-014-0672-7.

Makarova, K.S., Wolf, Y.I., Iranzo, J., Shmakov, S.A., Alkhnbashi, O.S., Brouns, S.J.J., Charpentier, E., Cheng, D., Haft, D.H., Horvath, P., Moineau, S., Mojica, F.J.M., Scott, D., Shah, S.A., Siksnys, V., Terns, M.P., Venclovas, Č., White, M.F., Yakunin, A.F., Yan, W., Zhang, F., Garrett, R.A., Backofen, R., van der Oost, J., Barrangou, R., Koonin, E.V., 2020. Evolutionary classification of CRISPR-Cas systems: a burst of class 2 and derived variants. *Nat Rev Microbiol* **18**, 67–83. https://doi.org/10.1038/s41579-019-0299-x.

Makky, S., Dawoud, A., Safwat, A., Abdelsattar, A.S., Rezk, N., El-Shibiny, A., 2021. The bacteriophage decides own tracks: When they are with or against the bacteria. *Current Research in Microbial Sciences* **2**, 100050. https://doi.org/10.1016/j.crmicr.2021.100050.

Malki, K., Kula, A., Bruder, K., Sible, E., Hatzopoulos, T., Steidel, S., Watkins, S.C., Putonti, C., 2015. Bacteriophages isolated from Lake Michigan demonstrate broad host-range across several bacterial phyla. *Virol J* **12**, 164. https://doi.org/10.1186/s12985-015-0395-0.

Manning, A.J., Kuehn, M.J., 2011. Contribution of bacterial outer membrane vesicles to innate bacterial defense. *BMC Microbiol* **11**, 258. https://doi.org/10.1186/1471-2180-11-258.

Mäntynen, S., Laanto, E., Oksanen, H.M., Poranen, M.M., Díaz-Muñoz, S.L., 2021. Black box of phage–bacterium interactions: exploring alternative phage infection strategies. *Open Biol.* **11**, 210188. https://doi.org/10.1098/rsob.210188.

Marie, D., Brussaard, C.P.D., Thyrhaug, R., Bratbak, G., Vaulot, D., 1999. Enumeration of Marine Viruses in Culture and Natural Samples by Flow Cytometry. *Applied and Environmental Microbiology* **65**, 45–52. https://doi.org/10.1128/AEM.65.1.45-52.1999.

Marz, M., Beerenwinkel, N., Drosten, C., Fricke, M., Frishman, D., Hofacker, I.L., Hoffmann, D., Middendorf, M., Rattei, T., Stadler, P.F., Töpfer, A., 2014. Challenges in RNA virus bioinformatics. *Bioinformatics* **30**, 1793–1799. https://doi.org/10.1093/bioinformatics/btu105.

Mathurin, F.A., Åström, M.E., Laaksoharju, M., Kalinowski, B.E., Tullborg, E.-L., 2012. Effect of tunnel excavation on source and mixing of groundwater in a coastal granitoidic fracture network. *Environ Sci Technol* **46**, 12779–12786.

https://doi.org/10.1021/es301722b.

Matsko, N., Klinov, D., Manykin, A., Demin, V., Klimenko, S., 2001. Atomic force microscopy analysis of bacteriophages ΦKZ and T4. *Microscopy* **50**, 417–422. https://doi.org/10.1093/jmicro/50.5.417.

Maxwell, K.L., Garcia, B., Bondy-Denomy, J., Bona, D., Hidalgo-Reyes, Y., Davidson, A.R., 2016. The solution structure of an anti-CRISPR protein. *Nat Commun* **7**, 13134. https://doi.org/10.1038/ncomms13134.

McDaniel, L.D., delaRosa, M., Paul, J.H., 2006. Temperate and lytic cyanophages from the Gulf of Mexico. *Journal of the Marine Biological Association of the United Kingdom* **86**, 517–527. https://doi.org/10.1017/S0025315406013427.

Medvedeva, S., Liu, Y., Koonin, E.V., Severinov, K., Prangishvili, D., Krupovic, M., 2019. Virus-borne mini-CRISPR arrays are involved in interviral conflicts. *Nat Commun* **10**, 5204. https://doi.org/10.1038/s41467-019-13205-2.

Meier-Kolthoff, J.P., Auch, A.F., Klenk, H.-P., Göker, M., 2013. Genome sequence-based species delimitation with confidence intervals and improved distance functions. *BMC Bioinformatics* **14**, 60. https://doi.org/10.1186/1471-2105-14-60.

Meier-Kolthoff, J.P., Göker, M., 2017. VICTOR: genome-based phylogeny and classification of prokaryotic viruses. *Bioinformatics* **33**, 3396–3404. https://doi.org/10.1093/bioinformatics/btx440.

Michaelis, W., Seifert, R., Nauhaus, K., Treude, T., Thiel, V., Blumenberg, M., Knittel, K., Gieseke, A., Peterknecht, K., Pape, T., Boetius, A., Amann, R., Jørgensen, B.B., Widdel, F., Peckmann, J., Pimenov, N.V., Gulin, M.B., 2002. Microbial reefs in the Black Sea fueled by anaerobic oxidation of methane. *Science* **297**, 1013–1015. https://doi.org/10.1126/science.1072502.

Michas, A., Harir, M., Lucio, M., Vestergaard, G., Himmelberg, A., Schmitt-Kopplin, P., Lueders, T., Hatzinikolaou, D.G., Schöler, A., Rabus, R., Schloter, M., 2020. Sulfate Alters the Competition Among Microbiome Members of Sediments Chronically Exposed to Asphalt. *Frontiers in Microbiology* **11**. https://doi.org/10.3389/fmicb.2020.556793.

Middelboe, M., Glud, R., Filippini, M., 2011. Viral abundance and activity in the deep sub-seafloor biosphere. *Aquat. Microb. Ecol.* **63**, 1–8. https://doi.org/10.3354/ame01485

Miettinen, H., Bomberg, M., Vikman, M., 2018. Acetate Activates Deep Subsurface Fracture Fluid Microbial Communities in Olkiluoto, Finland. *Geosciences* **8**, 399. https://doi.org/10.3390/geosciences8110399.

Milne, R.G., Trautner, T.A., 1967. Thin sectioning and electron microscopy of SP50 bacteriophage adsorbed to Bacillus subtilis. *Journal of Ultrastructure Research* **20**, 267–276. https://doi.org/10.1016/S0022-5320(67)90287-0.

Mochizuki, T., Krupovic, M., Pehau-Arnaudet, G., Sako, Y., Forterre, P., Prangishvili, D., 2012. Archaeal virus with exceptional virion architecture and the largest single-stranded DNA genome. *Proceedings of the National Academy of Sciences* **109**, 13386–13391. https://doi.org/10.1073/pnas.1203668109.

Mohamed Zuki, F., Edyvean, R.G.J., Pourzolfaghar, H., Kasim, N., 2021. Modeling of the Van Der Waals Forces during the Adhesion of Capsule-Shaped Bacteria to Flat Surfaces. *Biomimetics (Basel)* **6**, 5. https://doi.org/10.3390/biomimetics6010005.

Moissl, C., Rachel, R., Briegel, A., Engelhardt, H., Huber, R., 2005. The unique structure of archaeal 'hami', highly complex cell appendages with nano-grappling hooks. *Mol Microbiol* **56**, 361–370. https://doi.org/10.1111/j.1365-2958.2005.04294.x.

Moissl, C., Rudolph, C., Huber, R., 2002. Natural Communities of Novel Archaea and Bacteria with a String-of-Pearls-Like Morphology: Molecular Analysis of the Bacterial Partners. *Appl Environ Microbiol* **68**, 933–937.

https://doi.org/10.1128/AEM.68.2.933-937.2002.
Moissl, C., Rudolph, C., Rachel, R., Koch, M., Huber, R., 2003. In situ growth of the novel SM1 euryarchaeon from a string-of-pearls-like microbial community in its cold biotope, its physical separation and insights into its structure and physiology. *Archives of Microbiology* **180**, 211–217. https://doi.org/10.1007/s00203-003-0580-1.
Mojica, K.D.A., Brussaard, C.P.D., 2014. Factors affecting virus dynamics and microbial host–virus interactions in marine environments. *FEMS Microbiology Ecology* **89**, 495–515. https://doi.org/10.1111/1574-6941.12343.
Moller, A.G., Liang, C., 2017. MetaCRAST: reference-guided extraction of CRISPR spacers from unassembled metagenomes. *PeerJ* **5**, e3788. https://doi.org/10.7717/peerj.3788.
Møller, S., Sternberg, C., Andersen, J.B., Christensen, B.B., Ramos, J.L., Givskov, M., Molin, S., 1998. In situ gene expression in mixed-culture biofilms: evidence of metabolic interactions between community members. *Appl Environ Microbiol* **64**, 721–732. https://doi.org/10.1128/AEM.64.2.721-732.1998.
Molnár, J., Magyar, B., Schneider, G., Laczi, K., Valappil, S.K., Kovács, Á.L., Nagy, I.K., Rákhely, G., Kovács, T., 2020. Identification of a novel archaea virus, detected in hydrocarbon polluted Hungarian and Canadian samples. *PLoS One* **15**, e0231864. https://doi.org/10.1371/journal.pone.0231864.
Momper, L., Jungbluth, S.P., Lee, M.D., Amend, J.P., 2017. Energy and carbon metabolisms in a deep terrestrial subsurface fluid microbial community. *ISME J* **11**, 2319–2333. https://doi.org/10.1038/ismej.2017.94.
Monsees, I., Turzynski, V., Esser, S.P., Soares, A., Timmermann, L.I., Weidenbach, K., Banas, J., Kloster, M., Beszteri, B., Schmitz, R.A., Probst, A.J., 2022. Label-Free Raman Microspectroscopy for Identifying Prokaryotic Virocells. *mSystems* **7**, e01505-21. https://doi.org/10.1128/msystems.01505-21.
Moraru, C., Lam, P., Fuchs, B.M., Kuypers, M.M.M., Amann, R., 2010. GeneFISH - an in situ technique for linking gene presence and cell identity in environmental microorganisms: GeneFISH in environmental microorganisms. *Environmental Microbiology* **12**, 3057–3073. https://doi.org/10.1111/j.1462-2920.2010.02281.x.
Moraru, C., Varsani, A., Kropinski, A.M., 2020. VIRIDIC-A Novel Tool to Calculate the Intergenomic Similarities of Prokaryote-Infecting Viruses. *Viruses* **12**, E1268. https://doi.org/10.3390/v12111268.
Morita, R.Y., 1999. Is H 2 the Universal Energy Source for Long-Term Survival? *Microbial Ecology* **38**, 307–320. https://doi.org/10.1007/s002489901002.
Müller, T., Sakin, V., Müller, B., 2019. A Spotlight on Viruses—Application of Click Chemistry to Visualize Virus-Cell Interactions. *Molecules* **24**, 481. https://doi.org/10.3390/molecules24030481.
Munson-McGee, J., Snyder, J., Young, M., 2018. Archaeal Viruses from High-Temperature Environments. *Genes* **9**, 128. https://doi.org/10.3390/genes9030128.
Munson-McGee, J.H., Rooney, C., Young, M.J., 2019. An Uncultivated Virus Infecting a Nanoarchaeal Parasite in the Hot Springs of Yellowstone National Park. *J Virol* **94**, e01213-19, /jvi/94/3/JVI.01213-19.atom. https://doi.org/10.1128/JVI.01213-19.

N

Nagasaki, K., Yamaguchi, M., 1998. Effect of temperature on the algicidal activity and the stability of HaV (Heterosigma akashiwo virus). *Aquat. Microb. Ecol.* **15**, 211–216. https://doi.org/10.3354/ame015211.
Nasukawa, T., Uchiyama, J., Taharaguchi, S., Ota, S., Ujihara, T., Matsuzaki, S., Murakami, H., Mizukami, K., Sakaguchi, M., 2017. Virus purification by CsCl density gradient

using general centrifugation. *Arch Virol* **162**, 3523–3528. https://doi.org/10.1007/s00705-017-3513-z.

Noble, R., Fuhrman, J., 1998. Use of SYBR Green I for rapid epifluorescence counts of marine viruses and bacteria. *Aquat. Microb. Ecol.* **14**, 113–118. https://doi.org/10.3354/ame014113.

Nonnenmacher, M., O'Boyle, M.P., Wickramasinghe, H.K., 1991. Kelvin probe force microscopy. *Appl. Phys. Lett.* **58**, 2921–2923. https://doi.org/10.1063/1.105227.

Norrby, E., 1983. The morphology of virus particles. Classification of viruses. In 'Textbook of Medical Virology'. Elsevier, pp. 4–16. https://doi.org/10.1016/B978-0-407-00253-1.50007-4.

Nunoura, T., Takaki, Y., Kakuta, J., Nishi, S., Sugahara, J., Kazama, H., Chee, G.-J., Hattori, M., Kanai, A., Atomi, H., Takai, K., Takami, H., 2011. Insights into the evolution of Archaea and eukaryotic protein modifier systems revealed by the genome of a novel archaeal group. *Nucleic Acids Res* **39**, 3204–3223. https://doi.org/10.1093/nar/gkq1228.

Nuppunen-Puputti, M., Purkamo, L., Kietäväinen, R., Nyyssönen, M., Itävaara, M., Ahonen, L., Kukkonen, I., Bomberg, M., 2018. Rare Biosphere Archaea Assimilate Acetate in Precambrian Terrestrial Subsurface at 2.2 km Depth. *Geosciences* **8**, 418. https://doi.org/10.3390/geosciences8110418.

Nurk, S., Meleshko, D., Korobeynikov, A., Pevzner, P.A., 2017. metaSPAdes: a new versatile metagenomic assembler. *Genome Res* **27**, 824–834. https://doi.org/10.1101/gr.213959.116.

Nyyssönen, M., Hultman, J., Ahonen, L., Kukkonen, I., Paulin, L., Laine, P., Itävaara, M., Auvinen, P., 2014. Taxonomically and functionally diverse microbial communities in deep crystalline rocks of the Fennoscandian shield. *ISME J* **8**, 126–138. https://doi.org/10.1038/ismej.2013.125.

O

O'Connell, S.P., Lehman, R.M., Snoeyenbos-West, O., Winston, V.D., Cummings, D.E., Watwood, M.E., Colwell, F.S., 2003. Detection of Euryarchaeota and Crenarchaeota in an oxic basalt aquifer. *FEMS Microbiol Ecol* **44**, 165–173. https://doi.org/10.1016/S0168-6496(02)00465-8.

Olm, M.R., Crits-Christoph, A., Bouma-Gregson, K., Firek, B.A., Morowitz, M.J., Banfield, J.F., 2021. inStrain profiles population microdiversity from metagenomic data and sensitively detects shared microbial strains. *Nat Biotechnol* **39**, 727–736. https://doi.org/10.1038/s41587-020-00797-0.

P

Paez-Espino, D., Eloe-Fadrosh, E.A., Pavlopoulos, G.A., Thomas, A.D., Huntemann, M., Mikhailova, N., Rubin, E., Ivanova, N.N., Kyrpides, N.C., 2016. Uncovering Earth's virome. *Nature* **536**, 425–430. https://doi.org/10.1038/nature19094.

Pan, D., Nolan, J., Williams, K.H., Robbins, M.J., Weber, K.A., 2017. Abundance and Distribution of Microbial Cells and Viruses in an Alluvial Aquifer. *Front. Microbiol.* **8**, 1199. https://doi.org/10.3389/fmicb.2017.01199.

Papadopoulos, J.S., Agarwala, R., 2007. COBALT: constraint-based alignment tool for multiple protein sequences. *Bioinformatics* **23**, 1073–1079. https://doi.org/10.1093/bioinformatics/btm076.

Parada, A.E., Needham, D.M., Fuhrman, J.A., 2016. Every base matters: assessing small

subunit rRNA primers for marine microbiomes with mock communities, time series and global field samples: Primers for marine microbiome studies. *Environ Microbiol* **18**, 1403–1414. https://doi.org/10.1111/1462-2920.13023.

Parikka, K.J., Le Romancer, M., Wauters, N., Jacquet, S., 2017. Deciphering the virus-to-prokaryote ratio (VPR): insights into virus-host relationships in a variety of ecosystems: Deciphering the virus-to-prokaryote ratio. *Biol Rev* **92**, 1081–1100. https://doi.org/10.1111/brv.12271.

Parkes, R.J., Cragg, B.A., Wellsbury, P., 2000. Recent studies on bacterial populations and processes in subseafloor sediments: A review. *Hydrogeology Journal* **8**, 11–28. https://doi.org/10.1007/PL00010971.

Paul, J.H., 2008. Prophages in marine bacteria: dangerous molecular time bombs or the key to survival in the seas? *ISME J* **2**, 579–589. https://doi.org/10.1038/ismej.2008.35.

Pauly, M.D., Bautista, M.A., Black, J.A., Whitaker, R.J., 2019a. Diversified local CRISPR-Cas immunity to viruses of Sulfolobus islandicus. *Philos Trans R Soc Lond B Biol Sci* **374**, 20180093. https://doi.org/10.1098/rstb.2018.0093.

Pauly, M.D., Bautista, M.A., Black, J.A., Whitaker, R.J., 2019b. Diversified local CRISPR-Cas immunity to viruses of *Sulfolobus islandicus*. *Phil. Trans. R. Soc. B* **374**, 20180093. https://doi.org/10.1098/rstb.2018.0093.

Pawluk, A., Bondy-Denomy, J., Cheung, V.H.W., Maxwell, K.L., Davidson, A.R., 2014. A New Group of Phage Anti-CRISPR Genes Inhibits the Type I-E CRISPR-Cas System of Pseudomonas aeruginosa. *mBio* **5**, e00896-14. https://doi.org/10.1128/mBio.00896-14.

Payet, J.P., Suttle, C.A., 2013. To kill or not to kill: The balance between lytic and lysogenic viral infection is driven by trophic status. *Limnol. Oceanogr.* **58**, 465–474. https://doi.org/10.4319/lo.2013.58.2.0465.

Pedersen, K., Arlinger, J., Eriksson, S., Hallbeck, A., Hallbeck, L., Johansson, J., 2008. Numbers, biomass and cultivable diversity of microbial populations relate to depth and borehole-specific conditions in groundwater from depths of 4–450 m in Olkiluoto, Finland. *ISME J* **2**, 760–775. https://doi.org/10.1038/ismej.2008.43.

Peduzzi, P., 2016. Virus ecology of fluvial systems: a blank spot on the map? *Biol Rev* **91**, 937–949. https://doi.org/10.1111/brv.12202.

Peduzzi, P., Agis, M., Luef, B., 2013. Evaluation of confocal laser scanning microscopy for enumeration of virus-like particles in aquatic systems. *Environ Monit Assess* **185**, 5411–5418. https://doi.org/10.1007/s10661-012-2955-8.

Peduzzi, P., Weinbauer, M.G., 1993. Effect of concentrating the virus-rich 2-2nm size fraction of seawater on the formation of algal flocs (marine snow). *Limnol. Oceanogr.* **38**, 1562–1565. https://doi.org/10.4319/lo.1993.38.7.1562.

Penesyan, A., Paulsen, I.T., Kjelleberg, S., Gillings, M.R., 2021. Three faces of biofilms: a microbial lifestyle, a nascent multicellular organism, and an incubator for diversity. *npj Biofilms Microbiomes* **7**, 80. https://doi.org/10.1038/s41522-021-00251-2.

Perras, A.K., Daum, B., Ziegler, C., Takahashi, L.K., Ahmed, M., Wanner, G., Klingl, A., Leitinger, G., Kolb-Lenz, D., Gribaldo, S., Auerbach, A., Mora, M., Probst, A.J., Bellack, A., Moissl-Eichinger, C., 2015. S-layers at second glance? Altiarchaeal grappling hooks (hami) resemble archaeal S-layer proteins in structure and sequence. *Front Microbiol* **6**, 543. https://doi.org/10.3389/fmicb.2015.00543.

Pfister, P., Wasserfallen, A., Stettler, R., Leisinger, T., 1998. Molecular analysis of Methanobacterium phage psiM2. *Mol Microbiol* **30**, 233–244. https://doi.org/10.1046/j.1365-2958.1998.01073.x.

Phelps, T.J., Murphy, E.M., Pfiffner, S.M., White, D.C., 1994. Comparison between geochemical and biological estimates of subsurface microbial activities. *Microb Ecol*

28, 335–349. https://doi.org/10.1007/BF00662027.

Philosof, A., Yutin, N., Flores-Uribe, J., Sharon, I., Koonin, E.V., Béjà, O., 2017. Novel Abundant Oceanic Viruses of Uncultured Marine Group II Euryarchaeota. *Curr Biol* **27**, 1362–1368. https://doi.org/10.1016/j.cub.2017.03.052.

Pietilä, M.K., Atanasova, N.S., Manole, V., Liljeroos, L., Butcher, S.J., Oksanen, H.M., Bamford, D.H., 2012. Virion Architecture Unifies Globally Distributed Pleolipoviruses Infecting Halophilic Archaea. *J Virol* **86**, 5067–5079. https://doi.org/10.1128/JVI.06915-11.

Pietilä, M.K., Demina, T.A., Atanasova, N.S., Oksanen, H.M., Bamford, D.H., 2014. Archaeal viruses and bacteriophages: comparisons and contrasts. *Trends in Microbiology* **22**, 334–344. https://doi.org/10.1016/j.tim.2014.02.007.

Pietilä, M.K., Laurinavičius, S., Sund, J., Roine, E., Bamford, D.H., 2010. The Single-Stranded DNA Genome of Novel Archaeal Virus Halorubrum Pleomorphic Virus 1 Is Enclosed in the Envelope Decorated with Glycoprotein Spikes. *J Virol* **84**, 788–798. https://doi.org/10.1128/JVI.01347-09.

Pietilä, M.K., Roine, E., Paulin, L., Kalkkinen, N., Bamford, D.H., 2009. An ssDNA virus infecting archaea: a new lineage of viruses with a membrane envelope. *Molecular Microbiology* **72**, 307–319. https://doi.org/10.1111/j.1365-2958.2009.06642.x.

Pietilä, M.K., Roine, E., Sencilo, A., Bamford, D.H., Oksanen, H.M., 2016. Pleolipoviridae, a newly proposed family comprising archaeal pleomorphic viruses with single-stranded or double-stranded DNA genomes. *Arch Virol* **161**, 249–256. https://doi.org/10.1007/s00705-015-2613-x.

Pina, S., Creus, A., Gonzaález, N., Gironeés, R., Felip, M., Sommaruga, R., 1998. Abundance, morphology and distribution of planktonic virus-like particles in two high-mountain lakes. *J Plankton Res* **20**, 2413–2421. https://doi.org/10.1093/plankt/20.12.2413.

Pires, D.P., Melo, L.D.R., Azeredo, J., 2021. Understanding the Complex Phage-Host Interactions in Biofilm Communities. *Annu. Rev. Virol.* **8**, 73–94. https://doi.org/10.1146/annurev-virology-091919-074222.

Potter, S.C., Luciani, A., Eddy, S.R., Park, Y., Lopez, R., Finn, R.D., 2018. HMMER web server: 2018 update. *Nucleic Acids Res* **46**, W200–W204. https://doi.org/10.1093/nar/gky448.

Prangishvili, D., Arnold, H.P., Götz, D., Ziese, U., Holz, I., Kristjansson, J.K., Zillig, W., 1999. A novel virus family, the Rudiviridae: Structure, virus-host interactions and genome variability of the sulfolobus viruses SIRV1 and SIRV2. *Genetics* **152**, 1387–1396. https://doi.org/10.1093/genetics/152.4.1387.

Prangishvili, D., Bamford, D.H., Forterre, P., Iranzo, J., Koonin, E.V., Krupovic, M., 2017. The enigmatic archaeal virosphere. *Nat Rev Microbiol* **15**, 724–739. https://doi.org/10.1038/nrmicro.2017.125.

Prangishvili, D., Forterre, P., Garrett, R.A., 2006a. Viruses of the Archaea: a unifying view. *Nat Rev Microbiol* **4**, 837–848. https://doi.org/10.1038/nrmicro1527.

Prangishvili, D., Garrett, R.A., Koonin, E.V., 2006b. Evolutionary genomics of archaeal viruses: Unique viral genomes in the third domain of life. *Virus Research* **117**, 52–67. https://doi.org/10.1016/j.virusres.2006.01.007.

Prangishvili, D., Vestergaard, G., Häring, M., Aramayo, R., Basta, T., Rachel, R., Garrett, R.A., 2006c. Structural and Genomic Properties of the Hyperthermophilic Archaeal Virus ATV with an Extracellular Stage of the Reproductive Cycle. *Journal of Molecular Biology* **359**, 1203–1216. https://doi.org/10.1016/j.jmb.2006.04.027.

Prata, C., Ribeiro, A., Cunha, Â., Gomes, Newton.C.M., Almeida, A., 2012. Ultracentrifugation as a direct method to concentrate viruses in environmental waters:

virus-like particle enumeration as a new approach to determine the efficiency of recovery. *J. Environ. Monit.* **14**, 64–70. https://doi.org/10.1039/C1EM10603A.

Price, M.N., Dehal, P.S., Arkin, A.P., 2010. FastTree 2--approximately maximum-likelihood trees for large alignments. *PLoS One* **5**, e9490. https://doi.org/10.1371/journal.pone.0009490.

Probst, A., Moissl-Eichinger, C., 2015. "Altiarchaeales": Uncultivated Archaea from the Subsurface. *Life* **5**, 1381–1395. https://doi.org/10.3390/life5021381.

Probst, A.J., Birarda, G., Holman, H.-Y.N., DeSantis, T.Z., Wanner, G., Andersen, G.L., Perras, A.K., Meck, S., Völkel, J., Bechtel, H.A., Wirth, R., Moissl-Eichinger, C., 2014a. Coupling Genetic and Chemical Microbiome Profiling Reveals Heterogeneity of Archaeome and Bacteriome in Subsurface Biofilms That Are Dominated by the Same Archaeal Species. *PLoS ONE* **9**, e99801. https://doi.org/10.1371/journal.pone.0099801.

Probst, A.J., Elling, F.J., Castelle, C.J., Zhu, Q., Elvert, M., Birarda, G., Holman, H.-Y.N., Lane, K.R., Ladd, B., Ryan, M.C., Woyke, T., Hinrichs, K.-U., Banfield, J.F., 2020. Lipid analysis of CO2-rich subsurface aquifers suggests an autotrophy-based deep biosphere with lysolipids enriched in CPR bacteria. *ISME J* **14**, 1547–1560. https://doi.org/10.1038/s41396-020-0624-4.

Probst, A.J., Holman, H.-Y.N., DeSantis, T.Z., Andersen, G.L., Birarda, G., Bechtel, H.A., Piceno, Y.M., Sonnleitner, M., Venkateswaran, K., Moissl-Eichinger, C., 2013. Tackling the minority: sulfate-reducing bacteria in an archaea-dominated subsurface biofilm. *ISME J* **7**, 635–651. https://doi.org/10.1038/ismej.2012.133.

Probst, A.J., Ladd, B., Jarett, J.K., Geller-McGrath, D.E., Sieber, C.M.K., Emerson, J.B., Anantharaman, K., Thomas, B.C., Malmstrom, R.R., Stieglmeier, M., Klingl, A., Woyke, T., Ryan, M.C., Banfield, J.F., 2018. Differential depth distribution of microbial function and putative symbionts through sediment-hosted aquifers in the deep terrestrial subsurface. *Nat Microbiol* **3**, 328–336. https://doi.org/10.1038/s41564-017-0098-y.

Probst, A.J., Weinmaier, T., Raymann, K., Perras, A., Emerson, J.B., Rattei, T., Wanner, G., Klingl, A., Berg, I.A., Yoshinaga, M., Viehweger, B., Hinrichs, K.-U., Thomas, B.C., Meck, S., Auerbach, A.K., Heise, M., Schintlmeister, A., Schmid, M., Wagner, M., Gribaldo, S., Banfield, J.F., Moissl-Eichinger, C., 2014b. Biology of a widespread uncultivated archaeon that contributes to carbon fixation in the subsurface. *Nat Commun* **5**, 5497. https://doi.org/10.1038/ncomms6497.

Proctor, L., Fuhrman, J., 1992. Mortality of marine bacteria in response to enrichments of the virus size fraction from seawater. *Mar. Ecol. Prog. Ser.* **87**, 283–293. https://doi.org/10.3354/meps087283.

Proctor, L.M., 1997. Advances in the study of marine viruses. *Microsc Res Tech* **37**, 136–161. https://doi.org/10.1002/(SICI)1097-0029(19970415)37:2<136::AID-JEMT3>3.0.CO;2-M.

Purkamo, L., Kietäväinen, R., Miettinen, H., Sohlberg, E., Kukkonen, I., Itävaara, M., Bomberg, M., 2018. Diversity and functionality of archaeal, bacterial and fungal communities in deep Archaean bedrock groundwater. *FEMS Microbiol Ecol* **94**. https://doi.org/10.1093/femsec/fiy116.

Q

Quast, C., Pruesse, E., Yilmaz, P., Gerken, J., Schweer, T., Yarza, P., Peplies, J., Glöckner, F.O., 2013. The SILVA ribosomal RNA gene database project: improved data processing and web-based tools. *Nucleic Acids Res* **41**, D590-596.

https://doi.org/10.1093/nar/gks1219.
Quemin, E.R.J., Chlanda, P., Sachse, M., Forterre, P., Prangishvili, D., Krupovic, M., 2016. Eukaryotic-Like Virus Budding in Archaea. *mBio* **7**, e01439-16. https://doi.org/10.1128/mBio.01439-16.

R

R Core Team (2019). R: A language and environment for statistical computing. R Foundation for Statistical Computing, Vienna, Austria. https://www.R-project.org/.
R Core Team (2022). R: A language and environment for statistical computing. R Foundation for Statistical Computing, Vienna, Austria. https://www.R-project.org/.
Rachel, R., Bettstetter, M., Hedlund, B.P., Häring, M., Kessler, A., Stetter, K.O., Prangishvili, D., 2002. Remarkable morphological diversity of viruses and virus-like particles in hot terrestrial environments. *Archives of Virology* **147**, 2419–2429. https://doi.org/10.1007/s00705-002-0895-2.
Rahlff, J., Turzynski, V., Esser, S.P., Monsees, I., Bornemann, T.L.V., Figueroa-Gonzalez, P.A., Schulz, F., Woyke, T., Klingl, A., Moraru, C., Probst, A.J., 2021. Lytic archaeal viruses infect abundant primary producers in Earth's crust. *Nat Commun* **12**, 4642. https://doi.org/10.1038/s41467-021-24803-4.
Rambaut A. 2006. FigTree, a graphical viewer of phylogenetic trees and as a program for producing publication-ready figures. http://tree.bio.ed.ac.uk/software/figtree/. [Software].
Rastogi, G., Stetler, L.D., Peyton, B.M., Sani, R.K., 2009. Molecular analysis of prokaryotic diversity in the deep subsurface of the former Homestake gold mine, South Dakota, USA. *J Microbiol.* **47**, 371–384. https://doi.org/10.1007/s12275-008-0249-1.
Rath, D., Amlinger, L., Rath, A., Lundgren, M., 2015. The CRISPR-Cas immune system: Biology, mechanisms and applications. *Biochimie*, Special Issue: Regulatory RNAs **117**, 119–128. https://doi.org/10.1016/j.biochi.2015.03.025.
Rauch, B.J., Silvis, M.R., Hultquist, J.F., Waters, C.S., McGregor, M.J., Krogan, N.J., Bondy-Denomy, J., 2017. Inhibition of CRISPR-Cas9 with Bacteriophage Proteins. *Cell* **168**, 150-158.e10. https://doi.org/10.1016/j.cell.2016.12.009.
Refardt, D., 2011. Within-host competition determines reproductive success of temperate bacteriophages. *ISME J* **5**, 1451–1460. https://doi.org/10.1038/ismej.2011.30.
Reith, F., 2011. Life in the deep subsurface. *Geology* **39**, 287–288. https://doi.org/10.1130/focus032011.
Remmert, M., Biegert, A., Hauser, A., Söding, J., 2011. HHblits: lightning-fast iterative protein sequence searching by HMM-HMM alignment. *Nat Methods* **9**, 173–175. https://doi.org/10.1038/nmeth.1818.
Rempfert, K.R., Miller, H.M., Bompard, N., Nothaft, D., Matter, J.M., Kelemen, P., Fierer, N., Templeton, A.S., 2017. Geological and Geochemical Controls on Subsurface Microbial Life in the Samail Ophiolite, Oman. *Frontiers in Microbiology* **8**. https://doi.org/10.3389/fmicb.2017.00056.
Ren, J., Ahlgren, N.A., Lu, Y.Y., Fuhrman, J.A., Sun, F., 2017. VirFinder: a novel k-mer based tool for identifying viral sequences from assembled metagenomic data. *Microbiome* **5**, 69. https://doi.org/10.1186/s40168-017-0283-5.
Reyes-Robles, T., Dillard, R.S., Cairns, L.S., Silva-Valenzuela, C.A., Housman, M., Ali, A., Wright, E.R., Camilli, A., 2018. Vibrio cholerae Outer Membrane Vesicles Inhibit Bacteriophage Infection. *J Bacteriol* **200**, e00792-17. https://doi.org/10.1128/JB.00792-17.
Reynolds, E.S., 1963. The use of lead citrate at high pH as an electron-opaque stain in

electron microscopy. *Journal of Cell Biology* **17**, 208–212. https://doi.org/10.1083/jcb.17.1.208.

Rinke, C., Schwientek, P., Sczyrba, A., Ivanova, N.N., Anderson, I.J., Cheng, J.-F., Darling, A., Malfatti, S., Swan, B.K., Gies, E.A., Dodsworth, J.A., Hedlund, B.P., Tsiamis, G., Sievert, S.M., Liu, W.-T., Eisen, J.A., Hallam, S.J., Kyrpides, N.C., Stepanauskas, R., Rubin, E.M., Hugenholtz, P., Woyke, T., 2013. Insights into the phylogeny and coding potential of microbial dark matter. *Nature* **499**, 431–437. https://doi.org/10.1038/nature12352.

Ripp, S., Miller, R.V., 1997. The role of pseudolysogeny in bacteriophage-host interactions in a natural freshwater environment. *Microbiology* **143**, 2065–2070. https://doi.org/10.1099/00221287-143-6-2065.

Roberts, I.S., 1996. The biochemistry and genetics of capsular polysaccharide production in bacteria. *Annu Rev Microbiol* **50**, 285–315. https://doi.org/10.1146/annurev.micro.50.1.285.

Rodrigues, R.A.L., Andrade, A.C.D.S.P., Boratto, P.V. de M., Trindade, G. de S., Kroon, E.G., Abrahão, J.S., 2017. An Anthropocentric View of the Virosphere-Host Relationship. *Front Microbiol* **8**, 1673. https://doi.org/10.3389/fmicb.2017.01673.

Roux, S., Adriaenssens, E.M., Dutilh, B.E., Koonin, E.V., Kropinski, A.M., Krupovic, M., Kuhn, J.H., Lavigne, R., Brister, J.R., Varsani, A., Amid, C., Aziz, R.K., Bordenstein, S.R., Bork, P., Breitbart, M., Cochrane, G.R., Daly, R.A., Desnues, C., Duhaime, M.B., Emerson, J.B., Enault, F., Fuhrman, J.A., Hingamp, P., Hugenholtz, P., Hurwitz, B.L., Ivanova, N.N., Labonté, J.M., Lee, K.-B., Malmstrom, R.R., Martinez-Garcia, M., Mizrachi, I.K., Ogata, H., Páez-Espino, D., Petit, M.-A., Putonti, C., Rattei, T., Reyes, A., Rodriguez-Valera, F., Rosario, K., Schriml, L., Schulz, F., Steward, G.F., Sullivan, M.B., Sunagawa, S., Suttle, C.A., Temperton, B., Tringe, S.G., Thurber, R.V., Webster, N.S., Whiteson, K.L., Wilhelm, S.W., Wommack, K.E., Woyke, T., Wrighton, K.C., Yilmaz, P., Yoshida, T., Young, M.J., Yutin, N., Allen, L.Z., Kyrpides, N.C., Eloe-Fadrosh, E.A., 2019. Minimum Information about an Uncultivated Virus Genome (MIUViG). *Nat Biotechnol* **37**, 29–37. https://doi.org/10.1038/nbt.4306.

Roux, S., Brum, J.R., Dutilh, B.E., Sunagawa, S., Duhaime, M.B., Loy, A., Poulos, B.T., Solonenko, N., Lara, E., Poulain, J., Pesant, S., Kandels-Lewis, S., Dimier, C., Picheral, M., Searson, S., Cruaud, C., Alberti, A., Duarte, C.M., Gasol, J.M., Vaqué, D., Tara Oceans Coordinators, Bork, P., Acinas, S.G., Wincker, P., Sullivan, M.B., 2016. Ecogenomics and potential biogeochemical impacts of globally abundant ocean viruses. *Nature* **537**, 689–693. https://doi.org/10.1038/nature19366.

Roux, S., Enault, F., Hurwitz, B.L., Sullivan, M.B., 2015. VirSorter: mining viral signal from microbial genomic data. *PeerJ* **3**, e985. https://doi.org/10.7717/peerj.985.

Rowe, J., Saxton, M., Cottrell, M., DeBruyn, J., Berg, G., Kirchman, D., Hutchins, D., Wilhelm, S., 2008. Constraints on viral production in the Sargasso Sea and North Atlantic. *Aquat. Microb. Ecol.* **52**, 233–244. https://doi.org/10.3354/ame01231.

Rudolph, C., Moissl, C., Henneberger, R., Huber, R., 2004. Ecology and microbial structures of archaeal/bacterial strings-of-pearls communities and archaeal relatives thriving in cold sulfidic springs. *FEMS Microbiology Ecology* **50**, 1–11. https://doi.org/10.1016/j.femsec.2004.05.006.

Rudolph, C., Wanner, G., Huber, R., 2001. Natural Communities of Novel Archaea and Bacteria Growing in Cold Sulfurous Springs with a String-of-Pearls-Like Morphology. *Appl Environ Microbiol* **67**, 2336–2344. https://doi.org/10.1128/AEM.67.5.2336-2344.2001.

S

Sauer, K., Stoodley, P., Goeres, D.M., Hall-Stoodley, L., Burmølle, M., Stewart, P.S., Bjarnsholt, T., 2022. The biofilm life cycle: expanding the conceptual model of biofilm formation. *Nat Rev Microbiol* **20**, 608–620. https://doi.org/10.1038/s41579-022-00767-0.

Schippers, A., Neretin, L.N., Kallmeyer, J., Ferdelman, T.G., Cragg, B.A., John Parkes, R., Jørgensen, B.B., 2005. Prokaryotic cells of the deep sub-seafloor biosphere identified as living bacteria. *Nature* **433**, 861–864. https://doi.org/10.1038/nature03302.

Schlitzer, R., 2015. Data Analysis and Visualization with Ocean Data View. *CMOS Bulletin SCMO* **43**, 9–13.

Schwank, K., Bornemann, T.L.V., Dombrowski, N., Spang, A., Banfield, J.F., Probst, A.J., 2019. An archaeal symbiont-host association from the deep terrestrial subsurface. *ISME J* **13**, 2135–2139. https://doi.org/10.1038/s41396-019-0421-0.

Secor, P.R., Sweere, J.M., Michaels, L.A., Malkovskiy, A.V., Lazzareschi, D., Katznelson, E., Rajadas, J., Birnbaum, M.E., Arrigoni, A., Braun, K.R., Evanko, S.P., Stevens, D.A., Kaminsky, W., Singh, P.K., Parks, W.C., Bollyky, P.L., 2015. Filamentous Bacteriophage Promote Biofilm Assembly and Function. *Cell Host & Microbe* **18**, 549–559. https://doi.org/10.1016/j.chom.2015.10.013.

Shannon, P., Markiel, A., Ozier, O., Baliga, N.S., Wang, J.T., Ramage, D., Amin, N., Schwikowski, B., Ideker, T., 2003. Cytoscape: a software environment for integrated models of biomolecular interaction networks. *Genome Res* **13**, 2498–2504. https://doi.org/10.1101/gr.1239303.

Sharma, A., Schmidt, M., Kiesel, B., Mahato, N.K., Cralle, L., Singh, Y., Richnow, H.H., Gilbert, J.A., Arnold, W., Lal, R., 2018. Bacterial and Archaeal Viruses of Himalayan Hot Springs at Manikaran Modulate Host Genomes. *Front. Microbiol.* **9**, 3095. https://doi.org/10.3389/fmicb.2018.03095.

Sharon, I., Alperovitch, A., Rohwer, F., Haynes, M., Glaser, F., Atamna-Ismaeel, N., Pinter, R.Y., Partensky, F., Koonin, E.V., Wolf, Y.I., Nelson, N., Béjà, O., 2009. Photosystem I gene cassettes are present in marine virus genomes. *Nature* **461**, 258–262. https://doi.org/10.1038/nature08284.

Sharrar, A.M., Flood, B.E., Bailey, J.V., Jones, D.S., Biddanda, B.A., Ruberg, S.A., Marcus, D.N., Dick, G.J., 2017. Novel Large Sulfur Bacteria in the Metagenomes of Groundwater-Fed Chemosynthetic Microbial Mats in the Lake Huron Basin. *Front Microbiol* **8**, 791. https://doi.org/10.3389/fmicb.2017.00791.

Shekhawat, G.S., 2005. Nanoscale Imaging of Buried Structures via Scanning Near-Field Ultrasound Holography. *Science* **310**, 89–92. https://doi.org/10.1126/science.1117694.

Short, C.M., Suttle, C.A., 2005. Nearly identical bacteriophage structural gene sequences are widely distributed in both marine and freshwater environments. *Appl Environ Microbiol* **71**, 480–486. https://doi.org/10.1128/AEM.71.1.480-486.2005.

Silas, S., Lucas-Elio, P., Jackson, S.A., Aroca-Crevillén, A., Hansen, L.L., Fineran, P.C., Fire, A.Z., Sánchez-Amat, A., 2017. Type III CRISPR-Cas systems can provide redundancy to counteract viral escape from type I systems. *Elife* **6**, e27601. https://doi.org/10.7554/eLife.27601.

Sillankorva, S., Neubauer, P., Azeredo, J., 2008. Pseudomonas fluorescens biofilms subjected to phage phiIBB-PF7A. *BMC Biotechnology* **8**, 79. https://doi.org/10.1186/1472-6750-8-79.

Silveira, C.B., Rohwer, F.L., 2016. Piggyback-the-Winner in host-associated microbial communities. *npj Biofilms Microbiomes* **2**, 16010. https://doi.org/10.1038/npjbiofilms.2016.10.

Smith, D.M., 2004. Challenges to the Worldwide Supply of Helium in the Next Decade. In 'AIP Conference Proceedings'. Presented at the Advances in Cryogenic Engineering: Transactions of the Cryogenic Engineering Conference - CEC, AIP, Anchorage, Alaska (USA), pp. 119–138. https://doi.org/10.1063/1.1774674.

Söding, J., Biegert, A., Lupas, A.N., 2005. The HHpred interactive server for protein homology detection and structure prediction. *Nucleic Acids Res* **33**, W244-248. https://doi.org/10.1093/nar/gki408.

Soler, N., Krupovic, M., Marguet, E., Forterre, P., 2015. Membrane vesicles in natural environments: a major challenge in viral ecology. *ISME J* **9**, 793–796. https://doi.org/10.1038/ismej.2014.184.

Srinivasiah, S., Bhavsar, J., Thapar, K., Liles, M., Schoenfeld, T., Wommack, K.E., 2008. Phages across the biosphere: contrasts of viruses in soil and aquatic environments. *Research in Microbiology* **159**, 349–357. https://doi.org/10.1016/j.resmic.2008.04.010.

Stedman, K.M., DeYoung, M., Saha, M., Sherman, M.B., Morais, M.C., 2015. Structural insights into the architecture of the hyperthermophilic Fusellovirus SSV1. *Virology* **474**, 105–109. https://doi.org/10.1016/j.virol.2014.10.014.

Stevens, T., 1997. Lithoautotrophy in the subsurface: Table 1. *FEMS Microbiol Rev* **20**, 327–337. https://doi.org/10.1111/j.1574-6976.1997.tb00318.x.

Stevens, T.O., McKinley, J.P., 1995. Lithoautotrophic Microbial Ecosystems in Deep Basalt Aquifers. *Science* **270**, 450–455. https://doi.org/10.1126/science.270.5235.450.

Storesund, J.E., Erga, S.R., Ray, J.L., Thingstad, T.F., Sandaa, R.-A., 2015. Top-down and bottom-up control on bacterial diversity in a western Norwegian deep-silled fjord. *FEMS Microbiology Ecology* **91**, fiv076. https://doi.org/10.1093/femsec/fiv076.

Sun, G., Xiao, J., Wang, H., Gong, C., Pan, Y., Yan, S., Wang, Y., 2014. Efficient purification and concentration of viruses from a large body of high turbidity seawater. *MethodsX* **1**, 197–206. https://doi.org/10.1016/j.mex.2014.09.001.

Sutherland, I., 2001. The biofilm matrix – an immobilized but dynamic microbial environment. *Trends in Microbiology* **9**, 222–227. https://doi.org/10.1016/S0966-842X(01)02012-1.

Sutherland, I.W., Hughes, K.A., Skillman, L.C., Tait, K., 2004. The interaction of phage and biofilms. *FEMS Microbiology Letters* **232**, 1–6. https://doi.org/10.1016/S0378-1097(04)00041-2.

Suttle, C.A., 2007. Marine viruses — major players in the global ecosystem. *Nat Rev Microbiol* **5**, 801–812. https://doi.org/10.1038/nrmicro1750.

Suttle, C.A., 2005. Viruses in the sea. *Nature* **437**, 356–361. https://doi.org/10.1038/nature04160.

Suttle, S.W., 1999. Viruses and Nutrient Cycles in the Sea **49**, 8.

Suzek, B.E., Huang, H., McGarvey, P., Mazumder, R., Wu, C.H., 2007. UniRef: comprehensive and non-redundant UniProt reference clusters. *Bioinformatics* **23**, 1282–1288. https://doi.org/10.1093/bioinformatics/btm098.

Suzuki, T., Iwasaki, T., Uzawa, T., Hara, K., Nemoto, N., Kon, T., Ueki, T., Yamagishi, A., Oshima, T., 2002. Sulfolobus tokodaii sp. nov. (f. Sulfolobus sp. strain 7), a new member of the genus Sulfolobus isolated from Beppu Hot Springs, Japan. *Extremophiles : life under extreme conditions* **6**, 39–44. https://doi.org/10.1007/s007920100221.

T

Takai, K., Moser, D.P., DeFlaun, M., Onstott, T.C., Fredrickson, J.K., 2001. Archaeal

diversity in waters from deep South African gold mines. *Appl Environ Microbiol* **67**, 5750–5760. https://doi.org/10.1128/AEM.67.21.5750-5760.2001.

Teira, E., Reinthaler, T., Pernthaler, A., Pernthaler, J., Herndl, G.J., 2004. Combining Catalyzed Reporter Deposition-Fluorescence In Situ Hybridization and Microautoradiography To Detect Substrate Utilization by Bacteria and Archaea in the Deep Ocean. *Applied and Environmental Microbiology* **70**, 4411–4414. https://doi.org/10.1128/AEM.70.7.4411-4414.2004.

Teske, A., Biddle, J.F., Edgcomb, V.P., Schippers, A., 2013. Deep subsurface microbiology: a guide to the research topic papers. *Front. Microbiol.* **4**. https://doi.org/10.3389/fmicb.2013.00122.

Teske, A.P., 2005. The deep subsurface biosphere is alive and well. *Trends in Microbiology* **13**, 402–404. https://doi.org/10.1016/j.tim.2005.07.004.

Thingstad, T., Lignell, R., 1997. Theoretical models for the control of bacterial growth rate, abundance, diversity and carbon demand. *Aquat. Microb. Ecol.* **13**, 19–27. https://doi.org/10.3354/ame013019.

Thingstad, T.F., 2000. Elements of a theory for the mechanisms controlling abundance, diversity, and biogeochemical role of lytic bacterial viruses in aquatic systems. *Limnol. Oceanogr.* **45**, 1320–1328. https://doi.org/10.4319/lo.2000.45.6.1320.

Thiroux, S., Dupont, S., Nesbø, C.L., Bienvenu, N., Krupovic, M., L'Haridon, S., Marie, D., Forterre, P., Godfroy, A., Geslin, C., 2021. The first head-tailed virus, MFTV1, infecting hyperthermophilic methanogenic deep-sea archaea. *Environ Microbiol* **23**, 3614–3626. https://doi.org/10.1111/1462-2920.15271.

Thurber, R.V., Haynes, M., Breitbart, M., Wegley, L., Rohwer, F., 2009. Laboratory procedures to generate viral metagenomes. *Nat Protoc* **4**, 470–483. https://doi.org/10.1038/nprot.2009.10.

Tokuyasu, K.T., 1973. A technique for ultracryotomy of cell suspensions and tissues. *J Cell Biol* **57**, 551–565. https://doi.org/10.1083/jcb.57.2.551.

Tolker-Nielsen, T., 2015. Biofilm Development. *Microbiol Spectr* **3**, MB-0001-2014. https://doi.org/10.1128/microbiolspec.MB-0001-2014.

Torrella, F., Morita, R.Y., 1979. Evidence by Electron Micrographs for a High Incidence of Bacteriophage Particles in the Waters of Yaquina Bay, Oregon: Ecological and Taxonomical Implicationst. *Appl Environ Microbiol* **37**, 5. https://doi.org/10.1128/aem.37.4.774-778.1979.

Trubl, G., Jang, H.B., Roux, S., Emerson, J.B., Solonenko, N., Vik, D.R., Solden, L., Ellenbogen, J., Runyon, A.T., Bolduc, B., Woodcroft, B.J., Saleska, S.R., Tyson, G.W., Wrighton, K.C., Sullivan, M.B., Rich, V.I., 2018. Soil Viruses Are Underexplored Players in Ecosystem Carbon Processing. *mSystems* **3**, e00076-18. https://doi.org/10.1128/mSystems.00076-18.

Tu, J., Park, T., Morado, D.R., Hughes, K.T., Molineux, I.J., Liu, J., 2017. Dual host specificity of phage SP6 is facilitated by tailspike rotation. *Virology* **507**, 206–215. https://doi.org/10.1016/j.virol.2017.04.017.

Turzynski, V., Monsees, I., Moraru, C., Probst, A.J., 2021. Imaging Techniques for Detecting Prokaryotic Viruses in Environmental Samples. *Viruses* **13**, 2126. https://doi.org/10.3390/v13112126.

Turzynski, V., Griesdorn, L., Moraru, C., Soares, A.R., Simon, S.A., Stach, T.L., Rahlff, J., Esser, S.P., Probst, A.J., 2023. Virus-Host Dynamics in Archaeal Groundwater Biofilms and the Associated Bacterial Community Composition. *Viruses* **15**, 910. https://doi.org/10.3390/v15040910.

Tyson, G.W., Banfield, J.F., 2005. Cultivating the uncultivated: a community genomics perspective. *Trends in Microbiology* **13**, 411–415.

https://doi.org/10.1016/j.tim.2005.07.003.

U

Untergasser, A., Cutcutache, I., Koressaar, T., Ye, J., Faircloth, B.C., Remm, M., Rozen, S.G., 2012. Primer3—new capabilities and interfaces. *Nucleic Acids Research* **40**, e115–e115. https://doi.org/10.1093/nar/gks596.

V

Vestergaard, G., Aramayo, R., Basta, T., Häring, M., Peng, X., Brügger, K., Chen, L., Rachel, R., Boisset, N., Garrett, R.A., Prangishvili, D., 2008. Structure of the Acidianus Filamentous Virus 3 and Comparative Genomics of Related Archaeal Lipothrixviruses. *J Virol* **82**, 371–381. https://doi.org/10.1128/JVI.01410-07.

Vidakovic, L., Singh, P.K., Hartmann, R., Nadell, C.D., Drescher, K., 2018. Dynamic biofilm architecture confers individual and collective mechanisms of viral protection. *Nat Microbiol* **3**, 26–31. https://doi.org/10.1038/s41564-017-0050-1.

Vijayakrishnan, S., McElwee, M., Loney, C., Rixon, F., Bhella, D., 2020. In situ structure of virus capsids within cell nuclei by correlative light and cryo-electron tomography. *Sci Rep* **10**, 17596. https://doi.org/10.1038/s41598-020-74104-x.

Vik, D.R., Roux, S., Brum, J.R., Bolduc, B., Emerson, J.B., Padilla, C.C., Stewart, F.J., Sullivan, M.B., 2017. Putative archaeal viruses from the mesopelagic ocean. *PeerJ* **5**, e3428. https://doi.org/10.7717/peerj.3428.

Vincent, F., Sheyn, U., Porat, Z., Schatz, D., Vardi, A., 2021. Visualizing active viral infection reveals diverse cell fates in synchronized algal bloom demise. *Proceedings of the National Academy of Sciences* **118**, e2021586118. https://doi.org/10.1073/pnas.2021586118.

Vincent, F., Sheyn, U., Porat, Z., Vardi, A., 2020. Visualizing active viral infection reveals diverse cell fates in synchronized algal bloom demise (preprint). Microbiology. https://doi.org/10.1101/2020.06.28.176719.

Visweswaran, G.R.R., Dijkstra, B.W., Kok, J., 2011. Murein and pseudomurein cell wall binding domains of bacteria and archaea—a comparative view. *Appl Microbiol Biotechnol* **92**, 921–928. https://doi.org/10.1007/s00253-011-3637-0.

Visweswaran, G.R.R., Dijkstra, B.W., Kok, J., 2010. Two Major Archaeal Pseudomurein Endoisopeptidases: PeiW and PeiP. *Archaea* **2010**, 480492. https://doi.org/10.1155/2010/480492.

W

Wagner, C., Reddy, V., Asturias, F., Khoshouei, M., Johnson, J.E., Manrique, P., Munson-McGee, J., Baumeister, W., Lawrence, C.M., Young, M.J., 2017. Isolation and Characterization of Metallosphaera Turreted Icosahedral Virus, a Founding Member of a New Family of Archaeal Viruses. *J. Virol.* **91**, e00925-17, /jvi/91/20/e00925-17.atom. https://doi.org/10.1128/JVI.00925-17.

Waldron, P.J., Petsch, S.T., Martini, A.M., Nüsslein, K., 2007. Salinity constraints on subsurface archaeal diversity and methanogenesis in sedimentary rock rich in organic matter. *Appl Environ Microbiol* **73**, 4171–4179. https://doi.org/10.1128/AEM.02810-06.

Wallner, G., Amann, R., Beisker, W., 1993. Optimizing fluorescent in situ hybridization with

rRNA-targeted oligonucleotide probes for flow cytometric identification of microorganisms. *Cytometry* **14**, 136–143. https://doi.org/10.1002/cyto.990140205.

Wang, H., Guo, Z., Feng, H., Chen, Y., Chen, X., Li, Z., Hernández-Ascencio, W., Dai, X., Zhang, Z., Zheng, X., Mora-López, M., Fu, Y., Zhang, C., Zhu, P., Huang, L., 2018. Novel Sulfolobus Virus with an Exceptional Capsid Architecture. *J Virol* **92**, e01727-17. https://doi.org/10.1128/JVI.01727-17.

Ward, B.W., Notte, J.A., Economou, N.P., 2006. Helium ion microscope: A new tool for nanoscale microscopy and metrology. *J. Vac. Sci. Technol. B* **24**, 2871. https://doi.org/10.1116/1.2357967.

Ward, J.A., Slater, G.F., Moser, D.P., Lin, L.-H., Lacrampe-Couloume, G., Bonin, A.S., Davidson, M., Hall, J.A., Mislowack, B., Bellamy, R.E.S., Onstott, T.C., Sherwood Lollar, B., 2004. Microbial hydrocarbon gases in the Witwatersrand Basin, South Africa: Implications for the deep biosphere. *Geochimica et Cosmochimica Acta* **68**, 3239–3250. https://doi.org/10.1016/j.gca.2004.02.020.

Watnick, P., Kolter, R., 2000. Biofilm, City of Microbes. *J Bacteriol* **182**, 2675–2679. https://doi.org/10.1128/JB.182.10.2675-2679.2000.

Watson, M.L., 1958. Staining of Tissue Sections for Electron Microscopy with Heavy Metals. *J Biophys Biochem Cytol* **4**, 475–478. https://doi.org/10.1083/jcb.4.6.727.

Webb, J.S., Givskov, M., Kjelleberg, S., 2003. Bacterial biofilms: prokaryotic adventures in multicellularity. *Current Opinion in Microbiology* **6**, 578–585. https://doi.org/10.1016/j.mib.2003.10.014.

Wegley, L., Edwards, R., Rodriguez-Brito, B., Liu, H., Rohwer, F., 2007. Metagenomic analysis of the microbial community associated with the coral Porites astreoides. *Environ Microbiol* **9**, 2707–2719. https://doi.org/10.1111/j.1462-2920.2007.01383.x.

Weidenbach, K., Nickel, L., Neve, H., Alkhnbashi, O.S., Künzel, S., Kupczok, A., Bauersachs, T., Cassidy, L., Tholey, A., Backofen, R., Schmitz, R.A., 2017. Methanosarcina Spherical Virus, a Novel Archaeal Lytic Virus Targeting Methanosarcina Strains. *J Virol* **91**, e00955-17. https://doi.org/10.1128/JVI.00955-17.

Weinbauer, M., Peduzzi, P., 1994. Frequency, size and distribution of bacteriophages in different marine bacterial morphotypes. *Mar. Ecol. Prog. Ser.* **108**, 11–20. https://doi.org/10.3354/meps108011.

Weinbauer, M., Suttle, C., 1997. Comparison of epifluorescence and transmission electron microscopy for counting viruses in natural marine waters. *Aquat. Microb. Ecol.* **13**, 225–232. https://doi.org/10.3354/ame013225.

Weinbauer, M.G., 2004. Ecology of prokaryotic viruses. *FEMS Microbiol Rev* **28**, 127–181. https://doi.org/10.1016/j.femsre.2003.08.001.

Weinbauer, M.G., Rassoulzadegan, F., 2004. Are viruses driving microbial diversification and diversity? *Environ Microbiol* **6**, 1–11. https://doi.org/10.1046/j.1462-2920.2003.00539.x.

Weitz, J.S., Li, G., Gulbudak, H., Cortez, M.H., Whitaker, R.J., 2019. Viral invasion fitness across a continuum from lysis to latency. *Virus Evolution* **5**, vez006. https://doi.org/10.1093/ve/vez006.

Wen, K., Ortmann, A.C., Suttle, C.A., 2004. Accurate Estimation of Viral Abundance by Epifluorescence Microscopy. *Applied and Environmental Microbiology* **70**, 3862–3867. https://doi.org/10.1128/AEM.70.7.3862-3867.2004.

Westmeijer, G., Mehrshad, M., Turner, S., Alakangas, L., Sachpazidou, V., Bunse, C., Pinhassi, J., Ketzer, M., Åström, M., Bertilsson, S., Dopson, M., 2022. Connectivity of Fennoscandian Shield terrestrial deep biosphere microbiomes with surface communities. *Commun Biol* **5**, 1–8. https://doi.org/10.1038/s42003-021-02980-8.

Whitman, W.B., Coleman, D.C., Wiebe, W.J., 1998. Prokaryotes: The unseen majority. *Proc.*

Natl. Acad. Sci. U.S.A. **95**, 6578–6583. https://doi.org/10.1073/pnas.95.12.6578.

Wickham, H., Averick, M., Bryan, J., Chang, W., McGowan, L.D., François, R., Grolemund, G., Hayes, A., Henry, L., Hester, J., Kuhn, M., Pedersen, T.L., Miller, E., Bache, S.M., Müller, K., Ooms, J., Robinson, D., Seidel, D.P., Spinu, V., Takahashi, K., Vaughan, D., Wilke, C., Woo, K., Yutani, H., 2019. Welcome to the Tidyverse. *J. Open Source Softw.* **4**, 1686. https://doi.org/10.21105/joss.01686.

Wickham 2016: Wickham, H. (2016). ggplot2: Elegant Graphics for Data Analysis. Springer-Verlag New York. ISBN 978-3-319-24277-4, https://ggplot2.tidyverse.org.

Wiegand, T., Karambelkar, S., Bondy-Denomy, J., Wiedenheft, B., 2020. Structures and Strategies of Anti-CRISPR-Mediated Immune Suppression. *Annual Review of Microbiology* **74**, 21–37. https://doi.org/10.1146/annurev-micro-020518-120107.

Wilhelm, S.W., Suttle, C.A., 1999. Viruses and Nutrient Cycles in the Sea: Viruses play critical roles in the structure and function of aquatic food webs. *BioScience* **49**, 781–788. https://doi.org/10.2307/1313569.

Wilkins, M.J., Daly, R.A., Mouser, P.J., Trexler, R., Sharma, S., Cole, D.R., Wrighton, K.C., Biddle, J.F., Denis, E.H., Fredrickson, J.K., Kieft, T.L., Onstott, T.C., Peterson, L., Pfiffner, S.M., Phelps, T.J., Schrenk, M.O., 2014. Trends and future challenges in sampling the deep terrestrial biosphere. *Front. Microbiol.* **5**. https://doi.org/10.3389/fmicb.2014.00481.

Wilkinson, J.F., 1958. The extracellualr polysaccharides of bacteria. *Bacteriol Rev* **22**, 46–73. https://doi.org/10.1128/br.22.1.46-73.1958.

Williamson, K.E., Fuhrmann, J.J., Wommack, K.E., Radosevich, M., 2017. Viruses in Soil Ecosystems: An Unknown Quantity Within an Unexplored Territory. *Annu. Rev. Virol.* **4**, 201–219. https://doi.org/10.1146/annurev-virology-101416-041639.

Williamson, K.E., Wommack, K.E., Radosevich, M., 2003. Sampling Natural Viral Communities from Soil for Culture-Independent Analyses. *AEM* **69**, 6628–6633. https://doi.org/10.1128/AEM.69.11.6628-6633.2003.

Williamson, S.J., Cary, S.C., Williamson, K.E., Helton, R.R., Bench, S.R., Winget, D., Wommack, K.E., 2008. Lysogenic virus–host interactions predominate at deep-sea diffuse-flow hydrothermal vents. *ISME J* **2**, 1112–1121. https://doi.org/10.1038/ismej.2008.73.

Williamson, S.J., Houchin, L.A., McDaniel, L., Paul, J.H., 2002. Seasonal Variation in Lysogeny as Depicted by Prophage Induction in Tampa Bay, Florida. *Appl Environ Microbiol* **68**, 4307–4314. https://doi.org/10.1128/AEM.68.9.4307-4314.2002.

Williamson, S.J., McLaughlin, M.R., Paul, J.H., 2001. Interaction of the ΦHSIC Virus with Its Host: Lysogeny or Pseudolysogeny? *Appl Environ Microbiol* **67**, 1682–1688. https://doi.org/10.1128/AEM.67.4.1682-1688.2001.

Wilson, W., Francis, I., Ryan, K., Davy, S., 2001. Temperature induction of viruses in symbiotic dinoflagellates. *Aquat. Microb. Ecol.* **25**, 99–102. https://doi.org/10.3354/ame025099.

Wimpenny, J.W.T., Colasanti, R., 1997. A unifying hypothesis for the structure of microbial biofilms based on cellular automaton models. *FEMS Microbiology Ecology* **22**, 1–16. https://doi.org/10.1111/j.1574-6941.1997.tb00351.x.

Winget, D.M., Helton, R.R., Williamson, K.E., Bench, S.R., Williamson, S.J., Wommack, K.E., 2011. Repeating patterns of virioplankton production within an estuarine ecosystem. *Proc Natl Acad Sci U S A* **108**, 11506–11511. https://doi.org/10.1073/pnas.1101907108.

Wirth, J., Young, M., 2022. Viruses in Subsurface Environments. *Annu. Rev. Virol.* **9**, 99–119. https://doi.org/10.1146/annurev-virology-093020-015957.

Wirth, J., Young, M., 2020. The intriguing world of archaeal viruses. *PLoS Pathog* **16**,

e1008574. https://doi.org/10.1371/journal.ppat.1008574.
Wolf, S., Fischer, M.A., Kupczok, A., Reetz, J., Kern, T., Schmitz, R.A., Rother, M., 2019. Characterization of the lytic archaeal virus Drs3 infecting Methanobacterium formicicum. *Arch Virol* **164**, 667–674. https://doi.org/10.1007/s00705-018-04120-w.
Wommack, K.E., Colwell, R.R., 2000. Virioplankton: Viruses in Aquatic Ecosystems. *Microbiology and Molecular Biology Reviews* **64**, 69–114. https://doi.org/10.1128/MMBR.64.1.69-114.2000.
Wommack, K.E., Sime-Ngando, T., Winget, D., Jamindar, S., Helton, R., 2010. Filtration-Based Methods for the Collection of Viral Concentrates from Large Water Samples. *Manual of Aquatic Viral Ecology (MAVE)* **12**. https://doi.org/10.4319/mave.2010.978-0-9845591-0-7.110.

X

Xiang, X., Chen, L., Huang, X., Luo, Y., She, Q., Huang, L., 2005. Sulfolobus tengchongensis Spindle-Shaped Virus STSV1: Virus-Host Interactions and Genomic Features. *J Virol* **79**, 8677–8686. https://doi.org/10.1128/JVI.79.14.8677-8686.2005.
Xiao, C., Kuznetsov, Y.G., Sun, S., Hafenstein, S.L., Kostyuchenko, V.A., Chipman, P.R., Suzan-Monti, M., Raoult, D., McPherson, A., Rossmann, M.G., 2009. Structural Studies of the Giant Mimivirus. *PLoS Biol* **7**, e1000092. https://doi.org/10.1371/journal.pbio.1000092.
Xu, Z., Huang, T., Min, D., Soteyome, T., Lan, H., Hong, W., Peng, F., Fu, X., Peng, G., Liu, J., Kjellerup, B.V., 2022. Regulatory network controls microbial biofilm development, with Candida albicans as a representative: from adhesion to dispersal. *Bioengineered* **13**, 253–267. https://doi.org/10.1080/21655979.2021.1996747.

Y

Yin, W., Wang, Y., Liu, L., He, J., 2019. Biofilms: The Microbial "Protective Clothing" in Extreme Environments. *Int J Mol Sci* **20**, 3423. https://doi.org/10.3390/ijms20143423.
Yu, Y., Yan, F., Chen, Y., Jin, C., Guo, J.-H., Chai, Y., 2016. Poly-γ-Glutamic Acids Contribute to Biofilm Formation and Plant Root Colonization in Selected Environmental Isolates of Bacillus subtilis. *Front. Microbiol.* **7**. https://doi.org/10.3389/fmicb.2016.01811.

Z

Zablocki, O., van Zyl, L.J., Kirby, B., Trindade, M., 2017. Diversity of dsDNA Viruses in a South African Hot Spring Assessed by Metagenomics and Microscopy. *Viruses* **9**. https://doi.org/10.3390/v9110348.
Zaremba-Niedzwiedzka, K., Caceres, E.F., Saw, J.H., Bäckström, D., Juzokaite, L., Vancaester, E., Seitz, K.W., Anantharaman, K., Starnawski, P., Kjeldsen, K.U., Stott, M.B., Nunoura, T., Banfield, J.F., Schramm, A., Baker, B.J., Spang, A., Ettema, T.J.G., 2017. Asgard archaea illuminate the origin of eukaryotic cellular complexity. *Nature* **541**, 353–358. https://doi.org/10.1038/nature21031.
Zhang, H., Ning, K., 2015. The Tara Oceans Project: New Opportunities and Greater Challenges Ahead. *Genomics, Proteomics & Bioinformatics* **13**, 275–277. https://doi.org/10.1016/j.gpb.2015.08.003.
Zhang, J., Mao, L., Zhang, L., Loh, K.-C., Dai, Y., Tong, Y.W., 2017. Metagenomic insight

into the microbial networks and metabolic mechanism in anaerobic digesters for food waste by incorporating activated carbon. *Sci Rep* **7**, 11293. https://doi.org/10.1038/s41598-017-11826-5.

Zhang, J., Zheng, X., Wang, H., Jiang, H., Dong, H., Huang, L., 2019. Novel *Sulfolobus* Fuselloviruses with Extensive Genomic Variations. *J Virol* **94**, e01624-19, /jvi/94/4/JVI.01624-19.atom. https://doi.org/10.1128/JVI.01624-19.

Zhang, X., Bishop, P.L., 2003. Biodegradability of biofilm extracellular polymeric substances. *Chemosphere* **50**, 63–69. https://doi.org/10.1016/S0045-6535(02)00319-3.

Zhen, X., Zhou, H., Ding, W., Zhou, B., Xu, X., Perčulija, V., Chen, C.-J., Chang, M.-X., Choudhary, M.I., Ouyang, S., 2019. Structural basis of AimP signaling molecule recognition by AimR in Spbeta group of bacteriophages. *Protein Cell* **10**, 131–136. https://doi.org/10.1007/s13238-018-0588-6.

Zillig, W., Kletzin, A., Schleper, C., Holz, I., Janekovic, D., Hain, J., Lanzendörfer, M., Kristjansson, J.K., 1993. Screening for Sulfolobales, their Plasmids and their Viruses in Icelandic Solfataras. *Systematic and Applied Microbiology* **16**, 609–628. https://doi.org/10.1016/S0723-2020(11)80333-4.

Zillig, W., Stetter, K.O., Wunderl, S., Schulz, W., Priess, H., Scholz, I., 1980. The Sulfolobus-"Caldariella" group: Taxonomy on the basis of the structure of DNA-dependent RNA polymerases. *Arch. Microbiol.* **125**, 259–269. https://doi.org/10.1007/BF00446886.

Zimmerman, A.E., Bachy, C., Ma, X., Roux, S., Jang, H.B., Sullivan, M.B., Waldbauer, J.R., Worden, A.Z., 2019. Closely related viruses of the marine picoeukaryotic alga *Ostreococcus lucimarinus* exhibit different ecological strategies. *Environ Microbiol* **21**, 2148–2170. https://doi.org/10.1111/1462-2920.14608.

Zimmermann, L., Stephens, A., Nam, S.-Z., Rau, D., Kübler, J., Lozajic, M., Gabler, F., Söding, J., Lupas, A.N., Alva, V., 2018. A Completely Reimplemented MPI Bioinformatics Toolkit with a New HHpred Server at its Core. *J Mol Biol* **430**, 2237–2243. https://doi.org/10.1016/j.jmb.2017.12.007.

Zucker, F., Bischoff, V., Olo Ndela, E., Heyerhoff, B., Poehlein, A., Freese, H.M., Roux, S., Simon, M., Enault, F., Moraru, C., 2022. New Microviridae isolated from Sulfitobacter reveals two cosmopolitan subfamilies of single-stranded DNA phages infecting marine and terrestrial Alphaproteobacteria. *Virus Evol* **8**, veac070. https://doi.org/10.1093/ve/veac070.

VII. Content of supporting CD

The supporting CD contains the Supplementary material for the publications listened in this dissertation. One manuscript (Turzynski et al., 2021) does not contain any supplemental material because it is a Review.

The folders on the CD are the following:

Table VII.1: Structure of the data on the supporting CD.

Folder name	Description of the content
Publication_Review_Turzynski_et_al_2021	This folder contains besides the publication also the Figures in TIFF format
Publication_Rahlff_Turzynski_et_al_2021	In this folder, the manuscript, the Supplementary Information, Supplementary Data, and Figures in TIFF format of the publication of Rahlff et al. (2021) can be found
Publication_Turzynski_et_al_2023	Here, all data for the publication of Turzynski et al. (2023) can be found, including the manuscript, Supplementary Material, Supplementary Information, Supplementary Tables, and Figures in TIFF format

In addition, all folders, the dissertation, and the respective imaging data can be found on our in-house server that belong to our AG Probst group: /BIFROST/NOVAC_Vicky/

Furthermore, all imaging and Nanopore data are uploaded on Figshare (https://figshare.com/) with the project title “Virus-host dynamics in archaeal groundwater biofilms and the associated bacterial community composition”. This corresponds to the manuscript of Turzynski et al. (2023) and also includes all raw data of the manuscript of Rahlff et al. (2021).

Microscopy images can also be found on our microscopy computer: D:\Users\zeiss\Desktop\Axio\Microscopy_Vicky

VIII. Eidesstattliche Erklärung

Ich erkläre hiermit an Eides statt, dass die vorliegende Arbeit ohne unzulässige Hilfe Dritter und ohne Benutzung anderer als der angegebenen Hilfsmittel angefertigt habe. Die aus anderen Quellen direkt oder indirekt übernommenen Daten und Konzepte sind unter Angabe des Literaturzitats gekennzeichnet.

Essen, 27.04.2023

Unterschrift: Victoria Turzynski